# Improving breast cancer outcome by preoperative systemic therapy and image-guided surgery

Mieog, J.S.D.

# Improving breast cancer outcome by preoperative systemic therapy and image-guided surgery

Sven Mieog

Printed by Optima Grafische Communicatie, Rotterdam

Cover design by Caro van Dijk

ISBN 978-94-6169-150-7

# Improving breast cancer outcome by preoperative systemic therapy and image-guided surgery

Proefschrift

ter verkrijging van
de graad van Doctor aan de Universiteit Leiden,
op gezag van de Rector Magnificus Prof. mr. P.F. van der Heijden,
volgens besluit van het college voor Promoties
te verdedigen op woensdag 26 oktober 2011
klokke 16.15 uur

door

Jan Sven David Mieog

geboren te Monster
in 1980

**Promotiecommissie**

| | |
|---|---|
| Promotor | Prof. dr. C.J.H. van de Velde |
| Co-promotor | Dr. A.L. Vahrmeijer |
| Overige leden | Prof. dr. C.W.G.M. Löwik<br>Prof. dr. J.W.R. Nortier<br>Prof. dr. M.J. van de Vijver (Universiteit van Amsterdam)<br>Dr. P.J.K. Kuppen<br>Dr. G.J. Liefers<br>Dr. V.T.H.B.M. Smit |

The author of this thesis is a MD-medical research trainee funded by the The Netherlands Organisation for Health Research and Development (grant nr. 92003526). The research described in this thesis was financially supported by the Center for Translational Molecular Medicine (CTMM, DeCoDe and MUSIS projects), the Dutch Cancer Society (KWF 2007-3968 and UL 2010-4732), and the Sacha Swarttouw-Hijmans Foundation.

Financial support by J.E. Jurriaanse Foundation, Pfizer, Novartis, Roche, Sanofi-Aventis, GSK, ChipSoft, Caliper Life Sciences, LI-COR Biosciences, PerkinElmer and Percuros for the publication of this thesis is gratefully acknowledged.

*Voor mijn ouders*

*Aan Anne*

# CONTENTS

# Chapter 1

## General introduction and outline of thesis

Breast cancer is the most common cancer in women and the leading cause of cancer death among females, accounting for 23% of the total cancer cases and 14% of cancer deaths.[1] In the Netherlands, 12.000 women are diagnosed with the disease annually and the lifetime risk of developing breast cancer is 12-13%. The incidence of breast cancer is still increasing, which likely results from changes in reproductive factors (including the increased use of postmenopausal hormone therapy) as well as an increased screening intensity.[2] Breast cancer is strongly related to age. Only 5% of all breast cancers occur in women under 40 years old.[3] The age distribution of breast cancer shows a bimodal characterization and early- and late-onset modes are observed near ages 50 and 70 years, respectively (Figure 1).[4] Over the last decades, mortality trends for breast cancer are declining. Currently, 90% of breast cancer patients are expected to survive at least five years. The increase in breast cancer survival seen since the mid-1970s has been attributed to improved systemic treatment. Nonetheless, surgery is still the cornerstone of the curative treatment of breast cancer.

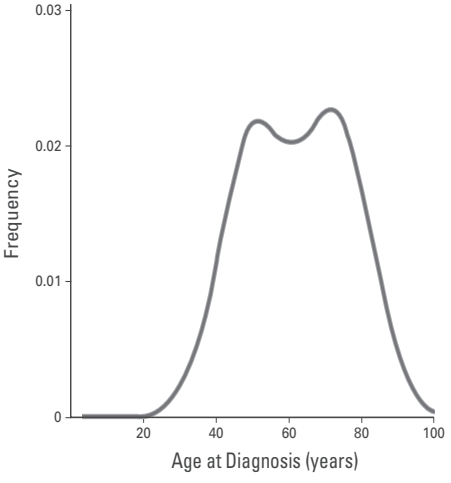


**Figure 1.** Bimodal age distribution at diagnosis for invasive female breast cancer cases (n = 94,813) in the National Cancer Institute's Surveillance, Epidemiology, and End Results Program during the years 1994 through 1997.[4]

## HISTORY OF BREAST CANCER SURGERY

The local treatment of breast cancer has undergone a dramatic paradigm shift during the last century, characterized by a more conservative surgical approach. The radical mastectomy, published in a landmark paper by Dr. William Halsted in 1894, was regarded as standard of care for every breast cancer patient regardless of any tumor characteristic or status of the axilla for several decades. As this operation included an *en bloc* excision of the breast gland, both pectoral muscles and all relevant lymph nodes, it was associated with a high morbidity.[5] In an attempt to decrease morbidity, the modified radical mastectomy was introduced, in which both pectoral muscles were spared and a less extensive axillary dissection was performed. The efficacy of both

operations was equal, while the morbidity was markedly decreased.[6,7] During the 1970s, the breast-conserving therapy was introduced, which comprised of a lumpectomy in combination with radiotherapy to the breast. While the survival rates were equal for mastectomy and lumpectomy,[8] the surgical morbidity and patients' self-image owing to better cosmetic outcome were ameliorated.[9, 10] In the 1990s, the sentinel lymph node procedure was introduced to further reduce surgical extent.[11] The sentinel lymph node procedure prevents the morbidity of an axillary lymph node dissection in lymph node negative patients. In line with this changing surgical approach of breast cancer, preoperative or neoadjuvant chemotherapy was introduced in early breast cancer to down size breast tumors in order to improve surgical possibilities and increase the rate of breast-conserving surgery.

## PART I: NEOADJUVANT SYSTEMIC THERAPY

Neoadjuvant chemotherapy in breast cancer treatment defines the use of cytotoxic chemotherapy before any local treatment, either surgery or radiotherapy. Although other terms such as 'primary', 'preoperative', 'induction', 'upfront' or 'initial' are perhaps more accurate descriptions, it was decided during the 2003 Consensus Conference to retain the more commonly used term 'neoadjuvant'.[12]

The use of neoadjuvant chemotherapy in breast cancer was introduced almost simultaneously with the establishment of adjuvant chemotherapy in the 1970s in patients with locally advanced disease in order to convert inoperable tumors into operable tumors. At present, neoadjuvant chemotherapy is the standard of care for patients with locally advanced and inflammatory breast cancer. Soon after reaching positive results in locally advanced breast cancer, randomized controlled trials were conducted to evaluate neoadjuvant chemotherapy in earlier, operable stages. A major benefit of neoadjuvant chemotherapy is the increase in breast conservation rate, which is associated with less morbidity and improved body image compared with complete breast removal. However, concerns exist on local control after down staging of the tumor and the delay of surgery in patients with tumors resistant to chemotherapy.

Besides an increase in breast conservation, an increase in overall survival was also anticipated with the use of neoadjuvant chemotherapy in early stage breast cancer. The rationale for this survival benefit was derived from several experimental studies, in which an increase in the proliferation index of residual tumor was shown after removal of the primary tumor, which resulted in acceleration of tumor growth.[13, 14] This increase in tumor growth was repressed by preoperative chemotherapy, which diminished the release of circulating growth factors and prolonged survival.[15] A more theoretical advantage is the Goldie–Coldman hypothesis, which proposes that, as a tumor cell population increases, an ever-expanding number of drug-resistant phenotypic variants arise that are more difficult to eradicate with chemotherapy.[16]

Moreover, early introduction of systemic therapy in the biological life of the tumor could tackle micrometastatic tumor cells several months earlier than in the adjuvant setting. Upon these considerations, it was reasoned that neoadjuvant chemotherapy might improve overall survival in early stage breast cancer patients.

Since the mid-1980s, several trials have been conducted to evaluate the efficiency of neoadjuvant chemotherapy compared with adjuvant chemotherapy in early stage breast cancer. In **Chapter 2**, a meta-analysis of these trials is performed in order to assess the overall effectiveness of neoadjuvant chemotherapy on clinical outcome.

**Prediction of tumor response to therapy: towards personalized treatment**

Neoadjuvant chemotherapy facilitates the *in vivo* monitoring of changes in tumor volume during systemic treatment. The achievement of complete eradication of local disease by systemic neoadjuvant therapy is strongly associated with a favorable long-term prognosis.[17] So, a pathological complete response during neoadjuvant therapy reflects chemosensitivity of distant micrometastasic disease. These findings have led to the use of pathological complete response as a surrogate marker for prognosis of survival and its use in clinical trials provides an early indication of drug activity. Moreover, the assessment of tumor response during neoadjuvant therapy is an excellent study model to identify predictive factors. A predictive factor is any clinical or biological characteristic associated with a response or lack of a response to a specific treatment. Identification of predictive factors may lead to more personalized treatment strategies.

In **Chapter 3**, predictive factors are identified that are capable of predicting pathological complete and overall clinical tumor response to preoperative anthracycline-based chemotherapy. For this, the pre-treatment core biopsies of women with operable breast cancer who enrolled in the European Organization for Research and Treatment of Cancer (EORTC) trial 10902 were used.

One of the most important predictive factors of tumor response to chemotherapy is the estrogen receptor (ER) status of the tumor. Several neoadjuvant chemotherapy studies have demonstrated that patients with ER negative tumors are more likely to achieve a pathological complete response than those with ER positive tumors.[18-20] Moreover, these studies found that, when patients with ER negative tumors achieved a pathological complete response, their survival was comparable to that of ER positive patients. Translating these results to the adjuvant setting, some authors have argued that chemotherapy should not be administrated to patients with node negative, ER positive breast cancer, but, instead, should be treated with hormonal treatment alone.

Young age (< 40 years) at the time of diagnosis of breast cancer is an independent factor of poor prognosis and current consensus guidelines have included young age as an absolute indication for adjuvant systemic chemotherapy irrespective of other tumor characteristics, such as stage, grade, or ER status.[21] However, young patients with hormone receptor positive breast cancer might receive limited benefit from

chemotherapy alone. Due to the fact that breast cancer at a young age is a relatively rare event and accounts for 5-7.5% of all cases, limited data on predictive and prognostic factors are available for this patient group. Therefore, concerns exist on the overtreatment with chemotherapy of these young patients. In particular the long-term toxicity of chemotherapy and the implications of possible fertility impairment and premature menopause are of concern in young women.[22] More refined knowledge of predictive and prognostic factors in young breast cancer patients will be of use in guiding systemic therapy in these women.

In **Chapter 4**, the effect of chemotherapy is studied in young patients with breast cancer in relation to hormone receptor status. In this study, the paraffin-embedded tumor material was used from a large cohort early stage breast cancer patients younger than 40 years who participated in one of four EORTC trials.

In **Chapter 5**, prognostic factors are identified in the above-described cohort and in the node negative subpopulation of which most patients did not receive chemotherapy.

**Resistance to therapy and breast cancer stem cells**

Despite recent advances in systemic therapy and radiotherapy, a significant proportion of early stage breast cancer patients still develop loco regional recurrences and distant metastases. Often, these recurrences occur after a considerable follow-up period. This phenomenon, referred as tumor dormancy, is a particular clinical problem in breast cancer, where disease recurrences are witnessed 20 years after initial curative treatment.[23] Recent biological research has provided evidence that the cancer stem cell theory might explain these treatment failures.

Cancer stem cells, defined as a small subset of tumor cells with stem cell-like features, including epithelial-to-mesenchymal transition, have the capacity of self-renewal and differentiation; giving rise to heterogeneous tumor cell population.[24] Various studies have shown that cancer stem cells have the ability to survive drugs and radiotherapy by a number of properties including high expression of ABC drug transporters, higher levels of DNA repair, and more anti-apoptotic traits.[25-27] Selective survival of cancer stem cells might provide opportunities for understanding treatment resistance and tumor dormancy. Several cancer stem cell markers have been suggested for breast cancer. However, expression of the detoxifying enzyme aldehyde dehydrogenase-1 (ALDH1) has shown the most promise as a clinically relevant prognostic cancer stem cell marker in breast cancer.[28-30]

Breast cancer stem cells could also provide a biological explanation for the well-known age-specific difference in breast cancer survival (Figure 1). Young age (< 65 years) is associated with more aggressive tumors with a relatively high risk of distant metastasis and loco-regional recurrence,[3] whereas old age is associated with more

indolent tumors.[31, 32] However, it is unknown whether the expression of ALDH1 is associated with age and has an influence on clinical outcome.

In **Chapter 6**, the age distribution of ALDH1 expression and its prognostic role in young and elderly patients was analyzed using the long-term follow-up data of a large cohort of breast cancer patients primarily treated with surgery at the Leiden University Medical Center.

To further elucidate the biological pathways involved in the formation and growth of cancer stem cells, the role of the putative coagulation protein tissue factor (TF) has been suggested. A large number of tumor types show tumoral expression of TF and the complex of TF and activated factor VII (TF:FVII) have been implicated in tumor growth and metastasis. TF exhibits its effect through a protease activated receptor-2 (PAR2)-dependent pathway, which results in proliferation, increased oncogene expression and cell migration. TF expression and the TF:FVII/PAR2 axis has been linked to cancer stem cells. However, the role of TF and its alternatively spliced isoform (asTF), which exhibit its role through an integrin-related pathway, have not been tested in breast cancer.

In **Chapter 7**, the expression of TF and asTF in early breast cancer was assessed as well as the association with clinicopathological characteristics, patient outcome and ALDH1 expression in the above-described cohort.

## PART II: IMAGE-GUIDED SURGERY

### Intraoperative tumor visualization

The main challenge in the surgical treatment of breast cancer is the complete removal of tumor tissue taking into account an adequate tumor-free margin and an acceptable cosmetic result. During breast-conserving surgery, the surgeon has to rely on palpation and visual inspection to discriminate tumor tissue from normal tissue. The distinction between tumor and normal tissue is often not evident, resulting in irradical resections in 5 to 40% of patients undergoing breast-conserving surgery, which requires additional resection or intensified radiotherapy regimens.[33-35] Particularly, after neoadjuvant chemotherapy the assessment of remnant cells may be difficult and tumor response can be either under- or overestimated owing to fibrosis, weakening of the tumor margins and resolution of edema. Local recurrence rates following breast-conservative therapy of 6.7 to 11% are reported,[36] which can be explained by remnant tumor tissue that is not identified during surgery. Loco regional recurrences are associated with a decrease in overall survival.[36] Therefore, there is a need for a diagnostic tool that can discriminate tumor tissue from normal tissue in real-time during surgery.

Optical imaging using near-infrared (NIR) fluorescence is a new technique that can be used to visualise structures in real-time during surgery. Advantages of

NIR fluorescent light (700-900nm) include high tissue penetration (millimetres to centimetres deep) and low autofluorescence, thereby providing sufficient contrast.[37] Because the human eye is insensitive to NIR wavelengths, the use of NIR light does not alter the surgical field. Several imaging systems have recently become available that are capable of visualizing NIR fluorescence in real-time (reviewed in [38]). Besides these imaging systems, tumor-targeted NIR fluorescent contrast agents ("probes") are necessary to visualize cancer cells. Various mechanisms are available for probes to target tumor cells: they can target increased metabolism, upregulated enzymes, or specific cell surface markers. Therefore, the use of NIR fluorescence imaging can be of great value in the intraoperative detection of critical anatomical structures and oncologic targets. The ultimate goal of NIR fluorescence imaging is a real-time visualization of cancer cells during surgery in order to achieve an increase of the radical resection rate and thereby an improvement in breast cancer outcome.

In **Chapter 8**, a novel, hand-held, intraoperative NIR fluorescence imaging system is tested. The minimal detection limits, resolving power and intraoperative utility are addressed in primary breast cancer and metastatic colorectal cancer in two syngeneic rat models.

In **Chapter 9**, the technique of NIR fluorescence imaging is assessed in a syngeneic breast cancer rat model using a protease-activated NIR probe and the accuracy is determined of intraoperative tumor detection to obtain an adequate tumor-free resection margin.

In **Chapter 10**, the technique of NIR fluorescence imaging is assessed in a syngeneic breast cancer rat model using monoclonal antibodies conjugated to a NIR fluorescence dye and its utility for image-guided resection is tested.

### Sentinel lymph node mapping

The sentinel lymph node (SLN) procedure, as introduced in the treatment of breast cancer by Giuliano *et al*,[11] is currently regarded as standard of care in staging of the axilla. The SLN is the first lymph node that receives lymphatic drainage from a tumor, and identification of the SLN and analysis for tumor involvement should predict the status of the remaining lymph nodes.

Despite widespread acceptance of SLN procedure, the current technique can be improved. The SLN procedure utilizes a gamma ray-emitting radiotracer or a blue dye or a combination. Radiocolloids require involvement of a nuclear medicine physician, can be difficult to localize with a handheld gamma probe and there is some exposure to ionizing radiation. Moreover, the time-window for SLN identification after injection of the radiocolloid is limited. Blue dyes cannot be seen easily through skin and fat and allow limited visualization of afferent lymphatic vessels and the SLN. Surgical time needed to complete the SLN procedure may take up to 30-45 minutes, in particular when identification is difficult, requiring extensive axillary exploration.

NIR fluorescence imaging using the NIR fluorescence agent indocyanine green has the potential to provide an alternative for, or an addition to, conventional techniques used for SLN mapping.[39] Indocyanine green (ICG) is currently the only clinically available NIR fluorophore that can be used for SLN mapping. Preclinically, ICG adsorbed to human serum albumin (ICG:HSA) improves its performance as a lymphatic tracer. The benefit of ICG:HSA for SLN mapping of breast cancer has not yet been assessed in a clinical trial.

In **Chapter 11**, the development of a miniaturized version of the fluorescence-assisted resection and exploration (FLARE) imaging system is described. Using this Mini-FLARE, preclinical and clinical optimization of the lymphatic tracer ICG:HSA was performed, followed by a more refined optimization in a phase II clinical trial. During this dose-escalating trial, the use of NIR fluorescence was directly compared with the combination of radioactive colloid and blue dye in breast cancer patients undergoing SLN mapping.

In **Chapter 12**, a double-blind, randomized clinical study is performed to determine if ICG:HSA has advantages over ICG alone in the SLN mapping in breast cancer.

Finally, **Chapter 13** includes a summary of this thesis as well as a general discussion. **Chapter 14** provides a summary in Dutch.

## REFERENCES


1. Jemal A, Bray F, Center MM, et al. Global cancer statistics. CA Cancer J Clin 2011 [cited 2011, Feb 25]; Available from: http://www.ncbi.nlm.nih.gov/pubmed/21296855.
2. Althuis MD, Dozier JM, Anderson WF, et al. Global trends in breast cancer incidence and mortality 1973-1997. Int J Epidemiol 2005; 34:405-12.
3. Anders CK, Johnson R, Litton J, et al. Breast cancer before age 40 years. Semin Oncol 2009; 36:237-49.
4. Anderson WF, Jatoi I, Sherman ME. Qualitative age interactions in breast cancer studies: mind the gap. J Clin Oncol 2009; 27:5308-11.
5. Halsted WS. I. The results of radical operations for the cure of carcinoma of the breast. Ann Surg 1907; 46:1-19.
6. Maddox WA, Carpenter JT, Jr., Laws HL, et al. A randomized prospective trial of radical (Halsted) mastectomy versus modified radical mastectomy in 311 breast cancer patients. Ann Surg 1983; 198:207-12.
7. Fisher B, Redmond C, Fisher ER, et al. Ten-year results of a randomized clinical trial comparing radical mastectomy and total mastectomy with or without radiation. N Engl J Med 1985; 312:674-81.
8. Yang SH, Yang KH, Li YP, et al. Breast conservation therapy for stage I or stage II breast cancer: a meta-analysis of randomized controlled trials. Ann Oncol 2008; 19:1039-44.
9. Tsai RJ, Dennis LK, Lynch CF, et al. The risk of developing arm lymphedema among breast cancer survivors: a meta-analysis of treatment factors. Ann Surg Oncol 2009; 16:1959-72.
10. Kiebert GM, de Haes JC, van de Velde CJ. The impact of breast-conserving treatment and mastectomy on the quality of life of early-stage breast cancer patients: a review. J Clin Oncol 1991; 9:1059-70.

11. Giuliano AE, Kirgan DM, Guenther JM, et al. Lymphatic mapping and sentinel lymphadenectomy for breast cancer. Ann Surg 1994; 220:391-8.
12. Schwartz GF, Hortobagyi GN. Proceedings of the consensus conference on neoadjuvant chemotherapy in carcinoma of the breast, April 26-28, 2003, Philadelphia, Pennsylvania. Cancer 2004; 100:2512-32.
13. Gunduz N, Fisher B, Saffer EA. Effect of surgical removal on the growth and kinetics of residual tumor. Cancer Res 1979; 39:3861-5.
14. Van Dierendonck JH, Keijzer R, Cornelisse CJ, et al. Surgically induced cytokinetic responses in experimental rat mammary tumor models. Cancer 1991; 68:759-67.
15. Fisher B, Gunduz N, Saffer EA. Influence of the interval between primary tumor removal and chemotherapy on kinetics and growth of metastases. Cancer Res 1983; 43:1488-92.
16. Goldie JH, Coldman AJ. A mathematic model for relating the drug sensitivity of tumors to their spontaneous mutation rate. Cancer Treat Rep 1979; 63:1727-33.
17. Wolmark N, Wang J, Mamounas E, et al. Preoperative chemotherapy in patients with operable breast cancer: nine-year results from National Surgical Adjuvant Breast and Bowel Project B-18. J Natl Cancer Inst Monogr 2001: 96-102.
18. Ring AE, Smith IE, Ashley S, et al. Oestrogen receptor status, pathological complete response and prognosis in patients receiving neoadjuvant chemotherapy for early breast cancer. Br J Cancer 2004; 91:2012-7.
19. Kuerer HM, Newman LA, Smith TL, et al. Clinical course of breast cancer patients with complete pathologic primary tumor and axillary lymph node response to doxorubicin-based neoadjuvant chemotherapy. J Clin Oncol 1999; 17:460-9.
20. Colleoni M, Bagnardi V, Rotmensz N, et al. Increasing steroid hormone receptors expression defines breast cancer subtypes non responsive to preoperative chemotherapy. Breast Cancer Res Treat 2009; 116:359-69.
21. Goldhirsch A, Gelber RD, Yothers G, et al. Adjuvant therapy for very young women with breast cancer: need for tailored treatments. J Natl Cancer Inst Monogr 2001:44-51.
22. Shannon C, Smith IE. Breast cancer in adolescents and young women. Eur J Cancer 2003; 39:2632-42.
23. Stearns AT, Hole D, George WD, et al. Comparison of breast cancer mortality rates with those of ovarian and colorectal carcinoma. Br J Surg 2007; 94:957-65.
24. Al-Hajj M, Wicha MS, Benito-Hernandez A, et al. Prospective identification of tumorigenic breast cancer cells. Proc Natl Acad Sci USA 2003; 100:3983-8.
25. Lou H, Dean M. Targeted therapy for cancer stem cells: the patched pathway and ABC transporters. Oncogene 2007; 26:1357-60.
26. Phillips TM, McBride WH, Pajonk F. The response of CD24(-/low)/CD44+ breast cancer-initiating cells to radiation. J Natl Cancer Inst 2006; 98:1777-85.
27. Gong C, Yao H, Liu Q, et al. Markers of tumor-initiating cells predict chemoresistance in breast cancer. PLoS One 2010; 5:e15630.
28. Ginestier C, Hur MH, Charafe-Jauffret E, et al. ALDH1 is a marker of normal and malignant human mammary stem cells and a predictor of poor clinical outcome. Cell Stem Cell 2007; 1:555-67.
29. Resetkova E, Reis-Filho JS, Jain RK, et al. Prognostic impact of ALDH1 in breast cancer: a story of stem cells and tumor microenvironment. Breast Cancer Res Treat 2010; 123:97-108.
30. Tanei T, Morimoto K, Shimazu K, et al. Association of breast cancer stem cells identified by aldehyde dehydrogenase 1 expression with resistance to sequential Paclitaxel and epirubicin-based chemotherapy for breast cancers. Clin Cancer Res 2009; 15:4234-41.
31. Diab SG, Elledge RM, Clark GM. Tumor characteristics and clinical outcome of elderly women with breast cancer. J Natl Cancer Inst 2000; 92:550-6.
32. Remvikos Y, Magdelenat H, Dutrillaux B. Genetic evolution of breast cancers. III: Age-dependent variations in the correlations between biological indicators of prognosis. Breast Cancer Res Treat 1995; 34:25-33.
33. Verkooijen HM, Borel Rinkes IH, Peeters PH, et al. Impact of stereotactic large-core needle biopsy on diagnosis and surgical treatment of nonpalpable breast cancer. Eur J Surg Oncol 2001; 27:244-9.
34. Mai KT, Yazdi HM, Isotalo PA. Resection margin status in lumpectomy specimens of infiltrating lobular carcinoma. Breast Cancer Res Treat 2000; 60:29-33.

35. Rizzo M, Iyengar R, Gabram SG, et al. The effects of additional tumor cavity sampling at the time of breast-conserving surgery on final margin status, volume of resection, and pathologist workload. Ann Surg Oncol 2010; 17:228-34.
36. Clarke M, Collins R, Darby S, et al. Effects of radiotherapy and of differences in the extent of surgery for early breast cancer on local recurrence and 15-year survival: an overview of the randomised trials. Lancet 2005; 366:2087-106.
37. Frangioni JV. New technologies for human cancer imaging. J Clin Oncol 2008; 26:4012-21.
38. Gioux S, Choi HS, Frangioni JV. Image-guided surgery using invisible near-infrared light: fundamentals of clinical translation. Mol Imaging 2010; 9:237-55.
39. Schaafsma BE, Mieog JS, Hutteman M, et al. The clinical use of indocyanine green as a near-infrared fluorescent contrast agent for image-guided oncologic surgery. J Surg Oncol 2011; 104:323-32.

# Part I

## Preoperative systemic therapy

# Part IA

## Preoperative therapy and personalized treatment

# Chapter 2

## Neoadjuvant chemotherapy for operable breast cancer: a Cochrane systematic review

Mieog JSD, van der Hage JA, van de Velde CJH

*Br J Surg 2007; 94:1189-200 and Cochrane Database Syst Rev 2007: CD005002*

## ABSTRACT

### Introduction

Neoadjuvant chemotherapy for early breast cancer can avoid mastectomy by shrinkage of tumor volume. Additional potential advantages are early introduction of systemic therapy, determination of chemosensitivity and early availability of prognostic information. However, concerns exist about local control after downsized surgery and the delay of local treatment in patients with tumors resistant to chemotherapy. This review assesses the effectiveness of neoadjuvant chemotherapy on clinical outcome.

### Methods

All randomized trials comparing neoadjuvant and adjuvant chemotherapy for early breast cancer were assessed for eligibility and quality, and data were extracted by two independent reviewers. Hazard ratios (HR) were derived for time-to-event outcomes directly or indirectly using the methods described by Parmar *et al*. Relative risks were derived for dichotomous outcomes. Meta-analyses were performed using fixed effect model.

### Results

Fourteen studies randomizing 5,500 women were eligible for analysis. Median follow-up ranged from 18 to 124 months. Eight studies described a satisfactory method of randomization. Overall survival was equivalent in both groups. In the neoadjuvant group, the mastectomy rate was lower (relative risk = 0.71, 95% CI = 0.67 to 0.75, $P < .0001$) without hampering local control (HR = 1.12, 95% CI = 0.92 to 1.37, $P = .25$). Neoadjuvant chemotherapy was associated fewer adverse effects. Pathological complete response is associated with better survival than residual disease (HR = 0.48, 95% CI = 0.33 to 0.69, $P < .0001$).

### Conclusion

Neoadjuvant chemotherapy is an established treatment option for early breast cancer in order to down stage surgical requirement, to evaluate chemosensitivity and to facilitate translational research.

## INTRODUCTION

Neoadjuvant, or preoperative, chemotherapy is the administration of chemotherapy before surgical treatment. Its use in breast cancer was introduced in the early 1980s in patients with locally advanced disease in order to convert inoperable into operable tumors.[1] Soon after achieving positive results in the locally advanced setting, randomized controlled trials were conducted to evaluate the technique for earlier, operable stages. A major benefit of neoadjuvant chemotherapy is its potential to increase breast conservation, which is associated with less morbidity and improved body image compared with complete breast removal.[2] However, there is concern about local control after down staging of the tumor and the delay to surgery in patients with tumors resistant to chemotherapy.

In their recently published meta-analysis on neoadjuvant and adjuvant chemotherapy, Mauri and colleagues[3] reported equivalent overall and disease-free survival rates, but an increased loco regional recurrence risk in the neoadjuvant group, particularly when surgery was withheld. However, this analysis excluded studies for which no peer-reviewed journal publication was available.[4] In addition, relative risks (RRs) for time-to-event data were used, whereas the hazard ratio (HR) would be a more appropriate statistic when individual patient data are not available.[5, 6] Furthermore, the change of local treatment in the neoadjuvant group was not assessed in a quantitative way and adverse effects were not analyzed. Finally, since the appearance of this publication, several studies have reported long-term follow-up results.

In the present report, the available evidence from randomized controlled trials is reviewed systematically to assess the effectiveness of neoadjuvant chemotherapy, compared with adjuvant chemotherapy, on treatment-related outcomes in women with operable breast cancer. The association between breast conservation surgery and loco regional recurrence is analyzed in detail. A substantial version of this review has appeared in the Cochrane Library.

## MATERIAL AND METHODS

### Search, selection and data collection

The Specialised Register maintained by the Editorial Base of the Cochrane Breast Cancer Group (CBCG) was searched using the codes 'early', 'locally advanced' and 'chemo'. The register includes both published and unpublished (including ongoing) trials and applies no language restrictions. Details of the search strategy are described in the Group's module in The Cochrane Library. Properly randomized controlled trials were selected that compared neoadjuvant with adjuvant chemotherapy in women with operable breast cancer (T1–3 N0–2 M0; American Joint Committee on Cancer stages

I–IIIA). Two independent reviewers assessed eligibility and quality, and extracted data from the included trials. Disagreements were resolved by consensus. Data were entered into Review Manager 4.2.7 and analyzed using Review Manager 1.0.2 (Cochrane Collaboration, Oxford, UK).

**Data analysis**

Time-to-event outcomes were overall survival and time to loco regional recurrence as first event, for which the HR is the most appropriate statistic.[5, 6] When possible, the HR and associated variances were extracted directly from the trial publication. If not reported, they were obtained indirectly using the methods described by Parmar *et al.*[7] and the Excel® (Microsoft, Redmond, Washington, USA) spreadsheet developed by Matthew Sydes (Cancer Division) in collaboration with the Meta-analysis Group of the Medical Research Council Clinical Trials Unit, London. To allow for immature follow-up, the numbers at risk were adjusted based on estimated minimum and maximum follow-up times. A pooled HR was obtained from the derived observed minus expected number of events and the variance for each trial using the fixed-effect model.[8] The pooled HR represents the overall risk of an event associated with neoadjuvant *versus* adjuvant chemotherapy.

The association between pathological complete response and overall survival was analyzed in the neoadjuvant treatment arm. Pathological complete response was defined as complete disappearance of invasive carcinoma on histological examination after chemotherapy. The survival rate of patients with a complete response was compared with that of patients with residual disease using the univariate meta-analysis technique described above.

For loco regional treatment, data were used from studies in which the treatment protocol allowed the derivation of differences in breast conservation rate, preferably after follow-up, between research and control arms to calculate RRs. Mastectomy was scored as an event. Patients with no information available on loco regional treatment were excluded from the analyses. In the neoadjuvant group, the change in originally planned local treatment strategy was analyzed and the local recurrence rate in patients with down staged breast conservation *versus* preplanned breast conservation was compared. For adverse effects, the number of World Health Organization grade III and IV events of postoperative complications, cardiotoxicity, chemotherapy-related infectious complications (leucopenia, neutropenia or infection), nausea and vomiting, and alopecia were extracted. For these outcomes, a pooled RR was obtained using the fixed-effect (Mantel–Haenszel) model. For clinical interpretation, the pooled RR was converted to risk difference and numbers needed to treat (NNT).

The $I^2$ statistic was used to test for heterogeneity across studies.[9] An $I^2$ value greater than 50% was considered to represent substantial heterogeneity. Subgroup analyses were conducted for treatment arm (neoadjuvant, 'sandwich') and loco

regional treatment (breast-conserving surgery, mastectomy, exclusive radiotherapy). $\chi^2$ tests for interaction were applied to these subgroup analyses.[10] Publication bias was tested by using funnel plots; an inverted symmetrical funnel plot assumes the absence of publication bias.[11]

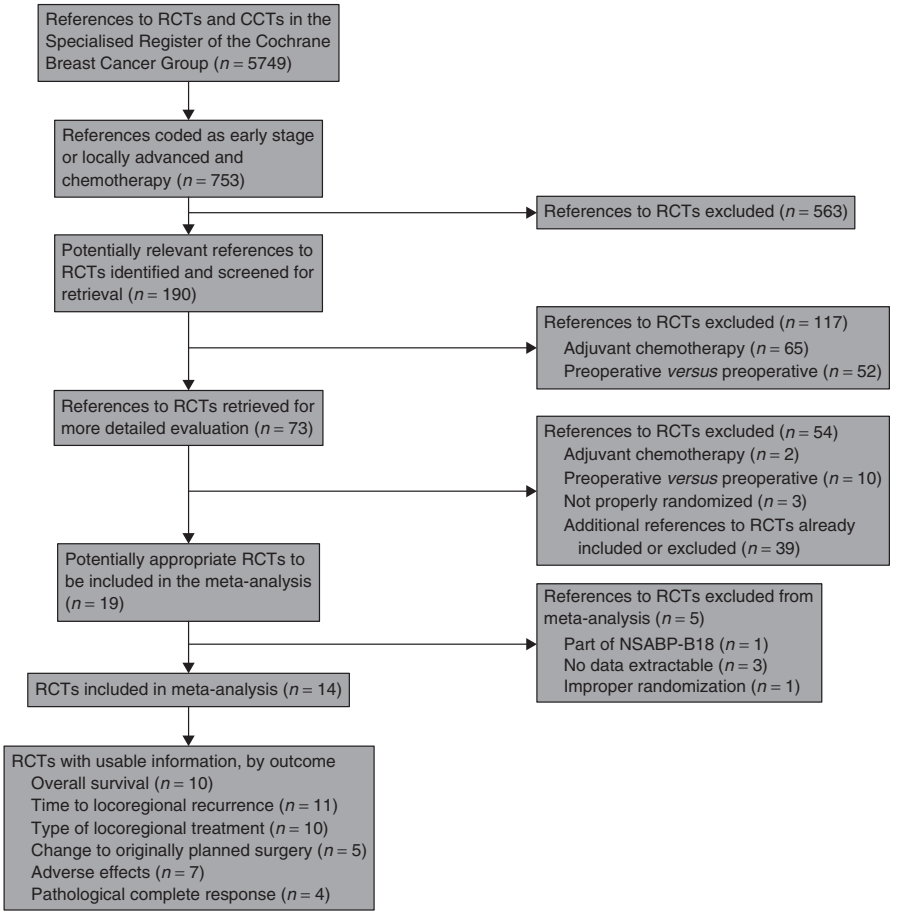


**Figure 1. Flow chart of papers assessed for analysis.** Search strategy applied 4 August 2005. RCT, randomized controlled trial; CCT, controlled clinical trial; NSABP, National Surgical Adjuvant Breast and Bowel Project.

# RESULTS

## Description of studies

On 4 August 2005, the Specialised Register of the CBCG contained 5,749 references of which 753 were identified during the search (Figure 1). After detailed evaluation of 73 references, 14 were included in this review (Table 1). In total, 5,500 women were randomized to either neoadjuvant or adjuvant chemotherapy. Median follow-

up ranged from 24 to 124 months. In eight studies, patients in the neoadjuvant arm received part of the chemotherapy courses after local treatment.[12, 15, 17, 19-21, 23, 24] In seven studies, tamoxifen was administered to eligible patients and started after surgery.[14, 16, 19, 20, 22, 23, 25] In one study, tamoxifen was administered before surgery.[23] Four studies gave both groups the same local treatment.[15, 19, 20, 24] Three studies administered preoperative radiotherapy.[17, 18, 24] Eight studies described a satisfactory method of randomization.[13, 14, 16, 19, 22-24] Six studies reported a satisfactory method of concealment of allocation.[15, 16, 21-23, 25] The randomization method was not reported in the remaining studies. Overall, 98.2% of the patients included in time-to-event outcomes were analyzed by intention to treat. For loco regional treatment, data on 5,292 (97.0%) of the 5,453 women randomized were available for analysis. For adverse effects, data on 3,382 (96.9%) of the 3,490 patients randomized were available for analysis.

**Table 1.** Characteristics of the included studies

| Study | Inclusion period | N | Stage | Type of chemotherapy* | Median follow-up (months) | Survival (%) | | Local recurrence (%) | | Mastectomy (%) | |
|---|---|---|---|---|---|---|---|---|---|---|---|
| | | | | | | Neo | Adj | Neo | Adj | Neo | Adj |
| ABCSG[12] | 1991-1999 | 423 | II-IIIA | CMF (3 of 6)[a] | n.a. | n.a. | n.a. | n.a. | n.a. | 33 | 41 |
| Bordeaux[13] | 1985-1989 | 272 | II-IIIA | EVM/MTV (6 of 6) | 124 | 62 | 59 | 23 | 9 | 55[b] | 100 |
| ECTO[14] | 1996-2002 | 902[c] | II-IIIA | AT + CMF (4 of 4) | 50 | 87 | 90 | 3 | 4 | 35 | 66 |
| Edinburgh[15] | n.a. | 79 | II-IIIA | CAP (4 of 6)[d] | n.a. | n.a. | n.a. | n.a. | n.a. | 100 | 100 |
| EORTC[16] | 1991-1999 | 698 | I-IIIA | FEC (4 of 4) | 120 | 65 | 66 | 14 | 13 | 63 | 77 |
| Institut Curie[17] | 1983-1986 | 196 | II-IIIA | FAC (2 of 6) | 54 | n.a. | n.a. | 18 | 20 | 23 | 36 |
| Institut Curie[18] | 1986-1990 | 414 | II-IIIA | FAC (2 of 6) | 105 | 65 | 60 | 27[e] | 19[e] | 37[f] | 35[f] |
| Japan[19] | 1995-1997 | 50 | II-III | FEC (2 of 5) | 24 | 84 | 80 | 10 | 8 | 100 | 100 |
| Lithuania[20] | 1994-1997 | 100 | II | CMF (2 of n.a.) | 42 | n.a. | n.a. | 2 | 6 | 0 | 0 |
| London[21] | 1990-1993 | 210 | I-IIIA | MMM (4 of 8)[d] | > 60 | 78 | 87 | 20 | 16 | 11 | 8 |
| NSABP[22] | 1988-1993 | 1523 | I-IIIA | AC (4 of 4) | 114[g] | 69 | 70 | 15 | 13 | 32 | 40 |
| Royal Marsden[23] | 1990-1995 | 309 | I-IIIA | MM(M) (4 of 4) | 112 | 70 | 63 | 9 | 6 | 11 | 22 |
| St Petersburg[24] | 1985-1990 | 271 | IIb-IIIa | TMF (1-2 of 6) | 53 | 86 | 78 | n.a. | n.a. | 100 | 100 |
| USA[25] | 1990-1998 | 53 | II | FLAC + G(M)-CSF (5 of 5) | 108 | 87 | 72 | 12 | 7 | 58 | 59 |

* Values in parentheses are number of courses given before operation as a proportion of total number of courses. a Lymph node-positive patients received three courses of epirubicin, cyclophosphamide after surgery. b After 10 year median follow-up initial rate was 37%. c Three-arm study; second postoperative arm included 453 patients. d Patients with estrogen-positive tumors received endocrine therapy. e After 5-year median follow-up. f After 5-year median follow-up. Initial rate was 18%. g Mean.

ABCSG, Austrian Breast and Colorectal Cancer Study Group; ECTO, European Cooperative Trial in Operable Breast Cancer; EORTC, European Organization for Research and Treatment of Cancer; NSABP, National Surgical Adjuvant Breast and Bowel Project. CMF, cyclophosphamide, methotrexate, fluorouracil; EVM/MTV, epirubicin, vincristine, methotrexate/mitomycin C, thiotepa, vindesine; AT, doxorubicin, paclitaxel; CAP, cyclophosphamide, doxorubicin, prednisolone; FEC, fluorouracil, epirubicin, cyclophosphamide; FAC, fluorouracil, doxorubicin, cyclophosphamide; MMM, mitozantrone, mitomycin C, methotrexate; AC, doxorubicin, cyclophosphamide; TMF, thiotepa, methotrexate, fluorouracil; FLAC, fluorouracil, leucovorin, doxorubicin, cyclophosphamide; GM-CSF, granulocyte–macrophage colony-stimulating factor; n.a., not available.

## Meta-analyses

### *Overall survival*

Ten studies reported overall survival data on 4,620 randomized women and 1,139 estimated deaths. There was no survival difference between neoadjuvant and adjuvant chemotherapy (HR = 0.98, 95% CI = 0.87 to 1.09; Figure 2). The associated funnel plot shows a symmetrical distribution (Figure 3). Of note, no study demonstrated a significant effect in favor of neoadjuvant or adjuvant chemotherapy.

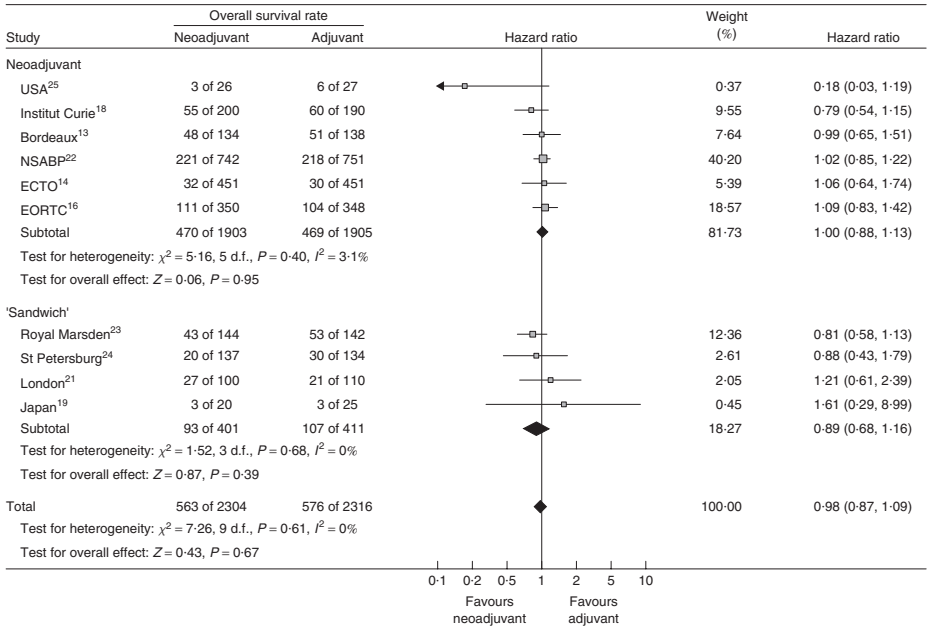


**Figure 2. Overall survival of patients who had neoadjuvant or adjuvant chemotherapy stratified by treatment arm protocol (neoadjuvant or 'sandwich').** Hazard ratios are given with 95% CI. NSABP, National Surgical Adjuvant Breast and Bowel Project; ECTO, European Cooperative Trial in Operable Breast Cancer; EORTC, European Organization for Research and Treatment of Cancer.

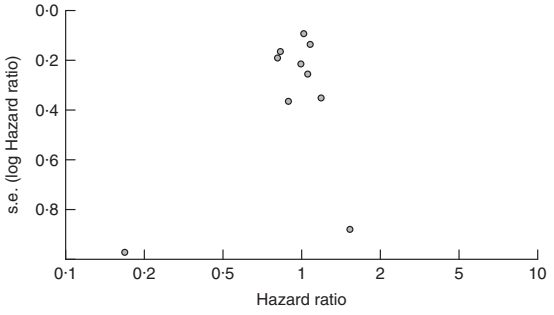


**Figure 3. Funnel plot of the studies reporting on overall survival.** The symmetrical distribution indicates a low risk of publication bias.

*Loco regional recurrence*

Eleven studies reported time to loco regional recurrence data on 5,041 randomized women and 570 estimated recurrences. There was a significant difference in favor of adjuvant chemotherapy (Figure 4). However, in three studies, more than one-third of patients received exclusive radiotherapy and no surgery after complete tumor regression.[13, 17, 18] The recurrence rates for these patients were reported separately in only one study.[13] In this study, after a 10-year follow-up, there was a loco regional recurrence rate of 30% when surgery was omitted after neoadjuvant chemotherapy. Therefore, it was decided to exclude these studies from the analysis of loco regional recurrence, because of inadequate loco regional treatment. After this exclusion, the remaining eight studies demonstrated no difference in loco regional recurrence rate between the neoadjuvant and adjuvant groups (HR = 1.12, 95% CI = 0.92 to 1.37, $P$ = .25).

When patients were analyzed according to type of surgery, loco regional recurrence rates were not influenced by the timing of chemotherapy in those who had breast-conserving surgery or women who underwent mastectomy (Figure 5). Two studies reported a non-significant increase in loco regional recurrence in patients

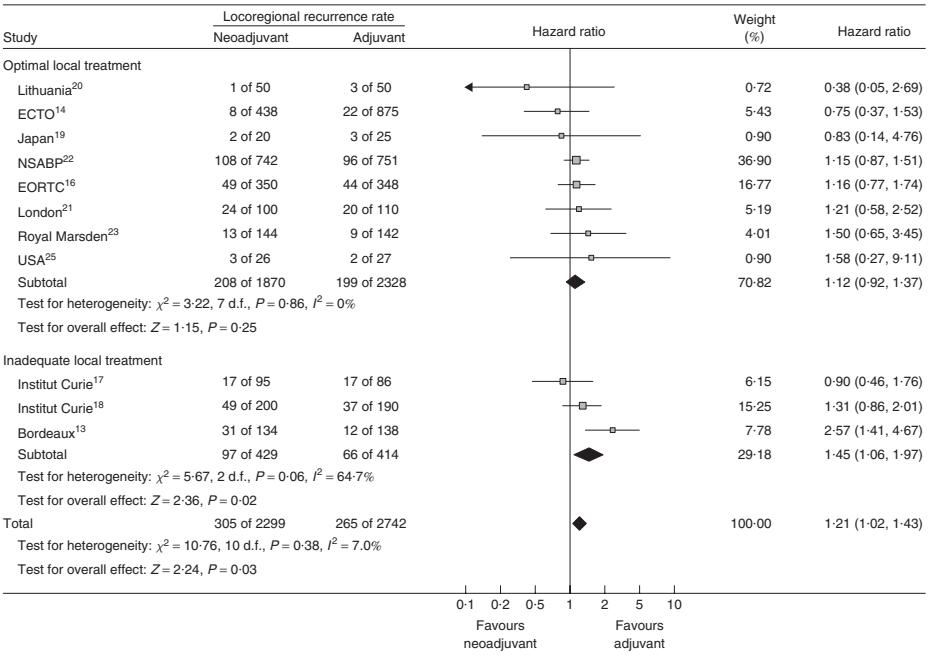


**Figure 4. Time to loco regional recurrence in patients who had neoadjuvant or adjuvant chemotherapy.** Hazard ratios are given with 95 per cent confidence intervals. The pooled result excluding three studies that omitted surgery in a vast proportion of patients showed a non-significant increase in the neoadjuvant group. This recurrence rate was lower than that in the three excluded trials ($\chi^2$ for difference = 1.66, 1 d.f., $P$ = .20). ECTO, European Cooperative Trial in Operable Breast Cancer; NSABP, National Surgical Adjuvant Breast and Bowel Project; EORTC, European Organization for Research and Treatment of Cancer.

who could be treated by breast-conserving surgery because of down staging of the tumor compared with patients for whom the initial plan before the administration of neoadjuvant chemotherapy was breast-conserving surgery (Figure 6).

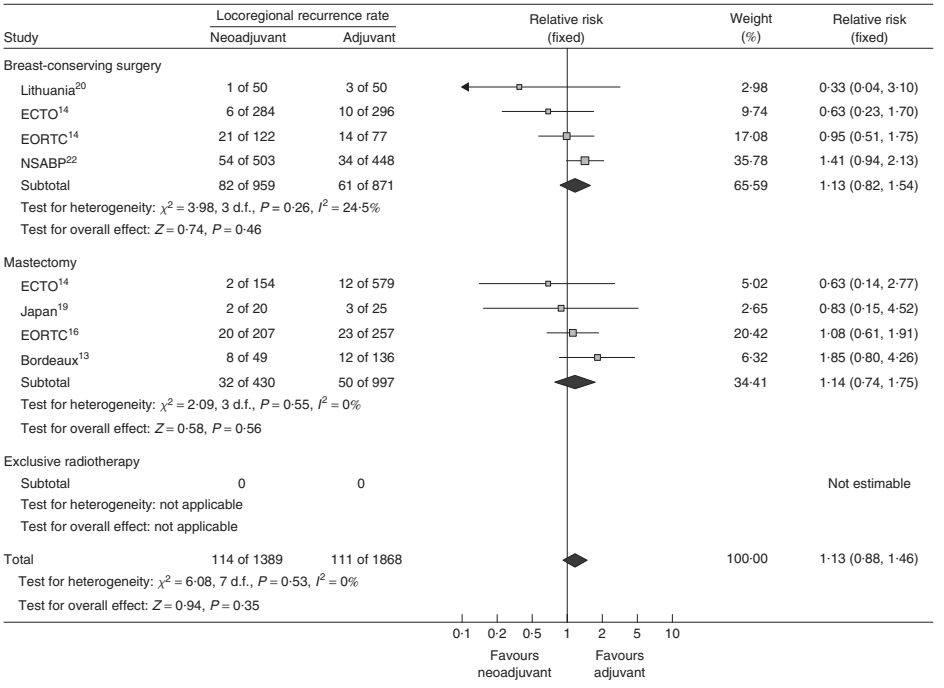


**Figure 5. Loco regional recurrence rates in patients who had neoadjuvant or adjuvant chemotherapy stratified by type of surgery.** Relative risks are given with 95% CI. There was no difference between breast-conserving surgery and mastectomy ($\chi^2$ = 0.01, 1 d.f., P = .92). ECTO, European Cooperative Trial in Operable Breast Cancer; EORTC, European Organization for Research and Treatment of Cancer; NSABP, National Surgical Adjuvant Breast and Bowel Project.

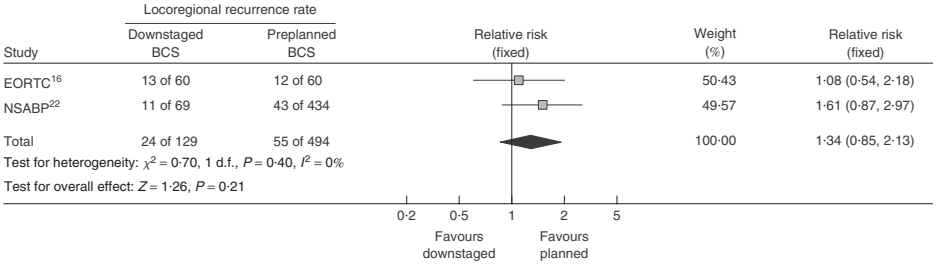


**Figure 6. Loco regional recurrence rates in the neoadjuvant group after down staged versus preplanned breast-conserving surgery (BCS).** Relative risks are given with 95% CI. The recurrence rate was non-significantly higher in the down staged group, represented by a risk difference of 7.5% (95% CI = 1.7 to 13.2); risk in adjuvant group was 11.1%. EORTC, European Organization for Research and Treatment of Cancer; NSABP, National Surgical Adjuvant Breast and Bowel Project.

*Loco regional treatment*

In ten studies, the protocol allowed derivation of differences in type of loco regional treatment after neoadjuvant chemotherapy. These studies contained 5,292 women of whom 2,395 underwent mastectomy (Figure 7). There was a statistically significant decrease in mastectomy rate in favor of neoadjuvant chemotherapy (RR = 0.71, 95% CI = 0.67 to 0.75, $P < .001$), representing a risk difference of 16.6% (95% CI = 15.1 to 18.1; NNT = 6). Two studies accounted for the substantial heterogeneity ($I^2 = 83.2\%$) in the forest plot. One study had an intensive chemotherapy regimen and achieved high response rates, allowing more conservative treatment.[14] In the other, all patients in the adjuvant chemotherapy arm underwent mastectomy as only those with tumors unsuitable for conservative treatment were included.[13] The remaining eight studies ($I^2 = 25.8\%$) showed a pooled RR of 0.82 (95% CI = 0.76 to 0.89, $P < .001$), representing a risk difference of 8.0% (95% CI = 6.3 to 9.7; NNT = 13).

Five studies reported the change in the originally planned local treatment after neoadjuvant chemotherapy (Table 2). Of the 1,549 assessable women, 397 (25.6%, 95% CI = 23.5 to 27.8) had their surgical treatment down staged; in 66 women (4.3%, 95% CI = 3.3 to 5.3) tumor progression necessitated more radical surgery than originally planned.

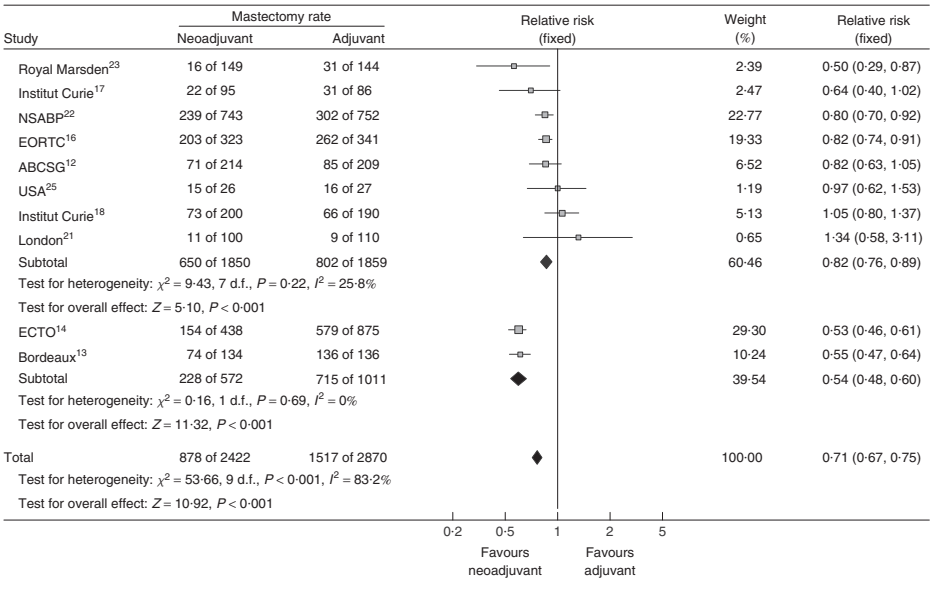


**Figure 7. Mastectomy rate in the neoadjuvant and adjuvant chemotherapy groups.** Two studies accounted for the substantial heterogeneity ($\chi^2$ for difference = 44.07, 1 d.f., $P < .001$). Neoadjuvant chemotherapy reduced the absolute mastectomy rate by 16.6% (95% CI = 15.1 to 18.1); risk in adjuvant group was 52.9%. NSABP, National Surgical Adjuvant Breast and Bowel Project; EORTC, European Organization for Research and Treatment of Cancer; ABCSG, Austrian Breast and Colorectal Cancer Study Group; ECTO, European Cooperative Trial in Operable Breast Cancer.

**Table 2.** Change of local treatment after neoadjuvant chemotherapy

| Study | BCS → BCS | Mast → Mast | Mast → BCS | Mast → RT | BCS → RT | BCS → Mast | Total |
|---|---|---|---|---|---|---|---|
| Bordeaux[13] | — | 49 | 40 | 44 | 0 | 0 | 133 |
| EORTC[16] | 60 | 190 | 60 | 0 | 0 | 14 | 324 |
| Institut Curie[18] | — | 36 | 62 | 102 | 0 | 0 | 200 |
| NSABP[22] | 435 | 187 | 69 | 0 | 0 | 52 | 743 |
| Royal Marsden[23] | 113 | 16 | 19 | 0 | 1 | 0 | 149 |
| Total | 608 | 478 | 250 | 146 | 1 | 66 | 1549 |

Surgical requirement was down staged in 397 women (25.6% (95% CI = 23.5 to 27.8)). BCS, breast-conserving surgery; Mast, modified radical mastectomy; RT, radiotherapy; EORTC, European Organization for Research and Treatment of Cancer; NSABP, National Surgical Adjuvant Breast and Bowel Project.

*Pathological complete response*

Four studies reported overall survival data in association with a pathological complete response in a total of 1,290 assessable women; there were 381 estimated deaths.[16, 22-24] In these studies the pathological complete response rate ranged from 4.0 to 29.2%. Patients with a pathological complete response had improved overall survival (HR = 0.48, 95% CI = 0.33 to 0.69, $P < .001$).

*Adverse effects*

Four studies reported infectious complications due to chemotherapy. The data set consisted of 327 events in 2,799 women. A significant decrease in the rate of such complications in the neoadjuvant chemotherapy group was demonstrated (RR = 0.69, 95% CI = 0.56 to 0.84, $P < .001$) with an absolute risk difference of 4.2% (95% CI = 2.3 to 5.6; NNT = 24; Figure 8). Cardiotoxicity events were less frequent in women receiving neoadjuvant chemotherapy (RR = 0.74, 95% CI = 0.53 to 1.04, $P = .08$).

## DISCUSSION

This review demonstrates that neoadjuvant chemotherapy results in overall survival rates equivalent to those associated with adjuvant chemotherapy, while permitting more breast-conserving therapy. Neoadjuvant treatment is associated with a decrease in adverse events and does not adversely affect loco regional control of disease. The findings relating to time-to-event data are in concordance with those of the earlier meta-analysis of Mauri and colleagues.[3] However, more studies were available for analysis in the present review and Cochrane Collaboration methodology was used.[6]

The present study, however, has some limitations. First, the maximum median follow-up of the included studies is 10 years, which may be too short to identify differences in clinical outcome. The latest Early Breast Cancer Trialists' Collaborative Group report demonstrated the importance of extended follow-up (15–20 years) in

early-stage breast cancer trials.[26] Furthermore, this report estimated that for every four recurrences one breast cancer death can be avoided over the next 15 years. Another limitation is that seven of the 11 studies reporting on loco regional recurrence provided this outcome as a RR instead of a HR,[13, 14, 18-20, 22, 25] thereby adversely affecting the accuracy of the pooled analysis. Third, the effect of neoadjuvant chemotherapy on breast conservation may be overestimated by detection and performance bias; the unblinded physician assessing tumor response may be more prone to advising breast-conserving therapy. Moreover, as time passes and recurrences develop, subsequent salvage mastectomies will decrease the breast conservation rate. Most studies reported only the initial breast conservation rates. Despite these limitations, the included studies were properly randomized and study quality was generally adequate. In addition, the funnel plot showed a symmetrical distribution suggesting a low risk of publication bias.

Neoadjuvant chemotherapy increases the breast conservation rate. It is well known that breast-conserving surgery is associated with a higher loco regional recurrence rate than mastectomy, without, however, affecting long-term overall survival.[27] The limited and non-significant increase in loco regional recurrence rate in the neoadjuvant group can, therefore, be explained by the increased breast conservation rate and the fact that a substantial proportion of patients in three studies had no surgery after neoadjuvant chemotherapy. To date, direct evidence of local recurrence after down staged surgery following neoadjuvant chemotherapy is still lacking. In the present analysis, no clear risk difference between down staged and preplanned conservative surgery could be found. However, this indirect comparison is based on limited data without correction for confounding effects.

This review demonstrates that the increased local recurrence rate associated with neoadjuvant treatment is greatly reduced after excluding studies in which patients received exclusive radiotherapy after complete tumor regression. This finding emphasizes the importance of incorporating surgery in the loco regional treatment strategy after neoadjuvant chemotherapy. Otherwise stated, the clinical assessment of tumor response by conventional means is insufficiently sensitive safely to withhold surgery. Recently, the introduction of magnetic resonance imaging (MRI) in the monitoring of tumor response has been shown to be of benefit in the assessment of surgical strategy after down staging by neoadjuvant chemotherapy.[28] However, concern exists about the higher false-positive rate of MRI.[29]

The rate of chemotherapy-related infectious complications was significantly lower in the neoadjuvant group. However, no obvious explanation is available. The actual number of chemotherapy courses received was equal in both treatment arms. It is possible that the immune system of patients who underwent primary surgery was already depressed as a result of surgical stress, making them more vulnerable to the negative effects of chemotherapy. In the neoadjuvant group, on the other hand,

patients were able to recover from the chemotherapy before they had surgery. The rate of cardiotoxicity also appeared to be lower in the neoadjuvant group. Known factors influencing cardiotoxicity are anthracycline use, taxane use, increasing age, previous cardiac disease and radiotherapy. The present analysis is driven by the European Cooperative Trial in Operable Breast Cancer (ECTO) 2005 study.[14] Because this study added a taxane to the anthracycline chemotherapy regimen, the assessment of cardiotoxicity was an important endpoint. No imbalance in prognostic variables or difference in method of assessment was found between the treatment arms. An additional literature search did not provide a satisfactory explanation for the reduced risk and, as it does not reach statistical significance, it may be explained simply by chance.

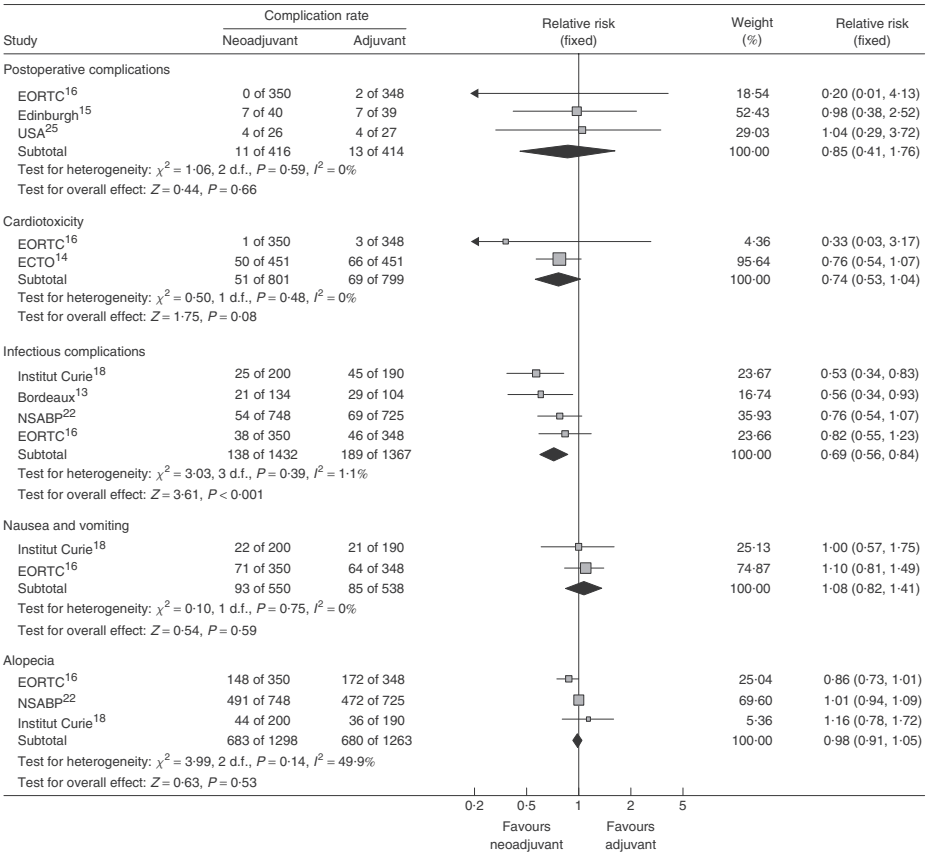


**Figure 8. Adverse effects in the neoadjuvant and adjuvant chemotherapy groups.** EORTC, European Organization for Research and Treatment of Cancer; ECTO, European Cooperative Trial in Operable Breast Cancer; NSABP, National Surgical Adjuvant Breast and Bowel Project.

Apart from higher breast conservation rates and fewer adverse effects, neoadjuvant chemotherapy facilitates monitoring of tumor response. By adjusting the

dose or switching to another drug in the case of treatment resistance, a patient may be saved the unnecessary burden of toxic side-effects.[30-32] This review suggests that neoadjuvant chemotherapy avoids a mastectomy in about 25% of patients. Conversely, a small percentage of patients (< 5%) originally suitable for breast conservation will require a mastectomy owing to disease progression while receiving neoadjuvant chemotherapy. This is an ethical concern. However, the included studies did not allow regimen change on tumor progression and it is reasonable to expect the percentage to be lower if switching to other cytotoxic drugs is permitted. Concerns might also be raised about the postoperative and thus 'blind' administration of chemotherapy to patients with tumors resistant to therapy. Such patients receive all chemotherapy courses while experiencing only the harmful side-effects, whereas resistance can be detected and adequately dealt with in the neoadjuvant setting. Although tumor response rate is an important predictor of survival, its role as a surrogate endpoint in clinical trials remains controversial.[33]

The introduction of neoadjuvant therapy has had a great impact on breast cancer research. The assessment of tumor behavior *in situ* during neoadjuvant therapy and the correlation of this behavior with clinical outcome is an excellent model with which to determine the predictive role of classical and molecular tumor characteristics. The ultimate goal of this translational research is the introduction of tailor-made treatment strategies based on individual risk profiles. Neoadjuvant therapy offers an excellent setting in which to determine the most efficient treatment approach for an individual patient.[34]

A suggested disadvantage of neoadjuvant chemotherapy is alteration of the lymphatic network, hampering the accuracy of sentinel lymph node biopsy.[35] However, a recently published meta-analysis has demonstrated equivalent accuracy of sentinel lymph node biopsy after neoadjuvant chemotherapy and primary surgery.[36] The apparent safety of this procedure after chemotherapy could decrease the need for axillary lymph node dissection, thereby reducing morbidity.[37] Whether this will affect prognosis, particularly in the situation of a clinically suspect axilla, remains unclear.

This systematic review demonstrates that neoadjuvant chemotherapy for early-stage breast cancer is safe. It induces tumor down staging and thereby an increase in breast conservation. Loco regional control of disease is not significantly influenced by neoadjuvant chemotherapy. Finally, it is an excellent tool with which to evaluate the tumor *in situ* and to facilitate translational research.

## ACKNOWLEDGEMENTS

This study was supported financially by a Dutch Cancer Society student grant. The authors thank Sharon Parker, Nicole Holcroft and Avinesh Pillai of the Cochrane Breast Cancer Group for their valuable help during protocol and review development.

They also thank the authors who kindly responded[12-14, 16, 18, 19, 21, 23] with special thanks to Patrick Therasse and Jan Bogaerts of the European Organization for Research and Treatment of Cancer (EORTC) for supplying updated data on the EORTC 10902 trial and to Janine van Nes, Leiden University Medical Center, for assistance in analyzing the data of this trial.

This paper is based on a Cochrane Review published in The Cochrane Library 2007, Issue 2 (see http://www.thecochranelibrary.com for information).

## REFERENCES

1. Kaufmann M, von Minckwitz G, Smith R, et al. International expert panel on the use of primary (preoperative) systemic treatment of operable breast cancer: review and recommendations. J Clin Oncol 2003; 21:2600-8.
2. Kiebert GM, de Haes JC, van de Velde CJ. The impact of breast-conserving treatment and mastectomy on the quality of life of early-stage breast cancer patients: a review. J Clin Oncol 1991; 9:1059-70.
3. Mauri D, Pavlidis N, Ioannidis JP. Neoadjuvant versus adjuvant systemic treatment in breast cancer: a meta-analysis. J Natl Cancer Inst 2005; 97:188-94.
4. McAuley L, Pham B, Tugwell P, Moher D. Does the inclusion of grey literature influence estimates of intervention effectiveness reported in meta-analyses? Lancet 2000; 356:1228-31.
5. Williamson PR, Smith CT, Hutton JL, Marson AG. Aggregate data meta-analysis with time-to-event outcomes. Stat Med 2002; 21:3337-51.
6. Higgins JPT, Green S (eds). Cochrane Handbook for Systematic Reviews of Interventions 4.2.6. In The Cochrane Library, Issue 4. John Wiley: Chichester, 2006.
7. Parmar MK, Torri V, Stewart L. Extracting summary statistics to perform meta-analyses of the published literature for survival endpoints. Stat Med 1998; 17:2815-34.
8. Yusuf S, Peto R, Lewis J, et al. Beta blockade during and after myocardial infarction: an overview of the randomized trials. Prog Cardiovasc Dis 1985; 27:335-71.
9. Higgins JP, Thompson SG. Quantifying heterogeneity in a meta-analysis. Stat Med 2002; 21:1539-58.
10. Deeks JJ, Altman DG, Bradburn MJ. Statistical methods for examining heterogeneity and combining results from several studies in meta-analysis. In Systematic Reviews in Health Care: Meta-Analysis in Context (2nd edn), Egger M, Davey Smith G, Altman DG (eds). BMJ Publication Group: London, 2001; 285-312.
11. Egger M, Davey Smith G, Schneider M, Minder C. Bias in meta-analysis detected by a simple, graphical test. BMJ 1997; 315:629-34.
12. Jakesz R. Comparison of pre- vs. postoperative chemotherapy in breast cancer patients: four-year results of Austrian Breast & Colorectal Cancer Study Group (ABCSG) Trial 7. J Clin Oncol (Meeting Abstracts) 2001; 20:Abstract 125.
13. Mauriac L, MacGrogan G, Avril A, et al. Neoadjuvant chemotherapy for operable breast carcinoma larger than 3 cm: a unicentre randomized trial with a 124-month median follow-up. Institut Bergonie Bordeaux Group Sein (IBBGS). Ann Oncol 1999; 10:47-52.
14. Gianni L, Baselga J, Eiermann W, et al. European Cooperative Trial in Operable Breast Cancer (ECTO): improved freedom from progression (FFP) from adding paclitaxel (T) to doxorubicin (A) followed by cyclophosphamide methotrexate and fluorouracil (CMF). J Clin Oncol (Meeting Abstracts) 2005; 23:Abstract 513.
15. Forouhi P, Dixon JM, Leonard RCF, Chetty U. Prospective randomized study of surgical morbidity following primary systemic therapy for breast cancer. Br J Surg 1995; 82:79-82.
16. van der Hage JA, van de Velde CJH, Julien JP, et al. Preoperative chemotherapy in primary operable breast cancer: results from the European Organization for Research and Treatment of Cancer trial 10902. J Clin Oncol 2001; 19:4224-37.

17. Scholl SM, Asselain B, Palangie T, et al. Neoadjuvant chemotherapy in operable breast cancer. Eur J Cancer 1991; 27:1668-71.
18. Broet P, Scholl SM, de la Rochefordiere A, et al. Short and long-term effects on survival in breast cancer patients treated by primary chemotherapy: an updated analysis of a randomized trial. Breast Cancer Res Treat 1999; 58:151-6.
19. Enomoto K, Ikeda T, Matsui A, Kitajima M, Koh J, Masamura S et al. Neoadjuvant therapy in stage II with T > 4 cm and stage III breast cancer. Eur J Cancer 1998; 34(Suppl 1):Abstract 33.
20. Ostapenko V, Pipiriene T, Valuckas K. Primary chemotherapy in conservative treatment of stage II breast cancer. Eur J Cancer 1998; 34(Suppl 1):Abstract 34.
21. Gazet JC, Ford HT, Gray R, et al. Estrogen-receptor-directed neoadjuvant therapy for breast cancer: results of a randomised trial using formestane and methotrexate, mitozantrone and mitomycin C (MMM) chemotherapy. Ann Oncol 2001; 12:685-91.
22. Wolmark N, Wang J, Mamounas E, et al. Preoperative chemotherapy in patients with operable breast cancer: nine-year results from National Surgical Adjuvant Breast and Bowel Project B-18. J Natl Cancer Inst Monogr 2001; 30:96-102.
23. Cleator SJ, Makris A, Ashley SE, et al. Good clinical response of breast cancers to neoadjuvant chemoendocrine therapy is associated with improved overall survival. Ann Oncol 2005; 16:267-72.
24. Semiglazov VF, Topuzov EE, Bavli JL, et al. Primary (neoadjuvant) chemotherapy and radiotherapy compared with primary radiotherapy alone in stage IIb-IIIa breast cancer. Ann Oncol 1994; 5:591-5.
25. Danforth DN Jr, Cowan K, Altemus R, et al. Preoperative FLAC/granulocyte-colony-stimulating factor chemotherapy for stage II breast cancer: a prospective randomized trial. Ann Surg Oncol 2003; 10:635-44.
26. Clarke M, Collins R, Darby S, et al. Effects of radiotherapy and of differences in the extent of surgery for early breast cancer on local recurrence and 15-year survival: an overview of the randomised trials. Lancet 2005; 366:2087-106.
27. Jatoi I, Proschan MA. Randomized trials of breast-conserving therapy versus mastectomy for primary breast cancer: a pooled analysis of updated results. Am J Clin Oncol 2005; 28:289-94.
28. Yeh E, Slanetz P, Kopans DB, et al. Prospective comparison of mammography, sonography, and MRI in patients undergoing neoadjuvant chemotherapy for palpable breast cancer. AJR Am J Roentgenol 2005; 184:868-77.
29. Rosen EL, Blackwell KL, Baker JA, et al. Accuracy of MRI in the detection of residual breast cancer after neoadjuvant chemotherapy. AJR Am J Roentgenol 2003; 181:1275-82.
30. von Minckwitz G, Blohmer JU, Raab G, et al. In vivo chemosensitivity-adapted pre-operative chemotherapy in patients with early-stage breast cancer: the GEPARTRIO pilot study. Ann Oncol 2005; 16:56-63.
31. Bear HD, Anderson S, Smith RE, et al. Sequential preoperative or postoperative docetaxel added to preoperative doxorubicin plus cyclophosphamide for operable breast cancer: National Surgical Adjuvant Breast and Bowel Project Protocol B-27. J Clin Oncol 2006; 24:2019-27.
32. Smith IC, Heys SD, Hutcheon AW, et al. Neoadjuvant chemotherapy in breast cancer: significantly enhanced response with docetaxel. J Clin Oncol 2002; 20:1456-66.
33. George SL. Response rate as an endpoint in clinical trials. J Natl Cancer Inst 2007; 99:98-9.
34. Jones RL, Smith IE. Neoadjuvant treatment for early-stage breast cancer: opportunities to assess tumour response. Lancet Oncol 2006; 7:869-74.
35. Kuerer HM, Hunt KK. The rationale for integration of lymphatic mapping and sentinel node biopsy in the management of breast cancer patients receiving neoadjuvant chemotherapy. Semin Breast Dis 2002; 5:80-7.
36. Xing Y, Foy M, Cox DD, et al. Meta-analysis of sentinel lymph node biopsy after preoperative chemotherapy in patients with breast cancer. Br J Surg 2006; 93:539-46.
37. Purushotham AD, Upponi S, Klevesath MB, et al. Morbidity after sentinel lymph-node biopsy in primary breast cancer: results from a randomized controlled trial. J Clin Oncol 2005; 23:4312-21.

# Chapter 3

## Tumor response to preoperative anthracycline-based chemotherapy in operable breast cancer: the predictive role of p53 expression

Mieog JSD, van der Hage JA, van de Vijver MJ, van de Velde CJH, and cooperating investigators of the European Organization for Research and Treatment of Cancer

*Eur J Cancer 2006; 42:1369-79*

# ABSTRACT

## Introduction

The aim of this retrospective study was to identify markers capable of predicting pathological complete (pCR) and overall clinical tumor response to preoperative anthracycline-based chemotherapy and clinical outcome in women with operable breast cancer.

## Methods

Therefore, we used the pre-treatment core biopsies from 107 patients who were enrolled in the EORTC trial 10902 to analyze tumor characteristics and the oncogenic markers Bcl-2, p53, ER, PgR, HER2, and p21. Median follow-up was 7 years (95% CI = 6.89 to 7.45).

## Results

pCR was seen in seven patients (6.5%) and was associated with improved overall survival (hazard ratio = 0.39, 95% CI = 0.05 to 2.56, *P* = .30). At multivariate logistic regression analysis, pCR was independently predicted by p53 overexpression estimated by immunohistochemistry (odds ratio (OR) = 16.83, 95% CI = 1.78 to 159.33, *P* = .01). Fifty-eight patients showed clinical tumor response (>50% decrease in tumor size), however responders experienced no benefit in clinical outcome. Clinical tumor response was independently predicted by p53 overexpression (OR = 5.57, 95% CI = 1.58 to 19.65, *P* = .008) and small clinical tumor size (OR = 10.26, 95% CI = 2.01 to 52.48, *P* = .005). At multivariate Cox regression analysis, negative pathological lymph node status, low tumor grade and use of tamoxifen showed improved overall survival.

## Conclusion

In conclusion, our data suggest p53 expression is of predictive significance in anthracycline-containing chemotherapeutic regimens.

# INTRODUCTION

Preoperative chemotherapy for large, but early stage breast cancer, has been subject of interest for over two decades. The efficacy of preoperative chemotherapy has been demonstrated in several prospective randomized trials showing similar survival and locoregional control rates in patients receiving preoperative chemotherapy and postoperative chemotherapy. Tumor down staging due to preoperative chemotherapy was found to increase breast-conserving therapy rates.[1 2]

Response of breast tumors following preoperative chemotherapy can be assessed either clinically or pathologically. Patients with responding tumors showed an improved overall and disease-free survival and particularly pathological complete response (complete disappearance of malignant cells on microscopic examination; pCR) is suggested as a surrogate marker for these clinical endpoints.[2-5]

Translational research using preoperative tumor tissue biopsies is an excellent study model to analyze the predictive value of different tumor characteristics for response to chemotherapy.[6] To date, a large number of oncogenic markers in breast cancer have been studied using classical survival analyses.[7 8] However, published data on the relation between tumor characteristics and pathological and clinical tumor response are still limited.

We have used data from a prospective randomized trial comparing pre- versus postoperative chemotherapy to study the correlation between pathological and clinical tumor response and patient and tumor characteristics. Tumor characteristics included oncogenic markers analyzed on pre-treatment biopsy specimens and classic tumor characteristics. In addition, we assessed the prognostic significance of these clinical characteristics including pathological and clinical tumor response on overall and distant disease-free survival.

# MATERIAL AND METHODS

## Study participants

All patients participated in a prospectively randomized trial (EORTC 10902) that compared preoperative chemotherapy versus the same chemotherapeutic regimen administered postoperatively in patients with operable breast cancer.[1] This trial accrued 698 women with early stage breast cancer between 1991 and 1999. The eligibility criteria for this trial have been described previously.[1] Efforts were made to obtain diagnostic biopsy material from all patients randomized to preoperative chemotherapy. For the present analysis, we included patients who had received preoperative chemotherapy with known pathological and clinical tumor response and from whom biopsy material were available for pathological evaluation. We used pre-treatment biopsy material for

immunohistochemical analyses in order to avoid interference of the chemotherapeutic regime on the expression levels of oncogenic markers.[9 10]

**Treatment**

Chemotherapy consisted of four cycles of preoperative fluorouracil 600 mg/m$^2$, epirubicin 60 mg/m$^2$, and cyclophosphamide 600 mg/m$^2$ (FEC) administered intravenously, at intervals of every 3 weeks. Surgical therapy followed within 4 weeks of the fourth course of chemotherapy. Surgery consisted of either a modified radical mastectomy or breast-conserving surgery (wide local excision of the tumor or quadrantectomy plus axillary dissection and adjuvant radiotherapy). Recommended guidelines for radiotherapy have been described previously.[1] If radiotherapy was indicated, it was administered after surgery. Patients older than 50 years also received tamoxifen 20 mg daily for at least 2 years, regardless of their estrogen receptor and nodal status.

**Pathological tumor response**

Surgical tumor specimens were examined for the presence of microscopic residual tumor. If no signs of residual malignant cells at the primary site were seen with histological examination, this was scored as a pathological complete response (pCR). The specimens still containing invasive malignant cells were graded as pINV.

**Clinical tumor response**

The tumor response classification system used in EORTC 10902 was according to the UICC.[11] Clinical tumor size was scored by the local investigators before the start of chemotherapy as well as at the time of surgery by both clinical examination and mammography. The product of the two greatest perpendicular diameters was used to compare tumor size before and after chemotherapy.

Clinical complete response (cCR) was defined as complete disappearance of all clinically detectable malignant disease by palpation and mammography. Clinical partial response (cPR) was defined as 50% decrease in total tumor size after four cycles of preoperative chemotherapy. An increase of 25% in tumor size after a minimum of two courses of preoperative chemotherapy was considered to be progressive disease (cPD). If patients did not meet one of the above-mentioned criteria after four cycles of chemotherapy, they were classified as having stable disease (cSD). For the purpose of this analysis, we distinguished between patients with overall clinical response (cCR and cPR) and patients with non-responding tumors (cSD and cPD).

### Histology and immunohistochemistry

Blocks were collected from core needle biopsies taken before the start of chemotherapy. All immunohistochemical analyses were performed in one reference laboratory by two pathologists who were unaware of the clinical outcome of the patients. Invasive carcinomas were histologically graded according to the method of Bloom and Richardson, adapted by Elston and Ellis.[12] Bcl-2 was assessed using Clone 124 (Boehringer Mannheim, Germany) and scored according to van Slooten and colleagues (staining 3 indicates positive status).[13] p53 accumulation was detected using Do-7 monoclonal antibody (NovaCastra, Newcastle on Tyne, United Kingdom) and a semi-quantitative system based on the sum of the mean staining intensity (0 to 3; none to strong) and an estimation of the percentage of positive cell nuclei (0 to 4; 0% to >75%); this allowed a sum score of 0 to 7, with staining 4 being considered positive.[14] Estrogen receptor status (ER) was estimated using the monoclonal antibody DAKO-ER 1D5 (Dako, Glostrup, Denmark; staining indicates positive status).[14] Progesterone receptor status (PgR) was measured using mPRI monoclonal antibody (Transbio, Paris, France; staining indicates positive status).[14] HER2 expression was assessed using the monoclonal antibody 3B5 (staining score 0, 1 and 2 indicates a negative result and 3 resembles a positive result).[15] p21 was measured using the monoclonal antibody EA10 (Calbiochem, Cambridge, MA, USA; 3 indicates a positive result).[13 14]

### Statistical analysis

Overall survival time was defined as the time between randomization and death from any cause. Distant disease-free survival was defined as the time between the date of randomization and the date of distant disease relapse or death from any cause whichever came first. Correlations between the two tumor response classification systems and patient and tumor characteristics were tested using the Pearson's Chi-square test or the Fisher's Exact test. A multivariate logistic regression model was fitted that was based on all characteristics that had a *P*-value up to .10 in the univariate analysis. The effect of patient and tumor characteristics on the survival endpoints was assessed using the Cox proportional hazards regression model to estimate hazard ratios and their 95% confidence intervals. A multivariate Cox regression model was fitted that was based on all characteristics that had a *P*-value up to .10 in the univariate analysis. Survival curves of the tumor response groups were estimated using the Kaplan-Meier technique. The statistical analyses were performed using SPSS software (SPSS Inc., Chicago, II, USA). A two-sided significance level of 0.05 was used.

# RESULTS

## Patient and tumor characteristics

EORTC 10902 trial randomized 350 patients to preoperative chemotherapy and 321 patients received this allocated treatment. Tumor response was assessable in 301 patients. For 194 of these patients no data was available on histological and immunohistochemical analyses. Thus, we were able to include 107 patients in this study. Patient and tumor characteristics are listed in Table 1.

**Table 1.** Patient and tumor characteristics

| Characteristic | N | % |
|---|---|---|
| **Age at diagnosis** | | |
| < 40 years | 11 | 10 |
| > 40 years | 96 | 90 |
| **Type of surgery** | | |
| Mastectomy | 57 | 53 |
| BCT | 50 | 47 |
| **Tamoxifen** | | |
| No | 59 | 55 |
| Yes | 48 | 45 |
| **Radiotherapy** | | |
| No | 20 | 19 |
| Yes | 87 | 81 |
| **Clinical tumor size**[a] | | |
| T1 | 18 | 17 |
| T2 | 64 | 60 |
| T3 | 21 | 19 |
| T4 | 4 | 3 |
| **Clinical tumor response**[b] | | |
| Complete | 7 | 7 |
| Partial | 51 | 48 |
| Stable disease | 47 | 44 |
| Progressive disease | 2 | 2 |
| **Pathological tumor size**[b] | | |
| pCR | 7 | 7 |
| pT1 | 43 | 40 |
| pT2 | 48 | 45 |
| pT3 | 7 | 7 |
| pT4 | 2 | 2 |
| **Clinical nodal status**[a] | | |
| Negative | 65 | 58 |
| Positive | 45 | 42 |
| **Pathological nodal status**[b] | | |
| Negative | 45 | 42 |
| Positive | 65 | 58 |
| **Grade**[a] | | |
| I | 13 | 12 |
| II | 69 | 64 |
| III | 19 | 18 |
| Unknown | 6 | 6 |
| **BCL-2 status**[a] | | |
| Negative | 25 | 23 |
| Positive | 59 | 55 |
| Unknown | 23 | 22 |
| **P53 status**[a] | | |
| negative | 73 | 68 |
| positive | 26 | 24 |
| unknown | 8 | 8 |
| **ER status**[a] | | |
| Negative | 21 | 20 |
| Positive | 71 | 66 |
| Unknown | 15 | 14 |
| **PgR status**[a] | | |
| Negative | 50 | 47 |
| Positive | 49 | 46 |
| Unknown | 8 | 7 |
| **HER2 status**[a] | | |
| Negative | 92 | 86 |
| Positive | 10 | 9 |
| Unknown | 5 | 5 |
| **P21 status**[a] | | |
| Negative | 45 | 42 |
| Positive | 47 | 44 |
| Unknown | 15 | 14 |

a Assessed prior to the delivery of chemotherapy.
b Assessed after the delivery of chemotherapy.
BCT, breast conservative treatment;
pCR, pathological complete response.

The median age at diagnosis was 49.8 years. Seven (6.5%) pathological complete responses following preoperative chemotherapy were seen and 58 (54%) patients had clinically responding tumors. All but one of the patients with pCR was clinically graded as responders. At the time of analysis, the median follow-up period was seven years (95% CI = 6.89 to 7.45); 31 (29%) patients have died and of the patients alive, 10 (9.3%) have experienced a distant relapse. Although otherwise stipulated in the treatment protocol, 9 (17%) women older than 50 years did not use tamoxifen and four (7.4%) women in the younger group did use tamoxifen.

## Prognostic value of pathological tumor response

The association of pCR with overall survival and distant disease-free survival is shown in Figure 1. Patients with a pCR had an overall survival rate after 7 years of 86% compared with 68% for patients with residual disease (pINV) on pathological examination (hazards ratio (HR) = 2.87, 95% CI = 0.39 to 21.14, $P = .30$). Patients with a pCR had a distant disease-free survival rate at 7 years follow-up of 86%, compared to 59% for patients with pINV (HR = 3.62, 95% CI = 0.50 to 26.33, $P = .21$).

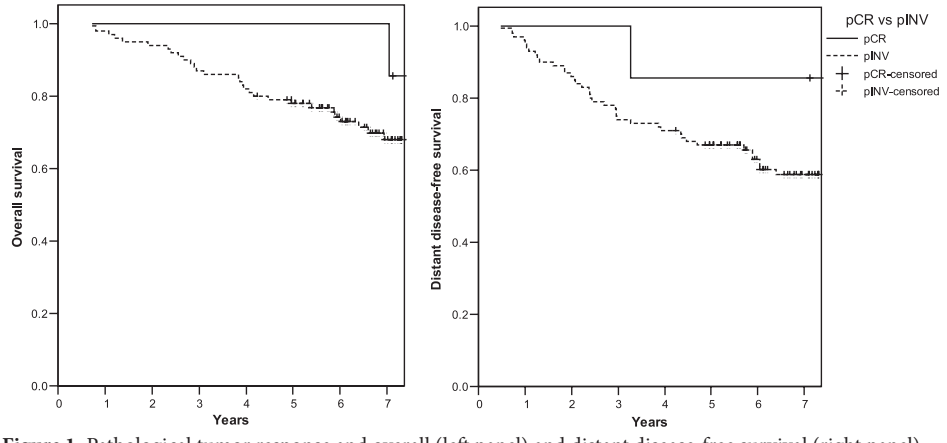


**Figure 1.** Pathological tumor response and overall (left panel) and distant disease-free survival (right panel). pCR = pathological complete response; pINV = invasive tumor cells on pathological examination.

## Prognostic value of clinical tumor response

Patients with a clinical tumor response had an overall survival rate after 7 years of 67% (Figure 2). Non-responders had an overall survival rate of 75% (HR = 0.71, 95% CI = 0.34 to 1.45, $P = .35$). Patients with clinical response had a distant disease-free survival rate after 7 years of 61% compared to 61% for patients with non-responding tumors (HR = 0.94, 95% CI = 0.51 to 1.74, $P = .84$; Figure 2).

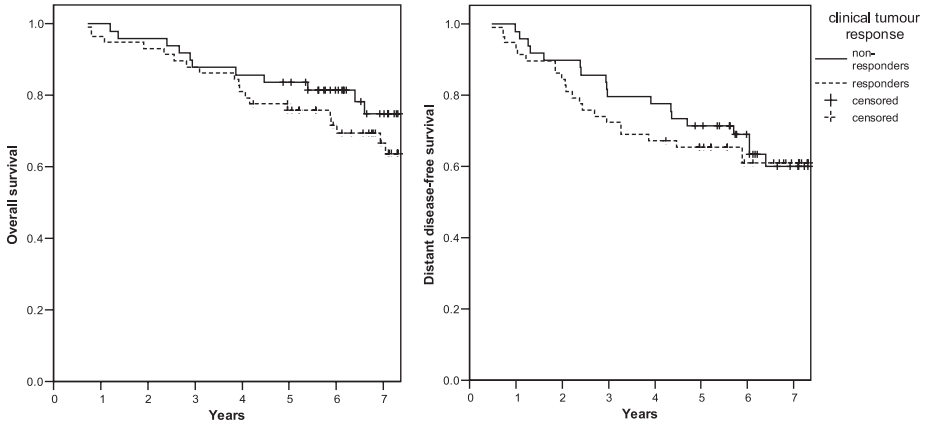


**Figure 2.** Clinical tumor response and overall (left panel) and distant disease-free survival (right panel).

## Predictive characteristics for pathological and clinical response

We assessed the predictive value of patient and tumor characteristics and expression of oncogenic markers in pre-treatment core needle biopsies. Table 2 lists the relationships between dichotomized characteristics and pathological and clinical tumor response. Pathological lymph node status and p53 status were significantly correlated with pathological tumor response. Including both variables in the multivariate analysis (Table 3) revealed an independent relationship of p53 overexpression with pCR (odds ratio (OR) = 16.83, 95% CI = 1.78 to 159.33, *P* = .01) and a non-significant association of negative pathological lymph node status. Clinical tumor response was predicted by clinical tumor size, tumor grade, p53 status, PgR status, and HER2 status (Table 2). At multivariate analysis, p53 overexpression (OR = 5.57, 95% CI = 1.58 to 19.65, *P* = .008) and small clinical tumor size (OR = 10.26, 95% CI = 2.01 to 52.48, P = .005) remained as independent predictive factors of clinical tumor response (Table 3).

**Table 3.** Multivariate logistic regression analysis of tumor characteristics and pathological complete tumor response (N = 99) and clinical response (N = 94)

| Characteristic | Pathological response | | | Clinical response | | |
|---|---|---|---|---|---|---|
| | OR | 95% CI | *P* | OR | 95% CI | *P* |
| **Lymph node negative**[a] | 8.47 | 0.88–81.82 | 0.07 | | | |
| **Positive p53 status**[b] | 16.83 | 1.78-159.33 | 0.01 | 5.57 | 1.58–19.65 | 0.008 |
| **Tumor size < 2 cm**[b] | | | | 10.26 | 2.01–52.48 | 0.005 |
| **Grade IIIa**[b] | | | | 1.58 | 0.41–6.13 | 0.51 |
| **Negative PgR status**[b] | | | | 2.37 | 0.89–6.31 | 0.08 |
| **Positive HER2 expression**[b] | | | | 2.93 | 0.47–18.14 | 0.25 |

a Assessed after to the delivery of chemotherapy. b Assessed prior the delivery of chemotherapy.

**Table 2.** Association of tumor response and patient and tumor characteristics

| Characteristic | Pathological response | | | | | Clinical response | | | | |
|---|---|---|---|---|---|---|---|---|---|---|
| | pCR | | pINV | | *P* | Responders | | Non-responders | | *P* |
| | N | % | N | % | | N | % | N | % | |
| **Age at diagnosis** | | | | | 1.00 | | | | | 0.22 |
| < 40 years | 0 | 0 | 11 | 100 | | 8 | 73 | 3 | 27 | |
| > 40 years | 7 | 7 | 89 | 93 | | 50 | 52 | 46 | 48 | |
| **Clinical tumor size** | | | | | 0.60 | | | | | 0.001 |
| < 2 cm | 0 | 0 | 18 | 100 | | 16 | 89 | 2 | 11 | |
| > 2 cm | 7 | 8 | 82 | 92 | | 42 | 47 | 47 | 53 | |
| **Clinical nodal status** | | | | | 1.00 | | | | | 0.43 |
| Negative | 4 | 7 | 58 | 93 | | 36 | 58 | 26 | 42 | |
| Positive | 3 | 7 | 42 | 93 | | 22 | 49 | 23 | 51 | |
| **Pathological nodal status** | | | | | 0.04 | | | | | 0.17 |
| Negative | 6 | 13 | 39 | 87 | | 28 | 62 | 17 | 38 | |
| Positive | 1 | 2 | 61 | 98 | | 30 | 48 | 32 | 52 | |
| **Histological grade** | | | | | 0.61 | | | | | 0.05 |
| I & II | 5 | 6 | 77 | 94 | | 40 | 49 | 42 | 51 | |
| III | 2 | 11 | 17 | 89 | | 14 | 74 | 5 | 26 | |
| **BCL-2 status** | | | | | 0.36 | | | | | 0.23 |
| Negative | 3 | 12 | 22 | 88 | | 15 | 60 | 10 | 40 | |
| Positive | 3 | 5 | 56 | 95 | | 27 | 46 | 32 | 54 | |
| **P53 status** | | | | | 0.004 | | | | | 0.001 |
| Negative | 1 | 1 | 72 | 99 | | 32 | 44 | 41 | 56 | |
| Positive | 5 | 19 | 21 | 81 | | 21 | 81 | 5 | 19 | |
| **ER status** | | | | | 0.13 | | | | | 0.13 |
| Negative | 3 | 14 | 18 | 86 | | 14 | 67 | 7 | 33 | |
| Positive | 3 | 4 | 68 | 96 | | 34 | 48 | 37 | 52 | |
| **PgR status** | | | | | 0.68 | | | | | 0.007 |
| Negative | 4 | 8 | 46 | 92 | | 33 | 66 | 17 | 34 | |
| Positive | 2 | 4 | 47 | 96 | | 19 | 39 | 30 | 61 | |
| **HER2 status** | | | | | 0.47 | | | | | 0.09 |
| Negative | 5 | 5 | 87 | 95 | | 46 | 50 | 46 | 50 | |
| Positive | 1 | 10 | 9 | 90 | | 8 | 80 | 2 | 20 | |
| **P21 status** | | | | | 1.00 | | | | | 0.53 |
| Negative | 3 | 7 | 42 | 93 | | 25 | 56 | 20 | 44 | |
| Positive | 3 | 6 | 44 | 94 | | 23 | 49 | 24 | 51 | |

pCR, pathological complete response; pINV, invasive tumor cells on pathological examination.

## Prognostic characteristics for overall survival and distant disease-free survival

Table 4 shows the prognostic value of patient and tumor characteristics in predicting clinical outcome. Significant prognostic variables for overall and distant disease-free survival were age, use of tamoxifen, and pathological lymph node status. In addition, histological tumor grade was significantly associated with overall survival. Overexpression of p53 was non-significantly related with poorer overall (HR = 1.72, 95% CI = 0.82 to 3.62, $P = .15$) and distant disease-free survival (HR = 1.39, 95% CI = 0.70 to 2.74, $P = .35$).

**Table 4.** Univariate Cox regression analyses for overall and distant disease-free survival

| Characteristic | Overall survival | | | | | Distant disease-free survival | | | | |
|---|---|---|---|---|---|---|---|---|---|---|
| | N/O | 7-year SR | HR | 95% CI | *P* | N/O | 7-year SR | HR | 95% CI | *P* |
| **Age at diagnosis** | | | | | 0.01 | | | | | 0.03 |
| < 40 years | 11/7 | 45 | 1.00 | | | 11/7 | 36 | 1.00 | | |
| > 40 years | 96/24 | 73 | 0.34 | 0.14–0.78 | | 96/34 | 64 | 0.40 | 0.18–0.92 | |
| **Surgery** | | | | | 0.62 | | | | | 0.29 |
| Mastectomy | 57/17 | 66 | 1.00 | | | 57/24 | 58 | 1.00 | | |
| Breast conserving | 50/14 | 74 | 0.83 | 0.41–1.69 | | 50/17 | 64 | 0.72 | 0.36–1.33 | |
| **Tamoxifen** | | | | | 0.01 | | | | | 0.01 |
| No | 59/24 | 60 | 1.00 | | | 59/30 | 48 | 1.00 | | |
| Yes | 48/7 | 84 | 0.34 | 0.15–0.79 | | 48/11 | 77 | 0.39 | 0.19–0.77 | |
| **Radiotherapy** | | | | | 0.11 | | | | | 0.32 |
| No | 20/8 | 56 | 1.00 | | | 20/9 | 51 | 1.00 | | |
| Yes | 87/23 | 74 | 0.52 | 0.23–1.16 | | 87/32 | 63 | 0.69 | 0.33–1.44 | |
| **Clinical tumor size** | | | | | 0.63 | | | | | 0.35 |
| < 2 cm | 18/4 | 72 | 1.00 | | | 18/5 | 67 | 1.00 | | |
| > 2 cm | 89/27 | 70 | 1.30 | 0.45–3.72 | | 89/36 | 59 | 1.57 | 0.61–4.00 | |
| **Clinical response** | | | | | 0.35 | | | | | 0.84 |
| Responders | 58/19 | 67 | 1.00 | | | 58/22 | 61 | 1.00 | | |
| Non-responders | 49/12 | 75 | 0.71 | 0.34–1.45 | | 49/19 | 61 | 0.94 | 0.51–1.74 | |
| **Pathological tumor size** | | | | | 0.35 | | | | | 0.26 |
| < 2 cm | 50/13 | 75 | 1.00 | | | 50/17 | 64 | 1.00 | | |
| > 2 cm | 57/18 | 66 | 1.41 | 0.69–2.88 | | 57/24 | 58 | 1.43 | 0.77–2.67 | |
| **Pathological response** | | | | | 0.30 | | | | | 0.21 |
| pCR | 7/1 | 86 | 1.00 | | | 7/1 | 86 | 1.00 | | |
| pINV | 100/30 | 68 | 2.87 | 0.39–21.14 | | 100/40 | 59 | 3.62 | 0.47–26.33 | |
| **Clinical nodal status** | | | | | 0.51 | | | | | 0.37 |
| Negative | 62/17 | 73 | 1.00 | | | 62/22 | 64 | 1.00 | | |
| Positive | 45/14 | 67 | 1.27 | 0.62–2.57 | | 45/19 | 56 | 1.33 | 0.72–2.55 | |
| **Pathological nodal status** | | | | | 0.01 | | | | | 0.00 |
| Negative | 45/8 | 84 | 1.00 | | | 45/8 | 81 | 1.00 | | |
| Positive | 62/23 | 61 | 2.82 | 1.23–6.44 | | 62/33 | 46 | 4.15 | 1.90–9.06 | |
| **Histological grade** | | | | | 0.05 | | | | | 0.23 |
| I & II | 82/20 | 74 | 1.00 | | | 82/29 | 64 | 1.00 | | |
| III | 19/9 | 55 | 2.23 | 1.01–4.91 | | 19/9 | 50 | 1.58 | 0.75–3.33 | |
| **BCL-2 status** | | | | | 0.30 | | | | | 0.12 |
| Negative | 25/8 | 70 | 1.00 | | | 25/11 | 54 | 1.00 | | |
| Positive | 59/12 | 79 | 0.62 | 0.26–1.53 | | 59/16 | 73 | 0.55 | 0.25–1.18 | |
| **P53 status** | | | | | 0.15 | | | | | 0.35 |
| Negative | 73/19 | 73 | 1.00 | | | 73/27 | 62 | 1.00 | | |
| Positive | 26/11 | 58 | 1.72 | 0.82–3.62 | | 26/12 | 52 | 1.39 | 0.70–2.74 | |
| **ER status** | | | | | 0.16 | | | | | 0.59 |
| Negative | 21/9 | 60 | 1.00 | | | 21/9 | 56 | 1.00 | | |
| Positive | 71/19 | 71 | 0.57 | 0.26–1.26 | | 71/27 | 61 | 0.81 | 0.38–1.74 | |
| **PgR status** | | | | | 0.14 | | | | | 0.16 |
| Negative | 50/19 | 62 | 1.00 | | | 50/23 | 52 | 1.00 | | |
| Positive | 49/12 | 75 | 0.58 | 0.28–1.19 | | 49/16 | 68 | 0.64 | 0.34–1.20 | |
| **HER2 status** | | | | | 0.87 | | | | | 0.74 |
| Negative | 92/27 | 70 | 1.00 | | | 92/37 | 59 | 1.00 | | |
| Positive | 10/3 | 69 | 1.11 | 0.34–3.66 | | 10/3 | 70 | 0.82 | 0.25–2.66 | |
| **P21 status** | | | | | 0.24 | | | | | 0.28 |
| Negative | 45/12 | 72 | 1.00 | | | 45/16 | 65 | 1.00 | | |
| Positive | 47/17 | 64 | 1.56 | 0.74–3.28 | | 47/12 | 53 | 1.44 | 0.75–2.76 | |

N/O, number of patients/ observed number of events; SR, survival rate; HR, hazard rate; pCR, pathological complete response; pINV, invasive tumor cells on pathological examination.

The prognostic factors found to be trend significant at univariate analyses were included in multivariate analyses to identify independent prognostic factors of overall and distant disease-free survival (Table 5). Negative pathological lymph node status and use of tamoxifen were both independently associated with improved overall and distant disease-free survival. In addition, histological tumor grade III was an independent prognostic factor of poorer overall survival.

## DISCUSSION

In this analysis, we demonstrated a significant independent association between p53 overexpression and pathological complete and clinical tumor response to 4 cycles of preoperative FEC. However, pCR as a prognostic factor for overall survival, as well as for distant disease-free survival, did not reach statistical significance in this patient population, although a clear trend was demonstrated (Figure 1). This finding is in accordance with other randomized controlled trials studying preoperative chemotherapy in primary operable breast cancer, while pCR in these studies was a significant prognostic factor.[2 16-18]

In this study, clinical tumor response showed no prognostic benefit (Figure 2). This result is in disagreement with other reports[2 16 17] and most probably resembles a selection bias as the data derived from our larger study population suggest an association of non-response with poorer overall survival (HR = 1.43, 95% CI = 0.91 to 2.24, $P$ = .12). However, the fact that clinical responders in the current group had no favorable prognosis implies that the results concerning the predictive value of characteristics for clinical response must be interpreted with caution. Moreover, determining clinical tumor response after preoperative chemotherapy is difficult and can be either under- or overestimated due to fibrosis, weakening of the tumor margins and resolution of edema, suggesting prognostic superiority of pathologically evaluated tumor response.[19-22]

Although pCR in our study was associated with p53 overexpression and higher survival rate, p53 overexpression was not translated in improved clinical outcome. In contrast, p53 overexpression was non-significantly related with poorer overall and distant disease-free survival. Hypothetically, the short-lived benefits of better response

**Table 5.** Multivariate Cox regression analyses of characteristics predicting for overall (N = 101) and distant disease-free survival (N = 107)

| Characteristic | Overall survival | | | Distant disease-free survival | | |
|---|---|---|---|---|---|---|
| | HR | 95% CI | *P* | HR | 95% CI | *P* |
| **Lymph node negative**[a] | 4.30 | 1.71–10.82 | 0.002 | 5.19 | 2.35–11.46 | 0.000 |
| **Use of tamoxifen** | 0.41 | 0.17–1.00 | 0.05 | 0.34 | 0.17–0.69 | 0.003 |
| **Age < 40 years** | 2.13 | 0.81–5.65 | 0.13 | 2.28 | 0.98–5.32 | 0.06 |
| **Grade IIIa**[b] | 3.02 | 1.28–7.12 | 0.01 | | | |

a Assessed after to the delivery of chemotherapy. b Assessed prior the delivery of chemotherapy.
HR, hazard ratio.

of p53 positive tumors may be overcast by rapid re-growth of micro-metastases after initial remission of the primary tumor, reflecting their aggressive biology. However, analysis of the hypothesis that survival in the pCR subgroup is dependent on p53 status was not possible due to the limited power of the current study.

p53, a nuclear protein, plays an essential role in the regulation of cell cycle and functions as a tumor suppressor. Breast cancer patients with p53 mutations or protein accumulation measured by immunohistochemistry in their tumors have worse survival.[23-26] Meanwhile, the literature of the predictive value of p53 status on tumor response to preoperative anthracycline-based chemotherapy is conflicting.[7] Most studies find no association between p53 expression and tumor response to anthracyclines.[27-32] Others have associated p53 overexpression with both resistance[14 33-35] and sensitivity[10 36] to preoperative anthracycline-based chemotherapy. Interpretation of the above literature is complicated since the definition of response varies across studies, the correlation between p53 protein accumulation and the presence of mutations is not absolute and numerous non-standardized immunohistochemistry techniques have been used, limiting the possibility to draw valid conclusions.[37]

The pathological lymph node status after preoperative chemotherapy is in our data an independent prognostic factor for both overall and distant disease-free survival. This finding has also been noted by others.[3 38-40] However, the pre-treatment clinical lymph node status was poorly correlated with clinical outcome. At the time this trial was conducted, the pre-treatment nodal status was determined by palpation only. Nowadays, imaging techniques such as ultrasound are more feasible in establishing nodal status.[41] Future trials should include this technique to provide more reliable information of the actual response of lymph node metastases to preoperative chemotherapy and to determine the subsequent prognostic significance of such a response.

At this time, it is not possible to select patient who will benefit from chemotherapy. However, data have begun to emerge from microarray studies which may lead to the introduction of tailored treatment strategies based upon custom-made risk profiles rather than the classic guidelines derived from traditional randomized clinical trials.[42-45]

In conclusion, our data derived from a prospective randomized trial suggest that p53 overexpression estimated by immunohistochemistry is an independent predictive factor of tumor response after preoperative anthracycline-based chemotherapy in operable breast cancer patients. However, this conclusion must be limited to the regime used in this trial (FE60C), which is probably suboptimal today.[46] Moreover, the relatively small sample size requires conformation in larger studies and the use of p53 measurements should be restricted to clinical trial settings. Prospectively derived data on the predictive and prognostic value of p53 is on the way from the neoadjuvant EORTC trial 10994.[47 48]

## ACKNOWLEDGEMENTS

We thank Hein Putter for his statistical support. Part of this work was financially supported by the EORTC Breast Cancer Group.

### Cooperating investigators and participating institutions

J-P. Julien, Centre Henri Becquerel, Rouen, France

M. Tubiana-Hulin, F. Bachelot, Centre René Huguenin, St Cloud, France

T. Delozier, Centre Regional François Baclesse, Caen, France

C.J.H. van de Velde, M.A. Nooy, Leiden University Medical Centre, Leiden, the Netherlands

H. Bonnefoi, Hopital Cantonal Universitaire de Geneve, Geneva, Switzerland

J.A. van Zyl, A.G. Muller, University of Stellenbosch, Tygerberg Hospital, Tygerberg, Republic of South Africa

S. Omar, National Cancer Institute, Cairo, Egypt

J. Jassem, J. Jaskiewicz, Medical University of Gdansk, Gdansk, Poland

J.J. Grau, Hospital Clinico y Provencial de Barcelona, Barcelona, Spain

D. Vukotic, Institute of Oncology and Radiology, Belgrade, Federal Republic of Yugoslavia

T. Cufer, M. Snoj, The Institute of Oncology, Ljubljana, Slovenia

O. Ivanova, V.F. Semiglazov, Petrov Research Institute of Oncology, St Petersburg, Russia

I. Varthalitis, Evangelismos Hospital, Athens, Greece

A. Ezzat, King Faisal Spec. Hospital and Research Center, Riyadh, Saudi Arabia

## REFERENCES

1. van der Hage JA, van de Velde CJH, Julien JP, et al. Preoperative chemotherapy in primary operable breast cancer: results from the European Organization for Research and Treatment of Cancer trial 10902. J Clin Oncol 2001; 19:4224-37.
2. Wolmark N, Wang J, Mamounas E, et al. Preoperative chemotherapy in patients with operable breast cancer: nine-year results from National Surgical Adjuvant Breast and Bowel Project B-18. J Natl Cancer Inst Monogr 2001: 96-102.
3. Bonadonna G, Valagussa P, Brambilla C, et al. Primary chemotherapy in operable breast cancer: eight-year experience at the Milan Cancer Institute. J Clin Oncol 1998; 16:93-100.
4. Kuerer HM, Newman LA, Smith TL, et al. Clinical course of breast cancer patients with complete pathologic primary tumor and axillary lymph node response to doxorubicin-based neoadjuvant chemotherapy. J Clin Oncol 1999; 17:460-9.
5. Chollet P, Amat S, Cure H, et al. Prognostic significance of a complete pathological response after induction chemotherapy in operable breast cancer. Br J Cancer 2002; 86:1041-6.
6. Fisher B, Mamounas EP. Preoperative chemotherapy: a model for studying the biology and therapy of primary breast cancer. J Clin Oncol 1995; 13:537-40.
7. Charfare H, Limongelli S, Purushotham AD. Neoadjuvant chemotherapy in breast cancer. Br J Surg 2005; 92:14-23.
8. Hamilton A, Piccart M. The contribution of molecular markers to the prediction of response in the treatment of breast cancer: a review of the literature on HER-2, p53 and BCL-2. Ann Oncol 2000; 11:647-63.

9. Makris A, Powles TJ, Allred DC, et al. Quantitative changes in cytological molecular markers during primary medical treatment of breast cancer: a pilot study. Breast Cancer Res Treat 1999; 53:51-9.
10. Faneyte IF, Schrama JG, Peterse JL, et al. Breast cancer response to neoadjuvant chemotherapy: predictive markers and relation with outcome. Br J Cancer 2003; 88:406-12.
11. Hayward JL, Carbone PP, Heuson JC, et al. Assessment of response to therapy in advanced breast cancer: a project of the Programme on Clinical Oncology of the International Union Against Cancer, Geneva, Switzerland. Cancer 1977; 39:1289-94.
12. Elston CW, Ellis IO. Pathological prognostic factors in breast cancer. I. The value of histological grade in breast cancer: experience from a large study with long-term follow-up. Histopathology 1991; 19:403-10.
13. van Slooten HJ, Clahsen PC, van Dierendonck JH, et al. Expression of Bcl-2 in node-negative breast cancer is associated with various prognostic factors, but does not predict response to one course of perioperative chemotherapy. Br J Cancer 1996; 74:78-85.
14. Clahsen PC, van de Velde CJH, Duval C, et al. p53 protein accumulation and response to adjuvant chemotherapy in premenopausal women with node-negative early breast cancer. J Clin Oncol 1998; 16:470-9.
15. van de Vijver MJ, Peterse JL, Mooi WJ, et al. Neu-protein overexpression in breast cancer. Association with comedo-type ductal carcinoma in situ and limited prognostic value in stage II breast cancer. N Engl J Med 1988; 319:1239-45.
16. Semiglazov VF, Topuzov EE, Bavli JL, et al. Primary (neoadjuvant) chemotherapy and radiotherapy compared with primary radiotherapy alone in stage IIb-IIIa breast cancer. Ann Oncol 1994; 5:591-5.
17. Cleator SJ, Makris A, Ashley SE, et al. Good clinical response of breast cancers to neoadjuvant chemoendocrine therapy is associated with improved overall survival. Ann Oncol 2005; 16:267-72.
18. Gianni L, Baselga J, Eiermann W, et al. European Cooperative Trial in Operable Breast Cancer (ECTO): Improved freedom from progression (FFP) from adding paclitaxel (T) to doxorubicin (A) followed by cyclophosphamide methotrexate and fluorouracil (CMF). ASCO Meeting Abstracts 2005; 23:513.
19. Abraham DC, Jones RC, Jones SE, et al. Evaluation of neoadjuvant chemotherapeutic response of locally advanced breast cancer by magnetic resonance imaging. Cancer 1996; 78:91-100.
20. Segel MC, Paulus DD, Hortobagyi GN. Advanced primary breast cancer: assessment at mammography of response to induction chemotherapy. Radiology 1988; 169:49-54.
21. Veronesi U, Bonadonna G, Zurrida S, et al. Conservation surgery after primary chemotherapy in large carcinomas of the breast. Ann Surg 1995; 222:612-8.
22. Vinnicombe SJ, MacVicar AD, Guy RL, et al. Primary breast cancer: mammographic changes after neoadjuvant chemotherapy, with pathologic correlation. Radiology 1996; 198:333-40.
23. Pharoah PD, Day NE, Caldas C. Somatic mutations in the p53 gene and prognosis in breast cancer: a meta-analysis. Br J Cancer 1999; 80:1968-73.
24. Thor AD, Moore DH, II, Edgerton SM, et al. Accumulation of p53 tumor suppressor gene protein: an independent marker of prognosis in breast cancers. J Natl Cancer Inst 1992; 84:845-55.
25. Allred DC, Clark GM, Elledge R, et al. Association of p53 protein expression with tumor cell proliferation rate and clinical outcome in node-negative breast cancer. J Natl Cancer Inst 1993; 85:200-6.
26. Yamashita H, Nishio M, Toyama T, et al. Coexistence of HER2 over-expression and p53 protein accumulation is a strong prognostic molecular marker in breast cancer. Breast Cancer Res 2004; 6:R24-R30.
27. Makris A, Powles TJ, Dowsett M, et al. Prediction of response to neoadjuvant chemoendocrine therapy in primary breast carcinomas. Clin Cancer Res 1997; 3:593-600.
28. MacGrogan G, Mauriac L, Durand M, et al. Primary chemotherapy in breast invasive carcinoma: predictive value of the immunohistochemical detection of hormonal receptors, p53, c-erbB-2, MiB1, pS2 and GST pi. Br J Cancer 1996; 74:1458-65.
29. Niskanen E, Blomqvist C, Franssila K, et al. Predictive value of c-erbB-2, p53, cathepsin-D and histology of the primary tumour in metastatic breast cancer. Br J Cancer 1997; 76:917-22.

30. Rozan S, Vincent-Salomon A, Zafrani B, et al. No significant predictive value of c-erbB-2 or p53 expression regarding sensitivity to primary chemotherapy or radiotherapy in breast cancer. Int J Cancer 1998; 79:27-33.
31. Mathieu MC, Koscielny S, Le Bihan ML, et al. p53 protein overexpression and chemosensitivity in breast cancer. Institut Gustave-Roussy Breast Cancer Group. Lancet 1995; 345:1182.
32. Jarvinen TA, Holli K, Kuukasjarvi T, et al. Predictive value of topoisomerase IIalpha and other prognostic factors for epirubicin chemotherapy in advanced breast cancer. Br J Cancer 1998; 77:2267-73.
33. Kandioler-Eckersberger D, Ludwig C, Rudas M, et al. TP53 mutation and p53 overexpression for prediction of response to neoadjuvant treatment in breast cancer patients. Clin Cancer Res 2000; 6:50-6.
34. Geisler S, Lonning PE, Aas T, et al. Influence of TP53 gene alterations and c-erbB-2 expression on the response to treatment with doxorubicin in locally advanced breast cancer. Cancer Res 2001; 61:2505-12.
35. Berns EM, Foekens JA, Vossen R, et al. Complete sequencing of TP53 predicts poor response to systemic therapy of advanced breast cancer. Cancer Res 2000; 60:2155-62.
36. Colleoni M, Orvieto E, Nole F, et al. Prediction of response to primary chemotherapy for operable breast cancer. Eur J Cancer 1999; 35:574-9.
37. Fitzgibbons PL, Page DL, Weaver D, et al. Prognostic factors in breast cancer. College of American Pathologists Consensus Statement 1999. Arch Pathol Lab Med 2000; 124:966-78.
38. Pierga JY, Mouret E, Dieras V, et al. Prognostic value of persistent node involvement after neoadjuvant chemotherapy in patients with operable breast cancer. Br J Cancer 2000; 83:1480-7.
39. Botti C, Vici P, Lopez M, et al. Prognostic value of lymph node metastases after neoadjuvant chemotherapy for large-sized operable carcinoma of the breast. J Am Coll Surg 1995; 181:202-8.
40. Rouzier R, Extra JM, Klijanienko J, et al. Incidence and prognostic significance of complete axillary downstaging after primary chemotherapy in breast cancer patients with T1 to T3 tumors and cytologically proven axillary metastatic lymph nodes. J Clin Oncol 2002; 20:1304-10.
41. Deurloo EE, Tanis PJ, Gilhuijs KG, et al. Reduction in the number of sentinel lymph node procedures by preoperative ultrasonography of the axilla in breast cancer. Eur J Cancer 2003; 39:1068-73.
42. Chang JC, Wooten EC, Tsimelzon A, et al. Gene expression profiling for the prediction of therapeutic response to docetaxel in patients with breast cancer. Lancet 2003; 362:362-9.
43. Ayers M, Symmans WF, Stec J, et al. Gene expression profiles predict complete pathologic response to neoadjuvant paclitaxel and fluorouracil, doxorubicin, and cyclophosphamide chemotherapy in breast cancer. J Clin Oncol 2004; 22:2284-93.
44. Gianni L, Zambetti M, Clark K, et al. Gene expression profiles in paraffin-embedded core biopsy tissue predict response to chemotherapy in women with locally advanced breast cancer. J Clin Oncol 2005; 23:7265-77.
45. Hannemann J, Oosterkamp HM, Bosch CA, et al. Changes in gene expression associated with response to neoadjuvant chemotherapy in breast cancer. J Clin Oncol 2005;23:3331-42.
46. Benefit of a high-dose epirubicin regimen in adjuvant chemotherapy for node-positive breast cancer patients with poor prognostic factors: 5-year follow-up results of French Adjuvant Study Group 05 randomized trial. J Clin Oncol 2001; 19:602-11.
47. Rutgers EJ, Meijnen P, Bonnefoi H. Clinical trials update of the European Organization for Research and Treatment of Cancer Breast Cancer Group. Breast Cancer Res 2004; 6:165-9.
48. Farmer P, Iggo R, Becette V, et al. High quality gene expression microarray data from a multicentre prospective trial: results of the first microarray analysis in the EORTC 10994/BIG 00-01 study. Eur J Canc Suppl 2004; 2:99.

# Chapter 4

# Efficacy of adjuvant chemotherapy according to hormone receptor status in young patients with breast cancer: a pooled analysis

van der Hage JA, Mieog JSD, van de Vijver MJ, van de Velde CJH, and cooperating investigators of the European Organization for Research and Treatment of Cancer

*Breast Cancer Res 2007; 9:R70*

## ABSTRACT

### Introduction

Breast cancer at a young age is associated with an unfavorable prognosis. Very young patients with breast cancer therefore are advised to undergo adjuvant chemotherapy irrespective of tumor stage or grade. However, chemotherapy alone may not be adequate in young patients with hormone receptor positive breast cancer. Therefore, we studied the effect of adjuvant chemotherapy in young patients with breast cancer in relation to hormone receptor status.

### Methods

Paraffin-embedded tumor material was collected from 480 early-stage breast cancer patients younger than 40 years who participated in one of four European Organization for Research and Treatment of Cancer trials. Using immunohistochemistry, we assessed estrogen receptor (ER) status and progesterone receptor (PgR) status in a standardized way. Endpoints in this study were overall survival (OS) and distant metastasis-free survival (DMFS). The median follow-up period was 7.3 years.

### Results

Overall, patients with ER positive tumors had better OS rates (hazard ratio (HR) = 0.63, 95% CI = 0.43 to 0.93, $P = .02$) compared with those with ER negative tumors. However, in the subgroup of patients who received chemotherapy, no significant difference in OS (HR = 0.87, 95% CI = 0.50 to 1.52, $P = .63$) and DMFS (HR = 1.36, 95% CI = 0.82 to 2.26, $P = .23$) was found between patients with ER positive tumors or those with ER negative tumors. These differences were similar for PgR status.

### Conclusion

Very young patients with hormone receptor positive tumors benefit less from adjuvant systemic chemotherapy than hormone receptor negative patients. These results confirm that chemotherapy alone cannot be considered optimal adjuvant systemic treatment in young breast cancer patients with hormone receptor positive tumors.

## INTRODUCTION

Breast cancer in premenopausal women is associated with worse outcome compared with postmenopausal patients.[1] Approximately 7% of women diagnosed with breast cancer are younger than 40 years old.[2] Very young women (that is, younger than 35 years old), especially, are at a high risk of developing distant metastases. Therefore, they are recommended to receive adjuvant systemic chemotherapy regardless of tumor stage or grade.[3] In addition, high local regional recurrence rates after breast-conserving therapy have been reported in young premenopausal patients with breast cancer.[4] Although it is clear that young age is an independent prognosticator of adverse outcome in breast cancer, controversies regarding the optimal treatment in this population exist.

Adjuvant systemic chemotherapy in premenopausal patients has been shown to improve survival,[1] but controversy about the role of chemotherapy in patients with hormone receptor positive tumors still exists. Aebi and colleagues clearly showed that the endocrine effects of chemotherapy alone might not be sufficient for very young patients with breast cancer.[5] In this study, it was shown that patients younger than 35 years with estrogen receptor (ER) positive tumors and treated with cyclophosphamide, methotrexate and 5-fluorouracil (CMF) had a significantly worse disease-free survival compared with ER negative patients.

To detect whether we could confirm these data by finding similar results, we studied the efficacy of chemotherapy in young patients with breast cancer according to ER status and progesterone receptor (PgR) status and selected patients aged younger than 40 years at the time of diagnosis from four European Organization for Research and Treatment of Cancer (EORTC) trials that were conducted by the EORTC Breast Cancer Group and Radiotherapy Group.

## MATERIAL AND METHODS

### Study participants

Data were collected from four EORTC trials. In total, 9,938 patients participated in these trials; 934 of these patients were 40 years old or younger at the time of diagnosis. The trial designs are summarized below.

EORTC trial 10801 (1980 to 1986, median follow-up 13.4 years) was conducted to assess the safety of breast-conserving treatment. In this trial, patients were randomly assigned between breast-conserving surgery combined with radiotherapy and radical mastectomy. Six cycles of adjuvant chemotherapy with cyclophosphamide 100 mg/m$^2$ given orally on days 1 to 14, methotrexate 40 mg/m$^2$ given intravenously on days 1 and 8, and 5-fluorouracil 600 mg/m$^2$ (CMF) given intravenously on days 1 and 8 were

indicated for all patients under the age of 55 with positive nodes. A total of 902 patients were randomly assigned.[6]

EORTC trial 10854 (1986 to 1991, median follow-up 10.8 years) studied the question of whether one course of perioperative chemotherapy given directly after surgery yields better results in terms of treatment outcome than surgery alone. Perioperative chemotherapy consisted of a single course of doxorubicin 50 mg/m$^2$, 5-fluorouracil 600 mg/m$^2$, and cyclophosphamide 600 mg/m$^2$ (FAC) administered intravenously within 36 hours after surgery. For axillary lymph node positive premenopausal patients in the perioperative chemotherapy group, adjuvant chemotherapy consisting of five cycles of CMF was recommended. For node positive patients younger than 50 years who did not receive perioperative chemotherapy, one conventional course of FAC followed by five cycles of CMF after surgery was recommended. Postmenopausal patients were recommended to receive tamoxifen. A total of 2,795 patients were included.[7]

EORTC trial 10902 (1991 to 1999, median follow-up 6.1 years) was set up to determine the value of preoperative chemotherapy. Patients were randomly assigned to receive four cycles of chemotherapy either before or after surgery. Chemotherapy consisted of four cycles of 5-fluorouracil 600 mg/m$^2$, epirubicin 60 mg/m$^2$, and cyclophosphamide 600 mg/m$^2$ (FEC) administered intravenously at 3-weekly intervals. In the preoperative chemotherapy group, surgical therapy followed within 4 weeks of the fourth course of chemotherapy. In the postoperative chemotherapy group, the first cycle was given within 36 hours after surgery. Patients not younger than 50 years received tamoxifen for 2 years. A total of 698 patients were randomly assigned.[8]

EORTC trial 22881 (1989 to 1996, median follow-up 5.1 years) was conducted to study the effect of an additional dose of 16 Gy radiation to the tumor bed among early stage breast cancer patients who received 50 Gy radiotherapy after lumpectomy. Patients with a microscopically incomplete resection were assigned to receive boost doses of 10 or 26 Gy. Premenopausal patients with axillary lymph node involvement received six cycles of adjuvant CMF, and all postmenopausal patients received tamoxifen 20 mg per day during at least 2 years. A total of 5,569 patients were enrolled.[9]

In all trials, if adjuvant chemotherapy was indicated, patients received either CMF or an anthracyclin-based regimen (FAC or FEC). Adjuvant hormonal therapy for premenopausal hormone receptor-positive patients was not yet recommended at the time these trials were conducted. In the two oldest trials, tamoxifen administration was not even recorded. This explains the high number of patients for whom no information was found on tamoxifen use. In the trials in which tamoxifen use was recorded, less than 5% of patients aged less than 40 years received tamoxifen. Therefore, we have to assume that only a very small fraction of the patient population in this study received tamoxifen.

### Hormone receptor staining

Paraffin-embedded tumor material was collected from 480 patients age less than 40 years. Tumors were histologically graded using hematoxylin and eosin slides as described previously.[10] Immunohistochemical staining for ER and PgR status was performed using a tissue microarray.[11-14] Three core biopsies were taken from each tumor block and inserted into a donor block. Immunohistochemical staining for ER was performed using the monoclonal antibody DAKO-ER, 1D5 (DakoCytomation Denmark A/S, Glostrup, Denmark), for PgR using the monoclonal antibody mPRI (TRANSBIO, Paris, France). Immunohistochemical staining was scored using a semiquantative system based on the percentage of positive nuclei. After the percentage of positive nuclei in three core biopsies was counted, the mean value was taken. For both ER and PgR, tumors with more than 10% of the tumor cells showing nuclear staining were considered positive.

### Statistical analysis

Analyses were performed for distant metastasis-free survival (DMFS) and overall survival (OS). DMFS was defined as the interval from time of randomization to time of distant metastasis or death, whichever came first. OS was defined as time from randomization to death from any cause. Survival curves were estimated using the Kaplan-Meier method. Differences in survival were analyzed using Cox proportional hazard models. The statistical analyses were performed using SPSS software (SPSS Inc., Chicago, IL, USA). A direct comparison of patients who received chemotherapy versus those who did not receive chemotherapy was not feasible. (This would have introduced a selection bias in this retrospective analysis as the vast majority of patients receiving chemotherapy had positive axillary lymph nodes.) Therefore, conclusions in this explorative analysis were based on indirect comparisons.

## RESULTS

### Participants

Paraffin-embedded tumor specimens were collected from 480 patients aged less than 40 years at the time of diagnosis (Table 1). For 12 patients, ER status could not be scored, and for 16 patients, PgR status could not be scored. Positive ER status and positive PgR status were found in 288 (60%) and 223 (46%) patients, respectively. Two hundred patients received prolonged adjuvant systemic chemotherapy, whereas 279 patients did not receive adjuvant systemic chemotherapy. Of the patients not receiving chemotherapy, 94% were node negative, whereas 85% of patients who did

**Table 1.** Characteristics of 480 breast cancer patients aged 40 years or younger

| Characteristic | N | % |
|---|---|---|
| **Pathological tumor size** | | |
| T1 | 292 | 61 |
| T2-3 | 151 | 31 |
| Missing | 37 | 8 |
| **Pathological nodal status** | | |
| Negative | 288 | 60 |
| Positive | 188 | 39 |
| Missing | 4 | 1 |
| **Surgery** | | |
| Breast conserving | 393 | 82 |
| Mastectomy | 86 | 18 |
| Missing | 1 | 0 |
| **Adjuvant chemotherapy** | | |
| No | 279 | 58 |
| Yes | 200 | 42 |
| Missing | 1 | 0 |
| *continued* | **N** | **%** |
| **Tamoxifen**[1] | | |
| No | 273 | 57 |
| Yes | 9 | 2[2] |
| Missing | 198 | 41 |
| **Histological grade** | | |
| I | 70 | 15 |
| II | 145 | 30 |
| III | 255 | 53 |
| Missing | 10 | 2 |
| **ER status** | | |
| Positive | 288 | 60 |
| Negative | 180 | 38 |
| Missing | 12 | 3 |
| **PgR status** | | |
| Positive | 223 | 46 |
| Negative | 241 | 50 |
| Missing | 16 | 3 |

[1] During the period of time in which these trials were conducted, tamoxifen was not routinely given to premenopausal patients with estrogen receptor positive tumors. [2] All patients who received tamoxifen had ER-positive tumors. ER, estrogen receptor; PgR, progesterone receptor.

receive chemotherapy were node positive. Characteristics related to adjuvant systemic chemotherapy treatment are listed in Table 2. At the time of the analysis, the median follow-up was 7.3 years, 106 (22%) patients had died, and 155 (32%) patients developed a distant recurrence or died. The distribution of events stratified by ER status is listed in Table 3.

**Table 3.** Distribution of events according to ER status and chemotherapy[1]

| | No adjuvant chemotherapy | | Adjuvant chemotherapy | |
|---|---|---|---|---|
| | **N** | **%** | **N** | **%** |
| **Deaths** (number of events = 106) | | | | |
| ER positive | 19 | 18 | 35 | 33 |
| ER negative | 29 | 27 | 19 | 18 |
| **Distant metastasis or death** (number of events = 155) | | | | |
| ER positive | 37 | 24 | 54 | 35 |
| ER negative | 38 | 25 | 21 | 14 |

[1]Missing data not shown. ER, estrogen receptor.

**Table 2.** Patient and tumor characteristics specified by adjuvant chemotherapy[1]

| Characteristic | No adjuvant chemotherapy (N = 279) | | Adjuvant chemotherapy (N = 200) | |
|---|---|---|---|---|
| | N | % | N | % |
| **ER status** | | | | |
| Positive | 161 | 58 | 126 | 63 |
| Anthracycline-based | | | 66 | |
| CMF | | | 60 | |
| Negative | 110 | 39 | 70 | 35 |
| Anthracycline-based | | | 48 | |
| CMF | | | 22 | |
| **PgR status** | | | | |
| Positive | 135 | 48 | 88 | 44 |
| Negative | 135 | 48 | 105 | 53 |
| **Tumor size** | | | | |
| < 2 cm | 187 | 67 | 105 | 53 |
| > 2 cm | 76 | 27 | 75 | 38 |
| **Nodal status** | | | | |
| Negative | 259 | 93 | 29 | 15 |
| Positive | 18 | 6 | 170 | 85 |
| **Surgery** | | | | |
| Breast conserving | 247 | 89 | 146 | 73 |
| Mastectomy | 32 | 11 | 53 | 27 |

[1]Missing data not shown. ER, estrogen receptor; CMF, cyclophosphamide, methotrexate, and 5-fluorouracil; PgR, progesterone receptor.

## Overall results

### *Estrogen receptor status*

Overall, patients with ER positive tumors had better OS rates compared with ER negative patients (hazard ratio (HR) = 0.63, 95% CI = 0.43 to 0.93, $P$ = .02; Figure 1A). Survival rates at 7 years were 82% for the ER positive group and 77% for the ER negative group. DMFS rates were 70% for the ER positive group and 66% for the ER negative group (HR = 0.90, 95% CI = 0.65 to 1.24, $P$ = .51; Figure 1B).

### *Progesterone receptor status*

PgR status yielded similar results: patients with PgR positive tumors had better OS (HR = 0.59, 95% CI = 0.40 to 0.88, $P$ = .01). However, for DMFS this difference was not of statistical significance (HR = 0.78, 95% CI = 0.57 to 1.01, $P$ = .14).

**Patients who did not receive prolonged adjuvant chemotherapy**

*Estrogen receptor status*

In patients who did not receive adjuvant systemic chemotherapy, positive ER status was associated with better OS (HR = 0.41, 95% CI = 0.23 to 0.74, $P < .01$; Figure 1C). Survival rates at 7 years were 90% for the ER positive group and 77% for the ER negative group. Also, DMFS rates at 7 years were significantly better for ER positive patients: 80% versus 64% (HR = 0.59, 95% CI = 0.37 to 0.92, $P = .02$; Figure 1D).

*Progesterone receptor status*

In patients who did not receive adjuvant systemic chemotherapy, positive PgR status was associated with better OS (HR = 0.44, 95% CI = 0.24 to 0.80, $P < .01$). Survival rates at 7 years were 88% for the PgR positive group and 75% for PgR negative group. DMFS rates at 7 years were 79% for PgR positive patients and 67% for PgR negative patients (HR = 0.66, 95% CI = 0.42 to 1.04, $P = .07$).

**Patients who received prolonged adjuvant systemic chemotherapy**

*Estrogen receptor status*

In the group of 200 patients who did receive adjuvant systemic chemotherapy, treatment outcome was not significantly different between ER positive and ER negative breast cancer patients. Survival rates at 7 years were 70% for the ER positive group and 75% for the ER negative group (HR = 0.87, 95% CI = 0.50 to 1.52, $P = .63$; Figure 1E), and DMFS rates were 59% for the ER positive group and 70% for the ER negative group (HR = 1.36, 95% CI = 0.82 to 2.26, $P = .23$; Figure 1F). No further subgroup analyses specified by type of chemotherapy were performed since these groups would have had insufficient numbers and events.

*Progesterone receptor status*

According to PgR status, no difference in treatment outcome for patients who have received adjuvant systemic chemotherapy was found. In both the PgR positive and PgR negative patient groups, the survival rate at 7 years was 72% (HR 0.84, 95% CI 0.49 to 1.43; $P = .51$). Also, DMFS rates did not differ significantly between the PgR positive group (59%) and the PgR negative group (64%; HR 1.02, 95% CI 0.65 to 1.60; $P = .93$).

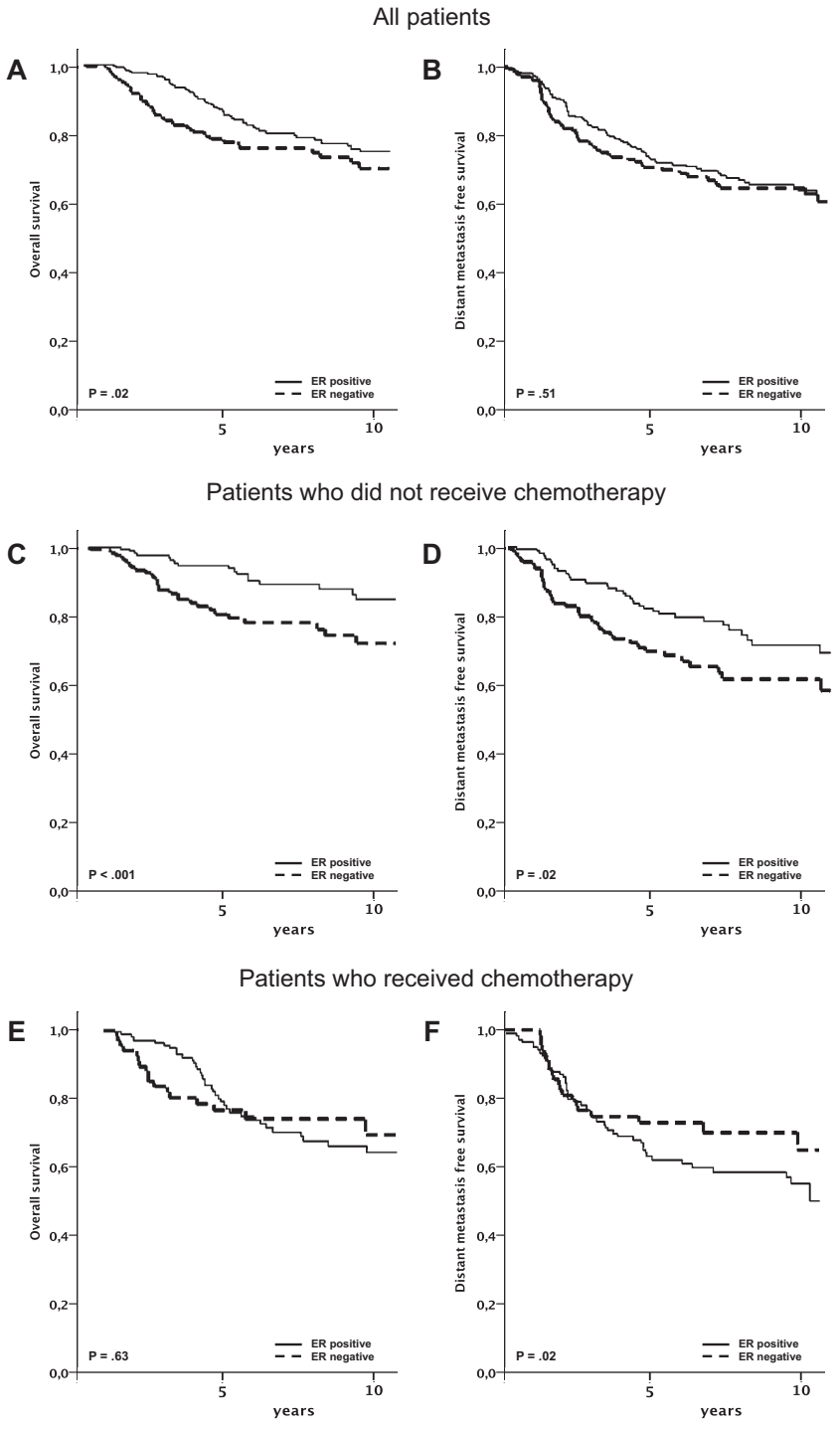


**Figure 1.** Overall and distant disease-free survival for all patients (A, B), patients who did not receive adjuvant chemotherapy (C, D) and patients who received chemotherapy (E, F) according to estrogen recepter status.

### Multivariate analysis

Multivariate Cox regression OS analyses were performed separately for ER status and PgR status. Other covariates included nodal status, tumor size, and the administration of prolonged adjuvant chemotherapy. Both ER status (relative risk (RR) = 1.65) and PgR status (RR = 1.56; data not shown) remained independent prognostic factors with a significant impact on OS (Table 4).

**Table 4.** Multivariate Cox regression analysis of overall survival

| Characteristic | Relative risk | 95% CI | *P* |
|---|---|---|---|
| **ER negative** | 1.65 | 1.09-2.50 | .02 |
| **Node positive** | 1.70 | 0.79-3.66 | .17 |
| **Tumor size > 2 cm** | 1.66 | 1.09-2.52 | .02 |
| **Adjuvant chemotherapy** | 1.02 | 0.48-2.17 | .96 |

ER, estrogen receptor.

## DISCUSSION

This pooled analysis of patients 40 years old or younger demonstrated that hormone receptor positive patients experienced no survival advantage of prolonged adjuvant CMF chemotherapy compared with hormone receptor negative patients. However, in patients who did not receive adjuvant chemotherapy, hormone receptor positive status was associated with improved survival rates compared with hormone receptor negative status. In overall multivariate analyses, both ER positive status and PgR positive status remained independent prognostic factors of overall survival.

Our study has some limitations. First, the current analysis retrospectively uses heterogeneous data from different randomized trials. Second, adjuvant CMF chemotherapy to a large extent has been replaced by anthracycline-containing chemotherapeutic regimens because of higher treatment efficacy in patients with breast cancer regardless of hormone receptor or menopausal status.[1] Also, taxanes are increasingly being used, showing additional survival benefits. Therefore, different effects might have been demonstrated when newer chemotherapy regimens were used throughout the included studies. Third, the direct comparison between administration of chemotherapy versus no chemotherapy in hormone receptor positive and hormone receptor negative patients would have been very interesting. However, the confounding effect of axillary lymph node status would have introduced a significant selection bias because the majority of patients who received chemotherapy had positive axillary lymph nodes. Nevertheless, in multivariate analysis including axillary lymph node status, tumor size, and the administration of prolonged adjuvant chemotherapy, hormone receptor status remained an independent prognostic factor for OS. Fourth, the survival curves of the ER positive and ER negative group depicted in Figure 1E (overall survival in patients receiving chemotherapy) are crossing. This implies that that the proportional

hazards assumption is not justified. The rapid decrease in survival benefit after a couple of years in the ER positive group may well be explained by the chemotherapy-induced amenorrhea and the associated low estrogen levels. Unfortunately, no information on the number of patients who have become amenorrheatic could be retrieved in order to test this hypothesis. Despite these limitations, this pooled analysis of four randomized controlled trials used individual patient data with renewed pathological analysis of hormone receptor status. Because less than 5% of the study population received tamoxifen, the effect of chemotherapy alone in hormone receptor positive patients could be well studied. By assessing hormone receptor status centrally, we have provided standardized measurements for all tumors in the study.

Adjuvant systemic chemotherapy is a well-established treatment modality in premenopausal breast cancer. In patients 35 years old or younger, administration of chemotherapy is advocated regardless of nodal status, tumor size, or grade.[3] However, the efficacy of chemotherapy in premenopausal patients with ER positive breast cancer has been questioned.[5] Our findings are in accordance with data from Aebi and colleagues,[5] who demonstrated that young premenopausal patients with breast cancer treated with adjuvant CMF chemotherapy had a higher risk of relapse and death than older premenopausal patients, especially if their tumors were ER positive. In addition, several neoadjuvant chemotherapy studies have demonstrated that patients with ER negative tumors are more likely to achieve a pathological complete response than those with ER positive tumors.[15-17] Moreover, these studies found that when patients with ER negative tumors achieved a pathological complete response their survival was comparable with that of ER positive patients.

To optimize adjuvant systemic treatment in premenopausal patients with breast cancer, several investigators have studied the role of ovarian suppression by luteinizing hormone-releasing hormone (LHRH) agonists. Recently, the Early Breast Cancer Overview group reported a meta-analysis of individual patient data on the use of LHRH agonists.[18] When chemotherapy alone was compared with chemotherapy in combination with an LHRH agonist, a difference between younger and older premenopausal women with hormone receptor positive disease was found. In patients 40 years old or younger, the addition of an LHRH agonist significantly reduced the risk of recurrence and death (HR = 0.74, $P = .01$). This effect was greatest in the group age younger than 35 years, whereas in the group older than 40 years, the addition of an LHRH agonist did not improve outcome. When chemotherapy alone was compared with LHRH agonist with or without tamoxifen in younger premenopausal patients with hormone receptor positive tumors, the endocrine therapy improved outcome (mortality HR = 0.82, $P = .15$). Conversely, in hormone receptor negative patients, the same comparison significantly favored treatment with chemotherapy (62.1% increased rate of recurrence or death; $P = .003$). To date, no trial has compared an LHRH agonist against chemotherapy with tamoxifen in both arms. This relevant and important issue

needs to be resolved. Although these results underline the fact that chemotherapy may be equivalent to hormonal ovarian suppression in terms of treatment outcome in hormone receptor positive patients, these results firmly demonstrate a beneficial effect of LHRH agonists as additional therapy, especially in young patients with breast cancer.

Three important ongoing trials are specifically investigating ovarian function suppression (Suppression of Ovarian Function Trial, or SOFT), an aromatase inhibitor (Tamoxifen and EXemestane Trial, or TEXT), and the need for chemotherapy (Premenopausal Endocrine Responsive CHEmotherapy, or PERCHE) in adjuvant treatment for young patients with hormone receptor-positive breast cancer.[19]

The 2005 St. Gallen Consensus Committee on adjuvant therapy for early-stage breast cancer recommended that the first consideration in treatment selection be endocrine responsiveness.[20] Three categories are identified: endocrine responsive, endocrine nonresponsive, and tumors of uncertain endocrine responsiveness. These categories refer to the groups of tumors that are responsive to endocrine therapies alone, chemotherapy alone, and chemotherapy and endocrine therapy combinations, respectively. The 2005 Panel viewed tamoxifen as a standard adjuvant treatment for premenopausal endocrine responsive patients. The combination of tamoxifen with an LHRH agonist is recommended for very young patients, especially in intermediate- and high-risk groups, and for premenopausal patients of any age at high risk, especially if chemotherapy did not induce amenorrhea. The use of aromatase inhibitors in premenopausal patients is not recommended outside of clinical trials, except when tamoxifen is contraindicated, especially in node positive disease. Chemotherapy in addition to hormone therapy is advised for endocrine responsive patients with node positive disease.

In this retrospective pooled analysis of four studies using heterogeneous chemotherapy regimens, we have demonstrated that treatment efficacy of adjuvant chemotherapy is less in young patients with hormone receptor positive tumors compared with young patients with hormone receptor negative tumors. Therefore, we conclude that chemotherapy alone is not a sufficient systemic treatment strategy in young patients with hormone receptor positive breast cancer. Hormone responsiveness is the key for tailoring therapy for young patients with breast cancer.

## REFERENCES

1. Early Breast Cancer Trialists' Collaborative G. Effects of chemotherapy and hormonal therapy for early breast cancer on recurrence and 15-year survival: an overview of the randomised trials. Lancet 2005; 365:1687-717.
2. Hankey BF, Miller B, Curtis R, et al. Trends in breast cancer in younger women in contrast to older women. J Natl Cancer Inst Monogr 1994:7-14.
3. Goldhirsch A, Gelber RD, Yothers G, et al. Adjuvant therapy for very young women with breast cancer: need for tailored treatments. J Natl Cancer Inst Monogr 2001:44-51.

4. Elkhuizen PH, van Slooten HJ, Clahsen PC, et al. High local recurrence risk after breast-conserving therapy in node-negative premenopausal breast cancer patients is greatly reduced by one course of perioperative chemotherapy: A European Organization for Research and Treatment of Cancer Breast Cancer Cooperative Group Study. J Clin Oncol 2000; 18:1075-83.
5. Aebi S, Gelber S, Castiglione-Gertsch M, et al. Is chemotherapy alone adequate for young women with oestrogen-receptor-positive breast cancer? Lancet 2000; 355:1869-74.
6. van Dongen JA, Voogd AC, Fentiman IS, et al. Long-term results of a randomized trial comparing breast-conserving therapy with mastectomy: European Organization for Research and Treatment of Cancer 10801 trial. J Natl Cancer Inst 2000; 92:1143-50.
7. van der Hage JA, van de Velde CJH, Julien JP, et al. Improved survival after one course of perioperative chemotherapy in early breast cancer patients. long-term results from the European Organization for Research and Treatment of Cancer (EORTC) Trial 10854. Eur J Cancer 2001; 37:2184-93.
8. van der Hage JA, van de Velde CJH, Julien JP, et al. Preoperative chemotherapy in primary operable breast cancer: results from the European Organization for Research and Treatment of Cancer trial 10902. J Clin Oncol 2001; 19:4224-37.
9. Bartelink H, Horiot JC, Poortmans P, et al. Recurrence rates after treatment of breast cancer with standard radiotherapy with or without additional radiation. N Engl J Med 2001; 345:1378-87.
10. Elston CW, Ellis IO. Pathological prognostic factors in breast cancer. I. The value of histological grade in breast cancer: experience from a large study with long-term follow-up. Histopathology 1991; 19:403-10.
11. Bubendorf L, Nocito A, Moch H, et al. Tissue microarray (TMA) technology: miniaturized pathology archives for high-throughput in situ studies. J Pathol 2001; 195:72-9.
12. Hoos A, Urist MJ, Stojadinovic A, et al. Validation of tissue microarrays for immunohistochemical profiling of cancer specimens using the example of human fibroblastic tumors. Am J Pathol 2001; 158:1245-51.
13. Mueller-Holzner E, Fink V, Frede T, et al. Immunohistochemical determination of HER2 expression in breast cancer from core biopsy specimens: a reliable predictor of HER2 status of the whole tumor. Breast Cancer Res Treat 2001; 69:13-9.
14. Kallioniemi OP, Wagner U, Kononen J, et al. Tissue microarray technology for high-throughput molecular profiling of cancer. Hum Mol Genet 2001; 10:657-62.
15. Ring AE, Smith IE, Ashley S, et al. Oestrogen receptor status, pathological complete response and prognosis in patients receiving neoadjuvant chemotherapy for early breast cancer. Br J Cancer 2004; 91:2012-7.
16. Colleoni M, Viale G, Zahrieh D, et al. Chemotherapy is more effective in patients with breast cancer not expressing steroid hormone receptors: a study of preoperative treatment. Clin Cancer Res 2004; 10:6622-8.
17. Kuerer HM, Newman LA, Smith TL, et al. Clinical course of breast cancer patients with complete pathologic primary tumor and axillary lymph node response to doxorubicin-based neoadjuvant chemotherapy. J Clin Oncol 1999; 17:460-9.
18. Cuzick J, Ambroisine L, Davidson N, et al. Use of luteinising-hormone-releasing hormone agonists as adjuvant treatment in premenopausal patients with hormone-receptor-positive breast cancer: a meta-analysis of individual patient data from randomised adjuvant trials. Lancet 2007; 369:1711-23.
19. Jonat W, Pritchard KI, Sainsbury R, et al. Trends in endocrine therapy and chemotherapy for early breast cancer: a focus on the premenopausal patient. J Cancer Res Clin Oncol 2006; 132:275-86.
20. Goldhirsch A, Glick JH, Gelber RD, et al. Meeting highlights: international expert consensus on the primary therapy of early breast cancer 2005. Ann Oncol 2005; 16:1569-83.

# Chapter 5

# Impact of established prognostic factors and molecular subtype in very young breast cancer patients: pooled analysis of four EORTC randomized controlled trials

van der Hage JA[1], Mieog JSD[1], van de Velde CJH, Putter H, Bartelink H, van de Vijver MJ.

[1] Shared first authorship

*Breast Cancer Res 2011; 13:R68*

## ABSTRACT

### Introduction

Young age at the time of diagnosis of breast cancer is an independent factor of poor prognosis. In many treatment guidelines, the recommendation is to treat young patients with adjuvant chemotherapy regardless of tumor characteristics. However, limited data on prognostic factors are available for young breast cancer patients. The purpose of this study was to determine the prognostic value of established clinical and pathological prognostic factors in young breast cancer patients.

### Methods

Data from four European Organisation for Research and Treatment of Cancer (EORTC) clinical trials were pooled, resulting in a dataset consisting of 9,938 early breast cancer patients with a median follow-up of 11 years. For 549 patients aged less than 40 years at the time of diagnosis, including 341 node negative patients who did not receive chemotherapy, paraffin tumor blocks were processed for immunohistochemistry using a tissue microarray. Cox proportional hazard analysis was applied to assess the association of clinical and pathological factors with overall and distant metastasis free survival.

### Results

For young patients, tumor size ($P = .01$), nodal status ($P = .006$) and molecular subtype ($P = .02$) were independent prognostic factors for overall survival. In the node negative subgroup, only molecular subtype was a prognostic factor for overall survival ($P = .02$). Young node negative patients bearing luminal A tumors had an overall survival rate of 94% after 10 years follow-up compared to 72% for patients with basal-type tumors.

### Conclusion

Molecular subtype is a strong independent prognostic factor in breast cancer patients younger than 40 years of age. These data support the use of established prognostic factors as a diagnostic tool to assess disease outcome and to plan systemic treatment strategies in young breast cancer patients.

## INTRODUCTION

The incidence of early stage breast cancer in young women is increasing. At present, breast cancer at a young age, that is, less than 40 years, accounts for approximately 5 to 7.5% of the total number of cases diagnosed each year in Western Europe and the US.[1-3] Based upon multiple retrospective analyses that demonstrated the unfavorable impact of young age on prognosis in breast cancer, several current consensus guidelines have included age under 35 years as an absolute indication for adjuvant systemic chemotherapy irrespective of other tumor characteristics.[4-6] These guidelines imply that for young patients with favorable tumor features such as small tumor size and negative axillary nodal status, adjuvant chemotherapy and hormonal therapy for patients with hormone receptor positive tumors is advised although absolute treatment benefits are not well known. Moreover, the long-term toxicity of adjuvant chemotherapy and the implications of possible fertility impairment and premature menopause are of particular concern in young women.[7] In addition to an increased risk of developing distant metastases, local recurrence rates after mastectomy or breast conserving therapy are also higher than in older patients,[5] and although an additional boost dose of radiotherapy after breast-conserving surgery decreases the risk of local recurrence especially in young women,[8] these loco-regional recurrence rates are still significantly higher compared with mastectomy in young patients.

Retrospective analyses have demonstrated breast cancer at a very young age to be associated with higher grade, estrogen receptor negative tumors, a more advanced stage of disease at the time of diagnosis, and the presence of BRCA-1 or -2 germline mutations.[9-13] Recent gene expression profiling studies showed that tumors of young women showed a higher probability of PI3K, Myc, and β-catenin deregulation and lower mRNA levels of estrogen receptor-α, estrogen receptor-β and progesterone receptor, but higher levels of HER2, and epidermal growth factor receptor.[14, 15]

More refined knowledge of prognostic factors in young breast cancer patients will be of use in guiding therapy, including adjuvant chemotherapy, in these women. The prognostic value of molecular subtype based on immunohistochemistry is uncertain within the group of young breast cancer patients. Therefore, we pooled the data of four randomized European Organisation for Research and Treatment of Cancer (EORTC) early stage breast cancer trials and collected and characterized tumor material of patients younger than 40 years in order to perform multivariate prognostic factor analyses.

# MATERIAL AND METHODS

## Study cohort

The data used in this study were obtained from four randomized phase III EORTC clinical trials that included patients with early stage breast cancer. The trials randomized between two types of loco-regional therapy and between different timing of the same type of systemic therapy. The detailed features of these trials have been described in detail previously.[16-19] The trial protocols are summarized below:

EORTC trial 10801 (1980 to 1986, median follow-up 13.4 years) was conducted in order to assess the safety of breast conserving treatment. Patients were randomized between breast conserving surgery combined with radiotherapy and modified radical mastectomy. Six cycles of adjuvant chemotherapy with cyclophosphamide 100 mg/m$^2$ given orally on days 1 to 14, methotrexate 40 mg/m$^2$ given intravenously on Days 1 and 8, and 5-fluorouracil 600 mg/m$^2$ (CMF) given intravenously on Days 1 and 8, were indicated for all node positive patients under the age of 55. No information was collected on hormonal therapy. A total number of 902 patients were randomized of which 113 patients aged less than 40 years at the time of diagnosis.[16]

EORTC trial 10854 (1986 to 1991, median follow-up 10.8 years) studied the question of whether one course of peri-operative chemotherapy given directly after surgery yields better results in terms of treatment outcome than surgery alone. Peri-operative chemotherapy consisted of one single course of doxorubicin 50 mg/m$^2$, 5-fluorouracil 600 mg/m$^2$, and cyclophosphamide 600 mg/m$^2$ (FAC), administered intravenously within 36 hours after surgery. Node positive premenopausal patients in the peri-operative chemotherapy group were recommended to receive an additional five cycles of CMF. Node positive premenopausal patients in the surgery alone group were advised to receive one conventional course of FAC followed by five cycles of CMF. Prolonged adjuvant systemic treatment was left to the discretion of the local investigators. A total number of 2,795 patients were included of which 396 patients aged less than 40 years at time of diagnosis.[17]

EORTC trial 10902 (1991 to 1999, median follow-up 10 years) was set up to compare pre-operative adjuvant chemotherapy with postoperative chemotherapy. Chemotherapy consisted of four cycles of 5-fluorouracil 600 mg/m$^2$, epirubicin 60 mg/m$^2$, and cyclophosphamide 600 mg/m$^2$ (FEC) administered intravenously, at three-weekly intervals. A total number of 698 patients were randomized of which 125 patients aged less than 40 years at time of diagnosis.[18, 20]

EORTC trial 22881 (1989 to 1996, median follow-up 10.8 years) studied the value of a boost dose after primary breast conserving surgery. Patients with stage I or II breast cancer who had undergone microscopically complete surgical removal of the tumor and axillary dissection were randomly assigned to undergo 50 Gy irradiation of

the whole breast with or without an additional dose of 16 Gy to the tumor bed. Patients with a microscopically incomplete excision were assigned to receive booster doses of 10 or 26 Gy. Patients with axillary lymph node involvement received adjuvant systemic therapy: premenopausal patients received chemotherapy (CMF, FEC, or FAC), and postmenopausal patients received tamoxifen. A total number of 5,569 patients were randomized of which 558 patients aged less than 40 years at time of diagnosis.[8, 19]

Adjuvant hormonal therapy for premenopausal hormone receptor positive patients was not yet recommended at the time these trials were conducted. In the oldest two trials, tamoxifen administration was not even recorded. In the trials where tamoxifen use was recorded, less than 5% of patients under 40 years received tamoxifen. Therefore, we assumed that only a very small fraction of the young patients in these studies received tamoxifen.

**Collection of tumor material and immunohistochemistry**

A request was sent to participating institutions to submit paraffin blocks containing a representative part of the tumor from all patients aged less than 40 years at the time of diagnosis except for those who had participated in EORTC trial 10902 and received neoadjuvant chemotherapy (this group of patients was excluded for this study to avoid the influence of down-staging by preoperative chemotherapy). Tumor tissue was collected and processed for immunohistochemistry using a tissue microarray. Three core biopsies of 0.6 mm were taken from every tumor specimen and placed in a so-called donor block. This procedure has been described previously.[21-24] A representative standard histological section from each individual tumor was stained with H&E to assess tumor type, to perform histological grading according to Elston and Ellis, and to assess the presence and extent of lymphangio invasion (none versus one to five versus more than five vessels).[25] ER, PgR, HER2 and P53 expression levels were assessed using immunohistochemistry. Detailed procedures have been described previously.[26-28] In summary, a tissue microarray slide was stained and scored counting the percentage of positive cells and taking the mean value of the three tumor biopsies. For ER expression, tumors with >1% of the tumor cells showing nuclear staining were considered positive. For PgR expression, tumors with >10% of the tumor cells showing nuclear staining were considered positive. For P53 accumulation, a semi-quantitative system was used based on the sum of the mean staining intensity (0 to 3; none to strong) and an estimation of the percentage of positive cell nuclei (0 to 4; 0% to >75%); this allowed a sum score of 0 to 7, with staining ≥4 being considered positive.[26, 27] HER2 expression was scored estimating the level of membranous staining (0, 1+, 2+, or 3+). Strong membranous staining in >30% of tumor cells (3+) was considered positive. The molecular breast cancer subtypes were approximated using histological grade and the ER, PgR, and HER2 status of the primary tumor. Patients were categorized as follows: luminal A (ER+ or PgR+ and HER2- and grade 1 or 2), luminal B (ER+ or PgR+ and

**Table 1.** Characteristics of study participants

| Characteristic | All patients (N = 549) | | Node negative (N = 341) | |
|---|---|---|---|---|
| | N | % | N | % |
| Age distribution | | | | |
| <30 years | 57 | 10 | 40 | 12 |
| 31 to 35 years | 178 | 32 | 107 | 31 |
| 35 to 40 years | 314 | 58 | 194 | 57 |
| Pathological tumor size | | | | |
| T1a-b | 37 | 7 | 30 | 10 |
| T1c | 296 | 60 | 241 | 64 |
| T2 | 158 | 32 | 82 | 26 |
| T3 | 6 | 1 | 2 | 1 |
| Missing | 32 | | 26 | |
| **Surgery** | | | | |
| Breast conserving | 446 | 81 | 299 | 88 |
| Mastectomy | 102 | 19 | 42 | 12 |
| **Adjuvant chemotherapy**[1] | | | | |
| No | 326 | 60 | 304 | 89 |
| Yes | 221 | 40 | 37 | 11 |
| **ER status** | | | | |
| Positive | 310 | 66 | 115 | 41 |
| Negative | 158 | 34 | 165 | 59 |
| Missing | 81 | | 61 | |
| **PgR status** | | | | |
| Positive | 223 | 48 | 141 | 51 |
| Negative | 241 | 52 | 136 | 49 |
| Missing | 85 | | 64 | |
| **Tumor type** | | | | |
| Ductal | 497 | 96 | 306 | 96 |
| Lobular | 17 | 3 | 10 | 3 |
| Other | 5 | 1 | 4 | 1 |
| Missing | 30 | | 21 | |
| **Histological grade** | | | | |
| I | 76 | 15 | 54 | 17 |
| II | 165 | 32 | 93 | 29 |
| III | 276 | 53 | 172 | 54 |
| Missing | 32 | | 22 | |
| **Lymphangio invasion** | | | | |
| None | 357 | 69 | 243 | 76 |
| 1-5 vessels | 86 | 17 | 49 | 15 |
| > 5 vessels | 76 | 14 | 27 | 9 |
| Missing | 30 | | 22 | |
| **HER2 status** | | | | |
| Negative | 346 | 74 | 216 | 63 |
| Positive | 119 | 26 | 64 | 19 |
| Missing | 84 | | 61 | |
| **P53 status** | | | | |
| Negative | 331 | 71 | 198 | 72 |
| Positive | 133 | 29 | 78 | 28 |
| Missing | 85 | | 65 | |

| *continued* | All patients (N = 549) | | Node negative (N = 341) | |
|---|---|---|---|---|
| | N | % | N | % |
| **Molecular subtype** | | | | |
| Luminal A | 154 | 34 | 79 | 29 |
| Luminal B | 157 | 34 | 86 | 32 |
| HER-2 | 35 | 8 | 90 | 34 |
| Basal (triple-negative) | 111 | 24 | 14 | 5 |
| Missing | 92 | | 72 | |

[1] EORTC trial 10854 randomized between one course of peri-operative chemotherapy which was not considered as prolonged chemotherapy. ER, estrogen receptor; HER2, human epidermal growth factor receptor 2; PgR, progesterone receptor.

HER2+; or ER+ or PgR+ and HER2- and grade 3), HER2 (ER- and PgR- and HER2+), and basal type (ER- and PgR- and HER2-). Estimations of tumor grade and protein expression levels were scored by two investigators (MJV and JAH) simultaneously who had to come to an agreement in case of different views.

## Statistical analyses

Data analysis was performed at the Leiden University Medical Center using SPSS for Mac (version 18.0; SPSS, Chicago, IL, USA). The $\chi^2$ test was used to compare the distribution of baseline characteristics among groups. Endpoints studied were overall survival and distant metastasis free survival. Overall survival time was defined as the time between randomization and death from any cause. Distant metastasis free survival time was defined as time to distant metastasis or death if the latter event occurred before a distant metastasis was diagnosed. Survival analyses were performed using the Kaplan Meier method. Covariates included patient age, and tumor- and treatment related characteristics. Tumor characteristics were tumor size, nodal status, histological grade, hormone receptor status, HER2 status, P53 status, molecular subtype and lymphangio invasion. Treatment characteristics were type of surgery and administration of chemotherapy. Tamoxifen use was not included because of the high rate of missing data for this variable. Cox proportional hazard regression models were used to estimate hazard ratios (HR) with 95% confidence intervals (CI). A multivariate Cox regression model was fitted that was based on all characteristics that had a *P*-value up to .10 in the univariate analysis. Variables determining molecular subtype were not included in multivariate analyses if molecular subtype was included. A 5% significance level was used and all tests are two-sided.

# RESULTS

## Prognostic factors in young patients

A total of 9,938 early stage breast cancer patients participated in the four trials. Of this dataset, 1,192 (12%) patients were aged less than 40 years at the time of diagnosis. Paraffin embedded tumor material was obtained and processed into a tissue microarray for 549 patients aged less than 40 years (Table 1). Median age of these patients was 36.8 years. Tumors were subdivided according to molecular subtype: 111 patients (24%) aged less than 40 years had triple-negative tumors, 154 (34%) patients had luminal A tumors, 157 (34%) had luminal B tumors and 35 (8%) had HER2 tumors. Twenty-nine percent of tumors were P53 positive (Table 1). At time of analysis, 143 of 549 patients had died and 64 patients had developed distant metastases and were still alive.

At univariate analysis, pathological tumor size, nodal status, histological grade, lymphangio invasion, progesterone receptor status, molecular subtype, type of surgery and adjuvant chemotherapy were significantly associated with overall and distant metastasis free survival (Supplementary Table 1). HER2 and P53 status did not show an association with overall or distant metastasis free survival and were not included at subsequent multivariate analysis. At multivariate analysis (Table 2), pathologic tumor size, nodal status, and molecular subtype remained the only independent prognostic factors for both overall survival and distant metastasis free survival. For distant metastasis free survival, molecular subtype was a trend-significant prognostic factor ($P = .06$; Table 2).

**Table 2.** Multivariate analysis of prognostic factors in 549 patients aged less than 40 years

| Characteristic | Overall survival | | | Distant disease-free survival | | |
|---|---|---|---|---|---|---|
| | HR | 95% CI | *P* | HR | 95% CI | *P* |
| **pT2 + pT3** | 1.68 | 1.12-2.52 | 0.01 | 1.61 | 1.14-2.25 | 0.006 |
| **Lymph node positive** | 2.62 | 1.31-5.23 | 0.006 | 2.21 | 1.24-3.96 | 0.008 |
| **Lymphangio invasion** | | | 0.75 | | | 0.73 |
| No vessels | 1 | | | 1 | | |
| 1 to 5 vessels | 0.93 | 0.53-1.62 | | 0.97 | 0.61-1.53 | |
| >5 vessels | 1.18 | 0.71-1.97 | | 1.17 | 0.75-1.83 | |
| **Molecular subtype** | | | 0.02 | | | 0.06 |
| Basal | 1 | | | 1 | | |
| Luminal A | 0.50 | 0.29-0.86 | | 0.69 | 0.44-1.08 | |
| HER2 | 0.42 | 0.17-1.04 | | 0.45 | 0.21-0.99 | |
| Luminal B | 0.92 | 0.56-1.48 | | 1.01 | 0.67-1.53 | |
| **Breast conserving therapy** | 0.76 | 0.47-1.24 | 0.27 | 0.81 | 0.53-1.23 | 0.33 |
| **Adjuvant chemotherapy** | 0.68 | 0.35-1.33 | 0.26 | 0.65 | 0.37-1.13 | 0.13 |

HR, hazard ratio; CI, confidence interval

**Prognostic factors in young node negative patients**

The subgroup of node negative patients aged less than 40 years consisted of 640 patients. Of 341 patients, tumor material was available for analysis (Table 1). Of these node negative patients, 304 (89%) patients did not receive adjuvant chemotherapy.

At univariate analysis, pathological tumor size, histological grade, ER status and molecular subtype were significantly associated with overall survival and distant metastasis free survival (Supplementary Table 2). In addition, PgR status and the administration of adjuvant chemotherapy were significantly associated with overall survival. Figure 1 shows the impact of molecular subtype, histological grade and pathological tumor size, respectively, on overall and distant metastasis free survival in the subgroup of node-negative patients aged less than 40 years. Ten-year survival rates for the molecular subtypes were 94% for luminal A, 93% for HER2, 78% for luminal B and 72% for basal (Figure 1). Of note, the overall survival rate for young patients bearing a grade I tumor was 92% at 11 years of follow-up, whereas patients with grade III tumors had a survival rate of 72% (Figure 1).

At multivariate analysis (Table 3), molecular subtype was associated with overall survival (overall $P = .02$; basal subtype versus luminal A subtype: HR = 0.22, 95% CI = 0.08 to 0.60, $P = .003$) and distant metastasis free survival (overall $P = .08$; basal subtype versus luminal A subtype: HR = 0.46, 95% CI = 0.25 to 0.85, $P = .013$).

## DISCUSSION

In this study, we performed a retrospective pooled analysis to gain further insight into tumor characteristics of young breast cancer patients. In young patients, molecular subtype was the strongest prognostic factor of the covariates studied, distinguishing young patients with a favorable prognosis from young patients with an unfavorable prognosis.

In our study, young node negative patients with luminal A and HER2 tumors had excellent long-term overall survival rates of 94% and 93%, respectively, and distant disease-free survival rates of 83% and 79%, respectively, at 10-year follow-up (Figure 1). Of note, only 3 out of 86 young node negative patients with luminal A tumors received adjuvant chemotherapy. Therefore, these data suggest that molecular subtype can be utilized in adjuvant treatment planning in young node negative patients. Recently, Cancello *et al*. showed that very young patients with basal, luminal B or HER2, but not luminal A breast cancer have a worse prognosis when compared with older patients with similar characteristics of disease.[29]

Several authors have previously described the independent prognostic role of histological grade in young breast cancer patients. Sundquist *et al.* showed that patients bearing histological grade III tumors had a poor overall survival of 41% at the 11-year follow-up in a Swedish cohort of 107 patients aged less than 40 years.[30]

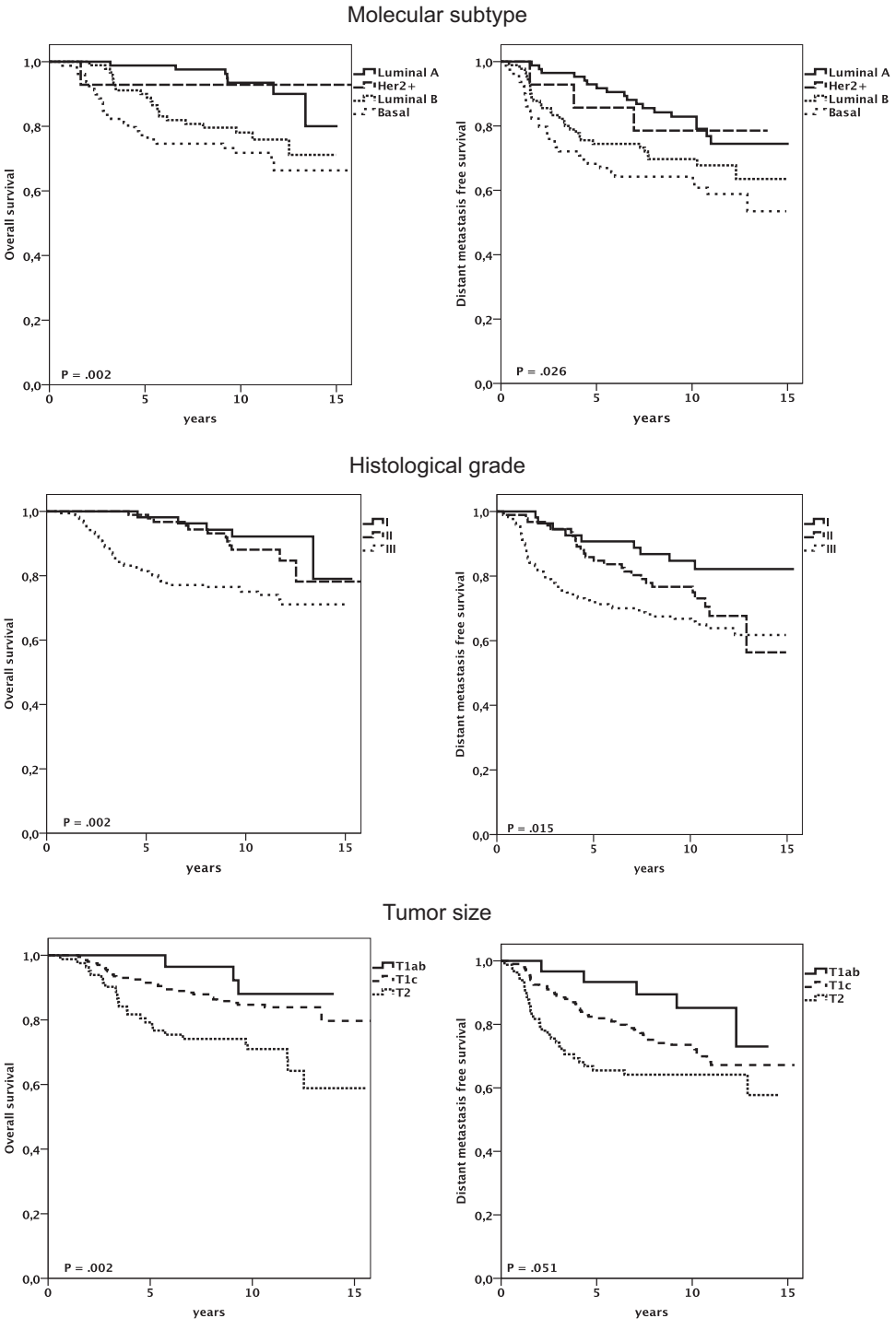


**Figure 1.** Overall and distant disease free survival for node negative patients aged less than 40 years stratified by molecular subtype, histological grade and tumor size.

Although histological grade was associated with overall survival, it did not reach statistical significance (Grade I versus III: HR = 4.19; 95% CI = 0.91 to 19.5). Kollias *et al.* demonstrated in a cohort of 2,879 patients that the worse prognosis of the age group younger than 35 years (N = 120) was explained by the higher proportion of histological grade III breast cancers in the young group.[31] In a recent study, high histological grade and young age were identified as the most important risk factors for local relapse.[32] Our study suggests that histological grade (as part of molecular subtype) is an important prognostic factor in young breast cancer patients.

Among the established prognostic and predictive factors in young breast cancer patients, the estrogen receptor status is of particular interest. Recently, we showed that adjuvant chemotherapy provides limited survival benefit in hormone receptor positive young breast cancer patients.[33] The Korean Breast Cancer Society recently reported that young age was associated with a greater probability of death in breast cancer patients.[34] When studied in more detail, the survival difference was only found in the hormone receptor positive group.[34] As these data were collected from 1992 onwards, young hormone receptor positive patients received tamoxifen, in contrast to the patients in our study who were treated before adjuvant tamoxifen treatment became a standard in a large proportion of breast cancer patients with hormone receptor positive disease. These observations suggest that tamoxifen therapy might provide less survival benefit in young hormone receptor positive breast cancer patients as compared to older hormone receptor positive breast cancer patients. However, several trials have suggested an equal effect of endocrine therapy as compared to chemotherapy in hormone receptor positive premenopausal breast cancer patients.[35, 36] In our data set of older EORTC trials, young hormone receptor positive patients did not receive hormonal therapy. Notwithstanding, in our study, young patients with luminal A tumors had an excellent prognosis, which might have been augmented with the administration of hormonal therapy.

The current study has a number of limitations. First, the study design was a retrospective analysis of four heterogeneous randomized trials that were not primarily

**Table 3.** Multivariate analysis of prognostic factors in 341 node negative patients aged less than 40 years

| Characteristic | Overall survival | | | Distant disease-free survival | | |
|---|---|---|---|---|---|---|
| | HR | 95% CI | *P* | HR | 95% CI | *P* |
| **pT2 + pT3** | 1.75 | 0.99-3.10 | 0.06 | 1.33 | 0.83-2.15 | 0.24 |
| **Molecular subtype** | | | 0.02 | | | 0.08 |
| Basal | 1 | | | 1 | | |
| Luminal A | 0.22 | 0.08-0.60 | | 0.46 | 0.25-0.85 | |
| HER2 | 0.25 | 0.03-1.85 | | 0.53 | 0.16-1.73 | |
| Luminal B | 0.87 | 0.48-1.59 | | 0.82 | 0.49-1.38 | |
| **Adjuvant chemotherapy** | 0.96 | 0.38-2.45 | 0.94 | | | |

HR, hazard ratio; CI, confidence interval

designed to test differences in outcome between young and old patients. Second, tumor material could not be collected for all patients aged less than 40 years and this could introduce selection bias. However, patient and traditional tumor characteristics were evenly distributed between the group for which tumor blocks were available and the group for which no tumor blocks could be collected (Supplementary Table 3). Third, information on tamoxifen use is largely missing. However, in the trials in which tamoxifen use was recorded, less than 5% of the patients younger than 40 years received tamoxifen. Despite these limitations, the current pooled analysis used individual patient data of four high-quality randomized controlled trials with renewed histopathological analysis to assess prognostic factors in young breast cancer patients. These data provide a robust estimate of the value of prognostic factors in young breast cancer patients. We believe our data justify a more critical view concerning current adjuvant chemotherapy guidelines in young low-risk breast cancer patients.

In conclusion, the established prognostic factors molecular subtype (including hormone receptor status, histological grade and HER2 receptor status), tumor size and nodal status remain independent prognostic factors on disease outcome in young breast cancer patients. In particular, molecular subtype was strongly associated with overall and distant metastasis free survival. Future treatment guidelines concerning young breast cancer patients should be refined based upon tumor characteristics, probably derived from microarray driven translational research projects, and not based upon age alone.[37-39]

## ACKNOWLEGDEMENT

We would like to thank Jan Bogaerts (EORTC, Brussels, Belgium) for his assistance in database construction.

## REFERENCES

1. Winchester DP. Breast cancer in young women. Surg Clin North Am 1996; 76:279-87.
2. Cancer Research UK: News & Resources [http://info.cancerresearchuk.org].
3. Dutch Cancer Centers [http://www.ikcnet.nl].
4. Goldhirsch A, Gelber RD, Yothers G, et al. Adjuvant therapy for very young women with breast cancer: need for tailored treatments. J Natl Cancer Inst Monogr 2001:44-51.
5. de Bock GH, van der Hage JA, Putter H, et al. Isolated loco-regional recurrence of breast cancer is more common in young patients and following breast conserving therapy: long-term results of European Organisation for Research and Treatment of Cancer studies. Eur J Cancer 2006; 42:351-6.
6. Elkhuizen PH, Voogd AC, van den Broek LC, et al. Risk factors for local recurrence after breast-conserving therapy for invasive carcinomas: a case-control study of histological factors and alterations in oncogene expression. Int J Radiat Oncol Biol Phys 1999; 45:73-83.
7. Shannon C, Smith IE. Breast cancer in adolescents and young women. Eur J Cancer 2003; 39:2632-42.

8. Bartelink H, Horiot JC, Poortmans P, et al. Recurrence rates after treatment of breast cancer with standard radiotherapy with or without additional radiation. N Engl J Med 2001; 345:1378-87.
9. Colleoni M, Rotmensz N, Robertson C, et al. Very young women (<35 years) with operable breast cancer: features of disease at presentation. Ann Oncol 2002; 13:273-9.
10. Maggard MA, O'Connell JB, Lane KE, et al. Do young breast cancer patients have worse outcomes? J Surg Res 2003; 113:109-13.
11. Choi DH, Lee MH, Bale AE, et al. Incidence of BRCA1 and BRCA2 mutations in young Korean breast cancer patients. J Clin Oncol 2004; 22:1638-45.
12. Loman N, Johannsson O, Kristoffersson U, et al. Family history of breast and ovarian cancers and BRCA1 and BRCA2 mutations in a population-based series of early-onset breast cancer. J Natl Cancer Inst 2001; 93:1215-23.
13. de Sanjose S, Leone M, Berez V, et al. Prevalence of BRCA1 and BRCA2 germline mutations in young breast cancer patients: a population-based study. Int J Cancer 2003; 106:588-93.
14. Anders CK, Acharya CR, Hsu DS, et al. Age-specific differences in oncogenic pathway deregulation seen in human breast tumors. PLoS ONE 2008; 3:e1373.
15. Anders CK, Hsu DS, Broadwater G, et al. Young age at diagnosis correlates with worse prognosis and defines a subset of breast cancers with shared patterns of gene expression. J Clin Oncol 2008; 26:3324-30.
16. van Dongen JA, Voogd AC, Fentiman IS, et al. Long-term results of a randomized trial comparing breast-conserving therapy with mastectomy: European Organization for Research and Treatment of Cancer 10801 trial. J Natl Cancer Inst 2000; 92:1143-50.
17. van der Hage JA, van de Velde CJH, Julien JP, et al. Improved survival after one course of perioperative chemotherapy in early breast cancer patients. long-term results from the European Organization for Research and Treatment of Cancer (EORTC) Trial 10854. Eur J Cancer 2001; 37:2184-93.
18. van der Hage JA, van de Velde CJH, Julien JP, et al. Preoperative chemotherapy in primary operable breast cancer: results from the European Organization for Research and Treatment of Cancer trial 10902. J Clin Oncol 2001; 19:4224-37.
19. Bartelink H, Horiot JC, Poortmans PM, et al. Impact of a higher radiation dose on local control and survival in breast-conserving therapy of early breast cancer: 10-year results of the randomized boost versus no boost EORTC 22881-10882 trial. J Clin Oncol 2007; 25:3259-65.
20. van Nes JGH, Van Der Hage JA, Bogaerts J, et al. After 10 years of follow-up, preoperative chemotherapy is still safe in operable breast cancer: Clinical and translational results from the European Organisation for Research and Treatment of Cancer Trial 10902. Eur J Cancer 2006; 4:149.
21. Bubendorf L, Nocito A, Moch H, et al. Tissue microarray (TMA) technology: miniaturized pathology archives for high-throughput in situ studies. J Pathol 2001; 195:72-9.
22. Hoos A, Urist MJ, Stojadinovic A, et al. Validation of tissue microarrays for immunohistochemical profiling of cancer specimens using the example of human fibroblastic tumors. Am J Pathol 2001; 158:1245-51.
23. Mueller-Holzner E, Fink V, Frede T, et al. Immunohistochemical determination of HER2 expression in breast cancer from core biopsy specimens: a reliable predictor of HER2 status of the whole tumor. Breast Cancer Res Treat 2001; 69:13-9.
24. Kallioniemi OP, Wagner U, Kononen J, et al. Tissue microarray technology for high-throughput molecular profiling of cancer. Hum Mol Genet 2001; 10:657-62.
25. Elston CW, Ellis IO. Pathological prognostic factors in breast cancer. I. The value of histological grade in breast cancer: experience from a large study with long-term follow-up. Histopathology 1991; 19:403-10.
26. van Slooten HJ, Clahsen PC, van Dierendonck JH, et al. Expression of Bcl-2 in node-negative breast cancer is associated with various prognostic factors, but does not predict response to one course of perioperative chemotherapy. Br J Cancer 1996; 74:78-85.
27. Clahsen PC, van de Velde CJH, Duval C, et al. p53 protein accumulation and response to adjuvant chemotherapy in premenopausal women with node-negative early breast cancer. J Clin Oncol 1998; 16:470-9.

28. van de Vijver MJ, Peterse JL, Mooi WJ, et al. Neu-protein overexpression in breast cancer. Association with comedo-type ductal carcinoma in situ and limited prognostic value in stage II breast cancer. N Engl J Med 1988; 319:1239-45.
29. Cancello G, Maisonneuve P, Rotmensz N, et al. Prognosis and adjuvant treatment effects in selected breast cancer subtypes of very young women (<35 years) with operable breast cancer. Ann Oncol 2010; 21:1974-81.
30. Sundquist M, Thorstenson S, Brudin L, et al. Incidence and prognosis in early onset breast cancer. Breast 2002; 11:30-5.
31. Kollias J, Elston CW, Ellis IO, et al. Early-onset breast cancer--histopathological and prognostic considerations. Br J Cancer 1997; 75:1318-23.
32. Jones HA, Antonini N, Hart AA, et al. Impact of pathological characteristics on local relapse after breast-conserving therapy: a subgroup analysis of the EORTC boost versus no boost trial. J Clin Oncol 2009; 27:4939-47.
33. van der Hage JA, Mieog JS, van de Vijver MJ, et al. Efficacy of adjuvant chemotherapy according to hormone receptor status in young patients with breast cancer: a pooled analysis. Breast Cancer Res 2007; 9:R70.
34. Ahn SH, Son BH, Kim SW, et al. Poor outcome of hormone receptor-positive breast cancer at very young age is due to tamoxifen resistance: nationwide survival data in Korea--a report from the Korean Breast Cancer Society. J Clin Oncol 2007; 25:2360-8.
35. Cuzick J, Ambroisine L, Davidson N, et al. Use of luteinising-hormone-releasing hormone agonists as adjuvant treatment in premenopausal patients with hormone-receptor-positive breast cancer: a meta-analysis of individual patient data from randomised adjuvant trials. Lancet 2007; 369:1711-23.
36. Jonat W, Pritchard KI, Sainsbury R, et al. Trends in endocrine therapy and chemotherapy for early breast cancer: a focus on the premenopausal patient. J Cancer Res Clin Oncol 2006; 132:275-86.
37. t Veer LJ, Dai H, van de Vijver MJ, et al. Gene expression profiling predicts clinical outcome of breast cancer. Nature 2002; 415:530-6.
38. van de Vijver MJ, He YD, van't Veer LJ, et al. A gene-expression signature as a predictor of survival in breast cancer. N Engl J Med 2002; 347:1999-2009.
39. Wang Y, Klijn JG, Zhang Y, et al. Gene-expression profiles to predict distant metastasis of lymph-node-negative primary breast cancer. Lancet 2005; 365:671-9.

## SUPPLEMENTARY DATA

**Supplementary Table 1.** Univariate analysis for prognostic factors in 549 patients aged less than 40 years

| Characteristic | Overall survival | | | Distant disease-free survival | | |
|---|---|---|---|---|---|---|
| | HR | 95% CI | *P* | HR | 95% CI | *P* |
| **pT2 + pT3** | 2.22 | 1.56-3.16 | <0.01 | 1.90 | 1.41-2.56 | <0.01 |
| **Lymph node positive** | 2.19 | 1.57-3.05 | <0.01 | 1.88 | 1.42-2.48 | <0.01 |
| **Histological grade** | | | <0.01 | | | <0.01 |
| I | 1 | | | 1 | | |
| II | 1.97 | 0.98-3.96 | | 2.13 | 1.23-3.70 | |
| III | 2.74 | 1.42-5.29 | | 2.27 | 1.34-3.85 | |
| **Lymphangio invasion** | | | 0.02 | | | 0.01 |
| No vessels | 1 | | | 1 | | |
| 1 to 5 vessels | 0.96 | 0.58-1.57 | | 0.97 | 0.64-1.47 | |
| > 5 vessels | 1.80 | 1.18-2.74 | | 1.71 | 1.18-2.47 | |
| **ER+** | 0.77 | 0.53-1.12 | 0.17 | 0.92 | 0.67-1.26 | 0.61 |
| **PgR+** | 0.67 | 0.47-0.97 | 0.03 | 0.80 | 0.59-1.09 | 0.16 |
| **HER2+** | 1.09 | 0.73-1.64 | 0.67 | 1.02 | 0.72-1.44 | 0.93 |

| | | | | | | |
|---|---|---|---|---|---|---|
| **Molecular subtype** | | | 0.06 | | | 0.15 |
| Basal | 1 | | | 1 | | |
| Luminal A | 0.56 | 0.34-0.92 | | 0.75 | 0.50-1.14 | |
| HER2 | 0.96 | 0.62-1.50 | | 1.07 | 0.73-1.58 | |
| Luminal B | 0.61 | 0.27-1.37 | | 0.60 | 0.29-1.24 | |
| **P53+** | 1.25 | 0.85-1.84 | 0.26 | 0.87 | 0.62-1.22 | 0.42 |
| **Breast conserving therapy** | 0.55 | 0.38-0.79 | <0.01 | 0.66 | 0.48-0.92 | 0.01 |
| **Adjuvant chemotherapy** | 1.87 | 1.34-2.61 | <0.01 | 1.55 | 1.17-2.05 | <0.01 |

HR, hazard ratio; CI, confidence interval; ER, estrogen receptor; PgR, progesterone receptor; HER2, human epidermal growth factor receptor 2.

**Supplementary Table 2.** Univariate analysis of prognostic factors in 341 node-negative patients aged less than 40 years.

| **Characteristic** | **Overall survival** | | | **Distant disease-free survival** | | |
|---|---|---|---|---|---|---|
| | **HR** | **95% CI** | ***P*** | **HR** | **95% CI** | ***P*** |
| **pT2 + pT3**[1] | 2.40 | 1.45-3.97 | <0.01 | 1.58 | 1.03-2.42 | 0.04 |
| **Histological grade** | | | <0.01 | | | 0.02 |
| I | 1 | | | 1 | | |
| II | 1.49 | 0.52-4.22 | 0.46 | 1.86 | 0.90-3.96 | 0.11 |
| III | 3.35 | 1.33-8.45 | <0.01 | 2.60 | 1.29-5.23 | <0.01 |
| **Lymphangio invasion** | | | 0.87 | | | 0.36 |
| No vessels | 1 | | | 1 | | |
| 1 to 5 vessels | 1.14 | 0.57-2.25 | | 1.24 | 0.72-2.14 | |
| > 5 vessels | 1.21 | 0.52-2.83 | | 1.55 | 0.80-3.01 | |
| **ER+** | 0.57 | 0.34-0.97 | 0.04 | 0.63 | 0.41-0.96 | 0.03 |
| **PgR+** | 0.56 | 0.32-0.95 | 0.03 | 0.71 | 0.46-1.08 | 0.11 |
| **HER2+** | 0.85 | 0.44-1.65 | 0.63 | 0.91 | 0.54-1.53 | 0.72 |
| **Molecular subtype** | | | <0.01 | | | 0.03 |
| Basal | 1 | | | 1 | | |
| Luminal A | 0.23 | 0.10-0.54 | | 0.43 | 0.24-0.76 | |
| HER2 | 0.72 | 0.40-1.30 | | 0.75 | 0.45-1.24 | |
| Luminal B | 0.22 | 0.03-1.59 | | 0.47 | 0.14-1.52 | |
| **P53+** | 1.41 | 0.80-2.48 | 0.24 | 0.90 | 0.57-1.47 | 0.68 |
| **Breast conserving therapy** | 0.92 | 0.45-1.85 | 0.81 | 1.31 | 0.68-2.52 | 0.41 |
| **Adjuvant chemotherapy**[2] | 1.97 | 1.03-3.76 | 0.04 | 1.12 | 0.60-2.08 | 0.72 |

[1] Two patients with pathological tumor size larger than 5 cm were excluded from the analysis. [2] 37 patients received adjuvant chemotherapy. HR, hazard ratio; CI, confidence interval; ER, estrogen receptor; PgR, progesterone receptor; HER2, human epidermal growth factor receptor 2.

**Supplementary Table 3.** Patient and tumor characteristics of patients aged < 40 years from whom tumor material was available for immunohistochemical analysis and of patients aged < 40 years from whom tumor material was not available.

| **Characteristic** | **Tumor material available (N = 549)** | | **Tumor material not available (N = 643)** | | ***P*** |
|---|---|---|---|---|---|
| | **N** | **%** | **N** | **%** | |
| **Clinical tumor size** | | | | | 0.31 |
| T1 | 219 | 40 | 245 | 39 | |
| T2 | 308 | 56 | 354 | 56 | |
| T3 | 20 | 4 | 35 | 5 | |
| Missing | 2 | | 9 | | |
| **Pathological nodal status** | | | | | 0.96 |
| Negative | 341 | 63 | 392 | 62 | |
| Positive | 204 | 37 | 236 | 38 | |
| Missing | 4 | | 15 | | |
| **Adjuvant chemotherapy** | | | | | 0.11 |
| No | 326 | 60 | 402 | 64 | |
| Yes | 221 | 40 | 225 | 36 | |
| Missing | 2 | | 16 | | |

# Part IB

## Resistance to therapy and cancer stem cells

# Chapter 6

# Age interactions in the prognostic role of the cancer stem cell marker aldehyde dehydrogenase-1 in breast cancer

Mieog JSD[1], de Kruijf EM[1], Bastiaannet E, Kuppen PJK, Sajet A, de Craen AJM, Smit VTHBM, van de Velde CJH, Liefers GJ

[1] Shared first authorship

*Submitted*

## ABSTRACT

### Introduction

The purpose of this study was to compare expression and prognostic effect of the breast cancer stem cell marker aldehyde dehydrogenase-1 (ALDH1) in young and elderly breast cancer patients.

### Methods

The study population (N = 574) consisted of all early breast cancer patients primarily treated with surgery in our center between 1985 and 1994. Median follow-up was 17.9 years (range: 0.1 to 23.5). Tissue microarray slides were immunohistochemically stained for ALDH1 expression and quantified by two independent observers who were blinded to clinical outcome. Assessment of the prognostic effect of ALDH1 expression was stratified according to age and systemic treatment.

### Results

Complete lack of expression of ALDH1 was found in 40% of tumors. With increasing age more tumors showed complete absence of ALDH1 expression ($P < .001$). In patients aged > 65 years, ALDH1 status was not associated with any clinical outcome. Conversely, in patients aged < 65 years, ALDH1 positivity was an independent risk factor of worse outcome for relapse free period (hazard ratio = 1.71, 95% CI = 1.09 to 2.68, $P = .021$) and relative survival (relative excess risks of death = 2.36, 95% CI = 1.22 to 3.68, $P = .016$). Ten-year relative survival risk was 57% in ALDH1 positive patients compared to 83% in ALDH1 negative patients.

### Conclusion

ALDH1 expression and its prognostic effect are age-dependent. Our results support the hypothesis that breast cancer biology is different in elderly patients compared to their younger counterparts and emphasizes the importance of taking into consideration age-specific interactions in breast cancer research.

## INTRODUCTION

Age at diagnosis of breast cancer is an important independent prognostic factor. Young age is associated with more aggressive tumors with a relatively high risk of distant metastasis and loco-regional recurrence,[1] whereas old age is associated with more indolent tumors.[2, 3] Although tumor characteristics differ considerably between age groups (including hormone receptor and human epidermal growth factor receptor 2 (HER2) status), these tumor characteristics can only account for part of the divergence in survival witnessed between age groups.[2] Little is known about the impact and significance of various prognostic and predictive factors in elderly as compared to their younger counterparts. As is the case with randomized trials, elderly are underrepresented in translational studies on molecular markers.[4, 5] This caveat is especially worrisome since studies show that the relative survival in elderly breast cancer patient is lower, despite more favorable tumor characteristics, which is probably due to the fact that these patients receive less aggressive treatment.[6] Molecular markers could aid to guide therapy in the fit elderly. Moreover, specific age-interactions might underlie pathophysiological processes in the development of primary breast cancer and subsequent local and distant metastases. Therefore, breast cancer researchers should account for age-specific differences.[4]

Recent evidence in tumor biology supports the cancer stem cell theory and may also provide a biological reason for the age-associated survival difference.[7] According to this theory, cancer stem cells, defined as a small subset of tumor cells with stem cell-like features including epithelial-to-mesenchymal transition, have the capacity to self-renewal and differentiation, giving rise to heterogeneous tumor cell population. Various putative markers of breast cancer stem cells have been proposed, including aldehyde dehydrogenase-1 (ALDH1) activity, CD44+/CD24-, CD133, and ITGA6.[7-10] In particular, ALDH1 expression has shown promise as a clinically relevant prognostic marker.[9, 11, 12] Moreover, various studies have shown that the subset of cancer stem cells is relatively resistant to chemo- and radiotherapy.[13, 14] Thereby, the subpopulation of cancer stem cells can provide both an explanation and a therapeutic target for poor-prognostic, treatment-resistant and recurrent breast cancer.

ALDH1 is a detoxifying enzyme responsible for the oxidation of intracellular aldehydes and thereby confers resistance to alkylating agents.[12, 15] This detoxifying capacity might underlie the longevity of stem cells by protecting against oxidative stress. Moreover, ALDH1 may have a role in early differentiation of stem cells and stem cell proliferation through its role in oxidizing retinol to retinoic acid, a modulator of cell proliferation.[15] ALDH1 expression is associated with unfavorable tumor characteristics in breast cancer, such as high grade, absence of hormone receptor expression, positive HER2 status and the basal-like molecular subtype.[9, 16-18]

To study whether the expression of the breast cancer stem cell marker ALDH1 is associated with age and has an influence on clinical outcome, we analyzed the age-

distribution of ALDH1 expression and its prognostic role in young and elderly patients using long-term follow-up data of a cohort of breast cancer patients primarily treated with surgery in our institution.

## MATERIAL AND METHODS

### Study cohort

The patient population comprised all non-metastasized breast cancer patients primarily treated with surgery in the Leiden University Medical Center between 1985 and 1994 with tumor material available (N = 574).[19] Patients with bilateral tumors or a prior history of cancer, other than basal cell carcinoma or cervical carcinoma *in situ*, were excluded. The following data were known: age, tumor grade, histological type, TNM stage, local and systemic therapy, locoregional or distant tumor recurrence, survival, and expression of estrogen receptor (ER), progesterone receptor (PgR) and human epidermal growth factor receptor 2 (HER2). All tumors were graded according to current pathological standards by an experienced breast cancer pathologist (V.S.). Median follow-up was 17.9 years (range: 0.01 to 23.5). Approval was obtained from the Leiden University Medical Center Medical Ethics Committee. All samples were handled in a coded fashion, according to National ethical guidelines ("Code for Proper Secondary Use of Human Tissue", Dutch Federation of Medical Scientific Societies).

### Assessment of ALDH1 expression

Mouse antibody against ALDH1 (611195, BD Biosciences) was used for immunohistochemistry. Tissue sections of 4 μm were cut from a previously constructed tissue microarray of formalin-fixed paraffin-embedded tumors of 574 patients from whom tumor material was available.[19] Immunohistochemical staining was performed according to previously described standard protocols.[19] Human liver tissue slides served as positive control. Negative controls were human liver tissue slides that did undergo the whole immunohistochemical staining without primary antibodies. Microscopic analysis of ALDH1 was assessed independently by two observers in a blinded manner. Absence and presence of ALDH1 activity was classified as 0% and 1-100% staining of tumor cells, respectively (Figure 1A).[9, 11]

### Statistical analysis

Statistical analyses were performed using the statistical packages SPSS (version 16.0 for Windows, Spps Inc, Chicago, IL, USA) and Stata (version 10.0 for Windows, StataCorp, College Station, TX, USA). Cohen's kappa coefficient was used to assess the

inter-observer agreement in quantification of ALDH1 expression. The $\chi^2$ test was used to evaluate associations between various clinicopathological parameters and ALDH1 expression. Relapse-free period was defined as the time from date of surgery until an event (locoregional recurrence and/or a distance recurrence, whichever came first). Relapse-free period is reported as cumulative incidence function, after accounting for death as competing risk.[20] The Kaplan–Meier method was used for survival plotting and log-rank test for comparison of relapse-free period curves. Cox proportional hazard analysis was used for univariate and multivariable analysis for relapse-free period. Relative survival was calculated by the Hakulinen method as the ratio of the survival observed among the cancer patients and the survival that would have been expected based on the corresponding (age, sex, and year) general population. National life tables were used to estimate expected survival. Relative excess risks of death were estimated using a multivariable generalized linear model with a Poisson distribution, based on collapsed relative survival data, using exact survival times.

Analyses were performed for all patients and stratified for age and systemic treatment. Age of 65 years at time of diagnosis was chosen as the cut-off point for age stratification.[21] An interaction term with age and ALDH1 status was introduced in Cox proportional hazard model to assess the interaction in prognostic effects of ALDH1 status for the age groups. Variables with a *P*-value of < .10 in univariate analysis were entered in multivariable analysis.

## RESULTS

### ALDH1 expression in patient cohort

Immunohistochemical data of ALDH1 expression were available for 496 of the 574 patients (86.4%). Of these patients, 326 (65.7%) were < 65 years at diagnosis and 170 (34.3%) were > 65 years at diagnosis. The Cohen's kappa coefficient for inter-observer agreement was 0.81. Complete lack of expression of ALDH1 of any tumor cell was found in 40.4% of the tumors. The association between ALDH1 status and age is shown in Figure 1B. ALDH1 expression was inversely correlated with age ($P = .0015$) and was significantly higher in patients aged < 65 years (65.3%) than in patients aged > 65 years (48.2%; $P < .001$). The association of ALDH1 expression with classic patient, tumor and treatment characteristics is shown in Table 1. In patients aged < 65 years, ALDH1 expression was significantly correlated with high histological grade and positive nodal status. In patients aged > 65 years, ALDH1 expression was significantly correlated with absence of estrogen receptor expression.

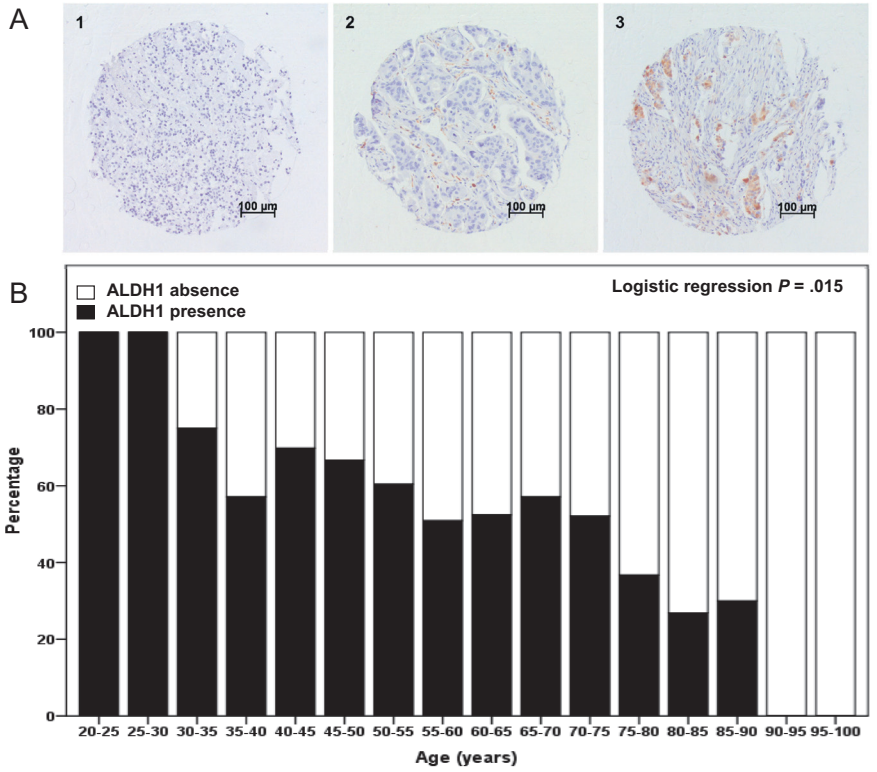


**Figure 1. ALDH1 expression and distribution over age groups. A.** Representative photographs of tissue microarray punches of human breast cancer specimens immunohistochemically stained for ALDH1 with representative examples of strong staining (left panel), intermediate staining (middle panel) and no staining (right panel). Bar represents 100 µm. **B.** ALDH1 status according to age (N = 496). Logistic regression *P*-value is shown.

## Impact of ALDH1 on survival

The association of ALDH1 status with relapse-free period and relative survival is shown in Figures 3 and 4, respectively. Analysis of relapse-free period showed a trend towards a significant association between ALDH1 status and clinical outcome for the whole population ($P = .10$; Figure 2A, D). In the group of patients aged younger than 65 years, a strong association was found between ALDH1 expression and poor clinical outcome ($P = .01$; Figure 2B). In the subgroup of younger patients who did not receive any systemic treatment, a comparable association was found ($P = .009$; Figure 2E). In this group, 52% of patients with ALDH1 positive tumors were relapse-free at 10 years follow-up compared to 72% of patients with ALDH1 negative tumors (absolute difference = 20%). Conversely, in the elderly patients, no association was found between ALDH1 status and clinical outcome ($P = .20$; Figure 2C, F). Interaction analysis demonstrated a statistically significant difference in the prognostic effect of ALDH1 status in young and elderly patients ($P = .007$).

**Table 1.** Association of ALDH1 status with clinicopathological charateristics, stratified by age*

| Characteristic | Patients < 65 years | | | | | Patients > 65 years | | | | |
|---|---|---|---|---|---|---|---|---|---|---|
| | ALDH1 negative | | ALDH1 positive | | | ALDH1 negative | | ALDH1 positive | | |
| | N | % | N | % | *P* | N | % | N | % | *P* |
| **Grade** | | | | | .02 | | | | | .79 |
| I | 19 | 17.3 | 18 | 8.5 | | 11 | 12.9 | 13 | 16.2 | |
| II | 58 | 52.7 | 103 | 48.6 | | 44 | 51.8 | 38 | 47.5 | |
| III | 33 | 30.0 | 91 | 42.9 | | 30 | 35.3 | 29 | 36.2 | |
| **Histological type** | | | | | .42 | | | | | .20 |
| Ductal | 103 | 92.8 | 191 | 90.1 | | 72 | 84.7 | 73 | 91.2 | |
| Lobular | 8 | 7.2 | 21 | 9.9 | | 13 | 15.3 | 7 | 8.7 | |
| **Tumor size** | | | | | .34 | | | | | .55 |
| T1 | 45 | 40.2 | 74 | 36.1 | | 27 | 31.0 | 24 | 31.6 | |
| T2 | 57 | 50.9 | 101 | 49.3 | | 48 | 55.2 | 37 | 48.7 | |
| T3/4 | 10 | 8.9 | 30 | 14.6 | | 12 | 13.8 | 15 | 19.7 | |
| **Nodal status** | | | | | .02 | | | | | .71 |
| Negative | 69 | 62.2 | 101 | 47.9 | | 46 | 56.1 | 46 | 59.0 | |
| Positive | 42 | 37.8 | 110 | 52.1 | | 36 | 43.9 | 32 | 41.0 | |
| **ER status** | | | | | .61 | | | | | .01 |
| Negative | 43 | 41.0 | 91 | 44.0 | | 16 | 19.0 | 30 | 38.0 | |
| Positive | 62 | 59.0 | 116 | 56.0 | | 68 | 81.0 | 49 | 62.0 | |
| **PgR status** | | | | | .77 | | | | | .08 |
| Negative | 48 | 47.1 | 84 | 40.6 | | 26 | 31.3 | 35 | 44.9 | |
| Positive | 54 | 52.9 | 123 | 59.4 | | 57 | 68.7 | 43 | 55.1 | |
| **HER2 status** | | | | | .99 | | | | | .80 |
| Negative | 67 | 87.0 | 153 | 86.9 | | 61 | 93.8 | 64 | 92.8 | |
| Positive | 10 | 13.0 | 23 | 13.1 | | 4 | 6.2 | 5 | 7.2 | |

* Missing data not shown. N, number of patients; ALDH1, aldehyde dehydrogenase 1; ER, estrogen receptor; PgR, progesterone receptor; HER2, human epidermal growth factor receptor 2

Analysis of relative survival showed a similar pattern as for relapse-free period: a strong association between ALDH1 positive tumors and poor relative survival in the younger patient group (Figure 3B, E) and no association between ALDH1 status and relative survival for elderly patients (Figure 3C, F). In the subgroup of younger patients who did not receive any systemic treatment, the 10-year relative survival rate was 57% in patients with ALDH1 positive tumors compared to 83% in patients with ALDH1 negative tumors (absolute difference = 26%, $P = .008$; Figure 3E). Interaction analysis demonstrated a statistically significant difference between the prognostic effect of ALDH1 status in young and elderly patients ($P = .047$).

Multivariable analyses were conducted for the patient groups that did not receive systemic treatment (276 young patients and 154 elderly patients). ALDH1 status remained an independent prognostic factor in the young patient group for both relapse-free period (hazard ratio = 1.71, 95% CI = 1.09 to 2.68, $P = .021$; Table 2) and relative survival (relative excess risks of death = 2.36, 95% CI = 1.22 to 3.68, $P = .016$; Table 3).

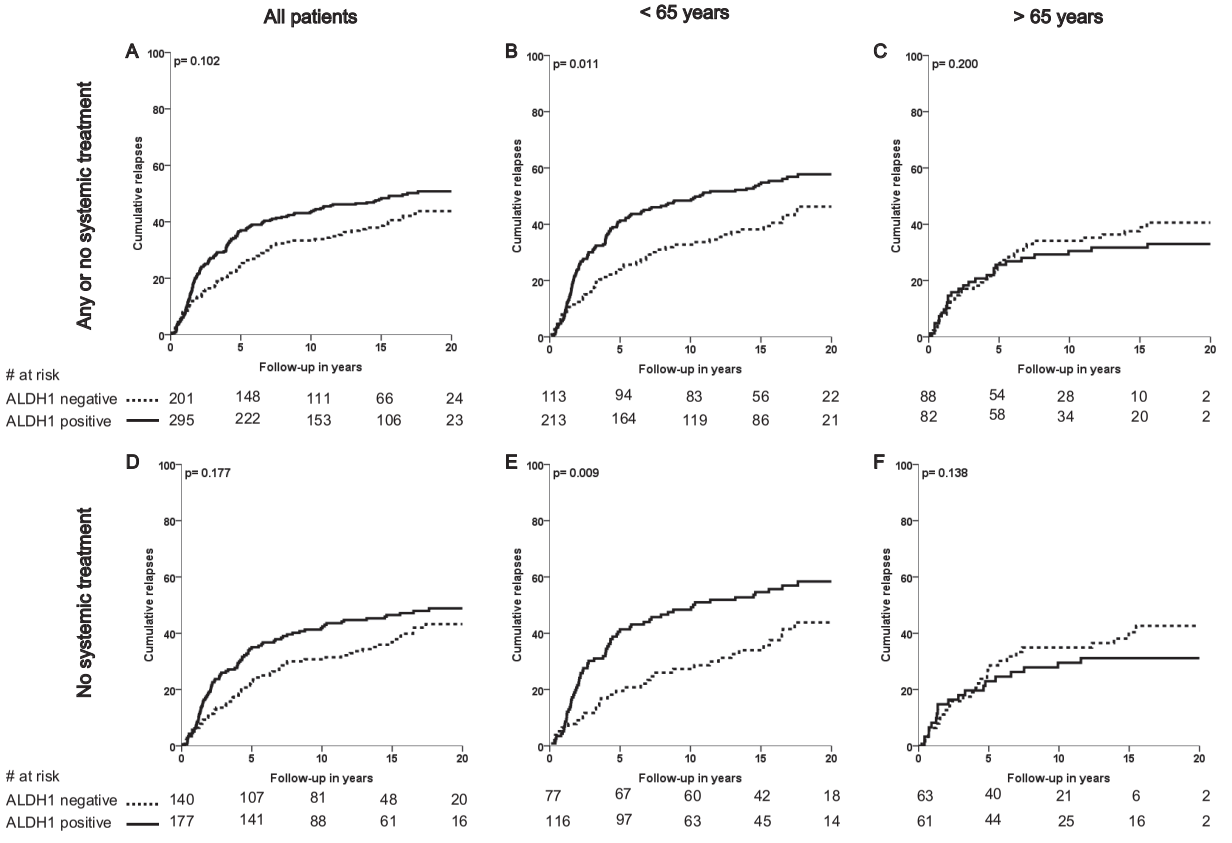


**Figure 2.** Relapse-free period according to ALDH1 status for all patients (A, D), for patients aged < 65 years (B, E) and for patients aged > 65 years (C, F); and for patients that did not receive systemic therapy (D-F). Log-rank *P*-values are shown in each graph.

**Table 2.** Univariate and multivariable analysis for relapse-free period stratified by age for patients naive to systemic treatment

| Characteristic | Patients < 65 years | | | | | | | Patients > 65 years | | | | | | |
|---|---|---|---|---|---|---|---|---|---|---|---|---|---|---|
| | | Univariate analysis | | | Multivariable analysis | | | | Univariate analysis | | | Multivariable analysis | | |
| | N | HR | 95% CI | *P* | HR | 95% CI | *P* | N | HR | 95% CI | *P* | HR | 95% CI | *P* |
| **Grade** | | | | .03 | | | 0.21 | | | | .01 | | | .29 |
| I | 31 | 1 | | | 1 | | | 24 | 1 | | | 1 | | |
| II | 131 | 1.45 | 0.76-2.75 | | 1.06 | 0.40-2.78 | | 74 | 1.73 | 0.66-4.58 | | 1.30 | 0.48-3.58 | |
| III | 75 | 2.17 | 1.12-4.20 | | 1.54 | 0.58-4.11 | | 44 | 3.66 | 1.39-9.61 | | 2.01 | 0.70-5.75 | |
| **Histological type** | | | | .54 | | | | | | | .53 | | | |
| Ductal | 223 | 1 | | | | | | 124 | 1 | | | | | |
| Other | 15 | 1.24 | 0.63-2.45 | | | | | 18 | 0.74 | 0.30-1.87 | | | | |
| **Tumor size** | | | | <.001 | | | 0.05 | | | | .03 | | | .90 |
| pT1 | 137 | 1 | | | 1 | | | 59 | 1 | | | 1 | | |
| pT2 | 109 | 1.66 | 1.16-2.37 | | 1.60 | 1.01-2.55 | | 71 | 2.23 | 1.22-4.09 | | 1.16 | 0.56-2.40 | |
| pT3/4 | 22 | 2.73 | 1.57-4.76 | | 2.04 | 1.07-3.88 | | 18 | 2.11 | 0.82-5.45 | | 1.23 | 0.42-3.63 | |
| **Nodal status** | | | | <.001 | | | <0.001 | | | | <.001 | | | <.001 |
| Negative | 204 | 1 | | | 1 | | | 109 | 1 | | | 1 | | |
| Positive | 69 | 4.25 | 3.02-5.99 | | 4.44 | 2.89-6.82 | | 36 | 3.94 | 2.28-6.82 | | 3.33 | 1.77-6.24 | |
| **ER status** | | | | .59 | | | | | | | .22 | | | |
| Negative | 87 | 1 | | | | | | 40 | 1 | | | | | |
| Positive | 126 | 0.90 | 0.66-1.32 | | | | | 95 | 1.53 | 0.78-2.98 | | | | |
| **PgR status** | | | | .78 | | | | | | | .78 | | | |
| Negative | 84 | 1 | | | | | | 55 | 1 | | | | | |
| Positive | 123 | 0.95 | 0.64-1.40 | | | | | 81 | 1.08 | 0.61-1.92 | | | | |
| **HER2 status** | | | | .26 | | | | | | | .05 | | | |
| Negative | 143 | 1 | | | | | | 105 | 1 | | | | | |
| Positive | 19 | 1.44 | 0.76-2.71 | | | | | 4 | 0.05 | 0.00-23.3 | | | | |
| **ALDH1 status** | | | | .01 | | | 0.02 | | | | .14 | | | |
| Negative | 77 | 1 | | | 1 | | | 63 | 1 | | | | | |
| Positive | 116 | 1.75 | 1.14-2.68 | | 1.71 | 1.09-2.68 | | 61 | 0.64 | 0.35-1.16 | | | | |

N, number of patients; HR, hazard ratio; ER, estrogen receptor; PgR, progesterone receptor; HER2, human epidermal growth factor receptor 2; ALDH1, aldehyde dehydrogenase1

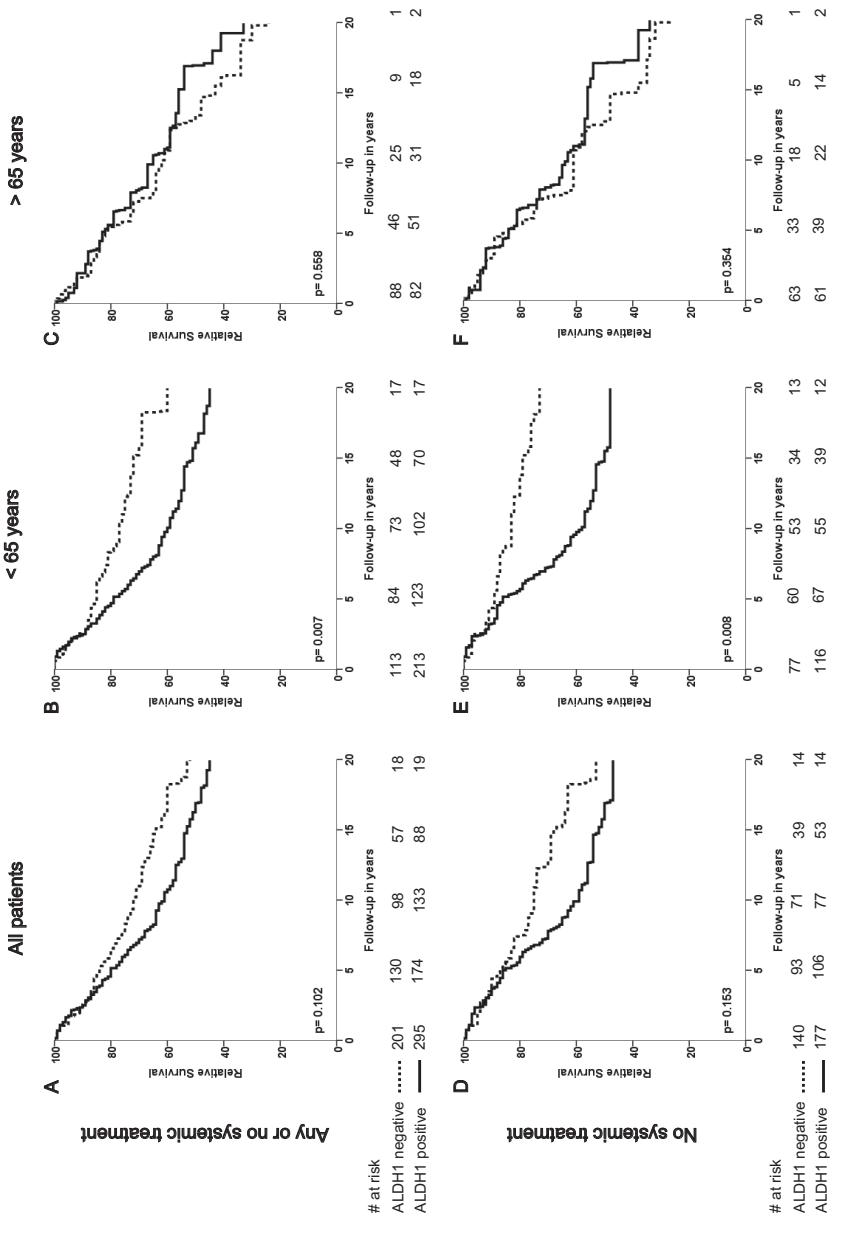


**Figure 3.** Relative survival according to ALDH1 status for all patients (A, D), for patients aged < 65 years (B, E) and for patients aged > 65 years (C, F); and for patients that did not receive systemic therapy (D-F). Log-rank *P*-values are shown in each graph.

**Table 3.** Univariate and multivariable analysis for relative survival stratified by age for patients naive to systemic treatment

| Characteristic | Patients < 65 years | | | | | | | Patients > 65 years | | | | | | |
|---|---|---|---|---|---|---|---|---|---|---|---|---|---|---|
| | | Univariate analysis | | | Multivariable analysis | | | | Univariate analysis | | | Multivariable analysis | | |
| | N | RER | 95% CI | *P* | RER | 95% CI | *P* | N | RER | 95% CI | *P* | RER | 95% CI | *P* |
| **Grade** | | | | .03 | | | .95 | | | | .34 | | | .29 |
| I | 31 | 1 | | | 1 | | | 24 | 1 | | | | | |
| II | 131 | 2.23 | 0.80-6.28 | | 1.24 | 0.31-5.03 | | 74 | 3.10 | 0.43-22.4 | | | | |
| III | 75 | 3.48 | 1.22-9.94 | | 1.27 | 0.30-5.45 | | 44 | 4.23 | 0.56-31.8 | | | | |
| **Histological type** | | | | .80 | | | | | | | .37 | | | |
| Ductal | 223 | 1 | | | | | | 124 | 1 | | | | | |
| Other | 15 | 1.12 | 0.46-2.71 | | | | | 18 | 1.49 | 0.62-3.61 | | | | |
| **Tumor size** | | | | <.001 | | | .33 | | | | .01 | | | .90 |
| pT1 | 137 | 1 | | | 1 | | | 59 | 1 | | | 1.00 | | |
| pT2 | 109 | 2.67 | 1.41-3.64 | | 1.42 | 0.73-2.76 | | 71 | 5.47 | 0.83-35.9 | | 4.26 | 0.71-25.4 | |
| pT3/4 | 22 | 4.26 | 2.29-7.94 | | 1.79 | 0.81-3.95 | | 18 | 13.2 | 1.90-92.1 | | 7.90 | 1.18-52.9 | |
| **Nodal status** | | | | <.001 | | | <.001 | | | | .02 | | | <.001 |
| Negative | 204 | 1 | | | 1 | | | 109 | 1 | | | 1.00 | | |
| Positive | 69 | 5.03 | 3.32-7.62 | | 5.82 | 3.16-10.7 | | 36 | 2.76 | 1.20-6.35 | | 1.48 | 0.56-3.92 | |
| **ER status** | | | | .11 | | | | | | | .91 | | | |
| Negative | 87 | 1 | | | | | | 40 | 1 | | | | | |
| Positive | 126 | 0.70 | 0.45-1.09 | | | | | 95 | 0.95 | 0.42-2.17 | | | | |
| **PgR status** | | | | .25 | | | | | | | .58 | | | |
| Negative | 84 | 1 | | | | | | 55 | 1 | | | | | |
| Positive | 123 | 0.77 | 0.49-1.21 | | | | | 81 | 0.80 | 0.36-1.77 | | | | |
| **HER2 status** | | | | .19 | | | | | | | .89 | | | |
| Negative | 143 | 1 | | | | | | 105 | 1 | | | | | |
| Positive | 19 | 1.57 | 0.80-3.09 | | | | | 4 | 0.85 | 0.09-8.40 | | | | |
| **ALDH1 status** | | | | .008 | | | .02 | | | | .35 | | | |
| Negative | 77 | 1 | | | 1 | | | 63 | 1 | | | | | |
| Positive | 116 | 2.12 | 1.22-3.68 | | 2.36 | 1.17-4.73 | | 61 | 0.68 | 0.30-1.53 | | | | |

N, number of patients; RER, relative excess risk; ER, estrogen receptor; PgR, progesterone receptor; HER2, human epidermal growth factor receptor 2; ALDH1, aldehyde dehydrogenase 1

## DISCUSSION

In this study, we demonstrated that the presence of ALDH1 expression is significantly higher in young breast cancer patients than in elderly patients. Moreover, we demonstrated that ALDH1 expression is an independent risk factor for decreased survival in young breast cancer patients, but not in elderly patients.

To the best of our knowledge, we are the first to show that expression of ALDH1 in tumors is age-dependent. A corresponding difference in the number of cancer stem cells might provide an explanation for known differences in survival between young and elderly breast cancer patients. A potential strength of our study is that it includes consecutive patients from one center, not biased by being part of a clinical trial. The age restriction of the majority of clinical trials prohibits inclusion of patients older than 70 year and, indeed, less than 10% of clinical trial participants is older than 65 years.[22] In our study, 34% of patients were 65 years or older at diagnosis of breast cancer. Therefore, our study was not hampered by lack of statistical power to analyse the effect of ALDH1 in the elderly.

We showed that ALDH1 expression has a qualitative age interaction effect. In our study, ALDH1 is a predictor of poor prognosis in young patients, but ALDH1 did not influence clinical outcome in elderly patients. Recently, Zhou *et al.* pooled the available data on the prognostic role of ALDH1 activity in breast cancer.[18] Their meta-analysis demonstrated that ALDH1 activity as assessed by immunohistochemistry was significantly associated with worse overall survival (unadjusted pooled relative risk, 2.83, 95% CI = 2.16 to 3.67; four patient cohorts including 1,158 patients).[18] However, the authors did not stratify for age. In other studies, no interaction was found between ALDH1 expression and age.[9, 13, 17] However, in these studies, an age of 40 or 50 year was used as a cut-off for age stratification. We used 65 years as a cut-off point as this may better match with the bimodal age distribution of breast cancer, which suggests that breast cancer is characterized by early- and late-onset tumor types with modes near ages 50 and 70 years.[4, 21] As argued by Anderson *et al.*, these modal ages do not suggest a sharp division of distinctive tumor categories, but rather reflect central tendencies for the age distributions of biologically distinct cancer populations.[4, 23] In line with this bimodal age distribution, a biological explanation of the qualitative age-interaction of the prognostic effect of ALDH1 expression might be that of a changing micro-environment in elderly patients, which may result in hampered signal transduction between tumor stem cells and the micro-environment. Moreover, changes in metabolic processes might limit the role of tumor stem cells in elderly patients. Increasing evidence from the field of epigenetics demonstrates that hypermethylation-induced repression of genes required for stem cell differentiation is linearly associated with age.[24] This suggests that, with increasing age, the role of tumor stem cells becomes more limited. Notwithstanding the need to clarify the underlying mechanism, this new finding on the age-dependent role of ALDH1 activity warrants further validation

and underlines the need of age stratification when assessing biomarkers and new therapies for breast cancer patients.

In conclusion, we demonstrated that expression of the putative breast cancer stem cell marker ALDH1 and its prognostic effect are age-dependent in breast cancer patients. We demonstrate, for the first time, the different prognostic impact of a molecular marker in elderly, which suggests that fundamentally different biological mechanisms underlie age-related breast cancer prognosis. Our results support the hypothesis that breast cancer biology of elderly patients and their younger counterparts is distinct and emphasizes the importance of analyzing and reporting age-specific effects in breast cancer research.

## REFERENCES


1. Anders CK, Johnson R, Litton J, et al. Breast cancer before age 40 years. Semin Oncol 2009; 36:237-49.
2. Diab SG, Elledge RM, Clark GM. Tumor characteristics and clinical outcome of elderly women with breast cancer. J Natl Cancer Inst 2000; 92:550-6.
3. Remvikos Y, Magdelenat H, Dutrillaux B. Genetic evolution of breast cancers. III: Age-dependent variations in the correlations between biological indicators of prognosis. Breast Cancer Res Treat 1995; 34:25-33.
4. Anderson WF, Jatoi I, Sherman ME. Qualitative age interactions in breast cancer studies: mind the gap. J Clin Oncol 2009; 27:5308-11.
5. Beadle BM, Woodward WA, Buchholz TA. The impact of age on outcome in early-stage breast cancer. Semin Radiat Oncol 2011; 21:26-34.
6. Bastiaannet E, Liefers GJ, de Craen AJ, et al. Breast cancer in elderly compared to younger patients in The Netherlands: stage at diagnosis, treatment and survival in 127,805 unselected patients. Breast Cancer Res Treat 2010; 124:801-7.
7. Al-Hajj M, Wicha MS, Benito-Hernandez A, et al. Prospective identification of tumorigenic breast cancer cells. Proc Natl Acad Sci USA 2003; 100:3983-8.
8. Cariati M, Naderi A, Brown JP, et al. Alpha-6 integrin is necessary for the tumourigenicity of a stem cell-like subpopulation within the MCF7 breast cancer cell line. Int J Cancer 2008; 122:298-304.
9. Ginestier C, Hur MH, Charafe-Jauffret E, et al. ALDH1 is a marker of normal and malignant human mammary stem cells and a predictor of poor clinical outcome. Cell Stem Cell 2007; 1:555-67.
10. Wright MH, Calcagno AM, Salcido CD, et al. Brca1 breast tumors contain distinct CD44+/CD24- and CD133+ cells with cancer stem cell characteristics. Breast Cancer Res 2008; 10:R10.
11. Resetkova E, Reis-Filho JS, Jain RK, et al. Prognostic impact of ALDH1 in breast cancer: a story of stem cells and tumor microenvironment. Breast Cancer Res Treat 2010; 123:97-108.
12. Tanei T, Morimoto K, Shimazu K, et al. Association of breast cancer stem cells identified by aldehyde dehydrogenase 1 expression with resistance to sequential Paclitaxel and epirubicin-based chemotherapy for breast cancers. Clin Cancer Res 2009; 15:4234-41.
13. Gong C, Yao H, Liu Q, et al. Markers of tumor-initiating cells predict chemoresistance in breast cancer. PLoS One 2010; 5:e15630.
14. Phillips TM, McBride WH, Pajonk F. The response of CD24(-/low)/CD44+ breast cancer-initiating cells to radiation. J Natl Cancer Inst 2006; 98:1777-85.
15. Huang EH, Hynes MJ, Zhang T, et al. Aldehyde dehydrogenase 1 is a marker for normal and malignant human colonic stem cells (SC) and tracks SC overpopulation during colon tumorigenesis. Cancer Res 2009; 69:3382-9.
16. Foulkes WD, Smith IE, Reis-Filho JS. Triple-negative breast cancer. N Engl J Med 2010; 363:1938-48.

17. Nalwoga H, Arnes JB, Wabinga H, et al. Expression of aldehyde dehydrogenase 1 (ALDH1) is associated with basal-like markers and features of aggressive tumours in African breast cancer. Br J Cancer 2010; 102:369-75.
18. Zhou L, Jiang Y, Yan T, et al. The prognostic role of cancer stem cells in breast cancer: a meta-analysis of published literatures. Breast Cancer Res Treat 2010; 122:795-801.
19. van Nes JG, de Kruijf EM, Faratian D, et al. COX2 expression in prognosis and in prediction to endocrine therapy in early breast cancer patients. Breast Cancer Res Treat 2011; 125:671-85.
20. Putter H, Fiocco M, Geskus RB. Tutorial in biostatistics: competing risks and multi-state models. Stat Med 2007; 26:2389-430.
21. Anderson WF, Jatoi I, Devesa SS. Distinct breast cancer incidence and prognostic patterns in the NCI's SEER program: suggesting a possible link between etiology and outcome. Breast Cancer Res Treat 2005; 90:127-37.
22. Hutchins LF, Unger JM, Crowley JJ, et al. Underrepresentation of patients 65 years of age or older in cancer-treatment trials. N Engl J Med 1999; 341:2061-7.
23. Anderson WF, Matsuno R. Breast cancer heterogeneity: a mixture of at least two main types? J Natl Cancer Inst 2006; 98:948-51.
24. Teschendorff AE, Menon U, Gentry-Maharaj A, et al. Age-dependent DNA methylation of genes that are suppressed in stem cells is a hallmark of cancer. Genome Res 2010; 20:440-6.

# Chapter 7

# Alternatively spliced and full-length tissue factor reveal a non-identical relationship to clinicopathological parameters in a large cohort of human breast cancer

van den Berg JW[1], Mieog JSD[1], de Kruijf EM, Wang J, Sajet A, Kuppen PJK, van de Velde CJH, Reitsma PH, Osanto S, Bogdanov VY, Versteeg HH, Liefers GJ

[1] Shared first authorship

# ABSTRACT

## Introduction

Alternatively spliced tissue factor (asTF) - a soluble variant of TF - influences tumor growth and angiogenesis in an integrin-dependent fashion, while full-length TF (flTF) stimulates angiogenesis via protease-activated receptor-2 (PAR2). Therefore, we investigated how TF isoforms relate to clinicopathology in human breast cancer.

## Methods

Tumor material and matched normal tissue of 574 breast cancer patients was obtained after primary surgery and assembled in tissue micro arrays, which were stained with antibodies specific for asTF and flTF. The percentage of positive tumor cells was independently scored by two observers. Patients in the first quartiles were deemed negative. Associations of TF expression with clinicopathological parameters and survival were calculated. Subcellular localization of asTF and flTF was investigated in transfected baby hamster kidney cells and human breast cancer sections.

## Results

asTF and flTF expression was found in virtually all breast cancer samples (> 95%), whereas normal tissue showed limited expression (asTF = 4%; flTF = 38%). asTF positive tumors were associated with poor histological differentiation and large tumors. flTF positive tumors were associated with poor histological differentiation and expression of the breast cancer stem cell marker ALDH1. asTF and flTF positivity did not influence clinical outcome. However, co-expression of flTF and ALDH1 resulted in poor relapse-free survival in patients younger than 65 years ($P$ = .004), whereas the opposite effect was noted in older patients ($P$ = .08). Unexpectedly, nuclei stained positive for asTF and confocal microscopy and biochemical fractionation confirmed that asTF, but not flTF, was localized in the perinuclear region.

## Conclusion

We demonstrated, in the largest cohort to date, expression of both TF isoforms to be common in human breast cancer and to be associated with unfavorable tumor characteristics. flTF and the VII:PAR2 pathway seems to play a role in breast cancer stem cell population. The differences in cellular localizations of asTF and flTF further support the notion that asTF acts through mechanisms distinct from flTF in cancer.

## INTRODUCTION

In the mid-nineteenth century, activation of coagulation was already observed to be tightly interwoven with cancer progression.[1] Patients suffering from various types of cancer frequently display Trousseau's syndrome, which is characterized by venous thrombosis of the upper and lower extremities. This thrombotic tendency is putatively caused by tumoral overexpression of full-length tissue factor (flTF), a 47 kDa transmembrane protein, on the surface of cancer cells.[2] Under physiological circumstances, flTF expression is limited to the surface of extravascular cells. Upon damage of the endothelium, flTF becomes exposed to the bloodstream and binds the blood-borne zymogen factor VII (FVII) and subsequently factors Xa, thrombin and fibrin are formed, thus resulting in a blood clot.[3] In a reciprocal manner, activation of coagulation also influences various stages of cancerous disease. The TF:FVIIa complex and thrombin have been implicated in tumor growth and metastasis.[4] For instance, flTF expression in colon cancer is associated with an increased risk of hepatic metastasis.[5] flTF expression in both colon and breast cancer has been suggested to promote tumor growth through modulation of angiogenesis.[6] Extensive research has uncovered that coagulation proteases activate so-called protease-activated receptors (PARs). The TF:FVIIa complex specifically activates PAR2 resulting in altered cell behavior such as proliferation, gene expression and migration.[7] In a spontaneous murine breast cancer model, activation of PAR2 by the TF:FVIIa complex was shown to enhance primary tumor growth via activation of the angiogenic switch.

In 2003, a natural occurring splicing variant of TF, alternatively spliced TF (asTF), was described which lacks exon 5. Due to this exon skipping, a frame shift occurs and hence asTF lacks a transmembrane region, but has a unique C-terminus, rendering asTF soluble.[8] Ever since its discovery, the role of asTF in coagulation has been debated,[9-11] however, an increasing body of evidence indicates that asTF may be involved in determining tumor biology and angiogenesis. In cervical cancer samples, asTF has been detected both on protein and mRNA level.[12] High levels of asTF mRNA confer an unfavorable outcome in non-small cell lung cancer,[13, 14] but in esophageal cancer, asTF mRNA levels did not affect outcome nor clinicopathology.[15] Experiments with murine cancer models revealed that tumor size of asTF-expressing tumors is larger and that those tumors display an enhanced number of tumor vessels.[16] Recently, our group reported that asTF drives angiogenesis in a non-proteolytic, integrin-ligating fashion. Human asTF activates $\alpha_6\beta_1$ and $\alpha_v\beta_3$ integrins on endothelial cells, thereby contributing to enhanced cell alignment and migration, respectively, which are indispensable in angiogenesis. In summary, these results suggest that tumor-derived asTF ligates integrins on endothelial cells in a paracrine manner, thus contributing to tumor angiogenesis.[12]

To date, clinical studies investigating the relation between asTF expression at protein level in tumor tissues and clinicopathological characteristics are lacking.

Furthermore, the relative contribution to cancer progression of the protease-mediated flTF axis and the integrin-mediated asTF axis is unclear. Apart from the contribution to tumor angiogenesis, previous studies showed that cancer stem cells are abundant in expression of flTF suggesting that the flTF:FVII:PAR2 axis in cancer stem cells fuels tumor growth and contributes to the maintenance of a chemotherapy resistant subset of tumor cells.[17-19] However, the relationship between flTF and cancer stem cells has not been validated in large patient studies nor in human breast cancer. Moreover, whether asTF has a function in cancer stem cell biology has not been investigated.

In this study, we employ a large cohort of human breast cancer samples with matched normal tissue and a long follow-up in order to clarify the relative contributions of TF isoforms to human breast cancer. Apart from classic clinicopathological parameters, we also investigated the relationship between TF isoforms and cancer stem cells. Moreover, we employed biochemical and microscopic techniques to characterize the tumoral and subcellular localization of asTF and flTF.

## MATERIAL AND METHODS

### Reagents

Normal goat serum and envision anti-rabbit HRP conjugate was purchased from DAKO (Glostrup, Denmark). The specific rabbit polyclonal human asTF antibody used in this study has been previously described and characterized.[8] A murine monoclonal anti human TF with an epitope against the AA encoded by exon 5 was purchased from American Diagnostica. RL-90 PDI and Histone 3 antibodies were purchased from AbCam (Cambridge, UK). Polyclonal goat-anti-human TF was a kind gift of Dr. W. Ruf (Scripps Institute, La Jolla, CA). Secondary antibodies directed against rabbit or mouse IgG with Alexa Fluor® fluorescent dyes were purchased from Invitrogen (Carlsbad, CA). Vectashield DAPI-containing mounting medium was purchased from Vector Labs (Burlingame, CA).

### Cell lines and vectors

Baby hamster kidney cells were kindly provided by Dr. W. Ruf. MCF-7 and MDA-MB-231 cells (ATCC, Manassas, VA) were cultured in DMEM (PAA GmbH, Pasching, Austria) supplemented with 10% fetal calf serum (Bodinco, Alkmaar, the Netherlands) and 50 μg/ml penicillin and 50 μg/ml streptomycin (PAA GmbH). ORFs for asTF (Baseclear) and flTF kind gift from Dr. W. Ruf were subcloned pcDNA3.1 (Invitrogen, Carlsbad, CA) vectors and used when appropriate. Transfections were performed with lipofectamine 2000 transfection reagent (Invitrogen) according to the manufacturer's protocol.

**Study cohort**

The patient population comprised all non-metastasized breast cancer patients primarily treated with surgery in the Leiden University Medical Center between 1985 and 1994 with tumor material available (N = 574).[20] Patients with bilateral tumors or a prior history of cancer, other than basal cell carcinoma or cervical carcinoma *in situ*, were excluded. The following data were known: age, tumor grade, histological type, TNM stage, local and systemic therapy, locoregional or distant tumor recurrence, survival, and expression of estrogen receptor (ER), progesterone receptor (PgR), human epidermal growth factor receptor 2 (HER2), and the breast cancer stem cell marker aldehyde dehydrogenase-1 (ALDH1). All tumors were graded according to current pathological standards. Of 371 patients (65%), normal mammary tissue was available for analysis. Median follow-up was 17.9 years (range: 0.01 to 23.5). Approval was obtained from the Leiden University Medical Center Medical Ethics Committee. All samples were handled in a coded fashion, according to National ethical guidelines ("Code for Proper Secondary Use of Human Tissue", Dutch Federation of Medical Scientific Societies).

**Assessment of expression of asTF and flTF**

Tissue sections of 4 μm were cut from a previously constructed tissue microarray of formalin-fixed paraffin-embedded tumors of 574 patients from whom tumor material was available and a tissue microarray of formalin-fixed paraffin-embedded normal corresponding mammary tissue of 371 patients. Immunohistochemical staining was performed according to standard procedures. Briefly, sections were deparaffinized, rehydrated and endogenous peroxidase activity was blocked with 0.3% $H_2O_2$ in MetOH. For asTF stainings, antigen retrieval was omitted whereas sections for flTF staining were subjected to antigen retrieval in sodium citrate buffer for 10 minutes at 100 °C. Sections were blocked for 1 hour with 10% normal goat serum in PBS/BSA 1% at room temperature. Then, sections were incubated overnight at 4 °C with 1 μg/ml anti-asTF or 20 μg/ml anti-flTF. Sections were washed in PBS, incubated for 30 minutes with Envision, washed and visualized in DAB solution. After counterstaining with hematoxillin, sections were dehydrated and covered. Human placenta tissue slides served as positive control, whereas placenta also served as a no primary control tissue for each staining procedure. The percentage of asTF and flTF positive tumor cells was scored by two observers in a blinded manner. Patients in the first quartiles were deemed negative.

**Immunofluorescent detection of asTF and flTF**

Tissue sections were processed and incubated with primary antibodies as mentioned above. After washing in PBS, sections were incubated with Alexa-488-labeled anti-

rabbit IgG and Alexa-546-labeled anti-mouse IgG for asTF and flTF, respectively. Sections were washed and mounted with DAPI-containing mounting medium. Pictures of the slides were obtained with a confocal laser scanning microscope (LSM510; Carl Zeiss Meditec, Jena, Germany) in a multitrack setting in which the slide is scanned multiple times with a fixed laser–filter pair. Alexa-488 was excited at 488 nm and detected with a 505 to 530 nm band-pass filter. Alexa-546 was excited at 543 nm and detected with a 560 to 615 nm band-pass filter. DAPI was excited at 358 nM and detected with a 455 to 470 nm band-pass filter. The computerized scans presented each fluorochrome signal with an artificial color: green for Alexa-488, red for Alexa-546 and blue for DAPI. All pictures were 512 × 512 pixels, 8-bit depth, and stack size 368.5 × 368.5 µm. A ×25 objective was used (PH2 Plan-NEOFluor 25×/0.80 Imm Korr; Carl Zeiss Meditec). Images were viewed and saved as merged images or as a set of two separate panels in LSM files.

### Cell fractionation

asTF- and flTF-transfected baby hamster kidney cells were grown to subconfluency, trypsinized and washed twice with PBS. 1.0 x $10^6$ cells were pelleted by centrifugation for 10 minutes at 1200 RPM at room temperature. The cell pellet was resuspended in 1 ml hypotonic buffer and cells were left on ice for 5 minutes. Then, 0.05% nonidet p-40 was added and cells were left on ice for 5 minutes for lysis of non-nuclear phospholipid membranes. The unlyzed nuclei were pelleted by centrifugation at 2000

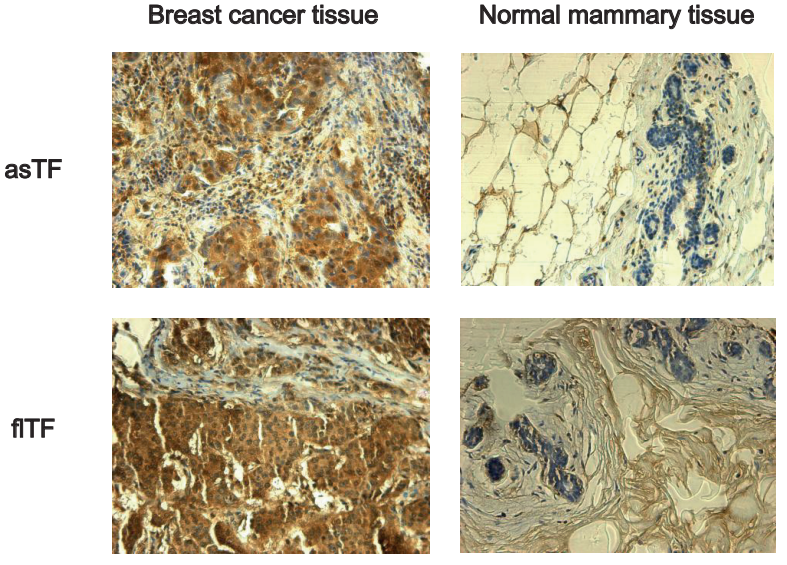


**Figure 1.** Representative photographs of tissue microarray punches of human breast cancer specimens (left panels) and matched normal mammary tissue (right panels) immunohistochemically stained for asTF (top panels) and flTF (bottom panels). A brown color indicates positive staining.

rpm for 10 minutes at 4 °C and washed three times with nonidet p-40. Proteins from the non-nuclear fraction were precipitated with 4 volumes of ice-cold acetone after which the obtained nuclear and non-nuclear pellets were resuspended in Laemmli buffer. Proteins were detected by western blot and purity of the fractions was assessed by blotting for protein disulfide isomerase (PDI) and Histone 3 as markers for the cytoplasmic and nuclear fractions, respectively.

### Statistical analysis

Statistical analyses were performed using the statistical packages SPSS (version 16.0 for Windows, Spps Inc, Chicago, IL) and Stata (version 10.0 for Windows, StataCorp, College Station, TX). Cohen's kappa coefficient was used to assess the inter-observer agreement in quantification of asTF and flTF expression. The Cohen's kappa coefficient was 0.85 and 0.87 for asTF and flTF, respectively. The $\chi^2$ test was used to evaluate associations between various clinicopathological parameters and asTF and flTF expression. Relapse-free period was defined as the time from date of surgery until an event (locoregional recurrence and/or a distance recurrence, whichever came first). Relapse-free period is reported as cumulative incidence function, after accounting for death as competing risk.[21] Relative survival was calculated by the Hakulinen method as the ratio of the survival observed among the cancer patients and the survival that would have been expected based on the corresponding (age, sex, and year) general population. National life tables were used to estimate expected survival. Relative excess risks of death were estimated using a multivariable generalized linear model with a Poisson distribution, based on collapsed relative survival data, using exact survival times. The Kaplan–Meier method was used for survival plotting and log-rank test for comparison of curves. Analyses were performed for all patients and stratified for age and ALDH1 status. Age of 65 years at time of diagnosis was chosen as the cut-off point for age stratification.[22] An interaction term with age and ALDH1 and flTF status was introduced in Cox proportional hazard model to assess the interaction in prognostic effects of ALDH1 status for the age groups.

## RESULTS

### asTF and flTF are abundantly, but differentially expressed in breast cancer

Expression of asTF and flTF was found in virtually all breast cancer samples, whereas normal mammary tissue showed limited expression (asTF = 4%, flTF = 38%; Figure 1). At the first quartile, 60% and 95% of tumor cells expressed asTF and flTF, respectively (Figure 2). The association of asTF and flTF expression with clinicopathological characteristics is shown in Table 1. Patients with an asTF positive tumor had tumors

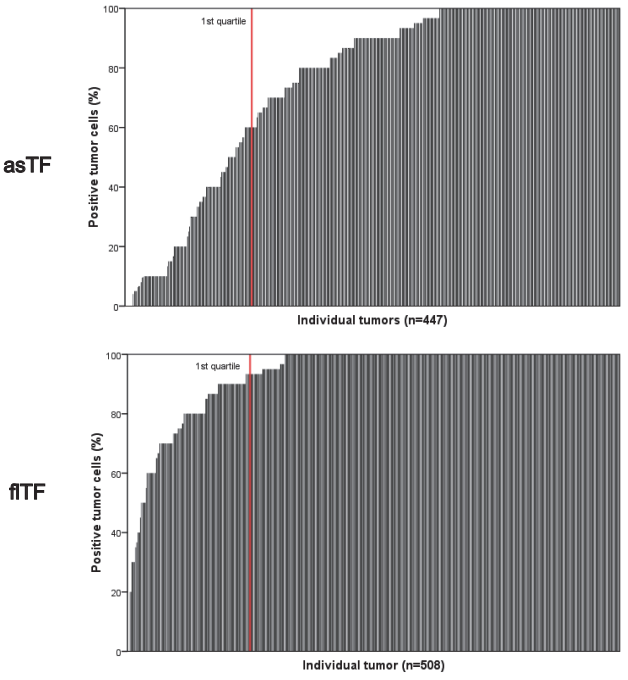


**Figure 2.** Bar chart indicating the number of positive tumor cells for each individual tumor for staining of asTF (top) and flTF (bottom). The red line marks the first quartile; these patients were deemed asTF or flTF negative.

with a higher histological grade compared to patients with an asTF negative tumor (odds ratio (OR) grade III vs. grade I = 3.88, 95% CI = 2.02 to 7.48, $P < .001$). Moreover, asTF positive tumors were larger in terms of tumor size (OR T3-4 vs. T1 = 2.18, 95% CI = 1.09 to 4.36, $P = .002$). Patients with a flTF positive tumor had tumors with a higher histological grade compared to patients with a flTF negative tumor (OR grade III vs. grade I = 3.12, 95% CI = 1.71 to 5.66, $P < .001$). However, flTF was not associated with tumor size (OR T3-4 vs. T1 = 1.6, 95% CI = 0.86 to 3.81, $P = .26$). flTF expression was highly associated with the expression of the breast cancer stem cell ALDH1 ($P = .001$), whereas asTF expression was not ($P = .84$). In addition, we unexpectedly noted a nuclear staining for asTF in breast cancer that was absent in placenta specimens and flTF-stained breast cancer specimens. As this unexpected staining pattern did not affect all nuclei, we regarded this to be a specific staining. High percentages of positive nuclei virtually coincided with high percentages of positive cytoplasm, which was reflected in a strong correlation ($P = .001$).

### asTF and flTF do not affect relapse-free period nor survival

The association of asTF and flTF status with relapse-free period and relative survival is shown in Figure 3. Analysis of relapse-free period showed no association between

**Table 1.** Association of asTF and flTF with patient and tumor characteristics

| | Total | | asTF | | | | | flTF | | | | |
|---|---|---|---|---|---|---|---|---|---|---|---|---|
| | | | Negative | | Positive | | *P* | Negative | | Positive | | *P* |
| | N | % | N | % | N | % | | N | % | N | % | |
| **Total** | 574 | 100 | 119 | 100 | 328 | 100 | | 157 | 100 | 351 | 100 | |
| **Age** | | | | | | | 0.03 | | | | | 0.71 |
| < 40 | 48 | 8.4 | 5 | 4.2 | 26 | 7.9 | | 15 | 9.6 | 26 | 7.4 | |
| 40-60 | 227 | 48.3 | 72 | 60.5 | 153 | 46.6 | | 75 | 47.8 | 171 | 48.7 | |
| > 60 | 249 | 43.4 | 42 | 35.3 | 149 | 45.4 | | 67 | 42.7 | 154 | 43.9 | |
| **Grade** | | | | | | | <0.001 | | | | | <0.001 |
| I | 80 | 14.2 | 26 | 22.2 | 28 | 8.6 | | 30 | 19.6 | 41 | 11.8 | |
| II | 282 | 49.9 | 58 | 49.6 | 159 | 48.9 | | 88 | 57.5 | 157 | 45.2 | |
| III | 203 | 35.9 | 33 | 28.2 | 138 | 42.5 | | 35 | 22.9 | 149 | 42.9 | |
| **Histology** | | | | | | | 0.39 | | | | | 0.18 |
| Ductal | 513 | 90.6 | 104 | 88.9 | 300 | 92.3 | | 133 | 86.9 | 320 | 92.2 | |
| Lobular | 53 | 9.4 | 13 | 11.1 | 25 | 7.7 | | 119 | 13.1 | 27 | 7.8 | |
| **T status** | | | | | | | 0.002 | | | | | 0.26 |
| T1 | 211 | 38.0 | 56 | 48.7 | 97 | 30.4 | | 64 | 42.1 | 120 | 35.1 | |
| T2 | 272 | 49.0 | 46 | 40.0 | 173 | 54.2 | | 71 | 46.7 | 171 | 50.0 | |
| T3-4 | 72 | 13.0 | 13 | 11.3 | 49 | 15.4 | | 17 | 11.2 | 51 | 14.9 | |
| **N status** | | | | | | | 0.62 | | | | | 0.18 |
| N0 | 307 | 55.1 | 64 | 54.7 | 166 | 52.0 | | 93 | 60.0 | 182 | 53.5 | |
| N1-3 | 250 | 44.9 | 53 | 45.3 | 153 | 48.0 | | 62 | 40.0 | 158 | 46.5 | |
| **ER status** | | | | | | | | | | | | 0.96 |
| Negative | 203 | 37.6 | 37 | 31.9 | 124 | 39.1 | 0.17 | 54 | 36.7 | 123 | 36.5 | |
| Positive | 337 | 62.4 | 79 | 68.1 | 193 | 60.9 | | 93 | 63.3 | 214 | 63.5 | |
| **PgR status** | | | | | | | 0.10 | | | | | 0.06 |
| Negative | 223 | 41.6 | 40 | 34.2 | 136 | 42.9 | | 50 | 34.0 | 144 | 43.0 | |
| Positive | 313 | 58.4 | 77 | 65.8 | 181 | 57.1 | | 97 | 66.0 | 191 | 57.0 | |
| **HER2 status** | | | | | | | 0.14 | | | | | 0.28 |
| Negative | 435 | 80.9 | 86 | 93.5 | 236 | 88.1 | | 105 | 92.1 | 244 | 88.4 | |
| Positive | 103 | 19.1 | 6 | 6.5 | 32 | 11.9 | | 9 | 7.9 | 32 | 11.6 | |
| **ALDH1 status** | | | | | | | 0.84 | | | | | 0.001 |
| Negative | 201 | 40.5 | 44 | 39.3 | 123 | 38.2 | | 74 | 50.7 | 105 | 34.1 | |
| Positive | 295 | 59.5 | 68 | 60.7 | 199 | 61.8 | | 72 | 49.3 | 203 | 65.9 | |

asTF, alternatively spliced tissue factor; flTF, full length tissue factor; T, tumor; N, Axillary lymph node; ER, estrogen receptor; PgR, progesterone receptor; HER2, human epidermal growth factor 2; ALDH1, aldehyde dehydrogenase 1

asTF and flTF expression and clinical outcome ($P$ = .38 and $P$ = .23, respectively). In this cohort, 55% of patients with asTF positive tumors was relapse-free at 10 year follow-up compared to 61% of patients with asTF negative tumors (absolute difference = 6%, $P$ = .38). 58% of patients with flTF positive tumors was relapse-free at 10 year follow-up compared to 63% of patients with flTF negative tumors (absolute difference = 5%, $P$ = .23). Analysis of relative survival showed a similar pattern (Figure 3).

## Age influences the prognostic role of flTF and ALDH1 co-expression

To further study the relationship between the breast cancer stem cell marker ALDH1 and the co- expression of flTF, the association of flTF status and ALDH1 status with relapse-free period was analyzed (Figure 4). Patients were grouped according to co-expression of ALDH1 and flTF versus one of both marker overexpressed or none overexpressed. Relapse-free period showed a trend towards a significant association between ALDH1 and flTF co-expression and poor clinical outcome for the whole

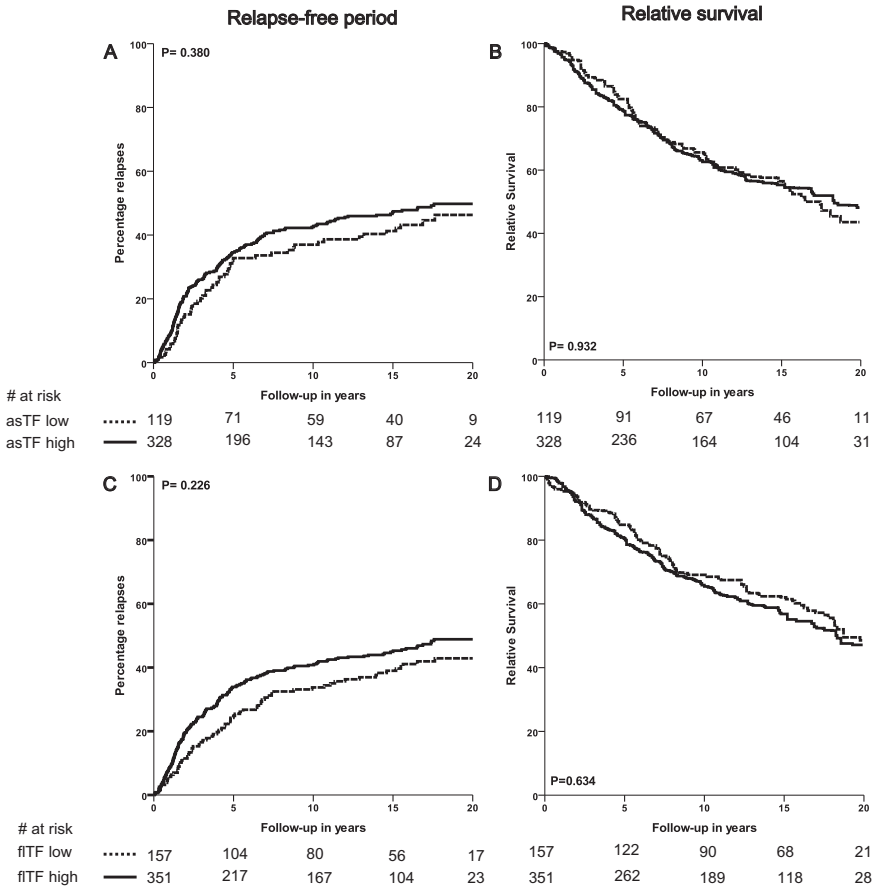


**Figure 3.** Expression of TF isoforms and association with relapse-free period (**A**, **C**) and relative survival (**B**, **D**). Log-rank *P*-values are shown in each graph.

population (*P* = .093; Figure 4A). In the group of patients aged younger than 65 years, a strong association was found between ALDH1 and flTF co-expression and poor relapse-free period (*P* = .004; Figure 4B) and 43% of patients with ALDH1 and flTF positive tumors was relapse-free at 10 year follow-up compared to 67% of patients without co-expressing tumors (absolute difference = 24%).

Conversely, in the group of patients aged older than 65 years, a trend towards an opposite effect of ALDH1 and flTF co-expression and improved clinical outcome was found (*P* = .084; Figure 4C). In this group, 71% of patients with ALDH1 and flTF positive tumors was relapse-free at 10 year follow-up compared to 53% of patients without co-expressing tumors (absolute difference = 18%; Figure 4C). Interaction analysis demonstrated a statistically significant difference in the prognostic effect of ALDH1 and flTF status in young and elderly patients (*P* = .003).

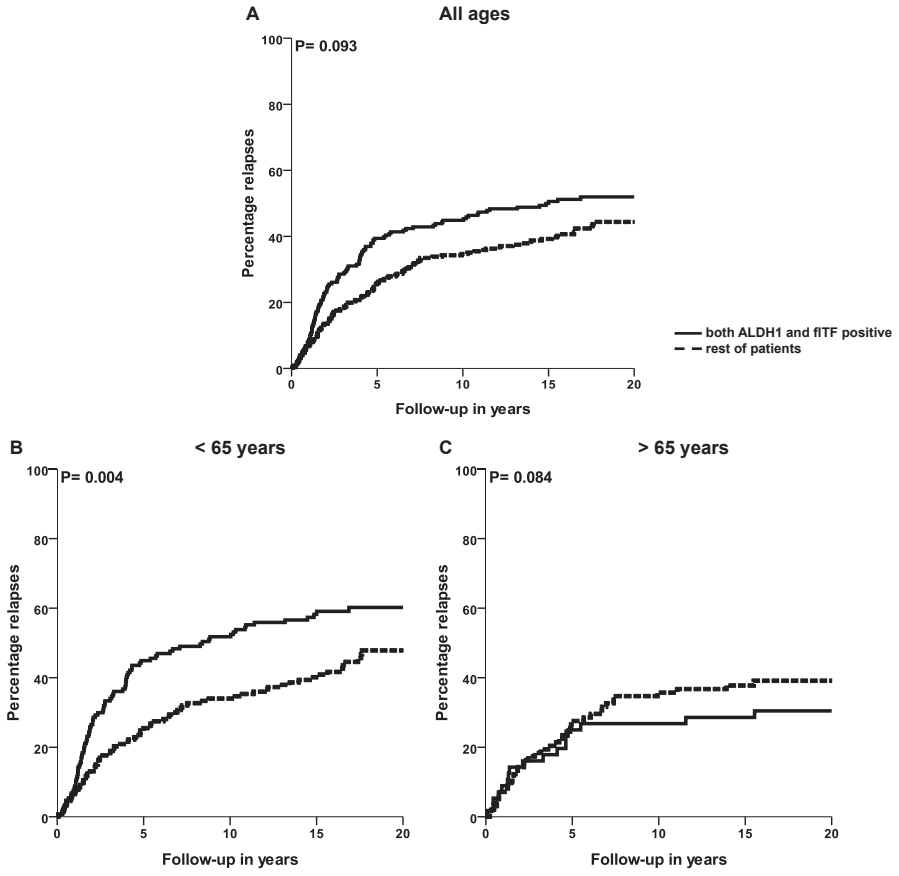


**Figure 4.** Relapse-free period according to flTF and ALDH1 co-expression for all patients (**A**), for patients aged < 65 years (**B**) and for patients aged > 65 years (**C**). Log- rank *P*-values are shown in each graph.

## asTF and flTF display different subcellular localizations

The observation of asTF specific positive staining nuclei in breast cancer specimen prompted us to confirm this unexpected localization of asTF. Confocal microscopy revealed that TF isoforms in human breast cancer show limited co-localization and rather have a different subcellular localization (Figure 5A). flTF as expected is located in the cytoplasm and on the cell membrane, whereas the asTF signal is most prominent adjacent to the cell's nucleus. Although co-localization of both isoforms could be expected, the number of cells displaying co-localization is limited. In transfected baby hamster kidney cells, asTF similarly localized to the perinuclear areas (Figure 5B). We confirmed the findings with confocal microscopy by cellular fractionation of asTF- or flTF-transfected baby hamster kidney cells (Figure 5C). Indeed, asTF was detectable in the nuclear fraction at 40 kDa, which is the expected weight of fully glycosylated asTF, and at 36 kDa, which putatively represents underglycolyated asTF.

## DISCUSSION

Since its discovery, the role of asTF in coagulation has been a matter of debate. However, a role for asTF in cancer has been suggested on basis of both experimental and small-scale patient studies. Recently, our group confirmed that asTF bears an angiogenic potential that acts through a different mechanism when compared to flTF. Earlier small-scale clinical studies indicated a relation between asTF mRNA levels and clinical outcome for several cancer types. Here, to our best knowledge, we are the first to report on the clinicopathologic associations of asTF at protein level in breast cancer using a large patient cohort with a long follow-up. Further, we were able to distinguish between TF isoforms by use of two isoform-specific antibodies. Moreover, we investigated the relative contribution of TF isoforms to breast cancer stem cells identified by ALDH1 expression.

In concordance with some previous small-scale clinical studies, we found both TF isoforms to be abundantly expressed in human breast cancer. A comparison with matched normal tissue from the same patients, led us to conclude that this expression pattern is specific for cancerous epithelia, since expression of both isoforms was considerably lower in normal epithelia. Moreover, asTF expression was almost absent in normal epithelia, further underlining that epithelial asTF expression may be a general phenomenon in breast cancer. Despite the near omnipresence of TF isoforms in breast cancer, we were able to correlate increasing percentages of asTF or flTF positive tumor cells with histological grade. Tumor size was only correlated with asTF, possibly reflecting that asTF has a differential effect on tumor size when compared to flTF.

As previous reports described striking effects of TF isoforms in murine cancer models on survival, we expected that the aforementioned correlations with clinicopathologic characteristics would result in a poor relapse-free and/or overall survival. Indeed, we found an impaired survival for patients with asTF or flTF positive tumors (absolute difference at 10 year follow-up was 6% and 5%, respectively), however, this finding did not reach statistical significance. A likely explanation for this finding is that TF isoforms heavily contribute to tumor growth in early tumorigenesis and are involved in the angiogenic switch, as reported in mouse studies. However, in the current group of patients, who were all operated in the pre-screening era, the process of tumor growth was already passed the stage of the angiogenic switch. Therefore, future research should focus on patients with small, non-palpable breast lumps to further elucidate the role of TF isoforms in human breast cancer tumorigenesis.

Unexpectedly, we observed a specific nuclear staining for asTF. To date, flTF has only been detected on the cell membrane and in the cytoplasm. The latter may reflect a large intracellular stock that can be employed for trafficking of flTF to the cell membrane in (patho)physiological situations when flTF is rapidly needed.[23] Further, the cellular secretion of asTF has been debated[11] and, although secretion of asTF is

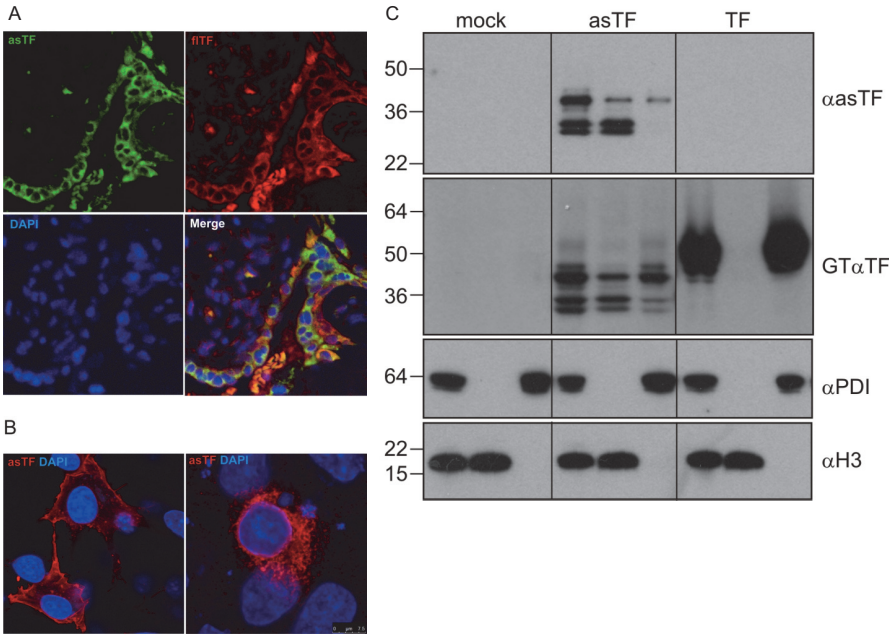


**Figure 5. Subcellular localization of asTF and flTF. A.** Confocal microscopy of TF isoforms in human breast cancer. Limited co-localization of asTF and flTF is found. flTF is located in the cytoplasm and on the cell membrane. asTF signal is most prominent adjacent to the cell's nucleus. **B.** In transfected baby hamster kidney cells, asTF is localized at the perinuclear areas. **C.** Western blot of cellular fractionated mock (left panel) and asTF (middle panel) and flTF (right panel) transfected baby hamster kidney cells demonstrates that asTF was detectable in the nuclear fraction and flTF in the cytoplasmic fraction. (40 kDa is expected weight of fully glycosylated asTF and 36 kDa is expected weight of underglycolyated asTF). Left lane, unfractionated cells. Middle lane, nuclear fraction. Right lane, cytoplasmic fraction. PDI, protein disulfide isomerase, marker of cytoplasmic fration. H3, histone 3, marker of nuclear fraction.

possible after proper stimuli,[24] it is not excluded that asTF accumulates intracellularly and promotes processes other than ligation of extracellular integrins. Future studies may prove an intracellular role for asTF other than its extracellular function of integrin ligation.

In this study, we demonstrated that tumors expressing the breast cancer stem cell marker ALDH1 are correlated with overexpression of flTF and not with asTF overexpression. Cancer stem cells, defined as a small subset of tumor cells with stem cell-like features including epithelial-to-mesenchymal transition, have the capacity of self-renewal and differentiation, giving rise to heterogeneous tumor cell population. Various studies have shown that cancer stem cells are relatively resistant to chemo- and radiotherapy, which might provide opportunities for understanding treatment resistance and tumor dormancy.[25, 26] The cancer stem cell marker ALDH1 expression has shown promise as a clinically relevant prognostic marker in breast cancer.[27-29] The current finding of the relation of flTF and ALDH1 sheds new light on the interaction between the tissue factor/protease activated receptor (TF:VII:PAR2) pathway and

the growth potential of the cancer stem cell subset. These observations are in line with others,[17-19] however, to the best of our knowledge, we are the first to investigate this relationship in breast cancer. Moreover, we demonstrated that asTF expression was not associated with ALDH1 expression. This finding suggests that the role of the asTF/integrin-dependent pathway is of limited, if any, role in the formation and maintenance of the breast cancer stem cell subset. Interestingly, co-expression of flTF and ALDH1 was shown to have a strong synergistic prognostic effect, which implies that flTF:FVII:PAR2 signaling but not asTF-mediated integrin ligation contributes to stem cell function. Recently, we found evidence for a strong age-dependent role of tumor stem cells in breast cancer and this synergistic relation between flTF and stem cells is even more dramatic in breast cancer patients younger than 65 years, whereas this relation inverses above 65 years. How age, the flTF:FVII:PAR2 axis and tumor stem cells mechanistically further relate is unclear, but the strong hormonal influence on flTF and FVII expression is likely to play a major role. In summary, our data suggest that the flTF:FVII:PAR2 pathway is important for the cancer stem cell population in early breast cancer. Therefore, modulation of the activity of this pathway might interfere with the cancer stem cell subset, which may subsequently improve patient survival.

In conclusion, differential TF isoform expression in breast cancer relates to different patient characteristics, which may reflect the different mechanisms of how TF isoforms modulate cancer biology. Targeting both TF isoforms may prove beneficial in early stages of tumor biology by counteracting tumor angiogenesis, especially by targeting asTF since its expression is rather tumor specific. On the other hand, targeting of the flTF:FVII:PAR2 axis may also improve patient outcome since this axis seems to be involved in the small subset of cancer stem cells, which are relatively resistance to current chemotherapeutic and radiotherapeutic regimens.

## REFERENCES

1. Trousseau A. Phlegmasia alba dolens. Clinique médicale de l'Hotel Dieu de Paris 3, 659-712. 1865. Baillière, J.B.
2. Forster Y, Meye A, Albrecht S, et al. Tissue specific expression and serum levels of human tissue factor in patients with urological cancer. Cancer Lett 2003; 193:65-73.
3. Monroe DM, Hoffman M. What does it take to make the perfect clot? Arterioscler Thromb Vasc Biol 2006; 26:41-8.
4. Versteeg HH, Ruf W. Emerging insights in tissue factor-dependent signaling events. Semin Thromb Hemost 2006; 32:24-32.
5. Seto S, Onodera H, Kaido T, et al. Tissue factor expression in human colorectal carcinoma: correlation with hepatic metastasis and impact on prognosis. Cancer 2000; 88:295-301.
6. Yu JL, May L, Lhotak V, et al. Oncogenic events regulate tissue factor expression in colorectal cancer cells: implications for tumor progression and angiogenesis. Blood 2005; 105:1734-41.
7. Schaffner F, Versteeg HH, Schillert A, et al. Cooperation of tissue factor cytoplasmic domain and PAR2 signaling in breast cancer development. Blood 2010; 116:6106-13.
8. Bogdanov VY, Balasubramanian V, Hathcock J, et al. Alternatively spliced human tissue factor: a circulating, soluble, thrombogenic protein. Nat Med 2003; 9:458-62.

9. Censarek P, Bobbe A, Grandoch M, et al. Alternatively spliced human tissue factor asHTF. is not pro-coagulant. Thromb Haemost 2007; 97:11- 4.
10. Szotowski B, Antoniak S, Rauch U. Alternatively spliced tissue factor: a previously unknown piece in the puzzle of hemostasis. Trends Cardiovasc Med 2006; 16:177-82.
11. Boing AN, Hau CM, Sturk A, et al. Human alternatively spliced tissue factor is not secreted and does not trigger coagulation. J Thromb Haemost 2009; 7:1423-6.
12. van den Berg YW, van den Hengel LG, Myers HR, et al. Alternatively spliced tissue factor induces angiogenesis through integrin ligation. Proc Natl Acad Sci USA 2009; 106:19497-502.
13. Goldin-Lang P, Tran QV, Fichtner I, et al. Tissue factor expression pattern in human non-small cell lung cancer tissues indicate increased blood thrombogenicity and tumor metastasis. Oncol Rep 2008; 20:123-8.
14. Rollin J, Regina S, Gruel Y. Tumour expression of alternatively spliced tissue factor is a prognostic marker in non-small cell lung cancer. J Thromb Haemost 2010; 8:607-10.
15. Ribeiro FS, Simao TA, Amoedo ND, et al. Evidence for increased expression of tissue factor and protease-activated receptor-1 in human esophageal cancer. Oncol Rep 2009; 21:1599-604.
16. Hobbs JE, Zakarija A, Cundiff DL, et al. Alternatively spliced human tissue factor promotes tumor growth and angiogenesis in a pancreatic cancer tumor model. Thromb Res 2007; 120:S13-21.
17. Milsom C, Anderson GM, Weitz JI, Rak J. Elevated tissue factor procoagulant activity in CD133-positive cancer cells. J Thromb Haemost 2007; 5:2550-2.
18. Milsom C, Magnus N, Meehan B, et al. Tissue factor and cancer stem cells: is there a linkage? Arterioscler Thromb Vasc Biol 2009; 29:2005-14.
19. Garnier D, Milsom C, Magnus N, et al. Role of the tissue factor pathway in the biology of tumor initiating cells. Thromb Res 2010; 125:S44-S50.
20. van Nes JG, de Kruijf EM, Faratian D, et al. COX2 expression in prognosis and in prediction to endocrine therapy in early breast cancer patients. Breast Cancer Res Treat 2011; 125:671-85.
21. Putter H, Fiocco M, Geskus RB. Tutorial in biostatistics: competing risks and multi-state models. Stat Med 2007; 26:2389-430.
22. Anderson WF, Jatoi I, Devesa SS. Distinct breast cancer incidence and prognostic patterns in the NCI's SEER program: suggesting a possible link between etiology and outcome. Breast Cancer Res Treat 2005; 90:127-37.
23. Mandal SK, Pendurthi UR, Rao LV. Cellular localization and trafficking of tissue factor. Blood 2006; 107:4746-53.
24. Szotowski B, Antoniak S, Poller W, et al. Procoagulant soluble tissue factor is released from endothelial cells in response to inflammatory cytokines. Circ Res 2005; 96:1233-9.
25. Gong C, Yao H, Liu Q, et al. Markers of tumor-initiating cells predict chemoresistance in breast cancer. PLoS One 2010; 5:e15630.
26. Phillips TM, McBride WH, Pajonk F. The response of CD24(-/low)/CD44+ breast cancer-initiating cells to radiation. J Natl Cancer Inst 2006; 98:1777-85.
27. Ginestier C, Hur MH, Charafe-Jauffret E, et al. ALDH1 is a marker of normal and malignant human mammary stem cells and a predictor of poor clinical outcome. Cell Stem Cell 2007; 1:555-67.
28. Resetkova E, Reis-Filho JS, Jain RK, et al. Prognostic impact of ALDH1 in breast cancer: a story of stem cells and tumor microenvironment. Breast Cancer Res Treat 2010; 123:97-108.
29. Tanei T, Morimoto K, Shimazu K, et al. Association of breast cancer stem cells identified by aldehyde dehydrogenase 1 expression with resistance to sequential paclitaxel and epirubicin-based chemotherapy for breast cancers. Clin Cancer Res 2009; 15:4234-41.

# Part II

## Image-guided surgery

# Part IIA

## Intraoperative tumor detection

# Chapter 8

## Novel intraoperative near-infrared fluorescence camera system for optical image-guided cancer surgery

Mieog JSD, Vahrmeijer AL, Hutteman M, van der Vorst JR, Drijfhout van Hooff M, Dijkstra J, Kuppen PJK, Keijzer R, Kaijzel EL, Que I, van de Velde CJH, Löwik CWGM

*Mol Imaging 2010; 9:223-31*

## ABSTRACT

### Introduction

Current methods of intraoperative tumor margin detection using palpation and visual inspection frequently result in incomplete resections, which is an important problem in surgical oncology. Therefore, real-time visualization of cancer cells is needed to increase the number of patients with a complete tumor resection. For this purpose, near-infrared (NIR) fluorescence imaging is a promising technique.

### Methods

Here, we describe a novel hand-held intraoperative NIR fluorescence camera system equipped with a 690 nm laser and validated its utility in detecting and guiding resection of cancer tissues in two syngeneic rat models. The camera system was calibrated using an activated cathepsin-sensing probe (ProSense).

### Results

Fluorescence intensity was strongly correlated with increased activated-probe concentration ($R^2 = 0.997$). During the intraoperative experiments, a camera exposure time of 10 ms was used which provided the optimal tumor-to-background ratio. Primary mammary tumors (N = 20 tumors) were successfully resected under direct fluorescent guidance. The tumor-to-background ratio was 2.34 using ProSense680 at 10 ms camera exposure time. The background fluorescence of abdominal organs in particular liver and kidney was high, thereby limiting the ability to detect peritoneal metastases with cathepsin-sensing probes in these regions.

### Conclusion

In conclusion, using this new camera system, we demonstrated its technical performance and intraoperative utility in guiding resection of tumors.

## INTRODUCTION

The main goal of surgical oncology is the complete and 'en-bloc' excision of tumors with adequate tumor-free margins whilst minimizing surgical morbidity. However, at present, intraoperative assessment of tumor margins is merely based on palpation and visual inspection, which frequently results in incomplete tumor resections (so-called R1 resections). For example, up to 40% of breast cancer patients treated with breast-conserving surgery needs to undergo secondary surgery due to involved tumor margins.[1] The local recurrence rate for primary or hepatic metastasis of colorectal carcinomas is 30-50% after curative intended surgery.[2, 3] Breast and colorectal cancer are amongst the most commonly diagnosed types of cancer worldwide with each type responsible for more than a million new cases and half a million deaths annually.[4] For patients suffering from these cancers, surgery is the cornerstone of curative intended therapy. It is therefore clear that new visualization techniques are needed to facilitate intraoperative assessment of the extent of the cancer tissue and to guide the subsequent surgical removal of these tumors with adequate margins.

Optical imaging using near-infrared (NIR) fluorescence light has recently emerged as a promising technique to visualize cancer cells during surgery.[5-9] Advantages of NIR fluorescence light (700-900 nm) include: high tissue penetration up to several centimeters deep, low autofluorescence providing sufficient signal-to-noise ratio, the current availability of NIR fluorescence probes and labels for conjugation to target tumor-specific molecules, and the insensitivity of human eyes to NIR wavelengths providing no interference with the surgical field.[6] Nonetheless, only a small number of fixed-geometry or hand-held fluorescence imaging systems have been developed with surgical oncology in mind.[10-15] These systems employ either a laser light source[10, 13] or light emitting diodes (LED)[11, 12] for NIR fluorescence excitation. Gutowski *et al.*[10] assessed the technique of intraoperative immunophotodetection using a prototype device (BFP Electronique, France). In this device, a cooled laser diode emitted light at 649 nm through a fiber-optic output. Ke *et al.*[13] used a custom built imaging system for intraoperative tumor detection, which employed two laser diodes at 660 nm (0.7mW/cm$^2$) and 785 nm (1.6mW/cm$^2$). Images were enhanced using an image intensifier tube. Kirsch *et al.*[14] described the use of a handheld device (Siemens Medical Solutions, USA), for which they described the molar detection limit. The Photodynamic Eye (PDE, Hamamatsu Photonics, Japan) uses LEDs and is designed for the detection of the clinically available probe indocyanine green and has been used in several clinical studies on lymph node mapping[12, 16, 17] and tumor imaging.[9] The system provides 1 mW/cm$^2$ of 760 nm excitation light. The FLARE™ imaging system has been used in preclinical[18-20] and clinical studies.[15] This system employs high power, cooled LEDs at 670 nm (4 mW/cm$^2$) and 760 nm (14 mW/cm$^2$) and also uses spectrally separate white light LEDs to illuminate the surgical field. This three-channel approach has the great advantage of displaying the NIR fluorescence signal in direct relation to the anatomical

landmarks by superimposing the NIR fluorescence image on the visible light image. However, the FLARE™ is significantly larger than other, hand-held systems.

All systems use charge-coupled devices (CCD) for signal registration. As the quantum efficiency of CCDs tends to diminish significantly in the NIR spectrum, the choice for a specific CCD is, besides excitation light and quality of optics, of importance for the detection limits of an imaging system. However, technical details such as illuminating power, detection capabilities of the camera, and resolving power are not clearly described for all of the above described camera systems. In order to determine an imaging system's contribution to the field of NIR fluorescence image-guided surgery, a system needs to be analyzed in a well-structured way for its technical capabilities (i.e. NIR excitation light production, detection limits) and its practical use (i.e. ergonomics, sterility).

Here, we describe the Fluobeam®, a novel, hand-held, intraoperative fluorescence camera system. The minimal detection limits, resolving power and intraoperative utility are addressed in primary breast cancer and metastatic colorectal cancer in two syngeneic rat models.

## MATERIAL AND METHODS

### Near-infrared fluorescence camera system

The Fluobeam® system (Fluoptics, Grenoble, France) is composed of a class 3B continuous wave laser (100 mW) emitting at 690 nm (Power Technology, USA) and supplied by a mains supply box (Mascot, Norway) continuously delivering 9V output current with a maximum of 4.5 A. The light from the excitation source is scattered using a diffuser in order to produce a homogeneous lightened field (6-8 cm diameter, field homogeneity > 30%) with an illumination power of 2.6 mW/cm$^2$. The animal is placed under the laser and illuminated by white light (Photonic Optics, China) filtered with a band-pass filter (350-650 nm) providing an irradiance of 7x10$^3$ lx at the animal level. The fluorescence signal is collected through a long pass filter (> 700 nm, OD-value at 690 nm is 3.5) by a digital 12-bit CCD camera (PCO Imaging, Germany) using a fixed-focus objective (Schneider Optische Werke GmbH, Germany). Camera exposure times are adjustable between 1 to 1000 ms. Camera exposure times of 10 ms and 20 ms provided the best contrast between tumor and background during surgical exploration for ProSense680 and ProSense750, respectively, and were used during both the *in vitro* and the *in vivo* part of this study. The spatial resolution of the Fluobeam is 0.17 mm/pixel at focus point. The resolving power of the system is 2.52 line pairs per mm, as determined using the USAF 1951 Target. The laser, the filtered white light illumination and the camera are suspended on a multi-angle adjustable arm which is positioned 20 cm above the point of focus allowing sufficient space for

surgical maneuvers (Figure 1). The system is operated by a desktop computer and the fluorescence signal is displayed in real-time on the computer screen.

### NIR fluorescence probe

The NIR fluorescence probes ProSense680 and ProSense750 (VisEn Medical, Woburn, USA) with peak absorbance of 680 and 750 nm, respectively, were used for fluorescent imaging. ProSense is an autoquenched fluorescent probe that converts from a non-fluorescent to a fluorescent state by proteolytic activation of lysosomal cysteine or serine proteases like cathepsin-B.[21]

### Calibration of camera system

For calibration of the Fluobeam camera system, 2 nmol Prosense (150 µl) was activated with 100 µl 0.25% trypsin-EDTA at 37 °C for 1 h.[14] The cleaved probe was diluted to a concentration of 128 nM and diluted 10 times on the ratio 1:2 in phosphate buffered saline and aliquoted into a 96 wells plate (Greiner Bio-one, #655090, suitable for fluorescent measurements). Subsequently, the samples were imaged with the Fluobeam at various camera exposure times. The experiment was performed for both ProSense680 and ProSense750. Phosphate buffered saline was used as negative control. In order to confirm the accuracy of dilution, the same samples were measured using the Odyssey NIR fluorescence scanning device (LI-COR Biosciences, USA).

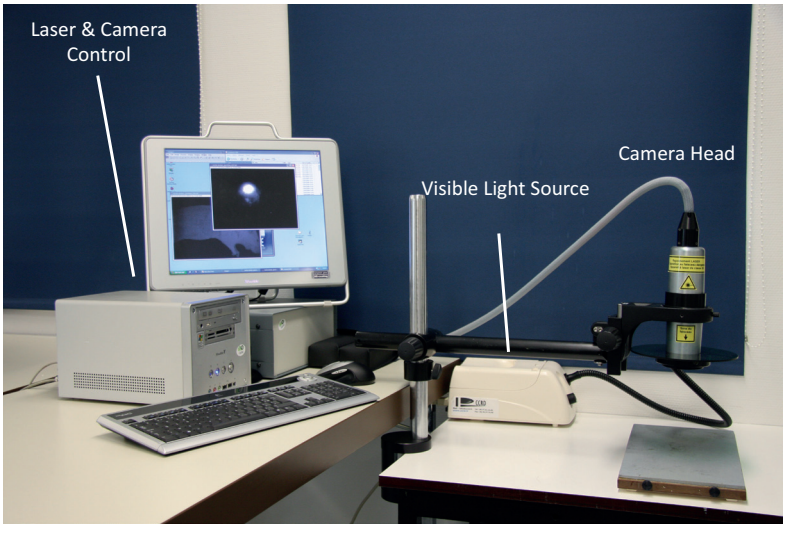


**Figure 1. The Fluobeam® intraoperative near-infrared camera system**

## Cell line experiments

The syngeneic MCR86 breast cancer rat cell line and the syngeneic CC531 colorectal cancer cell line were used for cell line experiments.[22, 23] Tumor cells were cultured in RPMI 1640 supplemented with 2 mM L-glutamine (Gibco, USA), 10% heat-inactivated fetal calf serum, 100 U/ml penicillin and 0.1 mg/ml streptomycin sulphate. Cells were harvested with a solution of 0.25% (w/v) EDTA and 0.25% (w/v) trypsin in HBSS (Sigma, St. Louis, MO, USA).

In order to determine the minimal number of tumor cells that could be detected, MCR86 and CC531 tumor cells were cultured in T75 culture flasks up to ¾ confluence and incubated in 20 ml medium with 10 nM ProSense680. After 24 h incubation with ProSense680, cells were washed, harvested as described above, washed in medium and adjusted to a suspension containing $1x10^6$ tumor cells per ml. This suspension was diluted 7 times on the ratio 1:2 in medium and aliquoted in 1.5 ml tubes. Tubes were centrifuged at 13,000 rpm for 5 minutes to generate cell pellets. Subsequently, the cell pellets were imaged with the Fluobeam at 10 ms camera exposure time. Tumor cells incubated with medium only served as negative control. This experiment was repeated three times for both the MCR86 and CC531 cell lines.

## Animal models

### *EMR86 breast cancer rat model*

The syngeneic transplantable EMR86 breast cancer model originated in a female WAG/Rij rat bearing a subcutaneously implanted estrogen pellet and is related to the MCR86 cell line. This model is developed by our research group.[24] Tumors are only induced and maintained in rats carrying estrogen pellets, whereas tumors transplanted into non-estrogenized animals never grow out. Fresh EMR86 tumor fragments of 1 $mm^3$ were subcutaneously implanted into the mammary fat pads at four sites in 4-6 months old female WAG/Rij rats (Charles River, the Netherlands). Simultaneously, an estrogen pellet was implanted subcutaneously in the intrascapular region of the neck. The in-house generated pellets consist of 2 by 3 mm silicone tubes containing 1.5 mg 17 beta-estradiol on a 1:3 cholesterol/ paraffin basis. Tumor volumes were estimated using digital calipers by measuring three orthogonal diameters of the tumor and multiplying this product by pi/6. After four weeks, tumors had reached of volume of approximately 1 $cm^3$.

### *CC531 colorectal cancer rat model*

In order to induce CC531 peritoneal metastases, CC531 cells were harvested as described above, washed three times in phosphate buffered saline and adjusted to a

suspension containing 2 x $10^6$ viable (trypan blue exclusion test) tumor cells per ml. The peritoneal cavity was inoculated with 2 x $10^6$ cells in 6-months old male WAG/Rij rats (Charles River, the Netherlands).[25] Two weeks after inoculation, small metastases of approximately 2 mm in diameter have originated in the abdominal cavity.

**Animal experiments**

All animals were housed in the animal facility of the Leiden University Medical Center. Pellet food and fresh tap water were provided *ad libitum*. The weight of the animals was followed throughout the experiment to monitor their general health state. Throughout imaging and surgical procedures, the animals were anesthetized with 5% isoflurane for induction and 2% isoflurane for maintenance in oxygen with a flow of 0.8 L/min and placed on animal bed with integrated nose mask. The Animal Welfare Committee of the Leiden University Medical Center approved these studies.

Rats were injected with ProSense (i.v., 10 nmol per animal) 24 hours before imaging. Before injection, autofluorescence of tumors, surrounding tissue and abdominal organs was determined. Rats were shaved to reduce absorption of the optical signal by fur. Animals were anesthetized with isoflurane as described above. Ethanol 70% was used as a disinfectant. EMR86 mammary tumors were removed by making an incision ventrally of the tumor and carefully dissecting the tumor with direct guidance of the real-time fluorescent signal. For the detection of CC531 intra-peritoneal metastases, a median laparotomy was performed followed by a systematic exploration of the small and large bowel along with the mesentery and peritoneal cavity. Metastases identified clinically or by fluorescence were carefully excised. Fluorescent intensity of tumors and abdominal organs was determined *in vivo* and *ex vivo* using the Fluobeam. Excised tumors were snap frozen in isopentane and stored at -80 °C or fixed in formaline and embedded in paraffin (FFPE) blocks. Frozen tissue sections of 20 μm or FFPE tumor sections of 4 μm were air-dried and stained with hematoxylin and eosin.

**Statistical analysis**

Fluobeam derived NIR fluorescence data were analyzed using the open-source software ImageJ by drawing regions of interest and measuring the fluorescent intensity of the 12-bit images.[26] For determination of detection limits, the fluorescent intensity of test samples was divided by the fluorescent intensity of the negative control. A ratio higher then 2 was considered as discriminative. For the animal experiments, regions of interest were drawn at the tumor and at the surrounding tissue within a range of 2 mm of the demarcation line of the tumor and the surrounding tissue. Statistical analysis and generation of graphs was performed using GraphPad Prism software (version 5.01, California, USA). Unless otherwise stated, mean fluorescent intensity

and associated standard deviations were reported. Pearson's correlation coefficients $R^2$ were used for the *in vitro* experiments. Unpaired and paired *t*-tests were used for testing differences of continuous variables between groups. Statistical tests were two-tailed and $P < .05$ was considered significant.

# RESULTS

## Calibration of camera system

Trypsin-activated ProSense680 and ProSense750 were used to calibrate the Fluobeam camera system (Figure 2A). Fluorescent intensity was linearly correlated with the concentration of activated ProSense680 and ProSense750 (correlation coefficient $R^2 = 0.997$ and 0.997, respectively). The dilution accuracy was confirmed using the Odyssey NIR fluorescence scanning device for both ProSense680 ($R^2 = 0.995$) and ProSense750 ($R^2 = 0.995$). At similar Fluobeam camera exposure times, fluorescent intensity of ProSense680 was on average 2.6 times higher than the fluorescent intensity of ProSense750. This reflects the better matching of the absorbance peak of ProSense680 with the 690 nm emitted by the laser of the Fluobeam. Therefore, ProSense680 was used in subsequent *in vitro* experiments. Camera exposure time was linearly correlated with fluorescent intensity ($R^2$ ranged between 0.997 and 1 for the different concentrations), indicating linearity of the camera system. During the *in vivo* experiments, the optimal fluorescent signal for tumor identification without saturated pixels was obtained at 10 ms camera exposure time. Therefore, a 10 ms camera exposure time was used during subsequent *in vitro* experiments using ProSense680. In order to quantify the sensitivity of the camera system, the minimal detectable concentration of

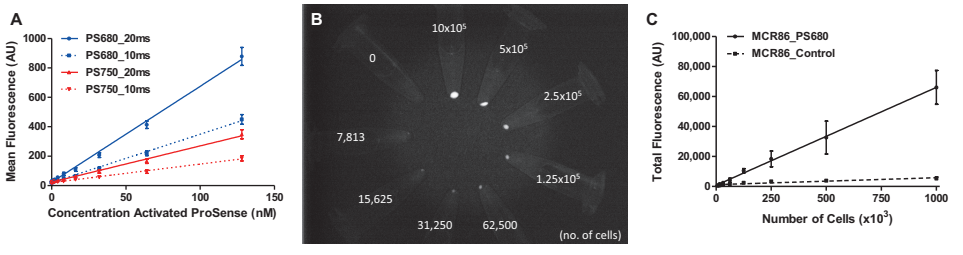


**Figure 2. Calibration of the Fluobeam® camera system. A.** The concentration of trypsin-activated ProSense680 and ProSense750 is plotted against the mean fluorescent intensity at 10 and 20 ms camera exposure times. **B.** NIR fluorescence Fluobeam image showing 1.5 ml tubes containing cell pellets of various amounts of cells of the MCR86 breast cancer cell line after 24 h incubation with 10 nM ProSense680. Camera exposure time was 10 ms. **C.** The number of MCR86 cells incubated with 10 nM ProSense680 is plotted against the total fluorescent intensity at 10 ms camera exposure time.

ProSense680 was determined at 10 ms camera exposure time, mimicking the *in vivo* situation. A signal-to-background ratio was calculated with phosphate buffered saline as background. A ratio of 2 was used as the cut-off. At these settings, the minimal detectable concentration of trypsin-activated ProSense680 was 9.3 ± 0.1 nM (Figure 2A). Therefore, a concentration of 10 nM was used in subsequent cell line experiments.

## Cell line experiments

In order to determine the minimal number of tumor cells that could be detected with the Fluobeam and ProSense680, cultured MCR86 and CC531 tumor cells were incubated in medium with 10 nM ProSense680. After 24 hours incubation, cells were aliquoted in 1.5 ml tubes at various cell concentrations, spun down and imaged with the Fluobeam (Figure 2B). The total fluorescence of the cell pellets was linearly correlated with the number of cells at 10 ms camera exposure time for both MCR86 ($R^2$ = 0.952; Figure 2C) and CC531 ($R^2$ = 0.989; data not shown). To determine the minimal detection limit, a signal-to-background ratio was calculated with medium only as background. A ratio of 2 was used as the cut-off. At 10 ms camera exposure time, the minimal detection limit of the Fluobeam was 20,400 ± 9,200 MCR86 cells and 12,800 ± 2,700 CC531 cells (data not shown). Cell pellets containing 20,000 cells are approximately 0.2 mm$^3$, reflecting sub-mm metastases.

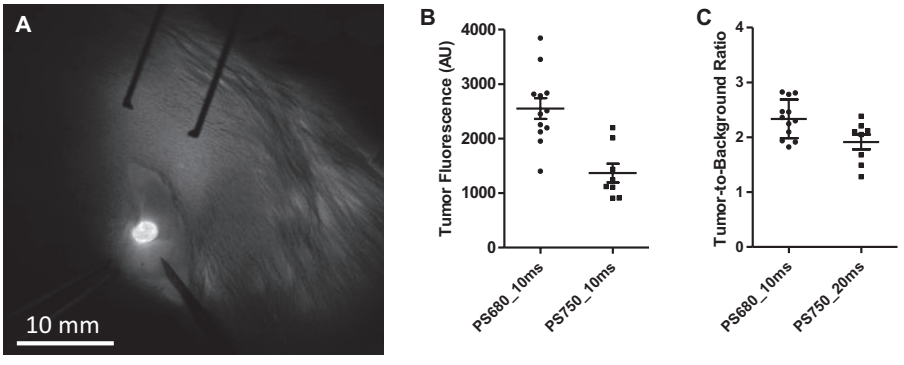


**Figure 3. Intraoperative NIR fluorescence guided resection of primary breast cancer using the Fluobeam® camera system. A.** NIR fluorescence image showing the intraoperative view of a 3.5-mm EMR86 breast tumor in a female rat 24 h after administration of 10 nmol ProSense680. Camera exposure time was 10 ms. **B.** The mean fluorescent intensity of breast tumors is plotted for ProSense680 (N = 12 tumors, 3 rats) and ProSense750 (N = 8 tumors, 3 rats). Camera exposure time was 10 ms. Horizontal lines represent mean ± SD. Fluorescent signal of the tumors was higher with ProSense680 than with ProSense750 ($t$ = 4.33, $P$ = .0004). **C.** The tumor-to-background ratio is plotted for both ProSense680 (N = 12 tumors, 3 rats) and ProSense750 (N = 8 tumors, 3 rats) for the camera exposure times that provided the optimal tumor-to-background ratio during surgery: 10 ms for ProSense680 and 20 ms for ProSense750. Horizontal lines represent mean ± SD. Tumor-to-background ratio was significantly higher for ProSense680 when compared to ProSense750 ($t$ = 2.53, $P$ = .021).

## Intraoperative imaging

*Primary breast cancer*

The syngeneic EMR86 breast cancer rat model was used to test the intraoperative application of the Fluobeam camera system. Primary breast tumors were induced in six female rats in the mammary fat pad. Twenty tumors were induced varying in size from 0.08 to 4.19 $cm^3$ (mean = 0.77 $cm^3$ ± 1.4). All tumors were successfully detected and resected under direct fluorescence guidance 24 hours after injection with ProSense680 (N = 12 tumors) or ProSense750 (N = 8 tumors, Figure 3). In concordance with the *in vitro* data, the fluorescent signal of the tumors was higher with ProSense680 (mean = 2552 ± 659.4) than with ProSense750 (mean = 1367 ± 489.9; $t = 4.33$, $P = .0004$; Figure 3B) at a 10 ms camera exposure time. During surgery, an optimal fluorescent contrast between tumor (unsaturated signal) and surrounding mammary fat pad was obtained using a 10 ms camera exposure time for ProSense680 and 20 ms for ProSense750. The signal of ProSense680 was stronger due to better matching with the 690 nm laser, as

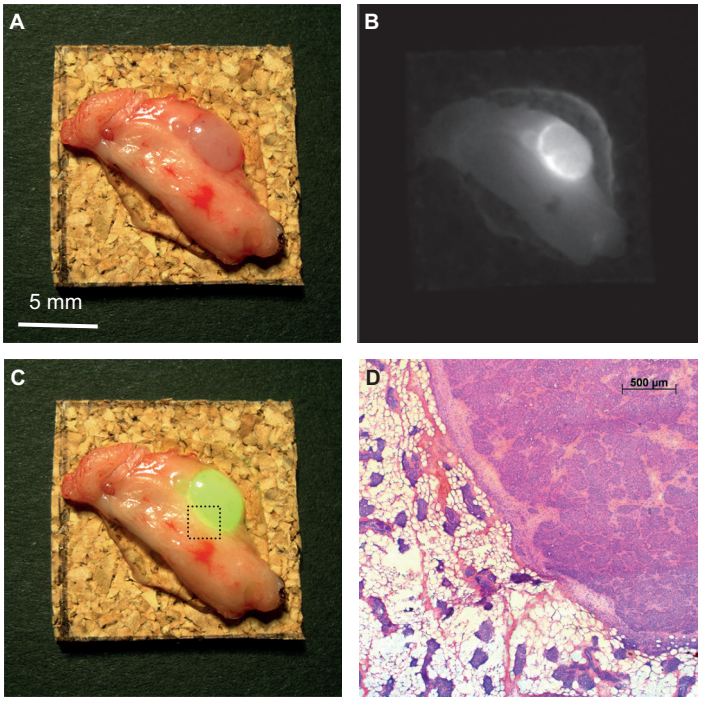


**Figure 4. NIR fluorescence imaging of excised primary breast cancer using the Fluobeam® camera system.** Shown are a color image (**A**), a NIR fluorescence image (**B**), and a pseudocolored green merge of the two images (**C**) of a sectioned 4-mm EMR86 breast tumor with surrounding mammary fat pad. The tumor was excised from a rat, which was injected with10 nmol ProSense680 24 h prior to imaging. Camera exposure time was 10 ms. **D.** H&E histological staining of a 20 µm frozen tissue section of the specimen from Figure 4C. Shown is the region indicated by the dashed square (25x magnification).

discussed above. Although the fluorescent intensity of tumor tissue was significantly higher than the surrounding mammary fat pad with both ProSense680 (paired $t$ = 12.52, $P$ < .0001, N = 12 tumors) and ProSense750 (paired $t$ = 6.29, $P$ = .0004, N = 8 tumors) using these camera exposure times, the tumor-to-background ratio was significantly higher for ProSense680 (2.34 ± 0.35) when compared to ProSense750 (1.91 ± 0.38; $t$ = 2.53, $P$ =.021; Figure 3C).

*Breast tumor margins*

In order to visualize the fluorescence of tumor margins, excised breast tumors were sectioned, imaged with the Fluobeam and processed for histopathology. In Figure 4, a typical example of a 4 mm large excised breast tumor is presented. A distinctive difference in fluorescence of the tumor tissue and surrounding mammary fat pad is shown which is confirmed in a fresh frozen tissue section after hematoxylin and eosin staining.

*Metastatic abdominal cancer*

To assess if the use of a protease-activatable probe could be used in tumor types located in the abdominal cavity, the fluorescence intensity of abdominal organs relevant in cancer surgery was measured with the Fluobeam in three rats before and after injection with ProSense680. Figure 5 demonstrates that liver, kidney, spleen, small bowel and

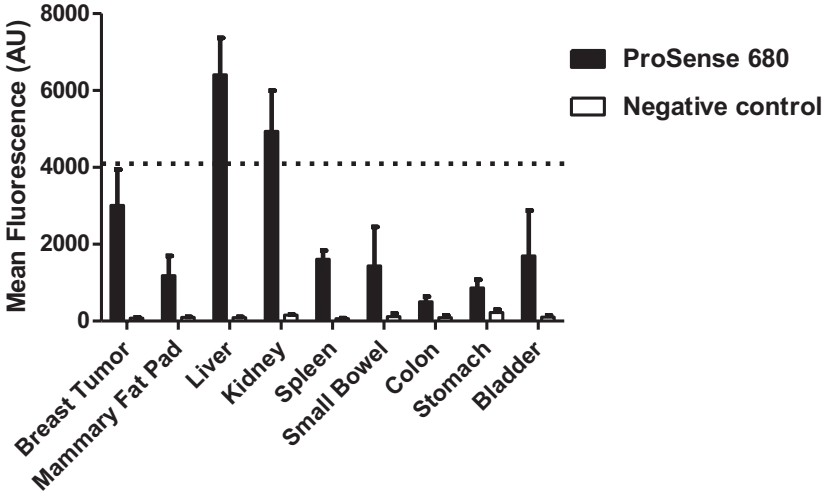


**Figure 5. *In vivo* fluorescence intensity of EMR86 breast tumors and abdominal organs.** Fluorescent intensity was measured using the Fluobeam® camera system in three rats bearing EMR86 breast tumors before and 24 h after administration of 10 nmol ProSense680. Camera exposure time was 10 ms. Bars represent mean ± SD. The signal for liver and kidney was saturated at 10 ms camera exposure times (dashed line). The plotted values are extrapolated from the non-saturated measurements at 5 ms camera exposure time.

bladder provide very high background fluorescence after injection of ProSense680. The fluorescent intensity of liver tissue was 69 times higher than in control rats ($t$ = 8.85, $P$ = .003) reflecting the high intrinsic cathepsin B activity of hepatocytes.[27] Also, the signal in the kidney was 32 times higher in the ProSense680 rats, particularly in the renal cortex, due to the intrinsic cathepsin B activity and the renal clearance of the probe ($t$ = 6.06, $P$ = .009).[28] Similar results were obtained with ProSense750.

These results suggest that protease-activatable probes are less useful for image-guided surgery of abdominally located tumors or metastases regardless of the protease activity and associated fluorescent intensity of those tumors.

To test the assumption that the use of ProSense in detecting abdominal tumors is limited, the syngeneic CC531 colorectal cancer rat model was used to induce intra-peritoneal tumors. Figure 6 shows a typical example of a rat bearing intra-peritoneal CC531 metastases imaged with the Fluobeam after injection with ProSense750. Although small peritoneal metastases could be detected on the mesentery of the small bowel (Figure 6A-B), one can not be sure to detect metastases in all parts of the bowel and in particular at the liver and kidney due to the high background fluorescence, as illustrated in Figure 6C.

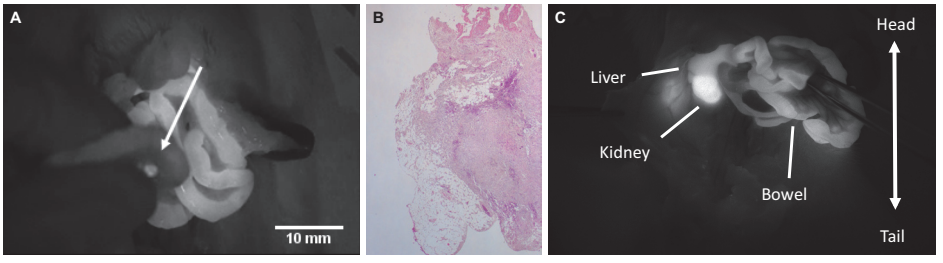


**Figure 6. Intraoperative NIR fluorescence imaging of colorectal CC531 peritoneal metastases using ProSense and the Fluobeam® camera system. A.** NIR fluorescence image showing a 3-mm fluorescent hotspot (arrow) located on the mesentery of the small bowel in a male rat injected with 10 nmol ProSense750. Camera exposure time was 20 ms. **B.** Corresponding H&E-stained formaline-fixed paraffine-embedded 4 µm tissue section confirms the presence of CC531 tumor cells (original magnification 25x). **C.** Intraoperative NIR fluorescence image showing the background fluorescence of the liver, kidney and small bowel in the same animal. Camera exposure time was 20 ms.

## DISCUSSION

A highly promising new development in surgical oncology is image-guided tumor resection using NIR fluorescenc imaging. The extent of the primary tumor as well as sites of regional disseminated disease can be detected in real-time. Using this new information, the surgical procedure can directly be adapted. Moreover, this technique provides a direct assessment of the resection plane after tumor removal to detect any residual cancer tissue, thereby reducing the number of patients with incomplete tumor resections. However, NIR fluorescence imaging with tumor-specific probes has not

been evaluated in humans. The main target of ProSense, the cysteine protease family (in particular cathepsin B) is upregulated in various human cancers including breast and colorectal cancer.[29-32] In the current pre-clinical study, we described the performance of a novel hand-held, intraoperative NIR fluorescence camera system based on a 690 nm laser and demonstrated its utility in detecting and guiding resection of primary and metastatic rat tumors using the cathepsin-activatable probe ProSense. Because the family of proteases is strongly conserved amongst mammals, it is expected that ProSense will be applicable for cancer patients.[29]

The efficacy of NIR fluorescence camera systems is determined by the interplay between the type of probe used, the probe concentration, tumor size and the camera exposure time. In this study, the cathepsin-activatable probe ProSense680 and ProSense750 were used to test the 690 nm laser-based Fluobeam camera system. Because of the better matching of ProSense680 with the 690 nm laser, the fluorescent signal was significantly higher using ProSense680 (Figure 2A). During the intraoperative experiments, 10 ms camera exposure time was found to be optimal in terms of tumor-to-background ratio for ProSense680. When assessed *in vitro*, the minimal detectable ProSense680 concentration at 10 ms camera exposure time was approximately 10 nM (Figure 2A). The minimal detectable number of tumor cells with 10 nM ProSense680 at 10 ms camera exposure time was approximately 20,000 for a breast cancer cell line and 13,000 for a colorectal cancer cell line. These cell numbers reflect sub-mm tumor depositions. When these settings were applied in the *in vivo* experiments, mammary tumors varying in size from 0.08 to 4.19 $cm^3$ could be detected and subsequently resected under direct fluorescent guidance after administration of 10 nmol ProSense680 with a clear demarcation of tumor margins (Figure 4). Fluorescence reflectance imaging is not inherently quantitative and quantification should always be performed relative to control tissue.[5] In this study, a tumor-to-background ratio of 2.34 was found for ProSense680. Tumor tissue was discriminated from the surrounding tissue by optimal thresholding without any further signal improvement techniques.[33]

In general, the ratio of the fluorescent intensity between tumor and surrounding tissue determines the applicability of protease-activatable probes in NIR fluorescence image-guided cancer surgery. In order to assess the applicability of the cathepsin-sensing probe in intraperitoneal metastases, the fluorescent intensity of abdominal organs were measured after the administration of ProSense680. In several abdominal organs the fluorescent intensity was markedly increased after injection of ProSense (Figure 5). For example, liver, kidney and intestine cells exploit an extensive cathepsin B activity and were highly fluorescent.[27] Therefore, cathepsin-activatable probes seem less useful for image-guided surgery of abdominally located tumors, even if tumors express high levels of cathepsin-B (Figure 6).

The currently available NIR fluorescence camera systems use either a laser[13, 14] or light emitting diode (LED)[11, 12, 19] illumination as a photon source for probe excitation.

The Fluobeam camera system is laser-based, which might possess logistic hurdles in terms of operator safety, although a distance of 18 cm away from the camera head is considered safe. However, LED illumination requires direct cooling at the camera head causing camera heads to be larger. Conversely, a fiber-guided laser source can be cooled outside the camera head, therefore the camera head can be smaller and a true hand-held system can be created. Direct comparison of various camera systems is necessary to test accuracy and efficacy parameters such as minimal detection limit, excitation power and signal-to-noise ratio in a standardized way, as presented here. Advantages of the Fluobeam system include its compact size, high resolving power and spatial resolution, user friendly and surgeon-oriented mode of operation, and the fact that the Fluobeam is commercially available. Moreover, the software incorporates the use of a dynamic threshold function, which could enhance the discrimination of tumor and normal tissue. Improvements of the Fluobeam could include the addition of a color video camera for visible light registration, as is already implemented in the LED-based FLARE™ system.[15]

Several new developments in optical imaging, such as fluorescence lifetime imaging,[34] frequency domain imaging and spatially modulated structured light[35] have the potential to increase tissue penetration and discriminatory power between fluorophores. These techniques are able to improve localization of an NIR fluorescence signal source and improve quantification of the fluorescence signal. These developments are expected to be integrated in intraoperative NIR fluorescence imaging devices within the next few years.

In conclusion, the ultimate goal of NIR fluorescence imaging is to provide surgical oncologists with a real-time tumor imaging technique to guide surgery for the complete and safe resection of cancer tissue. In this study, we described the technical details and performance of the Fluobeam intraoperative NIR fluorescence camera system. By using the Fluobeam and the activatable probe ProSense, we demonstrated that it is possible to resect tumors under fluorescence guidance. If these techniques will become available for clinical cancer treatment, surgical oncology will make a major step forward.

## ACKNOWLEGDEMENT

We want to thank Fluoptics (Grenoble, France) for providing us with the Fluobeam® system to perform the above described experiments and Gabi van Pelt for technical assistance. This study was performed within the framework of CTMM, the Center for Translational Molecular Medicine. DeCoDe project (grant 03O-101). This study was supported by the Sacha Swarttouw-Hijmans Foundation. J.S.D. Mieog is a MD-medical research trainee funded by the The Netherlands Organisation for Health Research and Development (grant nr. 92003526).

## REFERENCES


1. Verkooijen HM, Borel RI, Peeters PH, et al. Impact of stereotactic large-core needle biopsy on diagnosis and surgical treatment of nonpalpable breast cancer. Eur J Surg Oncol 2001; 27:244-9.
2. Nagtegaal ID, van de Velde CJ, Marijnen CA, et al. Low rectal cancer: a call for a change of approach in abdominoperineal resection. J Clin Oncol 2005; 23:9257-64.
3. Finch RJ, Malik HZ, Hamady ZZ, et al. Effect of type of resection on outcome of hepatic resection for colorectal metastases. Br J Surg 2007; 94:1242-8.
4. Ferlay J, Bray F, Pisani P, Parkin D. GLOBOCAN: Cancer Incidence, Mortality and Prevalence Worldwide. 1st edn. Lyon: IARCPress; 2001.
5. Weissleder R, Pittet MJ. Imaging in the era of molecular oncology. Nature 2008; 452:580-9.
6. Frangioni JV. New technologies for human cancer imaging. J Clin Oncol 2008; 26:4012-21.
7. Kaijzel EL, van der Pluijm G, Lowik CW. Whole-body optical imaging in animal models to assess cancer development and progression. Clin Cancer Res 2007; 13:3490-7.
8. Stepp H, Beck T, Pongratz T, et al. ALA and malignant glioma: fluorescence-guided resection and photodynamic treatment. J Environ Pathol Toxicol Oncol 2007; 26:157-64.
9. Ishizawa T, Fukushima N, Shibahara J, et al. Real-time identification of liver cancers by using indocyanine green fluorescent imaging. Cancer 2009; 115:2491-504.
10. Gutowski M, Carcenac M, Pourquier D, et al. Intraoperative immunophotodetection for radical resection of cancers: evaluation in an experimental model. Clin Cancer Res 2001; 7:1142-8.
11. De Grand AM, Frangioni JV. An operational near-infrared fluorescence imaging system prototype for large animal surgery. Technol Cancer Res Treat 2003; 2:553-62.
12. Kitai T, Inomoto T, Miwa M, Shikayama T. Fluorescence navigation with indocyanine green for detecting sentinel lymph nodes in breast cancer. Breast Cancer 2005; 12:211-5.
13. Ke S, Wen X, Gurfinkel M, et al. Near-infrared optical imaging of epidermal growth factor receptor in breast cancer xenografts. Cancer Res 2003; 63:7870-5.
14. Kirsch DG, Dinulescu DM, Miller JB, et al. A spatially and temporally restricted mouse model of soft tissue sarcoma. Nat Med 2007; 13:992-7.
15. Troyan SL, Kianzad V, Gibbs-Strauss SL, et al. The FLARE intraoperative near-infrared fluorescence imaging system: a first-in-human clinical trial in breast cancer sentinel lymph node mapping. Ann Surg Oncol 2009; 16:2943-52.
16. Murawa D, Hirche C, Dresel S, et al. Sentinel lymph node biopsy in breast cancer guided by indocyanine green fluorescence. Br J Surg 2009; 96:1289-94.
17. Noura S, Ohue M, Seki Y, et al. Feasibility of a lateral region sentinel node biopsy of lower rectal cancer guided by indocyanine green using a near-infrared camera system. Ann Surg Oncol 2010; 17:144-51.
18. Soltesz EG, Kim S, Kim SW, et al. Sentinel lymph node mapping of the gastrointestinal tract by using invisible light. Ann Surg Oncol 2006; 13:386-96.
19. Tanaka E, Choi HS, Fujii H, et al. Image-guided oncologic surgery using invisible light: completed pre-clinical development for sentinel lymph node mapping. Ann Surg Oncol 2006; 13:1671-81.
20. Matsui A, Lee BT, Winer JH, et al. Image-guided perforator flap design using invisible near-infrared light and validation with x-ray angiography. Ann Plast Surg 2009; 63:327-30.
21. Weissleder R, Tung CH, Mahmood U, Bogdanov A, Jr. In vivo imaging of tumors with protease-activated near-infrared fluorescent probes. Nat Biotechnol 1999; 17:375-8.
22. Marquet RL, Westbroek DL, Jeekel J. Interferon treatment of a transplantable rat colon adenocarcinoma: importance of tumor site. Int J Cancer 1984; 33:689-92.
23. van Dierendonck JH, Keijzer R, Cornelisse CJ, et al. Surgically induced cytokinetic responses in experimental rat mammary tumor models. Cancer 1991; 68:759-67.
24. Wijsman JH, Cornelisse CJ, Keijzer R, et al. A prolactin-dependent, metastasising rat mammary carcinoma as a model for endocrine-related tumour dormancy. Br J Cancer 1991; 64:463-8.
25. Lopes Cardozo AM, Gupta A, Koppe MJ, et al. Metastatic pattern of CC531 colon carcinoma cells in the abdominal cavity: an experimental model of peritoneal carcinomatosis in rats. Eur J Surg Oncol 2001; 27:359-63.
26. Rasband WS. ImageJ, U. S. National Institutes of Health, Bethesda, Maryland, USA, http://rsb.info.nih.gov/ij/. 2009.

27. Keppler D, Walter R, Perez C, et al. Increased expression of mature cathepsin B in aging rat liver. Cell Tissue Res 2000; 302:181-8.
28. Todorov V, Muller M, Kurtz A. Differential regulation of cathepsin B and prorenin gene expression in renal juxtaglomerular cells. Kidney Blood Press Res 2001; 24:75-8.
29. Mohamed MM, Sloane BF. Cysteine cathepsins: multifunctional enzymes in cancer. Nat Rev Cancer 2006; 6:764-75.
30. Harbeck N, Alt U, Berger U, et al. Prognostic impact of proteolytic factors (urokinase-type plasminogen activator, plasminogen activator inhibitor 1, and cathepsins B, D, and L) in primary breast cancer reflects effects of adjuvant systemic therapy. Clin Cancer Res 2001; 7:2757-64.
31. Parker BS, Ciocca DR, Bidwell BN, et al. Primary tumour expression of the cysteine cathepsin inhibitor Stefin A inhibits distant metastasis in breast cancer. J Pathol 2008; 214:337-46.
32. Kuester D, Lippert H, Roessner A, et al. The cathepsin family and their role in colorectal cancer. Pathol Res Pract 2008; 204:491-500.
33. Rosenfeld A, Kak A. Digital picture processing. 2nd edn. New York: Academic Press; 1982.
34. Kumar AT, Raymond SB, Bacskai BJ, et al. Comparison of frequency-domain and time-domain fluorescence lifetime tomography. Opt Lett 2008; 33:470-2.
35. Gioux S, Mazhar A, Cuccia DJ, et al. Three-dimensional surface profile intensity correction for spatially modulated imaging. J Biomed Opt 2009; 14:034045.

# Chapter 9

# Image-guided tumor resection using real-time near-infrared fluorescence in a syngeneic rat model of primary breast cancer

Mieog JSD, Hutteman M, van der Vorst JR, Kuppen PJK, Que I, Dijkstra J, Kaijzel EL, Prins F, Löwik CWGM, Smit VTHBM, van de Velde CJH, Vahrmeijer AL

*Breast Cancer Res Treat 2011; 128:679-89*

## ABSTRACT

### Introduction

Tumor involvement of resection margins is found in a large proportion of patients who undergo breast-conserving surgery. Near-infrared (NIR) fluorescence imaging is an experimental technique to visualize cancer cells during surgery.

### Methods

To determine the accuracy of real-time NIR fluorescence imaging in obtaining tumor-free resection margins, a protease-activatable NIR fluorescence probe and an intraoperative camera system were used in the EMR86 orthotopic syngeneic breast cancer rat model.

### Results

Influence of concentration, timing and number of tumor cells were tested in the MCR86 rat breast cancer cell line. These variables were significantly associated with NIR fluorescence probe activation. Dosing and tumor size were also significantly associated with fluorescence intensity in the EMR86 rat model, whereas time of imaging was not. Real-time NIR fluorescence guidance of tumor resection resulted in a complete resection of 17 out of 17 tumors with minimal excision of normal healthy tissue (mean minimum and a mean maximum tumor-free margin of 0.2 ± 0.2 mm and 1.3 ± 0.6 mm, respectively). Moreover, the technique enabled identification of remnant tumor tissue in the surgical cavity. Histological analysis revealed that the NIR fluorescence signal was highest at the invasive tumor border and in the stromal compartment of the tumor.

### Conclusion

NIR fluorescence detection of breast tumor margins was successful in a rat model. The present study suggests that clinical introduction of intraoperative NIR fluorescence imaging has the potential to increase the number of complete tumor resections in breast cancer patients undergoing breast-conserving surgery.

## INTRODUCTION

Incomplete tumor resections are an important clinical problem in breast cancer surgery. Tumor involvement of resection margins is found in 5-40% of patients who undergo breast-conserving surgery and these patients require additional surgery or intensified radiotherapy.[1-4] Furthermore, additional biopsies of the surgical cavity after primary resection have been shown to contain residual disease in 10% of patients with tumor-free specimen margins.[5] As a result, 5-year isolated local recurrences rates of 6.7-11% are reported in patients with tumor-free specimen margins treated with breast-conserving surgery and radiotherapy.[6] The occurrence of local relapse reduces the 15-year breast cancer specific and overall survival.[6] Consequently, increase of the radical resection rate will likely improve breast cancer outcome. Intraoperative real-time visualization of cancer cells is a promising method to achieve that goal.[7]

Near-infrared (NIR) fluorescence imaging is an experimental technique that can be used to visualize cancer cells during surgery. In current surgical practice, surgeons can only rely on palpation and visual inspection. Therefore, the use of NIR fluorescence imaging can be of great value, as already demonstrated in patients with glioma and liver cancer.[8-10] Advantages of NIR fluorescence light (700-900nm) include high tissue penetration (up to several centimeters deep) and low autofluorescence providing sufficient signal-to-background ratio.[11] Moreover, as the human eye is insensitive to NIR wavelengths, the use of NIR light will not interfere with the surgical field.

NIR fluorescence probes can target tumor cells through several mechanisms. For example, fluorophores can be conjugated to a tumor-specific antibody (e.g. directed to the Her-2/neu receptor), labeled to glucose derivates in order to visualize elevated metabolic rate, or autoquenched fluorophores can be activated by enzymatic cleavage in order to become fluorescent. The latter is of particular interest as certain enzyme systems are upregulated by a wide variety of cancer types, thus providing a more universally applicable NIR fluorescence probe. Proteolytic enzymes and in particular cathepsins from the cysteine protease family are a good candidate as they play essential roles in tumor growth, angiogenesis, resistance to apoptosis, and invasion.[12, 13] A member of this family, cathepsin B, is commonly active in the tumor microenvironment in various human cancers including breast cancer.[12, 14-16] Upregulated expression of cathepsin B is found in tumor, endothelial and immune cells, in particular macrophages.[13] Cathepsin B overexpression in human breast carcinomas is associated with poor differentiation, lymph node involvement, absence of estrogen receptor expression and impaired overall survival.[17, 18]

The protease-activatable NIR fluorescence probe ProSense (VisEn Medical, Woburn, USA) has been shown to detect a variety of tumors in nude or transgenic mice.[19-31] However, as tumor progression and metastasis are regulated by the surrounding microenvironment, it is important to use syngeneic animal models

that allow appropriate crosstalk at the invasive tumor border to study probes that are activated by proteolytic activity. Moreover, the use of a larger animal model such as the rat offers more challenges in terms of tissue penetration of NIR fluorescence probes.

Therefore, the aim of this study was to assess the technique of NIR fluorescence imaging in a syngeneic breast cancer rat model using ProSense and to determine the accuracy of intraoperative tumor detection to obtain an adequate tumor-free resection margin.

## MATERIAL AND METHODS

### Breast cancer cell line and culture conditions

The MCR86 cell line is a rapidly growing, syngeneic breast cancer cell line derived after subcutaneous transplantation of macroscopic lung tumors, which developed in a female WAG/Rij rat after intravenous inoculation of MCR83 breast cancer cells.[32] Tumor cells were cultured in RPMI 1640 supplemented with 2 mM L-glutamine (Gibco, Invitrogen Ltd, Carlsbad, USA), 10% heat-inactivated fetal calf serum, 100 U/ml penicillin and 0.1 mg/ml streptomycin sulphate.

### Breast cancer model and tumor induction

The related EMR86 model is a transplantable, hormone-dependent, metastasizing mammary carcinoma that originated in a female WAG/Rij rat bearing a subcutaneously implanted estrogen pellet and is developed by our research group (Figure 1A).[33] Tumors are only induced and maintained in rats carrying estrogen pellets, whereas tumors transplanted into non-estrogenized animals do not grow out. Removal of the estrogen pellet induces apoptosis and tumor regression (Figure 1B). EMR86 tumors are histologically classified as high-grade invasive ductaltype adenocarcinomas, with both a cribiform and a solid growth pattern. In large tumors areas, comedo type necrosis can be appreciated. Tumors have a stromal compartment of approximately 30% depending on tumor size (Figure 1C). EMR86 tumor cells show strong nuclear expression of the estrogen and progesterone receptor in more than 90% of cells, but stain negative for HER2/neu receptor (Figure 1D-F). Therefore, EMR86 tumors closely resemble the luminal A molecular subtype – the most prevalent subtype of human breast cancer.[34, 35]

For tumor induction, fresh EMR86 tumor fragments of 0.5-1 $mm^3$ were implanted in the mammary fat pad at four sites of female WAG/Rij rats (Charles River, Maastricht, the Netherlands) aging 4-6 months. (A stable cell line from EMR86 tumor has not yet been successfully established, therefore, tumor transplantation is used.) During the same session, an estrogen pellet was implanted subcutaneously in

the intrascapular region of the neck. The in-house generated pellets consist of 2 mm by 3 mm silicone tubes containing 1.5 mg 17 β-estradiol on a 1:3 cholesterol/paraffin basis. Tumor volumes were estimated twice weekly using digital calipers by measuring three orthogonal diameters of the tumor and multiplying this product by π/6. All rats were housed in the animal facility of the Leiden University Medical Center. Pellet food and fresh tap water were provided ad libitum. The weight of the animals was followed throughout the experiment to monitor their general health state. The Animal Welfare Committee of the Leiden University Medical Center approved the study. The study was conducted in concordance with the "Guidelines for the Welfare of Animals in Experimental Neoplasia" (Second Edition, 1997) available online at http://www.ncrn.org.uk/csg/animal_guides_text.pdf.

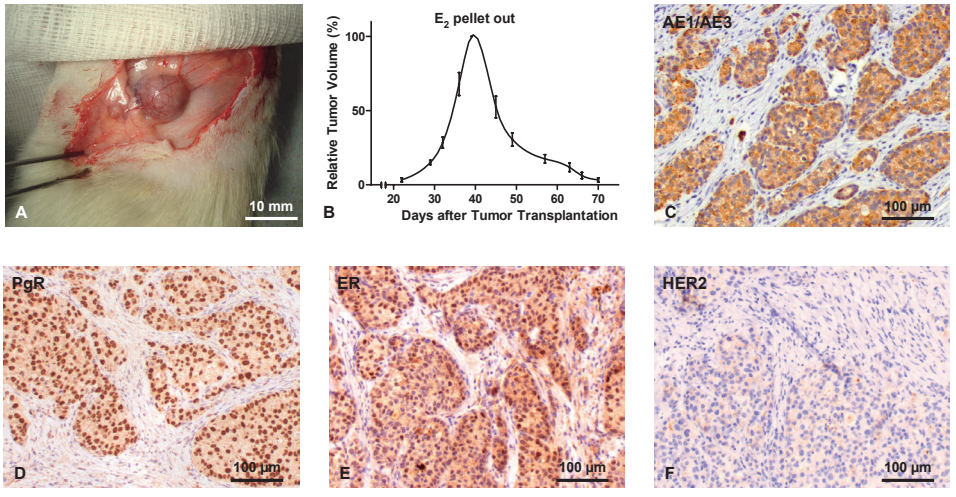


**Figure 1. Description of a syngeneic rat model of hormone-dependent breast cancer. A.** EMR86 breast tumors originate after transplantation of 0.5 mm3 fresh tumor fragments at the mammary fat path of female WAG/Rij rats. Shown is a tumor four weeks after transplantation. **B.** EMR86 tumors are only induced and maintained in rats carrying estrogen pellets. Removal of the estrogen pellet induces apoptosis and tumor regression (N = 16 tumors, 4 rats). **C.** EMR86 tumors are histologically classified as high-grade invasive ductal carcinomas, with both a cribiform and a solid growth pattern. Tumors have a stromal compartment of approximately 30% depending on tumor size. **D-F.** EMR86 tumor cells show strong nuclear expression of the estrogen and progesterone receptor in more than 90% of cells, but stain negative for HER2/neu receptor. Therefore, EMR86 tumors closely resemble the luminal A molecular subtype.

## NIR fluorescence probe

The commercially available, protease-activatable NIR fluorescence probes ProSense680 and ProSense750 were used (VisEn Medical). The probes consist of a synthetic graft polymer composed of poly-L-lysine that is sterically protected by multiple methoxypolyethylene glycol side chains and to which multiple fluorophores are attached.[19] In this non-activated state, the fluorophores are positioned in close proximity to one another, which results in mutual energy transfer and thus inhibition of fluorescence emission. After enzymatic cleavage of the backbone, the fluorophores

are released and regain their fluorescent characteristics. A number of cysteine proteases are involved in this process. Cathepsin B, and to a lesser degree cathepsin K, L, and S, has been demonstrated to be a major contributor to cleavage and activation of ProSense.[19] ProSense680 and ProSense750 have peak absorption of 680 nm and 750 nm, respectively. ProSense680 was selected for intraoperative studies and fluorescence microscopy because of the better matching of the laser of the intraoperative camera system with the peak excitation of ProSense680. ProSense750 was used for cell line experiments and non-invasive animal experiments because of the better spectral separation of autofluorescence signal.

**Intraoperative NIR fluorescence camera system**

The Fluobeam intraoperative NIR fluorescence camera system (Fluoptics, Grenoble, France) used in this study has been described previously by our group.[36, 37] Briefly, the system is composed of a class 3B laser (100 mW) emitting at 690 nm resulting in an illumination power of 2.6 mW/cm$^2$. Filtered white light (350-650 nm) provides an irradiance of 7x10$^3$ lx at the focus level. The emitted fluorescence is collected through a high pass filter (> 700 nm) by a 12 bits CCD camera resulting in a system spatial resolution of 0.17 mm/pixel.

**Experimental design**

*Cell line experiments*

For fluorescence measurements, tumor cells were harvested with a solution of 0.25% (w/v) EDTA and 0.25% (w/v) trypsin in Hanks' Buffered Salt Solution (Sigma-Aldrich, St. Louis, USA), washed three times in 0.9% phosphate buffered saline and 200 µL complete medium suspensions were made and transferred on a 96-well acrylate plate (Greiner Bio-one, Alphen aan de Rijn, the Netherlands, #655090; suitable for fluorescence measurements) and kept at 37 °C and 5% $CO_2$. At day 2, cells were washed and autoquenched ProSense750 (22.5 to 180 nM, 200 µl) was added. At day 3, cells were washed and 200 µl complete medium was added. Also, time-dependent studies were performed, during which ProSense750 was added at the indicated time-points (8 to 48 h). Fluorescence intensity was measured using the Odyssey NIR fluorescence scanning device (LI-COR Biosciences, Lincoln, USA). Overlying grids were drawn and fluorescence intensity was measured for each well using the Odyssey software (Version 2.1).

*Animal experiments*

Throughout injection, imaging and surgical procedures, rats were anaesthetized with inhalation of 2% mixture of isoflurane in oxygen. The rats were constantly monitored for the rate of the respiration and depth of anesthesia. Before imaging, rats were shaved to reduce absorption of the optical signal. A total of 20 rats bearing 77 primary mammary tumors varying in size from 0.01 to 1.8 $cm^3$ were used in this study.

In a dose- and time-dependent experiment, tumor-bearing rats (N = 9) were randomly assigned over three ProSense750 dose groups and intravenously injected with 2.5, 5 or 10 nmol ProSense750 (150 µl). Whole-body fluorescence was measured 24 h and 48 h after administration of ProSense750 using the IVIS Spectrum (Caliper LifeSciences, Hopkinton, USA), which allowed separation of the ProSense750 signal from the background fluorescence by means of spectral unmixing.[38] Acquisition settings were kept constant for the different dose groups and on the two consecutive days. Total photon counts per second were measured for each tumor using the Living Image software (Version 3.0, Caliper LifeSciences) and divided by the tumor volume as assessed by digital caliper measurement.

In an intraoperative experiment, tumor-bearing rats (N = 7) were operated under direct fluorescence guidance 24 h after intravenous administration of 10 nmol ProSense680 (150 µl). NIR fluorescence intensity of exposed tumors and surrounding tissues was measured with the Fluobeam intraoperative camera system. Tumor-to-background ratios were calculated by drawing regions of interest at the tumor and at the surrounding tissue by visual interpretation and subsequent measurement of fluorescent intensity using the open-source software ImageJ.[39] Merged visible light and NIR fluorescence light images were created using Adobe Photoshop CS3 Software (Version 10.0.1, Adobe Systems Inc., San Jose, USA). In order to determine sensitivity and specificity of the intraoperative NIR fluorescence technique, an attempt was made to completely remove all tumor tissue while removing as little as possible of the normal surrounding mammary fat pad tissue strictly based on the fluorescence signal in 5 of these 7 rats. Tumors were removed by sharp dissection. Excised tumors were inked with India ink, sliced in two or three parts depending on the size of the tumor and fixed overnight in 4% buffered formalin and embedded in paraffin (FFPE) blocks, mimicking the standard clinical workflow. After resection of the primary tumor, the surgical cavity was inspected with the Fluobeam to detect any remnant fluorescent tissue. After resection of all remnant fluorescent spots, random biopsies were taken of the surgical cavity from every quadrant in order to determine specificity of the technique. In one additional rat an irradical resection was performed intentionally to test the Fluobeam's ability to detect remnant tumor tissue. All specimens were fixed in formalin as described above. FFPE tumor sections of 4 µm were air-dried and stained with hematoxylin and eosin (H&E). The tumor size, the minimum and maximum

tumor-free margin and the presence of tumor in the random biopsies were determined by an experienced breast pathologist (V.T.H.B.M.S.).

**Fluorescence microscopy**

*Cell line experiments*

Time-dependent microscopic analysis of ProSense680 activation by cultured MCR86 cancer cells was performed using the LSM510 Zeiss confocal microscope (Jena, Germany, 40x/0,75w Ph2 ACHROPLAN objective). A 633 nm laser was used for fluorescence excitation and a 650 nm Long Pass for emission. Cells were cultured in 3.5 cm petri dishes incubated with 33.3 nM ProSense680 in 3 ml medium. Cells were kept at 37 °C and imaged for 4.5 hours.

*Ex vivo tumor imaging*

Freshly excised tumors with a wide rim of surrounding normal mammary tissue of rats injected with 10 nmol ProSense680 (N = 3) were halved. From one half, a 2 mm section was analyzed using the Odyssey scanning device at 21 µm resolution. Tumor border was defined as the outer rim of the tumor and its width was approximately 15% of the tumor diameter. The other half was snap-frozen on dry ice and stored at -80 °C. Unfixed 20 µm sections were measured for fluorescence using the Odyssey scanning device at 21 µm resolution. Processing of sections was performed under reduced light conditions to prevent photobleaching. Subsequently, the tissue sections were stained with H&E. The fluorescence image and the H&E image were merged using Adobe Photoshop enabling detailed analysis of the NIR fluorescence distribution along with the histological context.

**Statistical analysis**

Statistical analyses and generation of graphs were performed using GraphPad Prism software (Version 5.01, La Jolla, USA). Continuous variables were analyzed using the (paired) *t*-test for comparison of two groups and one-way analysis of variance (ANOVA) for comparison of more than two groups. To test the effect of two independent variables two-way ANOVA was used. Trend analysis and one-tailed planned comparisons between adjacent groups were conducted. When the assumption of homogeneity of variance was violated (Levene's test), the Brown-Forsythe *F*-ratio was reported. Pearson's correlation coefficients *R* were calculated for correlation analyses. All statistical tests were two-tailed and $P < .05$ was considered significant.

# RESULTS

## *In vitro* activation of ProSense by breast cancer rat cell line

The autoquenched NIR fluorescence probe ProSense680 was activated by MCR86 breast cancer cells within two hours. Microscopic analysis revealed an intracellular localization of activated ProSense680 (Figure 2A-B). Both incubation time ($F(3, 36) = 1615$, $P < .0001$) and concentration of ProSense750 ($F(3, 36) = 3704$, $P < .0001$) significantly influenced ProSense750 activation as measured by fluorescence intensity (two-way ANOVA, Fig. 2C). Also, there was an interaction between incubation time and ProSense750 concentration ($F(9, 36) = 230.4$, $P < .0001$), indicating that the difference in incubation time within ProSense750 concentration groups influenced ProSense750 activation. Furthermore, fluorescence intensity was highly correlated with number of MCR86 cells ($F(4, 10.97) = 39.13$, $P < .0001$, $R = 0.904$; Figure 2D).

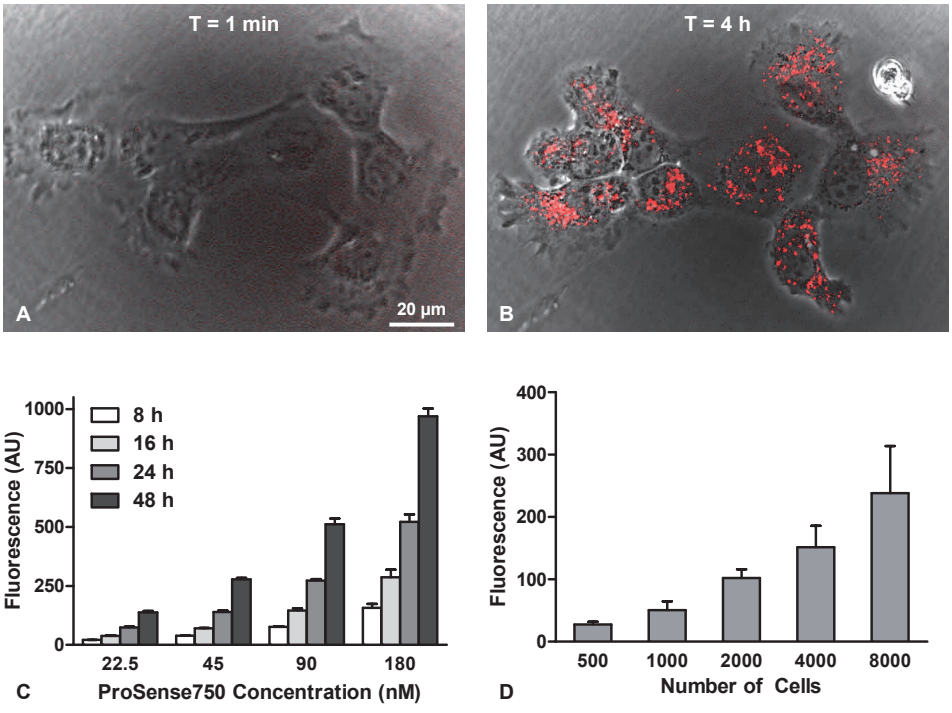


**Figure 2.** ***In vitro*** **activation of ProSense by syngeneic breast cancer rat cell line. A,B.** Fluorescence microscopy (LSM510 Zeiss confocal microscope, 40x objective) of a cluster of MCR86 cells, 1 minute (left panel) and 4.5 h (right panel) after incubation with ProSense680 (33.3 nM). **C.** ProSense750 concentration and incubation time both significantly influence NIR fluorescence intensity (4.000 MCR86 cells per well, two-way ANOVA, Odyssey scanner). Bars represent mean ± SEM (N = 4). **D.** NIR fluorescence intensity is positively correlated with number of MCR86 cells (45 nM ProSense750, 24 h incubation, $R = 0.890$, $P < .0001$, Odyssey scanner). Bars represent mean ± SEM (N = 8).

### *In vivo* activation of ProSense by syngeneic rat model of primary breast cancer

EMR86 breast tumors were successfully imaged percutaneously using the IVIS Spectrum after intravenous administration of ProSense750 (Figure 3A-B). To test the effect of ProSense750 dose and time of imaging on fluorescence intensity, nine rats (N = 35 mammary tumors, mean volume = 0.38 ± 0.36 $cm^3$) were randomly assigned to three ProSense750 dose groups and were imaged 24 h and 48 h post-injection. In concordance with the *in vitro* data, ProSense750 dose significantly influenced fluorescence intensity ($F(2,32) = 3.56$, $P = .04$, two-way ANOVA, Figure 3C). Of note, a substantial part of the tumors could not be identified in the 2.5 nmol dose group (24 h: 4 of 11 tumors, 48 h: 7 of 11 tumors) and the 5 nmol dose group (24 h: 2 of 12 tumors, 48 h: 3 of 12 tumors), whereas in the 10 nmol dose group all tumors were identified. In contrast to the *in vitro* data, time of imaging did not influence fluorescence intensity ($F(2,32) = 2.47$, $P = .13$, two-way ANOVA, Figure 3C). Furthermore, there was no interaction between time of imaging and ProSense750 dose ($F(2,32) = 1.06$, $P = .36$), indicating that the difference in time of imaging within dose groups did not influence fluorescence intensity. Based on these results, a dose of 10 nmol was selected for further *in vivo* testing. Imaging 24 h after ProSense administration was selected for practical purposes. With these settings, fluorescence intensity was significantly correlated with tumor volume ($R = 0.93$, $P < .0001$; Figure 3D), which was in concordance with the *in vitro* data.

### Intraoperative NIR fluorescence-guided resection of primary breast cancer

Using the Fluobeam intraoperative camera system, all primary breast tumors (N = 26 tumors, 7 rats) were successfully identified 24 h after intravenous administration of 10 nmol ProSense680 (Figure 4A). The technique provided a clear demarcation of tumor and surrounding mammary fat pad tissue with a mean tumor-to-background ratio of 2.35 ± 0.37 (paired $t = 14.95$, $P < .0001$, Figure 4B). To determine the accuracy of tumor margin detection of the intraoperative NIR fluorescence technique, 17 tumors (N = 5 rats) were resected completely under direct, real-time NIR fluorescence guidance, while removing as little as possible of the normal surrounding mammary fat pad tissue and processed for histopathological analysis (Figure 4C). All 17 tumors were completely excised with a mean minimum and a mean maximum tumor-free margin of 0.2 ± 0.2 mm and 1.3 ± 0.6 mm, respectively (Table 1). Mean pathological tumor size was 5.0 ± 2.1 mm. In two cases, after resection of the primary tumor, remnant fluorescent tissue was detected in the surgical cavity with the Fluobeam (Table 1). One specimen contained a lymph node with metastatic involvement and the other contained a reactive lymph node with abundant macrophage influx but no tumor involvement. This false-positive finding can be explained by the fact that macrophages show high cathepsin B expression.[13] After resection of all fluorescent spots, random biopsies were taken of the surgical cavity from every quadrant. None of the random

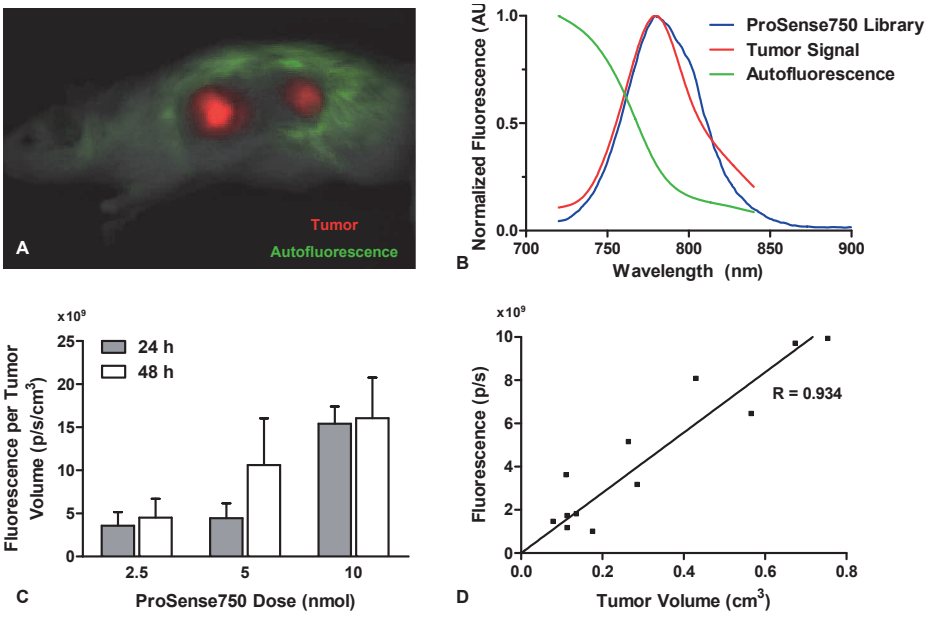


**Figure 3.** ***In vivo*** **activation of ProSense by syngeneic rat model of primary breast cancer. A.** Typical example of a spectral unmixed image of an EMR86 tumor-bearing female WAG/Rij rat, acquired 24 h after intravenous administration of 10 nmol ProSense750. Shown is the separation of the autofluorescence signal (pseudocolored green) and the ProSense750 signal (pseudocolored red; IVIS Spectrum). **B.** Emission curve plot of the spectrally unmixed fluorescence signals from **A.** demonstrates matching of the tumor signal (red line) with the predefined ProSense750 emission curve (blue line), confirming the localization of activated ProSense750 at the tumors. **C.** In a dose- and time-dependent experiment, nine tumor-bearing rats (N = 35 tumors) were randomized to three ProSense750 dose groups and imaged 24 h (grey bars) and 48 h (open bars) after intravenous administration of ProSense750 using the IVIS Spectrum. Bars represent mean ± SEM. **D.** Scatter plot of fluorescence intensity and tumor volume of the 10 nmol dose group imaged 24 h after intravenous administration of ProSense750 ($R$ = 0.934, $P$ < .0001, N = 12 tumors from 3 rats).

biopsies (N = 64, 5 rats) contained histologically any tumor cells. These results indicate an excellent accuracy of the technique. In one additional rat, an irradical resection was performed intentionally in order to show the Fluobeam's ability to detect remnant tumor tissue (Supplementary Figure 1). Remnant tumor tissue could be detected and subsequently resected under direct NIR fluorescence guidance.

## *Ex vivo* NIR fluorescence microscopy

In order to determine the histological localization of ProSense680, tumors were excised with a wide rim of normal mammary tissue 24 h after intravenous administration of 10 nmol ProSense680 (N = 12 tumors, 3 rats; Figure 5A). Fluorescence imaging of 2 mm thick, fresh tumor slices revealed that the NIR fluorescence intensity was 1.6 ± 0.3 times higher at the border of the tumor than at its center (paired $t$ = 4.99, $P$ = .0005, N = 12 tumors; Figure 5B). In order to obtain more detail about the histological localization of ProSense680, unfixed 20 µm frozen tissue sections were measured for

**Table 1.** Pathological assessment of inked resection margins after NIR fluorescence guided excision of primary breast cancer

| Rat | Tumor ID | Maximum ø Specimen (mm) | Maximum ø Tumor (mm) | Radical resection? | Minimum margin (mm) | Maximum margin (mm) | Remnant fluorescence tumor-positive? | Random non-fluorescence biopsies tumor-positive? |
|---|---|---|---|---|---|---|---|---|
| A | 1 | 7.4 | 3.8 | yes | <0.1 | 1.3 | 0 | 0/4 |
| | 2 | 2.8 | 0.8 | yes | <0.1 | 0.9 | 1/1[a] | 0/4 |
| | 3 | 8.8 | 4.8 | yes | 0.7 | 2.4 | 0 | 0/3 |
| B | 4 | 7.5 | 5.1 | yes | <0.1 | 1.4 | 0 | 0/4 |
| | 5 | 4.9 | 3.1 | yes | <0.1 | 1.0 | 0 | 0/4 |
| | 6 | 5.4 | 4.2 | yes | 0.1 | 1.0 | 0 | 0/4 |
| | 7 | 9.2 | 8.0 | yes | <0.1 | 1.0 | 0 | 0/4 |
| C | 8 | 9.1 | 7.9 | yes | <0.1 | 1.1 | 0 | 0/4 |
| | 9 | 8.9 | 5.7 | yes | 0.2 | 2.5 | 0 | 0/4 |
| | 10 | 9.7 | 7.7 | yes | <0.1 | 1.8 | 0 | 0/4 |
| D | 11 | 5.3 | 2.4 | yes | 0.4 | 1.6 | 0 | 0/3 |
| | 12 | 6.1 | 4.3 | yes | 0.2 | 1.0 | 0 | 0/4 |
| | 13 | 5.7 | 4.4 | yes | 0.2 | 1.5 | 0 | 0/4 |
| E | 14 | 8.2 | 6.9 | yes | <0.1 | 0.8 | 0 | 0/4 |
| | 15 | 8.3 | 7.3 | yes | <0.1 | 0.6 | 0 | 0/4 |
| | 16 | 7.3 | 5.6 | yes | 0.3 | 0.7 | 0 | 0/4 |
| | 17 | 6.6 | 3.0 | yes | <0.1 | 1.9 | 0/1[b] | 0/4 |
| **Mean ± SD** | | **7.1 ± 1.9** | **5.0 ± 2.1** | | 0.2 ± 0.2 | 1.3 ± 0.6 | 1/2 | 0/64 |

[a] Macrometastasis in lymph node
[b] Reactive lymph node with abundant macrophage influx

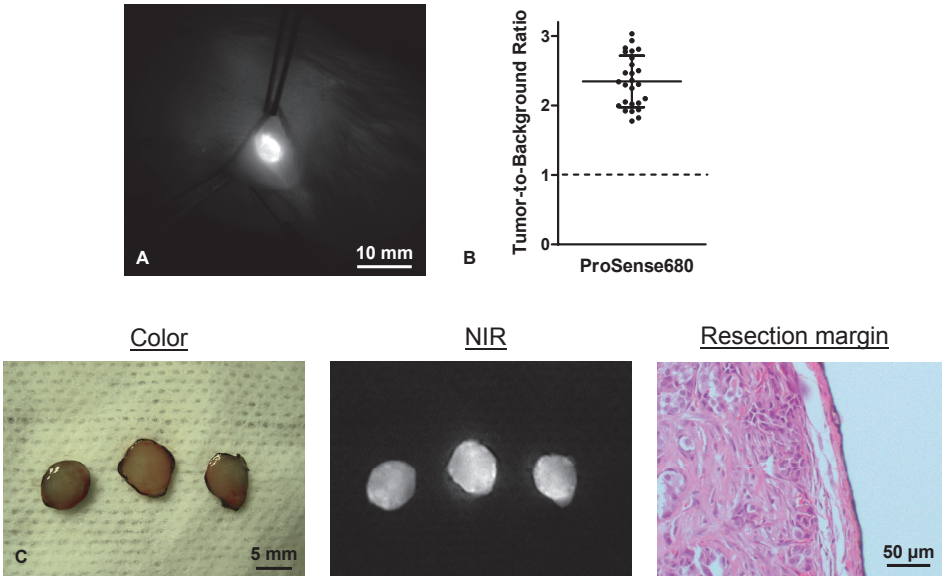


**Figure 4. Intraoperative NIR fluorescence-guided resection of primary breast cancer and pathological assessment. A.** Intraoperative NIR fluorescence image showing a 6-mm EMR86 breast tumor in a female WAG/Rij rat 24 h after intravenous administration of 10 nmol ProSense680 (Fluobeam camera system). Camera exposure time was 10 ms. **B.** Tumor-to-background ratios were determined *in vivo* in rats 24 h after intravenous administration of 10 nmol ProSense680 (N = 26 tumors, 7 rats). Fluobeam camera exposure time was 10 ms. Horizontal lines represent mean ± SD. Mean tumor-to-background ratio was 2.35 ± 0.37. **C.** *Ex vivo* color image (left panel), NIR fluorescence image (Fluobeam, middle panel) of 3 slices of an EMR86 tumor after resection and inking using India ink. The tumor was excised from a rat 24 h after intravenous administration of 10 nmol ProSense680. Camera exposure time was 10 ms. Resection margin of the tumor is shown after H&E staining of a 4 µm FFPE tissue section (right panel).

fluorescence using the Odyssey and subsequently stained with H&E (Figure 5C). These results showed that NIR fluorescence is mainly located in the stromal compartment of the breast tumors and in particular at the tumor border.

## DISCUSSION

In the current study, we demonstrated the feasibility of real-time intraoperative NIR fluorescence identification of breast tumors in a syngeneic orthotopic breast cancer rat model using the protease-activatable probe ProSense. In both the cell line and animal experiments, fluorescence intensity was strongly correlated with number of tumor cells, tumor size and ProSense dose. In contrast to the *in vitro* data, time of imaging (24 h vs. 48 h after administration of ProSense) did not significantly influence fluorescence intensity of breast tumors. This is likely a result of the relatively long blood half-life of ProSense (half-life in mice 18 h, VisEn Medical website) and may provide flexible operation planning in future clinical applications. Histological analysis demonstrated that NIR fluorescence intensity of tumors was highest at the invasive tumor border.

Resection of tumors under real-time NIR fluorescence guidance showed excellent accuracy of the technique in the intraoperative detection of tumor margins. These results suggest that clinical introduction of intraoperative NIR fluorescence imaging using a protease-activatable probe such as ProSense has the potential to increase the number of complete tumor resections in breast cancer patients undergoing breast-conserving surgery.

Previous studies in which NIR fluorescent and protease-activatable probes were tested have utilized xenograft or transgenic mouse models.[19-31] A limitation of many animal models of breast cancer is that, compared to the human situation, less normal mammary tissue is present in relation to tumor size. Therefore, these tumors are easily resected by removing all breast tissue. However, this approach does not resemble the principles underlying breast-conserving surgery. This study was performed using an orthotopic breast cancer model that is syngeneic to immunocompetent female WAG/Rij rats. In syngeneic models, tumors are grown in homologous species and in the strain in which the tumor has originated. Therefore, these models are more representative of the natural tumor-host interaction. Although no preclinical tumor model will contain all features of the complex biology of human cancer, this syngeneic model has several strengths, including its hormone-sensitivity, cribiform growth pattern and its ability to induce regression by estrogen pellet removal. Moreover, this model captures several important features of luminal A hormone-dependent, HER2/neu negative human breast cancer, which is the most predominant subtype of breast cancer.[34, 35] Another intrinsic limitation of animal models of surgical interventions is the potential occurrence of performance bias, because researchers carrying out the intervention can not be blinded to the allocated treatment. This form of bias may lead to flawed results.[40] To surpass these limitations in our study, a one-arm study design was chosen using small breast tumors (5.0 ± 2.1 mm). Tumors were excised based on the NIR fluorescence signal and examined by a breast pathologist using standard clinical methodology. Using this approach, all tumors were completely resected with a mean maximum tumor-free resection margin of 1.3 ± 0.6 mm, indicating that a minimal amount of normal mammary tissue was resected. Although syngeneic models provide a relevant tumor-host interaction, their major drawback is that the tumor cells are rodent, and therefore express the rodent homologues of the desired targets. However, the main target of ProSense, the cysteine protease family (most particular cathepsin B) is strongly conserved amongst mammals.[12] Upregulation of cathepsin B has been confirmed extensively in human breast cancer.[12, 14, 15, 41] It is therefore expected that this kind of protease-activated NIR fluorescence probes will be applicable for intraoperative NIR fluorescence imaging in a large proportion of breast cancer patients.

Analysis of the histological localization of activated ProSense demonstrated that the invasive tumor border exhibited the most intense NIR fluorescence signal. This observation is in concordance with immunohistological analysis of cathepsin B

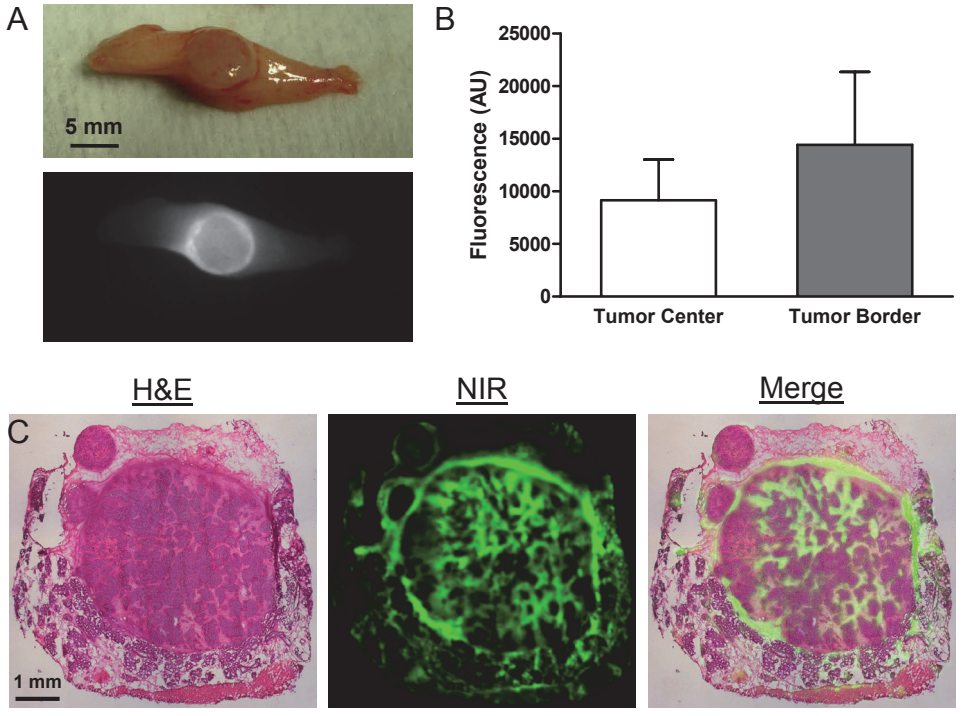


**Figure 5.** ***Ex vivo*** **NIR fluorescence microscopy of resected breast cancer. A.** *Ex vivo* color image (top panel) and NIR fluorescence image (Fluobeam, bottom panel) of an excised EMR86 tumor with surrounding normal mammary fat pad. Fluobeam camera exposure time was 10 ms. The tumor was excised from a rat 24 h after administration of 10 nmol ProSense680. **B.** Quantification of NIR fluorescence measurements of tumor tissue slices showed that the fluorescence signal was 1.6 ± 0.3 times higher at the border of the tumor than at its center (Odyssey scanner, paired $t$ = 4.99, $P$ = .0005, N = 12 tumors). **C.** Shown are a color image of H&E staining (left panel), a pseudocolored green NIR fluorescence image (middle panel; Odyssey scanner), and a merge of the two images (right panel) of a 20 µm frozen section of a 4-mm EMR86 breast tumor with surrounding mammary fat pad. The tumor was excised from a rat 24 h after administration of 10 nmol ProSense680.

reported by others[14, 24] and is in line with the pathophysiological role of cathepsins as reviewed by Gocheva.[42] Cathepsins promote tumor invasion through several possible mechanisms. First, they can directly cleave components of the extracellular matrix and basement membrane, essentially clearing a path for the migration of tumor cells away from the primary tumor. Second, at the cell membrane, cathepsins can direct a proteolytic cascade in which they activate other proteases such as matrix metalloproteinases and urokinase plasminogen activator, which in turn promotes tumor invasion. Third, cleavage of the cell adhesion protein, E-cadherin, at the cell surface can disrupt adherens junctions and thus facilitate cancer cell migration and invasion.[42] Apart from tumor border, NIR fluorescence was higher in the stromal compartment of the tumors. This finding is in concordance with Gounaris et al., who demonstrated that $CD11^+$ tumor-infiltrating macrophages accounted for 75% of the ProSense signal at FACS analysis.[29] In summary, as complete resection of breast tumors

requires adequate visualization of tumor margins, the increased activity of proteolytic enzymes at the invasive tumor border provides an excellent target for intraoperative NIR fluorescence-guided surgery.

Future clinical studies will have to provide proof-of-principle of intraoperative NIR fluorescence tumor detection. Currently, a number of intraoperative NIR fluorescence imaging systems are clinically available and have already been used for sentinel lymph node mapping.[43-45] It is expected that several tumor-targeting NIR fluorescent probes (such as ProSense) will receive regulatory approval within the next few years.

A therapeutic challenge of any new breast cancer imaging technology is the detection of occult tumor deposits in the breast. These tumor deposits could influence surgical decision making, but do not necessarily have a prognostic relevance, because postoperative radiation will eradicate these microscopic deposits in the vast majority of cases. For instance, in preoperative magnetic resonance imaging, the identification of additional tumor deposits is two to three times higher than the incidence of local recurrence, resulting in mastectomies that may not be beneficial to the patient.[46] Consequently, detection of tumor at the margins would be beneficial; detection of tumor deposits beyond the margins, below the cut edge of the lumpectomy cavity, could have the potential to increase surgical resection volume (or even mastectomy rates) without a benefit in survival. Since the maximum penetration depth for NIR fluorescence imaging is currently around 1 cm,[47] it is unlikely that intraoperative NIR fluorescence imaging will detect occult lesions at several centimeters distance from the primary tumor.

Sensitivity of NIR fluorescence is mostly dependent on photon absorption of the tissue, fluorescence excitation power of the light source and concentration of the NIR fluorophore in tissue. Required camera exposure times are inversely correlated with the amount of fluorescence signal. In the current study, camera exposure times of 2-20 ms were used. The field-of-view of the Fluobeam camera system is 7 cm of diameter. Therefore, the time needed to evaluate tumor margins and excision cavities is at most several seconds. Consequently, this real-time intraoperative technique is unlikely to prolong surgical time significantly.

In conclusion, this study provides preclinical validation of an innovative technique in which NIR fluorescence light is used to visualize breast tumors and to provide real-time guidance during subsequent resection. Clinical translation of these results might be very promising because of high accuracy of the technique, flexible surgical planning, increased proteolytic activity at the tumor border and upregulation of cathepsin B in a large proportion of breast cancer patients. Therefore, this study warrants clinical validation of this technique, once NIR fluorescence probes become available for clinical testing, with the ultimate goal to increase the radical resection rate of patients undergoing breast-conserving surgery.

## ACKNOWLEDGEMENTS

We want to thank Rob Keyzer and Anita Sajet for technical assistance and Fluoptics (Grenoble, France) for use of the Fluobeam® system. J.S.D. Mieog is a MD-medical research trainee funded by The Netherlands Organisation for Health Research and Development (grant nr. 92003526).

## REFERENCES

1. Mai KT, Yazdi HM, Isotalo PA. Resection margin status in lumpectomy specimens of infiltrating lobular carcinoma. Breast Cancer Res Treat 2000; 60:29-33.
2. Chagpar AB, Martin RC, Hagendoorn LJ, et al. Lumpectomy margins are affected by tumor size and histologic subtype but not by biopsy technique. Am J Surg 2004; 188:399-402.
3. Smitt MC, Horst K. Association of clinical and pathologic variables with lumpectomy surgical margin status after preoperative diagnosis or excisional biopsy of invasive breast cancer. Ann Surg Oncol 2007; 14:1040-4.
4. Rizzo M, Iyengar R, Gabram SG, et al. The effects of additional tumor cavity sampling at the time of breast-conserving surgery on final margin status, volume of resection, and pathologist workload. Ann Surg Oncol 2010; 17:228-34.
5. Hewes JC, Imkampe A, Haji A, et al. Importance of routine cavity sampling in breast conservation surgery. Br J Surg 2009; 96:47-53.
6. Clarke M, Collins R, Darby S, et al. Effects of radiotherapy and of differences in the extent of surgery for early breast cancer on local recurrence and 15-year survival: an overview of the randomised trials. Lancet 2005; 366:2087-106.
7. Nyirenda N, Farkas DL, Ramanujan VK. Preclinical evaluation of nuclear morphometry and tissue topology for breast carcinoma detection and margin assessment. Breast Cancer Res Treat 2011; 126:345-54.
8. Stepp H, Beck T, Pongratz T, et al. ALA and malignant glioma: fluorescence-guided resection and photodynamic treatment. J Environ Pathol Toxicol Oncol 2007; 26:157-64.
9. Ishizawa T, Fukushima N, Shibahara J, et al. Real-time identification of liver cancers by using indocyanine green fluorescent imaging. Cancer 2009; 115:2491-504.
10. Nguyen NQ, Biankin AV, Leong RW, et al. Real time intraoperative confocal laser microscopy-guided surgery. Ann Surg 2009; 249:735-7.
11. Frangioni JV. New technologies for human cancer imaging. J Clin Oncol 2008; 26:4012-21.
12. Mohamed MM, Sloane BF. Cysteine cathepsins: multifunctional enzymes in cancer. Nat.Rev. Cancer 2006; 6:764-75.
13. Gocheva V, Zeng W, Ke D, et al. Distinct roles for cysteine cathepsin genes in multistage tumorigenesis. Genes Dev 2006; 20:543-56.
14. Parker BS, Ciocca DR, Bidwell BN, et al. Primary tumour expression of the cysteine cathepsin inhibitor Stefin A inhibits distant metastasis in breast cancer. J Pathol 2008; 214:337-46.
15. Harbeck N, Alt U, Berger U, et al. Prognostic impact of proteolytic factors (urokinase-type plasminogen activator, plasminogen activator inhibitor 1, and cathepsins B, D, and L) in primary breast cancer reflects effects of adjuvant systemic therapy. Clin Cancer Res 2001; 7:2757-64.
16. Lah TT, Kokalj-Kunovar M, Strukelj B, et al. Stefins and lysosomal cathepsins B, L and D in human breast carcinoma. Int J Cancer 1992; 50:36-44.
17. Lah TT, Kos J, Blejec A, et al. The expression of lysosomal proteinases and their inhibitors in breast cancer: possible relationship to prognosis of the disease. Pathol Oncol Res 1997; 3:89-99.
18. Foekens JA, Kos J, Peters HA, et al. Prognostic significance of cathepsins B and L in primary human breast cancer. J Clin Oncol 1998; 16:1013-21.
19. Weissleder R, Tung CH, Mahmood U, et al. In vivo imaging of tumors with protease-activated near-infrared fluorescent probes. Nat Biotechnol 1999; 17:375-8.

20. Kirsch DG, Dinulescu DM, Miller JB, et al. A spatially and temporally restricted mouse model of soft tissue sarcoma. Nat Med 2007; 13:992-7.
21. Bremer C, Tung CH, Bogdanov A, Jr., et al. Imaging of differential protease expression in breast cancers for detection of aggressive tumor phenotypes. Radiology 2002; 222:814-8.
22. von Burstin J, Eser S, Seidler B, et al. Highly sensitive detection of early-stage pancreatic cancer by multimodal near-infrared molecular imaging in living mice. Int J Cancer 2008; 123:2138-47.
23. Sheth RA, Upadhyay R, Stangenberg L, et al. Improved detection of ovarian cancer metastases by intraoperative quantitative fluorescence protease imaging in a pre-clinical model. Gynecol Oncol 2009; 112:616-22.
24. Alencar H, Funovics MA, Figueiredo J, et al. Colonic adenocarcinomas: near-infrared microcatheter imaging of smart probes for early detection - study in mice. Radiology 2007; 244:232-8.
25. Bogdanov AA, Jr., Lin CP, Simonova M, et al. Cellular activation of the self-quenched fluorescent reporter probe in tumor microenvironment. Neoplasia. 2002; 4:228-36.
26. Niedre MJ, de Kleine RH, Aikawa E, et al. Early photon tomography allows fluorescence detection of lung carcinomas and disease progression in mice in vivo. Proc Natl Acad Sci USA 2008; 105:19126-31.
27. Ntziachristos V, Tung CH, Bremer C, et al. Fluorescence molecular tomography resolves protease activity in vivo. Nat Med 2002; 8:757-60.
28. Bremer C, Ntziachristos V, Weitkamp B, et al. Optical imaging of spontaneous breast tumors using protease sensing 'smart' optical probes. Invest Radiol 2005; 40:321-7.
29. Gounaris E, Tung CH, Restaino C, et al. Live imaging of cysteine-cathepsin activity reveals dynamics of focal inflammation, angiogenesis, and polyp growth. PLoS One. 2008; 3:e2916.
30. Grimm J, Kirsch DG, Windsor SD, et al. Use of gene expression profiling to direct in vivo molecular imaging of lung cancer. Proc Natl Acad Sci USA 2005; 102:14404-9.
31. Nguyen QT, Olson ES, Aguilera TA, et al. Surgery with molecular fluorescence imaging using activatable cell-penetrating peptides decreases residual cancer and improves survival. Proc Natl Acad Sci USA 2010; 107:4317-22.
32. van Dierendonck JH, Keijzer R, Cornelisse CJ, et al. Surgically induced cytokinetic responses in experimental rat mammary tumor models. Cancer 1991; 68:759-67.
33. Wijsman JH, Cornelisse CJ, Keijzer R, et al. A prolactin-dependent, metastasising rat mammary carcinoma as a model for endocrine-related tumour dormancy. Br J Cancer 1991; 64:463-8.
34. Sorlie T, Tibshirani R, Parker J, et al. Repeated observation of breast tumor subtypes in independent gene expression data sets. Proc Natl Acad Sci USA 2003; 100:8418-23.
35. Sihto H, Lundin J, Lehtimaki T, et al. Molecular subtypes of breast cancers detected in mammography screening and outside of screening. Clin Cancer Res 2008; 14:4103-10.
36. Mieog JS, Vahrmeijer AL, Hutteman M, et al. Novel intraoperative near-infrared fluorescence camera system for optical image-guided cancer surgery. Mol Imaging 2010; 9:223-31.
37. Keramidas M, Josserand V, Righini CA, et al. Intraoperative near-infrared image-guided surgery for peritoneal carcinomatosis in a preclinical experimental model. Br J Surg 2010; 97:737-43.
38. Mansfield JR, Hoyt C, Levenson RM. Visualization of microscopy-based spectral imaging data from multi-label tissue sections. Curr Protoc Mol Biol 2008; Chapter 14.
39. Rasband WS. ImageJ, U. S. National Institutes of Health, Bethesda, Maryland, USA, http://rsb.info.nih.gov/ij. 2009.
40. Juni P, Altman DG, Egger M. Systematic reviews in health care: Assessing the quality of controlled clinical trials. BMJ 2001; 323:42-6.
41. Kuester D, Lippert H, Roessner A, et al. The cathepsin family and their role in colorectal cancer. Pathol Res Pract 2008; 204:491-500.
42. Gocheva V, Joyce JA. Cysteine cathepsins and the cutting edge of cancer invasion. Cell Cycle 2007; 6:60-64.
43. Troyan SL, Kianzad V, Gibbs-Strauss SL, et al. The FLARE intraoperative near-infrared fluorescence imaging system: a first-in-human clinical trial in breast cancer sentinel lymph node mapping. Ann Surg Oncol 2009; 16:2943-52.
44. Hirche C, Murawa D, Mohr Z, et al. ICG fluorescence-guided sentinel node biopsy for axillary nodal staging in breast cancer. Breast Cancer Res Treat 2010; 121:373-8.

45. Kitai T, Inomoto T, Miwa M, et al. Fluorescence navigation with indocyanine green for detecting sentinel lymph nodes in breast cancer. Breast Cancer 2005; 12:211-5.
46. Bloom S, Morrow M. A clinical oncologic perspective on breast magnetic resonance imaging. Magn Reson Imaging Clin N Am 2010; 18:277-94.
47. De Grand AM, Lomnes SJ, Lee DS, et al. Tissue-like phantoms for near-infrared fluorescence imaging system assessment and the training of surgeons. J Biomed Opt. 2006; 11:014007.

## SUPPLEMENTARY DATA

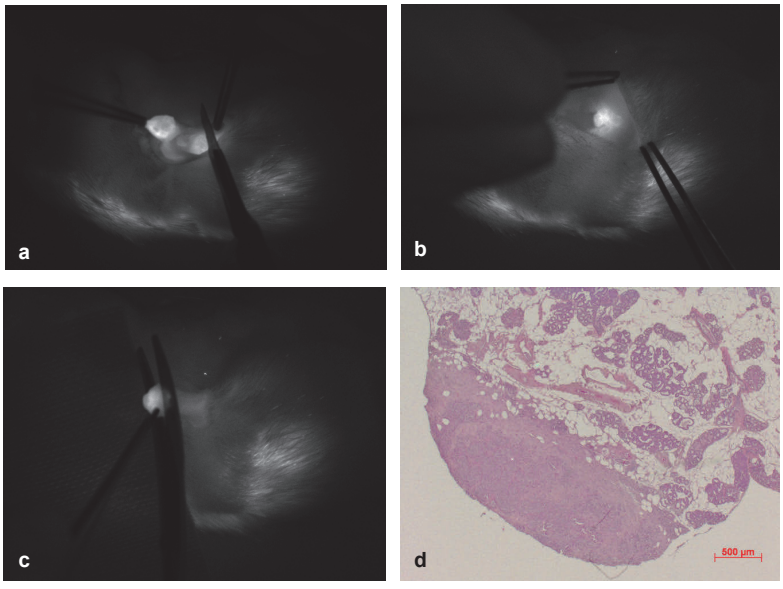


**Supplementary Figure 1. Intraoperative NIR fluorescence detection of irradical resection of pirmary breast cancer. A.** Intraoperative NIR fluorescence image of an intentionally irradical resection of an EMR86 tumor in a WAG/Rij rat 24 h after intravenous administration of 10 nmol ProSense680. **B.** A remnant fluorescent hotspot is readily visualized using intraoperative NIR fluorescence imaging. **C.** The identified fluorescent hotspot is resected under direct NIR fluorescence image-guidance. Camera exposure time was 10 ms. **D.** Resected hotspot is histologically confirmed as tumor tissue (H&E staining).

# Chapter 10

# Antibody-based intraoperative near-infrared fluorescence imaging of primary breast cancer in a syngeneic rat model

Mieog JSD[1], Hutteman M[1], van der Vorst JR, Schaafsma BE, Verbeek FPR, Boonstra MC, Löwik CWGM, Frangioni JV, van de Velde CJH, Kuppen PJK, Vahrmeijer AL

[1] Shared first authorship

## ABSTRACT

### Introduction

Incomplete tumor resections occur frequently in patients undergoing breast-conserving surgery. Intraoperative near-infrared (NIR) fluorescence imaging is a novel technique to assess the extent of disease during surgery. The current study aimed to investigate whether tumor-targeting monoclonal antibodies conjugated to a NIR fluorescence dye could detect primary breast carcinomas in a syngeneic rat model and be used for image-guided resection.

### Methods

The monoclonal mouse antibody MG1, directed against epithelial rat tumor cells, was conjugated to the NIR fluorescent IRDye™800-CW (MG1-CW800) and purified to homogeneity. The isotype-matched irrelevant antibody UPC10 was used as a control. Tumor specificity of MG1-CW800 was assessed using the MCR86 rat breast cancer cell line. *In vivo* tumor targeting was assessed in female WAG/Rij rats carrying EMR86 breast tumors. The Mini-FLARE imaging system was used for intraoperative image-guided resection of EMR86 tumors.

### Results

MG1-CW800 bound specifically to MCR86 tumor cells and could identify EMR86 breast tumors in rats using NIR fluorescence. The tumor-to-background ratio (TBR) was highest 24 h after intravenous administration (2.81 ± 0.74). Although UPC10-CW800 did not bound to MCR86 cells, clear tumor demarcation was observed after intravenous injection in EMR86 bearing rats (TBR = 2.95 ± 0.67). Using MG1-CW800, all tumors could be resected under direct image-guidance. MG1-CW800 signal corresponded with histological tumor demarcation.

### Conclusion

This study demonstrated that tumor-targeted antibodies conjugated to NIR fluorescence dyes can identify breast tumors in a syngeneic rat model. However, as the control antibody obtained similar *in vivo* results, the 'enhanced permability and retention effect' may be an important factor.

## INTRODUCTION

During breast-conserving surgery, the surgeon has to rely on palpation and visual inspection to discriminate tumor tissue from normal tissue. The distinction between tumor and normal tissue is often not evident, resulting in irradical resections in 5 to 40% of patients undergoing breast-conserving surgery, which requires additional resection or intensified radiotherapy regimens.[1-3] Local recurrence rates following breast-conservative therapy of 6.7 to 11% are reported,[4] which can be explained by remnant tumor tissue that is not identified during surgery. Loco regional recurrences are associated with a decrease in overall survival.[4] Therefore, there is a need for a diagnostic tool that can discriminate tumor tissue from normal tissue in real-time during surgery.

Near-infrared (NIR) fluorescence imaging is a technique that has the potential to fulfill this need. NIR light (700 – 900 nm) can penetrate millimeters to centimeters into tissue without the use of ionizing radiation.[5] Several imaging systems have recently become available that are capable of visualizing NIR fluorescence in real-time (reviewed in [6]). Besides these imaging systems, tumor-targeted NIR fluorescent contrast agents ("probes") are necessary to visualize cancer cells. Various mechanisms are available for probes to target tumor cells: they can target increased metabolism,[7] upregulated enzymes,[8-10] or specific cell surface markers.[11] Besides these targeted strategies, a non-targeted approach has been suggested that exploits the so-called 'enhanced permeability and retention (EPR) effect'.[12] The EPR effect is the phenomenon that macromolecules tend to accumulate in tumor tissue much more than they do in normal tissues, which is most probably due to fact that tumors have abnormal 'leaky' neovasculature having endothelial cells with wide fenestrations and lack of smooth muscle layer (Figure 1).

The current study focuses on the use of tumor-targeted antibodies for NIR fluorescence image-guided surgery. Ample clinical experience exists on the use of antibodies in breast cancer, which have been employed for diagnostic imaging,[13, 14] and therapeutic purposes.[15, 16] Moreover, preclinical studies have successfully exploited antibody-based NIR fluorescence tumor targeting.[17, 18] However, these studies were performed in transgenic animal models and lack an adequate isotype-matched control antibody. In this study, we used an antibody directed against epithelial rat tumors, which has been evaluated in a syngeneic rat model of colorectal cancer for the application of immunotherapy and radioimmunotherapy.[19-21] The aim of the current study was to construct an NIR fluorescent tumor-targeted antibody and to validate the intraoperative use of this probe during tumor resection and to compare it with the performance of an isotype-matched irrelevant antibody to control for the EPR effect.

# MATERIAL AND METHODS

## Animal model

All animals were housed in the animal facility of Leiden University Medical Center. Pellet food and fresh tap water were provided at libitum. The weight of the animals was followed throughout the experiment to monitor their general health state. Throughout imaging and surgical procedures, the animals were anesthetized with inhalation of 2% mixture of isoflurane in oxygen. The Animal Welfare Committee of the Leiden University Medical Center approved the study. The study was conducted in concordance with the "Guidelines for the Welfare of Animals in Experimental Neoplasia" (Second edition, 1997) available online at http://www.ncrn.org.uk/csg/animal_guides_text.pdf.

The EMR86 model is a hormone-dependent, transplantable, metastasizing mammary carcinoma that originated in a female WAG/Rij rat bearing a subcutenously implanted estrogen pellet and has been described previously.[9, 22] EMR86 tumor cells show strong nuclear expression of the estrogen and progesterone receptor, but stain negatively for the human epidermal growth factor receptor 2 (HER2/neu). Therefore, EMR86 tumors closely resemble the luminal A molecular subtype. Orthotopic breast tumors are induced after implantation of fresh EMR86 tumor fragments of 1 $mm^3$ into the mammary fat pad at four sites in 4 to 6 months old female WAG/Rij rats (Harlan, Horst, The Netherlands) with simultaneous implantation of an estrogen pellet in the intrascapular region of the neck. After four weeks, tumors reach a volume of approximately 1 $cm^3$, at which time point the experiments were conducted.

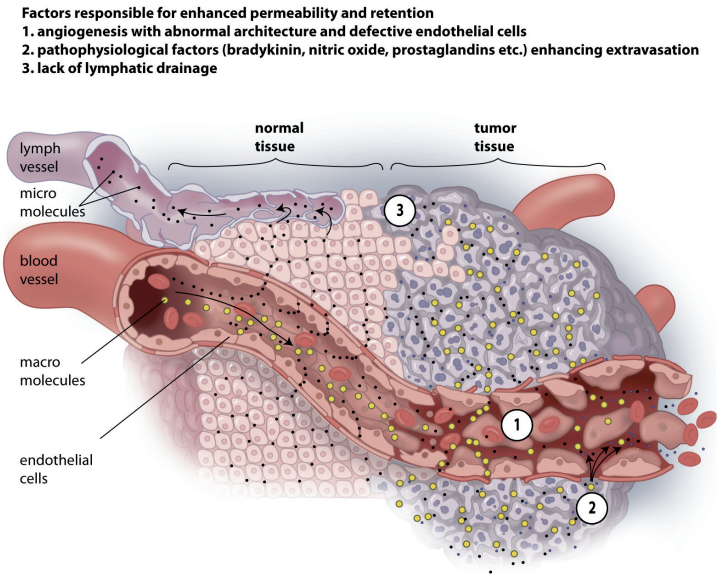


**Figure 1. Schematic representation of the 'enhanced permeability and retention effect'.**

**Immunohistochemistry and *in vivo* homing**

MG1 is an IgG2a mouse monoclonal antibody (Antibodies for Research Applications, Gouda, The Netherlands), which originated in Balb/c mice after immunization with CC531 colon adenocarcinoma cells that are syngeneic to WAG/Rij rats.[23] MG1 recognizes an 80 kDa cell surface antigen on rat cancer cells of epithelial origin, with minimal cross-reactivity with other tissues.[23] To assess the specificity of MG1 for EMR86 breast tumors, 4 μm cryosections of snap frozen EMR86 tumors were stained with MG1 as described previously.[23] The IgG2a mouse antibody UPC10 (Sigma Aldrich, Zwijndrecht, The Netherlands), which is directed against β-2-6-linked fructosan, was used as an isotype-matched irrelevant control antibody.[24]

*In vivo* homing of MG1 to EMR86 tumors was tested by injection of 200 μg of MG1 or UPC10 antibody in 500 μL PBS in the tail vein of EMR86 tumor bearing rats (N = 6 rats, 24 tumors). 24 h after injection, rats were sacrificed and tumors and organs were harvested and snap-frozen on dry ice. Frozen tissue was sectioned and stained as described above, with the exception that no primary antibody was applied.

**Construction of NIR fluorescence probes**

The NIR fluorescent IRDye 800CW-NHS (LI-COR, Lincoln, NE) was purchased as a dry powder and resuspended to 10 mM in anhydrous dimethyl sulfoxide (DMSO; Sigma Aldrich) under reduced light conditions and stored at -80 °C until used for conjugation.

Preservatives were removed from the solution containing MG1 antibodies using gel filtration chromatography with Zeba spin desalting columns with a cut-off of 7 kDa (Thermo Fisher Scientific, Etten-Leur, The Netherlands). The purified sample was then concentrated using Vivaspin columns (Sigma Aldrich) with a cut-off of 30 kDa and was reconstituted in phosphate-buffered saline (PBS) at pH 7.8. Antibody concentration was estimated using absorbance spectrometry (UltroSpec, Amersham, UK; $e_{280nm}$ = 180,000 $M^{-1}$ $cm^{-1}$).

IRDye 800CW-NHS was added dropwise to the purified MG1 solution, while maintaining a pH of 7.8. The reactant was gently shaken for 4 h at room temperature. Unreacted dye was separated from conjugated antibodies (MG1-CW800) by gel filtration chromatography with Zeba spin desalting columns with a cut-off of 7 kDa. The labeling ratio of the purified sample was then analyzed using absorbance spectrometry, using the extinction coefficients of MG1 ($e_{280nm}$ = 180,000 $M^{-1}$ $cm^{-1}$) and CW800 ($\varepsilon_{785nm}$ = 240,000 $M^{-1}$ $cm^{-1}$) in PBS, with correction for 6.5% of measured absorbance at 280 nm of CW800: Ratio = ($Abs_{785nm}$ / $\varepsilon_{785nm}$) / (($Abs_{280nm}$ – 0.065 * $Abs_{785nm}$) / $e_{280nm}$). The same protocol was applied to construct UPC10-CW800.

### *In vitro* confirmation of specificity of MG1-CW800

*In vitro* cell binding of the newly constructed NIR fluorescent probe MG1-CW800 was tested in the rat breast cancer cell line MCR86, which is recognized by MG1.[23] The characteristics of the cell line and the culture conditions as well as the methods for fluorescence measurements have been described previously.[9] In short, cultured tumor cells were harvested, washed and transferred to a 96-well acrylate plate (Greiner Bio-one, Alphen aan de Rijn, The Netherlands, #655090; suitable for fluorescence measurements). For the binding experiments, 16,000 cells were transferred per well, unless stated otherwise. After 24 h of incubation, cells were washed and MG1-CW800 (6.7 nM to 26.7 nM, 200 µl) was added. In a competitive blocking experiment, unconjugated MG1 was mixed with a fixed MG1-CW800 concentration in order to obtain concentrations of 6.7, 26.7 and 53.4 nM of unconjugated MG1 and 6.7 nM of MG1-CW800, and 200 µl of the mixtures was added to the cells. After incubation of 1 h, cells were washed and fluorescence intensity was measured using the Odyssey NIR fluorescence scanning device (LI-COR, Lincoln, NE). Overlying grids were drawn and integrated intensity was calculated for each well using the Odyssey software (Version 2.1; LI-COR, Lincoln, NE) and corrected for baseline fluorescence signal. UPC10 and UPC10-CW800 were used in a negative control experiment.

### *In vivo* tumor targeting

Tumor bearing rats (N = 14 rats, 55 tumors) were injected into the tail vein with 200 µg of MG1-CW800, UPC10-CW800 or unconjugated IRDye 800CW carboxylate (LI-COR). Rats were imaged at 24 h, 48 h and 120 h after injection of the NIR fluorescent probe using the IVIS Spectrum multispectral imager (Caliper LifeSciences, Hopkinton, MA), which allowed separation of the 800 nm signal from the rat's autofluorescence by means of spectral unmixing. Signal intensity of tumors and surrounding tissue were measured *in vivo*.

### Intraoperative NIR fluorescence imaging

Real-time intraoperative NIR fluorescence imaging was performed using the Mini-FLARE imaging system, which has been described previously.[25] Briefly, the system consists of two wavelength isolated light sources: a "white" light source, generating 22,600 lx of 400-650 nm light and a "near-infrared" light source, generating 7.7 mW $cm^{-2}$ of 760 nm light. Color video images and NIR fluorescence images are acquired simultaneously and displayed in real-time using custom optics and software. The system provides the surgeon with real-time images of color video, NIR fluorescence and a pseudocolored merge of the two for anatomical reference.

### Image-guided resection

Directed by time optimization experiments, EMR86 tumor bearing rats (N = 6 rats, 24 tumors) were injected with 200 µg of MG1-CW800 via tail vein injection and imaged 24 h thereafter. The Mini-FLARE was positioned at 30 cm above the animal. Guided by the NIR fluorescence images, a skin incision was made and the fluorescent hotspots were resected with a margin of approximately 0.5 cm non-fluorescent tissue. The surgical cavity was inspected for any remnant fluorescence, which, if present, was resected. NIR fluorescence intensity of organs was assessed *in vivo* for biodistribution analyses. Excised tumors were sliced in two parts and snap frozen on dry ice. Tumors were sectioned at 10 µm and air-dried. NIR fluorescence signal was measured using the Odyssey, after which the sections were stained with hematoxylin and eosin.

### Statistical analyses

Statistical analyses and generation of graphs were performed using GraphPad Prism software (Version 5.01, La Jolla, CA). Continuous variables were analyzed using the (paired) *t*-test for comparison of two groups. Homogeneity of variance was assessed using Levene's test. Pearson's correlation coefficients *R* were calculated for correlation analyses. All statistical tests were two-tailed and $P < .05$ was considered significant.

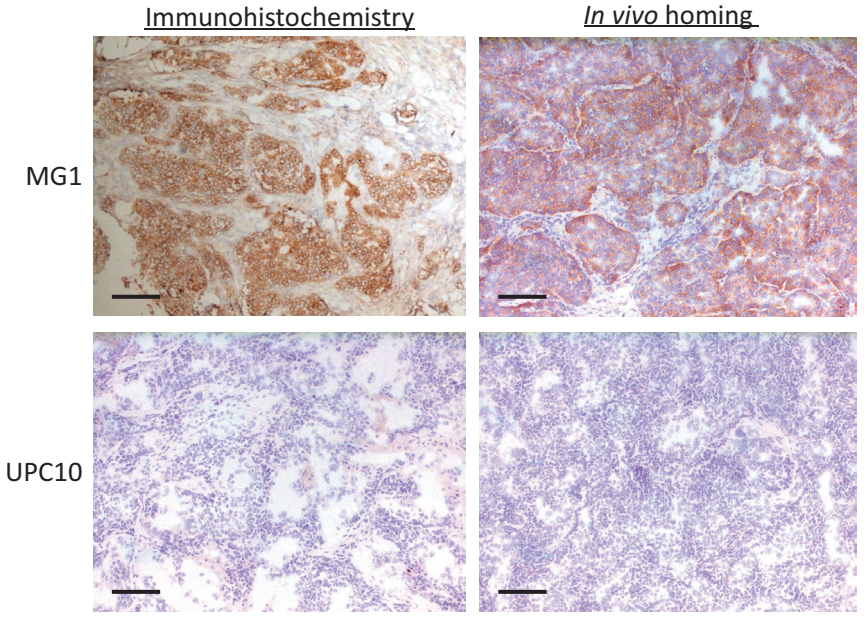


**Figure 2. Immunohistochemical confirmation of specificity of MG1 antibodies for EMR86 breast cancer tumors.** Incubation of frozen EMR86 sections with MG1 (upper left panel) and UPC10 antibodies (lower left panel). In a homing experiment, rats were intravenously infected with 200 µg MG1 or UPC10 antibody 24 h prior to resection of EMR86 tumors. Staining of frozen sections of these tumors showed presence of MG1 antibodies (upper right panel) and absence of UPC10 antibodies (lower right panel). Bars represent 100 µm.

# RESULTS

## Specificity of MG1 antibody for EMR86 breast tumors

Cryosections of EMR86 tumors showed clear staining with MG1 after immunohistochemistry and no staining with the UPC10 control antibody (Figure 2). Limited cross-reactivity with other tissues was observed (data not shown), similar to previous results in colorectal cancer.[23] To determine the *in vivo* binding capabilities of MG1 to EMR86 breast tumors, six tumor-bearing rats (N = 24 tumors) were i.v. injected with 200 µg of MG1 or UPC10 antibodies. The tumors were excised 24 h after injection. Immunohistochemical analyses showed adequate homing of the MG1 antibody to the tumors and no homing of the UPC10 antibody (Figure 2).

## Construction and *in vitro* testing of NIR fluorescent probes

To construct a NIR fluorescent probe, MG1 antibodies were conjugated to the NIR fluorescent IRDye 800CW. The resulting fluorescent antibody (MG1-CW800) was

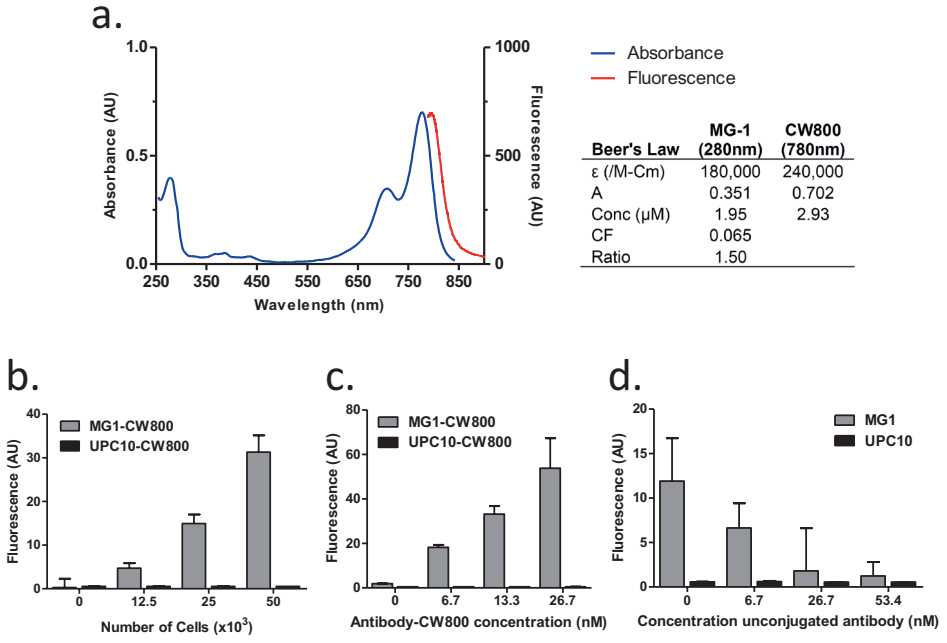


**Figure 3.** ***In vitro*** **characterization of MG1-CW800. A.** Absorbance and fluorescence spectra of MG1-CW800. Concentration and labeling ratio were determined using Beer-Lambert's law, as shown in the table. **B.** Fluorescence intensity was significantly correlated with the number of MCR86 breast cancer cells ($R = 0.98$, $P < .0001$). **C.** Fluorescence intensity was significantly correlated with the concentration of MG1-CW800 added to a fixed number of MCR86 cells (16,000 cells, $R = 0.95$, $P < .0001$). **D.** Specific binding was demonstrated by linear decrease of fluorescence intensity by adding increasing amounts of unlabeled MG1 ($R = -0.73$, $P = .003$).

separated from reaction products by gel filtration chromatography. The average number of fluorophores per antibody (labeling ratio) as estimated by absorbance spectrometry was 1.6 ± 0.4 (Figure 3A). To test if the binding capacities of MG1-CW800 were retained, cell line experiments were conducted (Figure 3B-D). UPC10-CW800 was used a control NIR fluorescent probe. Fluorescence intensity was significantly associated with number of cells ($R$ = 0.98, $P$ < .0001; Figure 3B) and the concentration of MG1-CW800 ($R$ = 0.95, $P$ < .0001; Figure 3C). Blocking of MG1-CW800 binding to MCR86 tumor cells was performed by adding escalating concentrations of unconjugated MG1. Fluorescence intensity was inversely correlated with the concentration of unconjugated MG1 ($R$ = -0.73, $P$ = .003; Figure 3D). UPC10-CW800 showed no binding with MCR86 cells (Figure 3B-D). These results demonstrated that the specific binding capacities of MG1-CW800 to MCR86 cells were preserved.

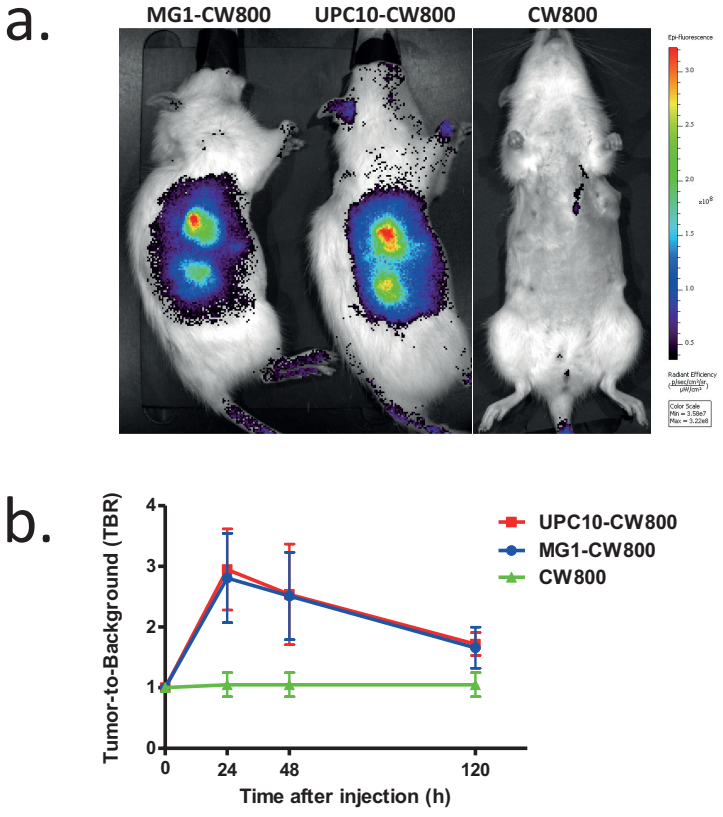


**Figure 4.** ***In vivo*** **NIR fluorescence detection of EMR86 tumors after intravenous injection of MG1-CW800 or UPC10-CW800. A.** *In vivo* imaging EMR86 tumor-bearing female WAG/Rij rats, 24 h after intravenous administration of 200 µg MG1-CW800 (left), 200 µg UPC10-CW800 (middle panel) or 2 nmol unconjugated IRDye 800CW carboxylate (right panel). Shown is the image after spectral unmixing (IVIS Spectrum). **B.** Tumor-to-background ratios were determined *in vivo* at t = 0, 24 h, 48 h and 120 h after administration of MG1-CW800, UPC10-CW800 and IRDye 800CW carboxylate using the IVIS Spectrum (N = 3 rats in each group).

### *In vivo* tumor targeting NIR fluorescent antibody MG1-CW800

The tumor-targeting properties of the NIR fluorescent antibody MG1-CW800 were tested in the EMR86 breast cancer rat model using the IVIS Spectrum imaging system (Figure 4). Both UPC10-CW800 and unconjugated IRDye 800CW carboxylate were used as a negative control. The tumor-to-background ratio's (TBR) were assessed at 24 h, 48 h and 120 h after injection (Figure 4B). The TBR of rats injected with MG1-CW800 peaked at the 24 h time point and the mean TBR was 2.81 ± 0.74. No significant difference was observed between the 24 h and 48 h time point ($t$ = 1.11, $P$ = .82). Imaging after 120 h resulted in a significantly lower TBR compared to the 24 h time point ($t$ = 4.30, $P$ = .001). Rats injected with UPC10-CW800 showed clear identification of tumors with a mean TBR at 24 h of 2.95 ± 0.67. Rats injected with unconjugated IRDye 800CW carboxylate showed no tumor demarcation. Based on these results, imaging 24 h after administration of fluorescent probe was selected for practical purposes.

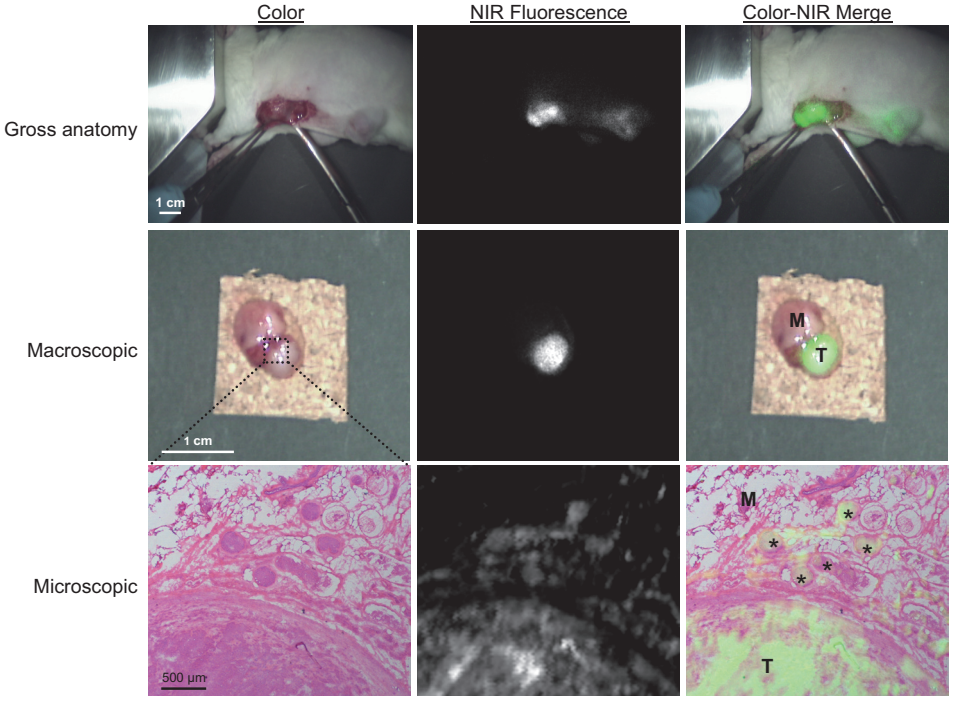


**Figure 5. Intraoperative and *ex vivo* tumor identification with NIR fluorescence.** Image-guided resection of an EMR86 breast tumor in a rat, 24 h after intravenous administration of 200 µg MG1-CW800 (upper row). Shown are a color image (left panel), NIR fluorescence image (middle panel) and a pseudocolored merge of the two (right panel) as shown in real-time during surgery (Mini-FLARE). *Ex vivo* NIR fluorescence analysis using the Mini-FLARE of resected specimens shows a clear demarcation of the tumor (T) from the surrounding mammary tissue (M; middle row). H&E staining and NIR fluorescence measurement (Odyssey) of cryosections of resected specimens reveal that MG1-CW800 localization corresponds with tumor areas (T = primary tumor, * = tumor satellites) as determined by histology. Surrounding mammary tissue (M) shows no NIR fluorescence (lower row).

### Intraoperative NIR fluorescence-guided resection of primary breast cancer

Using the Mini-FLARE intraoperative imaging system, all primary breast tumors (N = 24 tumors, 6 rats) were successfully identified 24 h after intravenous administration of 200 μg MG1-CW800 (Figure 5A). The technique provided a clear demarcation of tumor from surrounding mammary fat pad tissue ($t = 9.95$, $P < .0001$), with an average tumor-to-background ratio of 2.78 ± 0.74. After resection of the primary tumor under direct NIR fluorescence-guidance, no remnant fluorescence hotspots were detected. Histological analyses and fluorescence microscopy (at 800 nm) confirmed that the NIR fluorescent signal of MG1-CW800 corresponded with the presence of tumor cells (Figure 5B-C). In addition, immunohistochemical analysis confirmed that MG1 antibody was present at the cell surface of EMR86 tumor cells (data not shown). Next, the biodistribution of MG1-CW800 was assessed *in vivo* by quantifying the NIR fluorescence signal in selected organs of 6 rats 24 h after intravenous administration of 200 μg MG1-CW800 (data not shown). Because of the renal clearance of the NIR fluorescent probe, the kidney and the bladder showed attenuated fluorescent signal. Most organs, however, showed low fluorescent intensities. Conversely, the liver showed high fluorescence intensity.

## DISCUSSION

The current study demonstrated the construction of a NIR fluorescent tumor-targeted antibody (MG1-CW800) and its validation in a syngeneic rat model of breast cancer. *In vitro* characterization showed a linear increase of NIR fluorescence signal with increasing MG1-CW800 concentration and increasing cell concentration. Specificity of the binding was shown *in vitro* by blocking of the NIR fluorescence signal by addition of unlabeled antibody. During the *in vivo* experiments, all breast tumors could be clearly identified by NIR fluorescence after intravenous injection of MG1-CW800. Tumor demarcation as identified by intraoperative NIR fluorescence imaging corresponded to the histological findings.

*In vivo*, however, animals injected with the NIR fluorescent-labeled UPC10-CW800 isotype control antibody, showed similar tumor uptake as MG1-CW800. As UPC10-CW800 showed no specific binding *in vitro*, the *in vivo* tumor uptake can be attributed to the enhanced permeability and retention effect.[12] Previous studies using radiolabeled UPC10 demonstrated no tumor uptake.[24] The NIR fluorophore used in this study has a molecular weight of 1091 Da, whereas the radiolabel $^{111}$Indium has a molecular weight of 111 Da. A recently published study on novel NIR fluorophores has demonstrated the influence of the negative net charge of IRDye 800CW on biodistribution.[26] Future research should focus on the exploiting the effect of size and charge on tumor uptake, whilst minimizing background uptake.

Antibodies are a promising entity to provide contrast during NIR fluorescence image-guided surgery. In contrast to, for example, enzymatic targeting,[27, 28] an antibody targeting the correct antigen will target tumor cells itself, instead of surrounding tissue. Indeed, MG1 has been shown to stain virtually all tumor cells,[23] and similar results have been reported for antibodies against human targets.[29, 30] Several antibodies are available for clinical application,[15, 31, 32] with a multitude in the process of clinical approval. As the first fluorophores, including IRDye 800CW, are in the process of clinical approval,[33] it is expected that combining such a novel fluorophore with an already clinically available tumor-targeting agent (for example trastuzumab, bevacizumab and cetuximab) will encounter less roadblocks from bench to bedside.[34] Moreover, as these antibodies are already employed for novel adjuvant treatment options, as immunotherapy,[15, 31] radioimmunotherapy,[35] or pretargeted radioimmunotherapy,[36, 37] these antibodies have the potential to be used for both intraoperative tumor visualization and perioperative treatment of residual disease.

For an optimal tumor demarcation using NIR fluorescence probes, tumor binding needs to be maximized, while minimizing background uptake.[38] Therefore, an optimal tumor-targeting NIR fluorescent probe has a high affinity for the targeted ligand, has low non-specific uptake in non-targeted tissue, and unbound molecules are cleared rapidly from the body.[39] Antibodies as MG1 have a molecular weight of approximately 150 kDa and are therefore macromolecules, which have a relatively long blood half-life of 330 minutes.[40] In the current study, a high NIR fluorescence signal was observed in the liver, which could be caused by specific binding of the Fc region of the antibody and subsequent degradation of the immune complex by Kuppfer cells,[41] or aspecific binding by the liver parenchyma due to the surface charge and hydrodynamic diameter of MG1-CW800. Although the uptake in the liver would not directly hamper the ability to demarcate breast tumors (as opposed to intra-abdominal tumors, where this could be a significant impairment[42]), lower aspecific uptake will decrease the required dose and reduce potential side effects. Therefore, future studies will have to focus on smaller tumor-targeted entities (e.g. peptides,[43, 44] peptidomimetic molecules,[45-47] or antibody fragments[48]) that should be combined with optimized fluorophores, with minimal background uptake, to optimize biodistribution and clearance properties in order to maximize contrast with minimal dosing.[39]

In conclusion, this study shows the tumor-targeting capabilities of a newly constructed NIR fluorescent antibody and its use for intraoperative tumor demarcation of breast tumors, in a preclinical animal model. An aspecific isotype control antibody demonstrated similar *in vivo* tumor uptake, indicating the influence of the enhanced permeability and retention effect. The use of an antibody based tumor-targeting strategy permits the use of currently clinically available molecules, could enable combined use for visualization and treatment and therefore has the potential to be translated to the clinic in the foreseeable future.

## ACKNOWLEGDEMENTS

This work was supported in part by the Dutch Cancer Society grant UL2010-4732 and the Center for Translational Molecular Medicine (DeCoDe project, grant 03O-101). J.S.D. Mieog is a MD-medical research trainee funded by The Netherlands Organisation for Health Research and Development (grant nr. 92003526). We want to thank Rob Keyzer, Gabi van Pelt, Karien de Rooij and Isabel Mol for technical assistance and Lindsey Gendall for editing.

## REFERENCES

1. Verkooijen HM, Borel RI, Peeters PH, et al. Impact of stereotactic large-core needle biopsy on diagnosis and surgical treatment of nonpalpable breast cancer. Eur J Surg Oncol 2001; 27:244-9.
2. Mai KT, Yazdi HM, Isotalo PA. Resection margin status in lumpectomy specimens of infiltrating lobular carcinoma. Breast Cancer Res Treat 2000; 60:29-33.
3. Rizzo M, Iyengar R, Gabram SG, et al. The effects of additional tumor cavity sampling at the time of breast-conserving surgery on final margin status, volume of resection, and pathologist workload. Ann Surg Oncol 2010; 17:228-34.
4. Clarke M, Collins R, Darby S, et al. Effects of radiotherapy and of differences in the extent of surgery for early breast cancer on local recurrence and 15-year survival: an overview of the randomised trials. Lancet 2005; 366:2087-106.
5. Frangioni JV. In vivo near-infrared fluorescence imaging. Curr Opin Chem Biol 2003; 7:626-34.
6. Gioux S, Choi HS, Frangioni JV. Image-guided surgery using invisible near-infrared light: fundamentals of clinical translation. Mol Imaging 2010; 9:237-55.
7. Zhou H, Luby-Phelps K, Mickey BE, et al. Dynamic near-infrared optical imaging of 2-deoxyglucose uptake by intracranial glioma of athymic mice. PLoS One 2009; 4:e8051.
8. Weissleder R, Tung CH, Mahmood U, et al. In vivo imaging of tumors with protease-activated near-infrared fluorescent probes. Nat Biotechnol 1999; 17:375-8.
9. Mieog JS, Hutteman M, van der Vorst JR, et al. Image-guided tumor resection using real-time near-infrared fluorescence in a syngeneic rat model of primary breast cancer. Breast Cancer Res Treat 2011; 128:679-89.
10. Jiang T, Olson ES, Nguyen QT, et al. Tumor imaging by means of proteolytic activation of cell-penetrating peptides. Proc Natl Acad Sci USA 2004; 101:17867-72.
11. Backer MV, Levashova Z, Patel V, et al. Molecular imaging of VEGF receptors in angiogenic vasculature with single-chain VEGF-based probes. Nat Med 2007; 13:504-9.
12. Iyer AK, Khaled G, Fang J, et al. Exploiting the enhanced permeability and retention effect for tumor targeting. Drug Discov Today 2006; 11:812-8.
13. Dijkers EC, Oude Munnink TH, Kosterink JG, et al. Biodistribution of 89Zr-trastuzumab and PET imaging of HER2-positive lesions in patients with metastatic breast cancer. Clin Pharmacol Ther 2010; 87.
14. Oude Munnink TH, Nagengast WB, Brouwers AH, et al. Molecular imaging of breast cancer. Breast (Edinburgh, Scotland) 2009; 18 Suppl 3.
15. Hudis CA. Trastuzumab-mechanism of action and use in clinical practice. N Engl J Med 2007; 357:39-51.
16. Giampaglia M, Chiuri VE, Tinelli A, et al. Lapatinib in breast cancer: clinical experiences and future perspectives. Cancer Treat Rev 2010; 36 Suppl 3.
17. Ballou B, Fisher GW, Waggoner AS, et al. Tumor labeling in vivo using cyanine-conjugated monoclonal antibodies. Cancer immunology, immunotherapy: CII 1995; 41:257-63.
18. Ballou B, Fisher GW, Deng JS, et al. Cyanine fluorochrome-labeled antibodies in vivo: assessment of tumor imaging using Cy3, Cy5, Cy5.5, and Cy7. Cancer Detect Prev 1998; 22:251-7.

19. de Jong G, Hendriks T, Franssen G, et al. Adjuvant radioimmunotherapy after radiofrequency ablation of colorectal liver metastases in an experimental model. Eur J Surg Oncol 2011; 37:258-64.
20. de Jong GM, Hendriks T, Eek A, et al. Adjuvant radioimmunotherapy improves survival of rats after resection of colorectal liver metastases. Ann Surg 2011; 253:336-41.
21. Gelderman KA, Hakulinen J, Hagenaars M, et al. Membrane-bound complement regulatory proteins inhibit complement activation by an immunotherapeutic mAb in a syngeneic rat colorectal cancer model. Mol Immunol 2003; 40:13-23.
22. Wijsman JH, Cornelisse CJ, Keijzer R, et al. A prolactin-dependent, metastasising rat mammary carcinoma as a model for endocrine-related tumour dormancy. Br J Cancer 1991; 64:463-8.
23. Hagenaars M, Koelemij R, Ensink NG, et al. The development of novel mouse monoclonal antibodies against the CC531 rat colon adenocarcinoma. Clin Exp Metastasis 2000; 18:281-9.
24. de Jong GM, Hendriks T, Eek A, et al. Radioimmunotherapy improves survival of rats with microscopic liver metastases of colorectal origin. Ann Surg Oncol 2009; 16:2065-73.
25. Mieog JS, Troyan SL, Hutteman M, et al. Towards optimization of imaging system and lymphatic tracer for near-infrared fluorescent sentinel lymph node mapping in breast cancer. Ann Surg Oncol 2011; 18:2483-91.
26. Choi HS, Nasr K, Alyabyev S, et al. Synthesis and in vivo fate of zwitterionic near-infrared fluorophores. Angewandte Chemie 2011.
27. Bogyo M. Finding enzymes that are actively involved in cancer. Proc Natl Acad Sci USA 2010; 107:2379-80.
28. Kirsch DG, Dinulescu DM, Miller JB, et al. A spatially and temporally restricted mouse model of soft tissue sarcoma. Nat Med 2007; 13:992-7.
29. Packeisen J, Kaup-Franzen C, Knieriem HJ. Detection of surface antigen 17-1A in breast and colorectal cancer. Hybridoma 1999; 18:37-40.
30. Gottlinger HG, Funke I, Johnson JP, et al. The epithelial cell surface antigen 17-1A, a target for antibody-mediated tumor therapy: its biochemical nature, tissue distribution and recognition by different monoclonal antibodies. Int J Cancer 1986; 38:47-53.
31. Rini BI. Vascular endothelial growth factor-targeted therapy in renal cell carcinoma: current status and future directions. Clin Cancer Res 2007; 13:1098-106.
32. Van Cutsem E, Kohne CH, Hitre E, et al. Cetuximab and chemotherapy as initial treatment for metastatic colorectal cancer. N Engl J Med 2009; 360:1408-17.
33. Marshall MV, Draney D, Sevick-Muraca EM, et al. Single-dose intravenous toxicity study of IRDye 800CW in Sprague-Dawley rats. Mol Imaging Biol 2010; 12:583-94.
34. Frangioni JV. Translating in vivo diagnostics into clinical reality. Nat Biotechnol 2006; 24:909-13.
35. Liersch T, Meller J, Kulle B, et al. Phase II trial of carcinoembryonic antigen radioimmunotherapy with 131I-labetuzumab after salvage resection of colorectal metastases in the liver: five-year safety and efficacy results. J Clin Oncol 2005; 23:6763-70.
36. Kraeber-Bodere F, Rousseau C, Bodet-Milin C, et al. Targeting, toxicity, and efficacy of 2-step, pretargeted radioimmunotherapy using a chimeric bispecific antibody and 131I-labeled bivalent hapten in a phase I optimization clinical trial. J Nucl Med 2006; 47:247-55.
37. Orcutt KD, Ackerman ME, Cieslewicz M, et al. A modular IgG-scFv bispecific antibody topology. Protein Eng Des Sel 2010; 23:221-8.
38. Frangioni JV. The problem is background, not signal. Mol Imaging 2009; 8:303-4.
39. Choi HS, Liu W, Liu F, et al. Design considerations for tumour-targeted nanoparticles. Nat Nanotechnol 2010; 5:42-7.
40. Goel A, Colcher D, Baranowska-Kortylewicz J, et al. Genetically engineered tetravalent single-chain Fv of the pancarcinoma monoclonal antibody CC49: improved biodistribution and potential for therapeutic application. Cancer Res 2000; 60:6964-71.
41. Lovdal T, Andersen E, Brech A, et al. Fc receptor mediated endocytosis of small soluble immunoglobulin G immune complexes in Kupffer and endothelial cells from rat liver. J Cell Sci 2000; 113:3255-66.
42. Mieog JS, Vahrmeijer AL, Hutteman M, et al. Novel intraoperative near-infrared fluorescence camera system for optical image-guided cancer surgery. Mol Imaging 2010; 9:223-31.

43. Beer AJ, Niemeyer M, Carlsen J, et al. Patterns of alphavbeta3 expression in primary and metastatic human breast cancer as shown by 18F-Galacto-RGD PET. J Nucl Med 2008; 49:255-9.
44. Wu Y, Cai W, Chen X. Near-infrared fluorescence imaging of tumor integrin alpha v beta 3 expression with Cy7-labeled RGD multimers. Mol Imaging Biol 2006; 8:226-36.
45. Coleman PJ, Brashear KM, Askew BC, et al. Nonpeptide alphavbeta3 antagonists. Part 11: discovery and preclinical evaluation of potent alphavbeta3 antagonists for the prevention and treatment of osteoporosis. J Med Chem 2004; 47:4829-37.
46. Keramidas M, Josserand V, Righini CA, et al. Intraoperative near-infrared image-guided surgery for peritoneal carcinomatosis in a preclinical experimental model. Br J Surg 2010; 97:737-43.
47. Hutteman M, Mieog JS, van der Vorst JR, et al. Intraoperative near-infrared fluorescence imaging of colorectal metastases targeting integrin alpha(v)beta(3) expression in a syngeneic rat model. Eur J Surg Oncol 2011; 37:252-7.
48. Kampmeier F, Niesen J, Koers A, et al. Rapid optical imaging of EGF receptor expression with a single-chain antibody SNAP-tag fusion protein. Eur J Nucl Med Mol Imaging 2010; 37:1926-34.

# Part IIB

## Sentinel lymph node mapping

# Chapter 11

# Towards optimization of imaging system and lymphatic tracer for near-infrared fluorescent sentinel lymph node mapping in breast cancer

Mieog JSD[1], Troyan SL[1], Hutteman M[1], Donohue KJ, van der Vorst JR, Stockdale A, Liefers GJ, Choi HS, Gibbs-Strauss SL, Putter H, Gioux S, Kuppen PJK, Ashitate Y, Löwik CWGM, Smit VTHBM, Oketokoun R, Ngo LH, van de Velde CJH, Frangioni JV, Vahrmeijer AL

[1] Shared first authorship

*Ann Surg Oncol 2011; 18:2483-91*

## ABSTRACT

### Background

Near-infrared (NIR) fluorescent sentinel lymph node (SLN) mapping in breast cancer requires optimized imaging systems and lymphatic tracers.

### Methods

A small, portable version of the FLARE™ imaging system, termed Mini-FLARE™, was developed for capturing color video and two semi-independent channels of NIR fluorescence (700 nm and 800 nm) in real-time. Initial optimization of lymphatic tracer dose was performed using 35-kg Yorkshire pigs and a 6-patient pilot clinical trial. More refined optimization was performed in twenty-four consecutive breast cancer patients. All patients received the standard of care using $^{99m}$Technetium-nanocolloid and patent blue. In addition, 1.6 mL of indocyanine green adsorbed to human serum albumin (ICG:HSA) was injected directly after patent blue at the same location. Patients were allocated to one of eight escalating ICG:HSA concentration groups from 50 to 1000 μM.

### Results

The Mini-FLARE™ system was positioned easily in the operating room and could be used up to 13" from the patient. Mini-FLARE™ enabled visualization of lymphatic channels and SLNs in all patients. A total of 35 SLNs (mean = 1.45, range 1-3) were detected: 35 radioactive (100%), 30 blue (86%), and 35 NIR fluorescent (100%). Contrast agent quenching at the injection site and dilution within lymphatic channels were major contributors to signal strength of the SLN. Optimal injection dose of ICG:HSA ranged between 400 and 800 μM. No adverse reactions were observed.

### Conclusions

We describe the clinical translation of a new NIR fluorescence imaging system and define the optimal ICG:HSA dose range for SLN mapping in breast cancer.

## INTRODUCTION

Sentinel lymph node (SLN) mapping, as introduced for the management of breast cancer by Giuliano et al,[1] is currently regarded as the standard of care for staging of the axilla.[2] In general, a combination of radioactive colloid and blue dye is used. However, this exposes patients and caregivers to ionizing radiation, and blue dyes cannot be seen through skin and fatty tissue. Nonetheless, in recent trials, SLN identification rates of 95-97% are achieved when using this combination, and use of only one agent results in significantly lower identification rates.[3-6]

Recent preclinical and clinical data have demonstrated that near-infrared (NIR) fluorescence imaging using the NIR fluorescence agent indocyanine green (ICG) enables real-time transcutaneous and intraoperative visualization of lymphatic channels and detection of the SLN.[7-14] Therefore, NIR fluorescence imaging could provide an alternative for, or an addition to, conventional techniques used for SLN mapping. However, to date, clinical data are lacking a direct comparison of NIR fluorescence to the combination of radioactive tracer and blue dye. Also, even though ICG is the only fluorescent agent currently available in the clinic, it is not an optimal lymphatic tracer. Previous preclinical work has demonstrated that adsorption of ICG to human serum albumin (HSA, complex is ICG:HSA) increases the fluorescence intensity and the hydrodynamic diameter, thereby providing improved detection and better retention in the SLN.[15]

Recently, first-in-human clinical testing of ICG:HSA was performed.[14] The Fluorescence-Assisted Resection and Exploration (FLARE™) imaging system, developed by our group[14, 16] and used in the trial, is a general-purpose optical imaging platform that provides the surgeon with two independent NIR fluorescence channels (centered at 700 nm and 800 nm) to see otherwise invisible structures within the surgical field. The first generation of FLARE™ was large, expensive to build, and had a heavy imaging head that required a specially-designed articulated arm.[14] This prevented shipment of FLARE™ to researchers around the world, and therefore impeded efficient scientific investigation. During the first-in-human clinical testing of FLARE™, it also became apparent that contrast agents for SLN mapping were not yet optimal. The goals of the present study were to develop a miniaturized version of FLARE™, termed Mini-FLARE™, and to determine optimal lymphatic tracer dosing for SLN mapping in breast cancer.

# MATERIAL AND METHODS

## Mini-FLARE™ imaging system

A detailed description of the Mini-FLARE™ imaging system and *in vitro* characterization is available online at http://www.springerlink.com/content/r4712247933613tv/. For sterile usage in the operating room, a 0.118" thick acrylic splash shield having 95% optical transmission at 800 nm was hermetically bonded to a clear plastic drape and sterilized (Medical Technique, Inc., Tucson, USA).

## Preparation of indocyanine green adsorbed to human serum albumin

ICG (25-mg vials) was purchased from Pulsion Medical Systems (Munich, Germany) and was resuspended in 10 cc of sterile water for injection to yield a 2.5 mg/ml (3.2 mM) stock solution. Various amounts of this stock solution were transferred to a 50 cc vial of Cealb (20% human serum albumin (HSA) solution; Sanquin, Amsterdam, The Netherlands) to yield ICG in HSA (ICG:HSA) at a final concentration of 50 μM, 100 μM, 200 μM, 400 μM, 500 μM, 600 μM, 800 μM, or 1000 μM. To obtain a final concentration of 800 μM and 1000 μM, ICG was resuspended in 5 cc of sterile water, to yield a 6.4-mM stock solution prior to dilution.

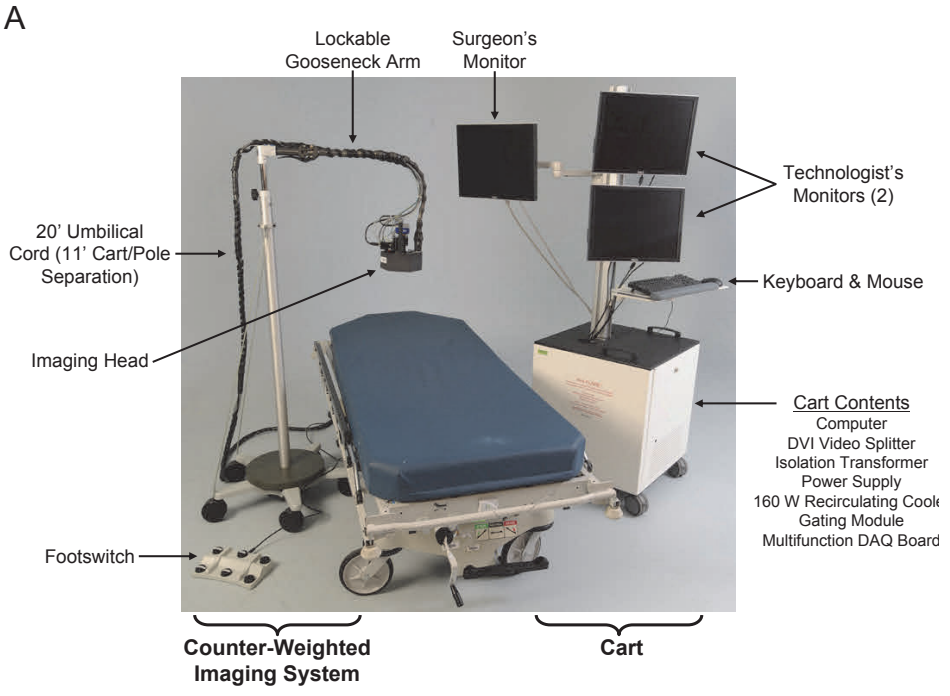

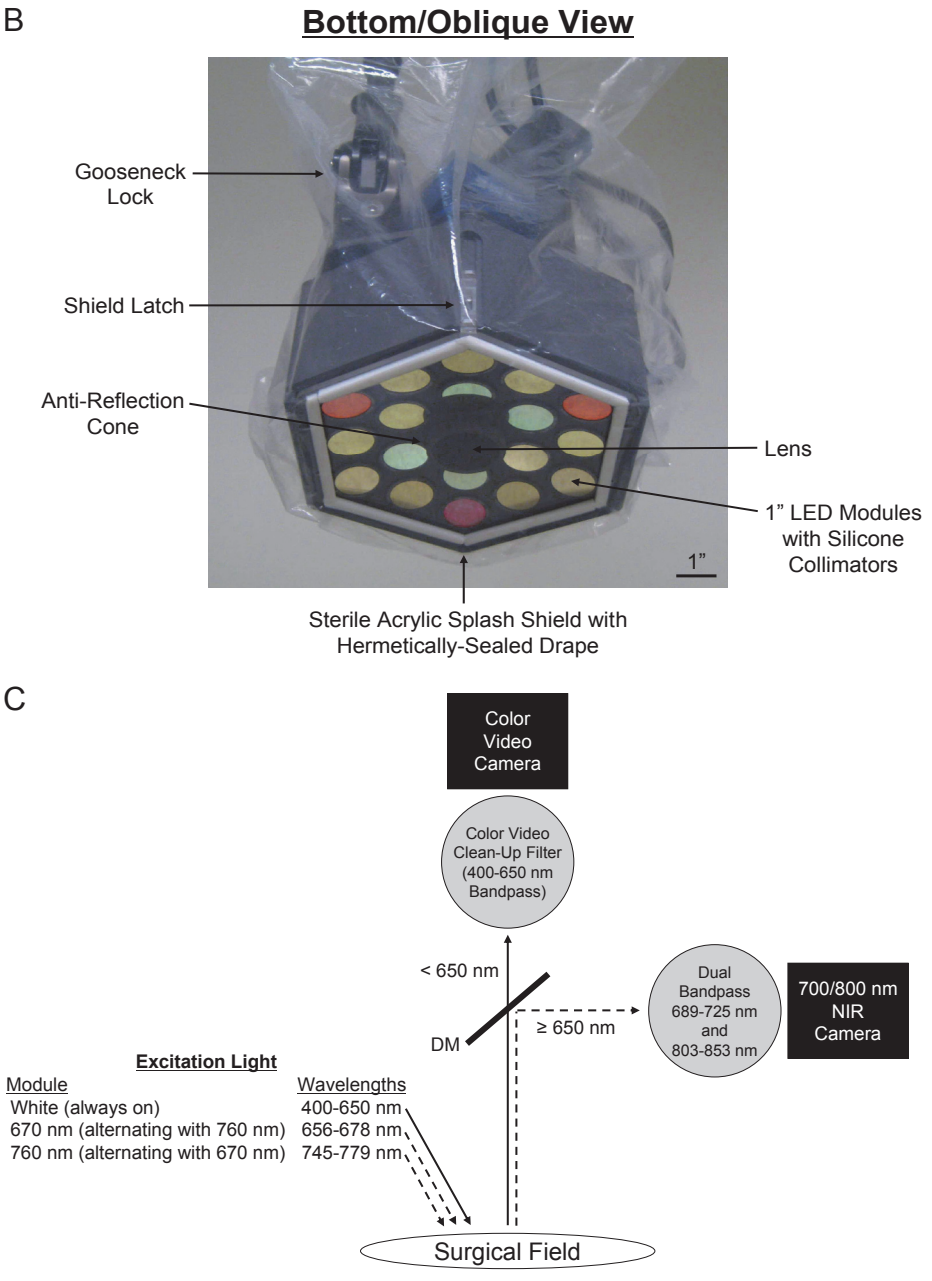


**Figure 1. The Mini-FLARE™ portable near-infrared fluorescence imaging system. A.** Imaging system composed of electronics/monitor cart and counter-weighted imaging system pole. **B.** Sterile drape/shield attached to the imaging head with other major parts identified. **C.** Excitation and emission light paths, and filtration for the Mini-FLARE™ imaging system. DM = 650 nm dichroic mirror.

**Pre-clinical characterization**

Animals were studied under the supervision of approved institutional protocol. Female Yorkshire pigs (E. M. Parsons and Sons, Hadley, USA) averaging 35 kg were induced with 4.4-mg/kg intramuscular Telazol (Fort Dodge Labs, Fort Dodge, USA), intubated, and maintained with 2% isoflurane (Baxter Healthcare, Deerfield, USA). Vital signs were monitored continuously. Excitation fluence rate for white light and 800-nm excitation light were 26,600 lux and 7.7 $mW/cm^2$, respectively. One hundred microliters of the specified ICG:HSA solution was injected intradermally. ICG concentration of the ICG:HSA complex was systematically increased from 10 μM to 500 μM to explore the counteracting effects of NIR fluorophore quenching at the injection site and NIR fluorophore dilution within the lymphatic channels.

**Dose-optimization clinical trial**

A 24-patient dose-escalation clinical trial was approved by the Medical Ethics Committee of the Leiden University Medical Center and was performed in accordance with the ethical standards of the Helsinki Declaration of 1975. All patients that had planned to undergo a SLN procedure for invasive breast cancer or extensive high-risk carcinoma *in situ* were eligible for participation in the study. Patients had clinically negative axillary nodes as assessed by palpation and ultrasonography. Exclusion criteria were pregnancy, lactation or an allergy to iodine, shellfish, or indocyanine green.

Twenty-four consecutive patients were included. All patients gave informed consent and were anonymized. Patients received the standard-of-care SLN procedure. For our institution, this implies one periareolar injection of approximately 100 MBq $^{99m}$Technetium-nanocolloid (mean ± S.D. = 99.6 ± 5.8 MBq) the day before surgery. Before the start of the operation, one mL of patent blue V was injected peritumorally or periareolarly. Choice of the injection site was left to the surgeon. Directly after patent blue injection, 1.6-mL ICG:HSA was administered as four injections at the same location as the patent blue injections. After surgical scrub and sterile covering of the operation field, NIR fluorescence imaging was performed with the imaging head of the Mini-FLARE™ at approximately 30 cm distance to the surgical field.

The surgical technique consisted of percutaneous assessment of NIR fluorescent signal in the breast and the axilla prior to skin incision. The location and length of the axillary skin incision was determined by the surgeon. Assessment of the surgical field using NIR fluorescence was applied continuously throughout the SLN procedure and surgical exploration. If the SLN was not easily detected by NIR fluorescence, the gamma probe was used to provide direction for surgical exploration. Camera exposure was between 5 to 250 msec as indicated. A SLN exhibiting a signal-to-background ratio (SBR) ≥ 1.1 *in situ* was considered positive by NIR fluorescence. Background

was chosen as an area within the surgical field, directly adjacent (within 1-2 cm) to the SLN.

Routine histopathological frozen analysis of SLNs was performed during surgery. If the patient participated in the After Mapping of the Axilla Radiotherapy or Surgery (AMAROS) trial and was randomized to the radiotherapy arm, no intraoperative frozen analysis was performed. SLNs were fixed in formalin and embedded in paraffin for routine hematoxylin, eosin, and immunohistopathological staining for AE1/AE3 at three levels, with an interval of 150-250 μm, according to the Dutch guidelines for SLN analysis. Patients underwent an axillary lymph node dissection if the SLN was found to contain metastases, except for those patients who participated in the radiotherapy arm of the AMAROS trial. If isolated tumor cells (ITCs) were found (< 0.2 mm), no axillary lymph node dissection was performed.

**Table 1.** Mini-FLARE™ imaging system specifications

| Category | Specification | Description |
|---|---|---|
| Physical | Size | Mobile Cart: 24" W x 24" D x 29" H; Mast Height: 76.5" |
| | Weights | Cart: 272 lbs, including all electronics<br>Arm: 95 lbs, including, stand, gooseneck, and imaging head<br>Imaging Head: 8.8 lbs. |
| | Arm and Stand | Flexible Arm; Reach: 27" – 64" from floor, 42" from center of stand. Center of stand up to 11 linear feet from cart |
| Electrical | Voltage and Plug | 120 V AC, 60 Hz; single NEMA 5-15 120 V/15 A AC plug |
| | Current | 5 A max |
| | Grounding | Isolation transformer for all components; redundant chassis grounding |
| | Leakage Current | < 300 μA (per AAMI/IEC #60601) |
| Sterility | Shield | Disposable acrylic shield with ≥95% transmission |
| | Drape | Disposable, custom-fit plastic drape bonded to shield |
| Light Source | Housing | Anodized aluminum with integrated liquid cooling |
| | Elements | Custom 25 mm circular LED arrays w/ integrated linear drivers |
| | Electronics | Custom control board with embedded microcontroller |
| | Fluence Rates | 26,600 lux white light (400-650 nm), 1.08 mW/cm$^2$ of 700 nm (656-678 nm) excitation light, 7.70 mW/cm$^2$ of 800 nm (745-779 nm) excitation light |
| Optics | Working Distance | 4" (10 cm) to 13" (32 cm) from patient (reverse telephoto) |
| | Field-of-View | 12 cm W x 9 cm H at 13" working distance |
| | Emission/ Reflectance Channels | Color Video (400-650 nm), 700 nm fluorescence (689-725 nm), 800 nm fluorescence (800-848 nm), all with simultaneous acquisition |
| | Pixel Resolution | 640 x 480 for each camera |
| | System Resolution | 320 x 320 μm (x,y) |
| | Display Refresh | Up to 15 Hz simultaneous acquisition on both cameras |
| | NIR Exposure Time | Adjustable from 100 μsec to 8 sec |
| Hands-Free | Optics | Automatic focus |
| | Control | 6-pedal footswitch |
| Monitors | Number | 3 cart-mounted 20": 2 for operator and 1 for surgeon |

### Statistical analysis

For statistical analysis, SPSS statistical software package (Version 16.0, Chicago, USA) was used. Graphs were generated using GraphPad Prism Software (Version 5.01, La Jolla, USA). To compare the SBR between concentration groups, a one-way analysis of variance (ANOVA) was performed with pairwise comparison with least square difference (LSD) adjustment for multiple testing. When the assumption of homogeneity of variance was violated (Levene's test), a log10 transformation was applied. All statistical tests were two-tailed and $P < .05$ was considered significant.

## RESULTS

### Design of the Mini-FLARE™ imaging system and *in vitro* characterization

The Mini-FLARE™ imaging system (Figure 1A) is composed of a small portable electronics cart and a counter-weighted pole stand that supports the imaging head. Unlike FLARE™, Mini-FLARE™ utilizes a flexible gooseneck arm, which permits positioning of the imaging head at extreme angles virtually anywhere over the surgical field. The only consumable for Mini-FLARE™ is a specially designed acrylic splash plate that is hermetically sealed to a plastic drape. Using sterile technique, the shield/drape is inserted into the imaging head, locked into place, and the drape is unfolded to encase the imaging head and imaging system pole stand (Figure 1B). Optical light paths for white light (i.e., color video images) and the two semi-independent NIR fluorescence channels, one centered at 700 nm emission and the other at 800 nm emission, are shown in Figure 1C.

Technical specifications of Mini-FLARE™ are detailed in Table 1. Of note, the working distance is up to 13" away from the patient, with field-of-view adjustable from 4.7" (12 cm) to 2" (5 cm) simply by moving the device toward or away from the surgical field. The cart occupies a volume of only 9.7 cu ft, and weighs only 272 lbs. A 6-pedal footswitch and autofocus circuit permit hands-free operation. The cost of all parts is ≈ $40,000.

### Pre-clinical optimization of NIR fluorescent lymphatic tracers

Our group has previously reported that ICG (and ICG:HSA) exhibits intense quenching (i.e., reduction of fluorescence emission) as its concentration is increased.[15] That is, increasing concentration actually decreases fluorescence, so there would theoretically be no benefit to injecting high concentration for SLN mapping. This effect is demonstrated vividly in Figure 2 (left panel), where the injection site becomes dramatically less fluorescent as concentration increases. As a general rule, if the

concentration is high enough to see green color at the injection site, ICG fluorescence is severely quenched.

Importantly, we have recently discovered that dilution of the injected NIR fluorophore as it travels through the lymphatic system and mixes with lymph counteracts the effect of quenching and results in signal in the SLN that increases with concentration, even when the injection site is barely fluorescent (Figure 2, right panel). This suggests that there will be an "optimal" concentration of injected NIR fluorophore such that final signal in the SLN is as high as possible.

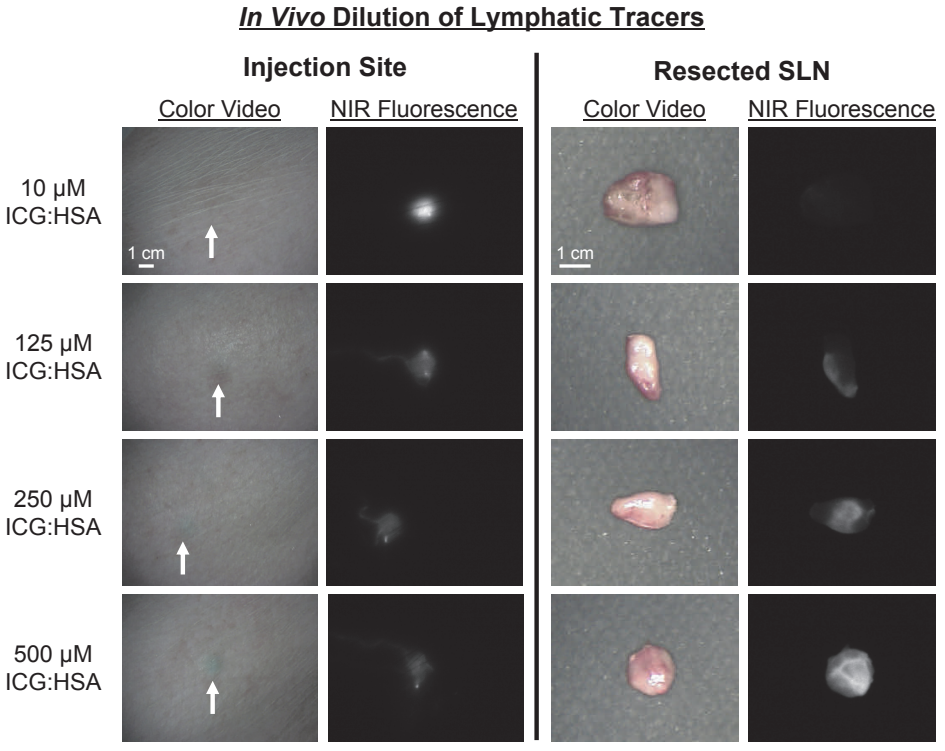


**Figure 2. Optimization of ICG:HSA dose as a function of the complex tradeoff between fluorescence quenching at the injection site and dilution of fluorophore in lymphatic channels.** Pre-clinical studies in Yorkshire pigs. Subcutaneous injection sites (left; white arrows) showing quenching and resected SLNs (right) showing NIR fluorophore dilution for increasing concentrations of ICG:HSA. For each are displayed color video (left columns) and 800 nm NIR fluorescence (right columns) images obtained using 760 nm excitation light at 7.7 mW/cm$^2$. All camera exposure times were 45 msec. Data are representative of N = 3 pigs.

## Optimization of ICG:HSA dose in breast cancer patients undergoing SLN mapping

This study aimed to test the feasibility of NIR fluorescence in SLN detection, using ICG:HSA and the Mini-FLARE™, in direct comparison with the conventional lymphatic tracers radiocolloid and patent blue. Twenty-four consecutive breast cancer

patients underwent standard-of-care SLN mapping with the addition of preoperative ICG:HSA injection and subsequent intraoperative NIR fluorescence imaging. Patient and tumor characteristics are provided in Table 2. Use of the Mini-FLARE™ during surgery did not interfere with the standard of care. Average time between ICG:HSA injection and skin incision was 16 ± 3 minutes (Table 3). In all patients (N = 24), NIR fluorescence imaging enabled visualization of the SLN (Figure 3). A total of 35 SLNs were identified, which were all radioactive and NIR fluorescent (Table 3). Five SLNs from four patients did not have blue staining from patent blue. In all patients, the NIR fluorescence signal in the SLN was detected before patent blue. Average time between skin incision and resection of the first SLN was 17 ± 5 minutes. After resection of all nodes detected using NIR fluorescence, the axilla was systematically inspected for any remaining radioactivity. No additional radioactive nodes were identified that were not detected by NIR fluorescence. No adverse reactions associated with the use of ICG:HSA or the Mini-FLARE™ occurred. Two patients experienced a wound infection requiring antibiotics and one patient underwent surgical re-exploration because of an expanding hematoma following axillary lymph node dissection (Table 3).

A second objective of this trial was to determine the optimal concentration of injected ICG:HSA for NIR fluorescence SLN mapping, i.e. which concentration provides the highest SBR in the SLN. Because ICG and ICG:HSA exhibit intense quenching as their concentrations are increased (typically above 50 μM), there would be theoretically no advantage of injecting higher doses of ICG:HSA. However, dilution of the lymphatic tracer occurs upon injection in the breast and uptake by the lymphatic system counteracting the quenching effect. To assess the relationship between the

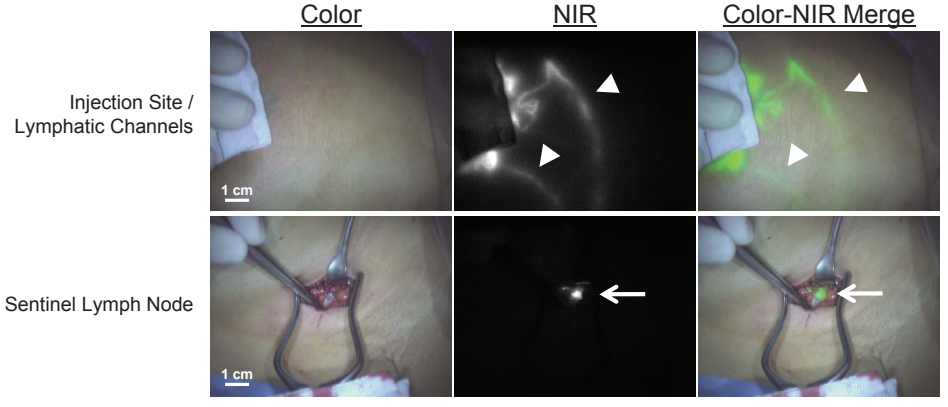


**Figure 3. Real-time NIR fluorescence imaging during sentinel lymph node mapping in women with breast cancer.** Shown are typical intraoperative results from a subject injected with 600 μM ICG:HSA demonstrating visualization of lymphatic channels (white arrowhead) of the breast running into the axilla from the partially covered periareolar injection site (top row) and detection of the sentinel lymph node (white arrow) in the axilla (bottom row). Camera exposure times were 67 msec (top row) and 20 msec (bottom row). 760 nm excitation fluence rate was ≈ 7.7 mW/cm$^2$ for all images.

concentration of injected NIR fluorescent lymphatic tracer and final SBR in the SLN, patients were allocated to eight ICG:HSA concentration groups ranging from 50 μM to 1000 μM. The concentration of ICG:HSA influenced the SBR and showed a normal distribution (Figure 4). The variances of the concentration groups were not equal (Levene's test, $P = .02$). A log10 transformation of the data could account for part of the unequal variances (Levene's test, $P = .05$). A one-way ANOVA with pairwise

**Table 2.** Patient and tumor characteristics

| Characteristic | N | % |
|---|---|---|
| Age (median, range) | 59.5 (33-81) | |
| Menopausal state | | |
| - Premenopausal | 5 | 21 |
| - Postmenopausal | 19 | 79 |
| Body Mass Index (median, range) | 25 (18-38) | |
| Skin type | | |
| - II | 4 | 17 |
| - III | 20 | 83 |
| Previous breast surgery [a] | 3 | 13 |
| Multifocality | 4 | 17 |
| Tumor side | | |
| - Left | 14 | 58 |
| - Right | 10 | 42 |
| Tumor localization | | |
| - Central | 5 | 21 |
| - Lower inner | 1 | 4 |
| - Lower outer | 1 | 4 |
| - Upper inner | 6 | 25 |
| - Upper outer | 11 | 46 |
| Type of operation | | |
| - Ablation | 9 | 38 |
| - Wide Local Excision | 15 | 63 |
| Pathological tumor size (median, range) | 15 (3-35) | |
| Histological type | | |
| - Infiltrating ductal adenocarcinoma | 18 | 75 |
| - Infiltrating lobular adenocarcinoma | 2 | 8 |
| - Ductal carcinoma *in situ* | 4 | 17 |
| Histological grade | | |
| - I | 3 | 13 |
| - II | 13 | 54 |
| - III | 8 | 33 |
| Receptor status [b] | | |
| - ER+ HER2- | 16 | 67 |
| - ER+ HER2+ | 3 | 13 |
| - ER- HER2- | 1 | 4 |
| - Missing [c] | 4 | 17 |

[a] Previous breast surgery (N = 3): silicone breast implantation, breast reduction and re-excision.
[b] HER2 status was determined using the chromogenic *in situ* hybridization (CISH) kit of Zymed (Invitrogen, Carlsbad, CA)
[c] Not applicable in four patients with ductal carcinoma *in situ*.

comparison with LSD adjustment for multiple comparison showed that the SBRs of the 400, 500, 600, and 800 μM concentration groups were significantly higher than of the 50, 100, 200, and 1000 μM concentration groups (200 vs. 400, $P = .001$; 200 vs. 500, $P = .001$; 200 vs. 600, $P < .0001$; 200 vs. 800, $P = .001$; 1000 vs. 400, 500, 600 and 800, all $P < .0001$). The SBRs of the 400, 500, 600, and 800 μM concentration groups were not significantly different, although a trend was found favoring the 600 μM concentration group (500 vs. 600, $P = .06$). The decline of the SBR in the 1000 μM concentration group was caused by decreased NIR fluorescence signal of the SLN (800 vs. 1000, $P = .001$), which suggests that quenching of ICG indeed occurred in the SLN.

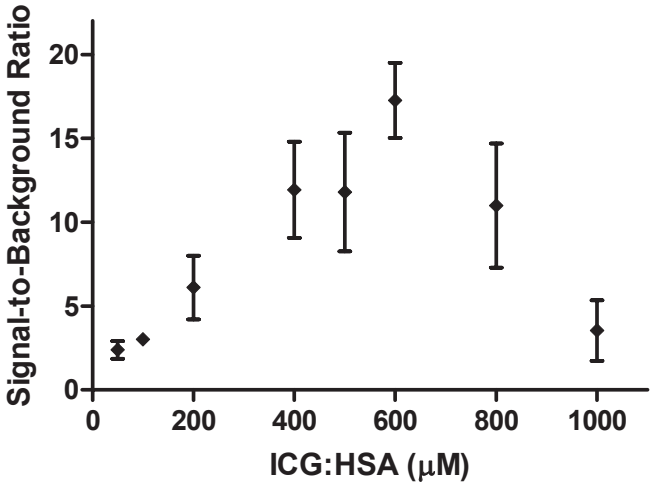


**Figure 4. Optimization of ICG:HSA concentration for breast cancer SLN mapping.** Signal-to-background ratio (mean ± S.D.) of the SLNs (ordinate) as a function of injected concentration of ICG:HSA (abscissa) in women undergoing SLN mapping for breast cancer. Statistical comparisons are as follows: 200 μM vs. 400 μM, $P = .001$; 200 μM vs. 500 μM, $P = .001$; 200 μM vs. 600 μM, $P < .0001$; 200 μM vs. 800 μM, $P = .001$; 1000 μM vs. 400, 500, 600 and 800 μM, all $P < .0001$). The SBRs of the 400, 500, 600 and 800 μM concentration groups were not significantly different, although a trend was found favoring the 600 μM concentration group (500 vs. 600, $P = .06$).

## DISCUSSION

Near-infrared (NIR) fluorescent light in the wavelength range of 700 to 900 nm is invisible to the human eye. It is also capable of penetrating millimeters into living tissue and is not obscured by autofluorescence. For these reasons, NIR fluorescent light is ideal for image-guided surgery. Indeed, several NIR fluorescence surgical imaging systems are already FDA-approved or are in the process of obtaining approval (reviewed in [17]). The Mini-FLARE™ camera system used in this study is capable of displaying NIR fluorescence signal in relation to the surgical anatomy and illuminates the surgical field with white light. This enabled the surgeon to perform surgery under direct image guidance.

NIR fluorescence optical imaging using Mini-FLARE™ offers the advantages of real-time, continuous, high-resolution, and high sensitivity detection of SLNs, without the need for ionizing radiation. Because NIR light is invisible, there is no staining of the surgical field as with blue dyes, and the class of chemicals in which ICG belongs has a remarkable safety record in humans. ICG:HSA adds approximately $150 to the cost of a case, but if future studies show that the blue dye and/or Tc-99m sulfur colloid can be eliminated when using NIR fluorescence, a much larger savings will offset this cost. And, the surgeon can perform the injection procedure only minutes before SLN identification and resection. Although a technologist was used in this first-in-human study, Mini-FLARE™ is equipped with hand-free operation and there is virtually no learning curve because unlike other SLN techniques, the lymphatic tracer can be visualized in real-time throughout the procedure.

**Table 3.** SLN identification results

| Characteristic | N | % |
|---|---|---|
| Injection site patent blue and ICG:HSA | | |
| - Periareolar | 20 | 83 |
| - Peritumoral | 4 | 17 |
| | | |
| SLN detection | | |
| - Number of SLNs identified | 35 | |
| - Average number of SLNs identified (range) | 1.45 (1-3) | |
| Method of detection | | |
| - Radioactive | 35 | 100 |
| - Blue | 30 | 86 |
| - Near-infrared fluorescence | 35 | 100 |
| | | |
| Average time between injection of ICG:HSA and skin incision (S.D.) | 16 minutes ± 3 | |
| Average time between skin incision and SLN resection (S.D.) | 17 minutes ± 5 | |
| | | |
| Histology | | |
| - Negative | 26 | 74 |
| - Isolated tumor cells | 3 | 9 |
| - Micrometastases | 0 | 0 |
| - Macrometastases | 6 | 17 |
| | | |
| Axillary treatment | | |
| - None | 16 | 67 |
| - Axillary lymph node dissection | 5 | 21 |
| - Axillary radiotherapy | 3 | 13 |
| Complications | | |
| - No | 21 | 87 |
| - Yes | 3 [a] | 13 |

Abbreviations: ICG:HSA = indocyanine green adsorbed to human serum albumin, SLN = sentinel lymph node, S.D. = standard deviation

[a] Two patients experienced postoperative wound infection requiring treatment with antibiotics and one patient underwent surgical re-exploration because of an expanding hematoma following axillary lymph node dissection.

An important objective of the study was to optimize NIR fluorescent contrast agent dose for breast cancer SLN mapping. The only clinically available NIR fluorescent lymphatic tracer, albeit approved for other indications, is ICG.[7, 11, 13, 18, 19] We have previously proposed simple mixing of ICG and HSA (ICG:HSA) prior to injection[14, 15] because ICG is a small molecule and like blue dyes can pass through SLNs, and exhibit a relatively low quantum yield in aqueous environments.[15] Indeed, the product insert for ICG notes that it rapidly binds albumin when injected intravenously, so pre-mixing merely improves kinetics. Importantly, though, pre-mixing increases quantum yield (i.e., brightness) 3-fold and also results in a final hydrodynamic diameter (≈ 7 nm) that is better retained in the SLN.[15]

NIR fluorescent signal in the SLN is a complex function of the concentration of the injected NIR lymphatic tracer, the distance between the injection site and the SLN, the volume of ultra-filtrate within the lymphatic channels encountered by the NIR fluorophore, and retention of the NIR fluorophore by the SLN. Of these, only the injection concentration can be controlled. Our study suggested that an optimal ICG:HSA concentration is in the range 400 μM and 800 μM. In the 1000 μM concentration group, the fluorescence intensity of the SLN and the SBR decreased rapidly, most likely due to quenching. Furthermore, since lymphatic vessels could be visualized percutaneously and directly after incision, particularly in the optimal dose range groups, a more efficient identification of SLNs was facilitated. This is of particular benefit for lymph nodes located deeper in the axilla, which exceed the 1-2 cm depth limit of the technology. These nodes could often be located by following the NIR fluorescent signal of the afferent lymphatic tract.

The accuracy of SLN identification using ICG fluorescence was similar to that using conventional radioisotope scanning, as both techniques identified all SLNs and no additional fluorescent lymph nodes were identified. However, blue dye identification was not successful in 5 of 35 (14%) SLNs. These results suggest that patent blue staining can be replaced by NIR fluorescence using ICG:HSA. Replacing patent blue has the additional advantage of absent tattooing of the breast and visual alteration of the surgical field. Moreover, the intrinsic dark color of patent blue dye can obscure the fluorescence intensity of any fluorescent lymphatic tracer. Indeed, *in vitro* tests using a fixed ICG:HSA concentration showed that addition of patent blue dye decreased NIR fluorescence of ICG:HSA (data not shown). An as yet unanswered question is whether radioisotope scanning can be omitted from the SLN procedure. A larger trial to address whether NIR fluorescence imaging alone can replace blue dyes and/or radiocolloids is ongoing.

In summary, this study demonstrated feasibility and accuracy of NIR fluorescence imaging using ICG:HSA and the Mini-FLARE™ imaging system for SLN mapping in breast cancer patients. The optimal dose of injected ICG:HSA lies between 400 μM and 800 μM and can be chosen based on local preparation preferences. For example, in the United States, a dose of 500 μM is most convenient since it requires minimal manipulation of albumin volumes.

## ACKNOWLEDGEMENTS

The BIDMC study team thanks Barbara L. Clough and Mireille Rosenberg for clinical trial preparation, Keith V. Belken from the BIDMC Investigational Pharmacy, Judith Hirshfield-Bartek for assistance with patient medical histories, Sunil Gupta for technical assistance with the imaging system, Lorissa A. Moffitt and Lindsey Gendall for editing, and Eugenia Trabucchi for administrative support.

The Leiden study team thanks Gemma Ranke, Elly Krol-Warmerdam, Annemarie Voet-van den Brink, Gerlinda van Gent-de Bruijn (Breast Cancer Unit) and Linda van der Hulst (Central Pharmacy). Part of the study protocol was written during the 10th ECCO-AACR-ASCO Workshop on Methods in Clinical Cancer Research (Flims, Switzerland).

We thank the following individuals and companies for their contributions to this project: Gordon Row (Yankee Modern Engineering), Kelly Stockwell and Paul Millman (Chroma Technology), David Comeau and Robert Waitt (Albright Technologies), Bob Zinter, Gary Avery, Phil Dillon, Will Barker, Craig Shaffer, and Ed Schultz (Qioptiq), Jeffrey Thumm (Duke River Engineering), Colin Johnson (LAE Technologies), Robert Eastlund (Graftek Imaging), John Fortini (Lauzon Manufacturing), Steve Huchro (Solid State Cooling), Clay Sakewitz, Johnny Fraga, and Will Richards (Design and Assembly Concepts), Ken Thomas and Fernando Irizarry (Sure Design), Paul Bistline and Phil Bonnette (Medical Technique, Inc.), Amy King (Civco), and Jim Cuthbertson (Nashua Circuits).

This study was supported in part by the following grants from the National Institutes of Health (National Cancer Institute) to JVF: NIH Bioengineering Research Partnership grant #R01-CA-115296 (JVF), Quick Trials for Imaging grant #R21-CA-130297 (JVF), Nuts Ohra Fund (ALV), the Maurits and Anna de Kock Foundation (ALV), and the American Women's Club of The Hague. JSDM is a MD-medical research trainee funded by The Netherlands Organisation for Health Research and Development (grant nr. 92003526).

## REFERENCES


1. Giuliano AE, Kirgan DM, Guenther JM, et al. Lymphatic mapping and sentinel lymphadenectomy for breast cancer. Ann Surg 1994; 220:391-8.
2. Cox CE, Pendas S, Cox JM, et al. Guidelines for sentinel node biopsy and lymphatic mapping of patients with breast cancer. Ann Surg 1998; 227:645-51.
3. Goyal A, Newcombe RG, Chhabra A, et al. Factors affecting failed localisation and false-negative rates of sentinel node biopsy in breast cancer - results of the ALMANAC validation phase. Breast Cancer Res Treat 2006; 99:203-8.
4. Krag DN, Anderson SJ, Julian TB, et al. Technical outcomes of sentinel-lymph-node resection and conventional axillary-lymph-node dissection in patients with clinically node-negative breast cancer: results from the NSABP B-32 randomised phase III trial. Lancet Oncol 2007; 8:881-8.
5. Straver ME, Meijnen P, van Tienhoven G, et al. Sentinel node identification rate and nodal involvement in the EORTC 10981-22023 AMAROS trial. Ann Surg Oncol 2010; 17:1854-61.
6. Zavagno G, De Salvo GL, Scalco G, et al. A Randomized clinical trial on sentinel lymph node biopsy versus axillary lymph node dissection in breast cancer: results of the Sentinella/GIVOM trial. Ann Surg 2008; 247:207-13.
7. Hirche C, Murawa D, Mohr Z, et al. ICG fluorescence-guided sentinel node biopsy for axillary nodal staging in breast cancer. Breast Cancer Res Treat 2010; 121:373-8.
8. Hojo T, Nagao T, Kikuyama M, et al. Evaluation of sentinel node biopsy by combined fluorescent and dye method and lymph flow for breast cancer. Breast 2010; 19:210-3.
9. Kitai T, Inomoto T, Miwa M, et al. Fluorescence navigation with indocyanine green for detecting sentinel lymph nodes in breast cancer. Breast Cancer 2005; 12:211-5.
10. Murawa D, Hirche C, Dresel S, et al. Sentinel lymph node biopsy in breast cancer guided by indocyanine green fluorescence. Br J Surg 2009; 96:1289-94.
11. Sevick-Muraca EM, Sharma R, Rasmussen JC, et al. Imaging of lymph flow in breast cancer patients after microdose administration of a near-infrared fluorophore: feasibility study. Radiology 2008; 246:734-41.
12. Tagaya N, Yamazaki R, Nakagawa A, et al. Intraoperative identification of sentinel lymph nodes by near-infrared fluorescence imaging in patients with breast cancer. Am J Surg 2008; 195:850-3.
13. Tanaka E, Chen FY, Flaumenhaft R, et al. Real-time assessment of cardiac perfusion, coronary angiography, and acute intravascular thrombi using dual-channel near-infrared fluorescence imaging. J Thorac Cardiovasc Surg 2009; 138:133-40.
14. Troyan SL, Kianzad V, Gibbs-Strauss SL, et al. The FLARE intraoperative near-infrared fluorescence imaging system: a first-in-human clinical trial in breast cancer sentinel lymph node mapping. Ann Surg Oncol 2009; 16:2943-52.
15. Ohnishi S, Lomnes SJ, Laurence RG, et al. Organic alternatives to quantum dots for intraoperative near-infrared fluorescent sentinel lymph node mapping. Mol Imaging 2005; 4:172-81.
16. Gioux S, Kianzad V, Ciocan R, et al. High-power, computer-controlled, light-emitting diode-based light sources for fluorescence imaging and image-guided surgery. Mol Imaging 2009; 8:156-65.
17. Gioux S, Choi HS, Frangioni JV. Image-guided surgery using invisible near-infrared light: fundamentals of clinical translation. Mol Imaging 2010; 9:237-55.
18. Kusano M, Tajima Y, Yamazaki K, et al. Sentinel node mapping guided by indocyanine green fluorescence imaging: a new method for sentinel node navigation surgery in gastrointestinal cancer. Dig Surg 2008; 25:103-8.
19. Yamashita S, Tokuishi K, Anami K, et al. Video-assisted thoracoscopic indocyanine green fluorescence imaging system shows sentinel lymph nodes in non-small-cell lung cancer. J Thorac Cardiovasc Surg 2011; 141:141-4.

# Chapter 12

# Randomized, double-blind comparison of indocyanine green with or without albumin premixing for near-infrared fluorescence imaging of sentinel lymph nodes in breast cancer patients

Hutteman M[1], Mieog JSD[1], van der Vorst JR, Liefers GJ, Putter H, Löwik CWGM, Frangioni JV, van de Velde CJH, Vahrmeijer AL

[1] Shared first authorship

*Breast Cancer Res Treat 2011; 127:163-70*

## ABSTRACT

### Introduction

Near-infrared (NIR) fluorescence imaging has the potential to improve sentinel lymph node (SLN) mapping in breast cancer. Indocyanine green (ICG) is currently the only clinically available fluorophore that can be used for SLN mapping. Preclinically, ICG adsorbed to human serum albumin (ICG:HSA) improves its performance as a lymphatic tracer in some anatomical sites. The benefit of ICG:HSA for SLN mapping of breast cancer has not yet been assessed in a clinical trial.

### Methods

We performed a double-blind, randomized study to determine if ICG:HSA has advantages over ICG alone. The primary endpoint was the fluorescence brightness, defined as the signal-to-background ratio (SBR), of identified SLNs. Clinical trial subjects were 18 consecutive breast cancer patients scheduled to undergo SLN biopsy. All patients received standard of care using $^{99m}$Technetium-nanocolloid and patent blue. Patients were randomly assigned to receive 1.6 mL of 500 μM ICG:HSA or ICG that was injected periareolarly directly after patent blue. The Mini-Fluorescence-Assisted Resection and Exploration (Mini-FLARE) imaging system was used for NIR fluorescence detection and quantitation.

### Results

SLN mapping was successful in all patients. Patient, tumor and treatment characteristics were equally distributed over the treatment groups. No significant difference was found in SBR between the ICG:HSA group and the ICG alone group (8.4 vs. 11.3, respectively, $P = .18$). In both groups, the average number of detected SLNs was 1.4 ± 0.5 SLNs per patient ($P = .74$).

### Conclusion

This study shows that there is no direct benefit of premixing ICG with HSA prior to injection for SLN mapping in breast cancer patients, thereby reducing the cost and complexity of the procedure. With these optimized parameters that eliminate the necessity of HSA, larger trials can now be performed to determine patient benefit.

## INTRODUCTION

Sentinel lymph node (SLN) mapping is currently regarded as standard of care in staging of the axilla in breast cancer patients with clinically negative axillary lymph nodes.[1] In general, a combination of radioactive colloid and blue dye is used for SLN mapping. Using this combination, identification rates of 95% to 97% are achieved.[2-5] The use of only one of these two detection methods results in significantly lower identification rates.[2-5] Both detection methods possess certain disadvantages. Radioactive colloids require involvement of a nuclear medicine physician, can be difficult to localize with a handheld gamma probe, and the time-window for SLN identification is limited due to the short half-life (6 hours) of $^{99m}$Technetium. Blue dyes cannot be seen through skin and fatty tissue, and permit only limited visualization of afferent lymphatic vessels and the SLN.

Optical imaging using the near-infrared (NIR) fluorescence lymphatic tracer indocyanine green (ICG) enables real-time transcutaneous and intraoperative visualization of lymphatic channels and SLNs.[6-13] Therefore, NIR fluorescence imaging could provide an alternative for, or an addition to, conventional techniques used for SLN mapping. Recently, our group has demonstrated that NIR fluorescence performed equally well as the combination of radioactive colloid and blue dye in SLN mapping of breast cancer patients.[14]

ICG is currently the only clinically available NIR lymphatic tracer. However, due to its relatively low fluorescence brightness and its small hydrodynamic diameter, which permits flow through the SLN to higher tier nodes, it is not an optimal lymphatic tracer. Preclinical work has demonstrated that adsorption of ICG to human serum albumin (HSA, complex is ICG:HSA), by simply mixing it, increases the fluorescence intensity and the hydrodynamic diameter, thereby providing improved detection and better retention in the SLN in certain anatomical sites, such as the intestine.[15] Another parameter that must be considered when using ICG or ICG:HSA is the effect of fluorescence quenching, which results in a decrease in fluorescence intensity as the concentration of ICG (or ICG:HSA) is increased above 50 μM. The use of 50 μM ICG for SLN imaging, however, is suboptimal, because ICG will be diluted once taken up by the lymphatic system. To assess the magnitude of this *in vivo* dilution effect, our group has conducted a dose-finding study to demonstrate that the optimal concentration of ICG:HSA for NIR-based SLN mapping in breast cancer patients lies between 400 μM and 800 μM.[14]

A theoretical disadvantage of the use of ICG alone is poor retention of the lymphatic tracer in the SLN, which as a consequence results in fluorescent staining of higher tier nodes and background staining of the axilla. Although not compared directly, studies using ICG alone reported a higher average number of identified SLNs (range = 1.8-5.4; aggregate average = 3.4),[6-10] than with the use of ICG:HSA (aggregate: 1.5).[11, 14] However, comparison of these data is difficult because the concentration of

ICG used was significantly higher (typically 6.4 mM) than in the trials using ICG:HSA (10 μM to 1000 μM).

Although we have obtained good results with the use of ICG:HSA for SLN mapping in breast cancer patients, the use of albumin adds cost and complexity to the procedure. Moreover, the use of human blood products, such as HSA, poses regulatory hurdles in certain countries, such as the United States. Therefore, the use of ICG alone would be favorable. After intravenous administration, ICG binds rapidly and completely to plasma proteins.[16] Lymph fluid has a similar protein constitution as serum, albeit in a lower concentration (20.6 g/L for lymph fluid versus 73.7 g/L for plasma).[17] After intradermal or subcutaneous injection, ICG could theoretically bind to these proteins, eliminating the need for premixing ICG and HSA. We therefore hypothesized that ICG alone could render the same fluorescence intensity in SLNs as ICG:HSA, and tested this hypothesis in a double-blind randomized trial.

## MATERIAL AND METHODS

### Preparation of indocyanine green adsorbed to human serum albumin

ICG (25 mg vials) was purchased from Pulsion Medical Systems (Munich, Germany) and was resuspended in 10 cc of sterile water for injection to yield a 2.5 mg/ml (3.2 mM) stock solution. To obtain a 500 μM dilution, 7.8 mL of the 3.2 mM ICG solution was diluted in 50 cc vial of sterile water for injection or 50 cc vial of Cealb (20% human serum albumin, Sanquin, Amsterdam, The Netherlands) for the preparation of ICG alone or ICG:HSA, respectively. Prior to the addition of ICG, 7.8 mL was drawn from the 50 cc vials. In a previous study, we determined that the optimal dose of ICG:HSA lies between 400 μM and 800 μM.[14] A dose of 500 μM was chosen because it requires minimal manipulation of ICG and albumin volumes.

### Intraoperative near-infrared imaging system (Mini-FLARE)

SLN mapping was performed using the Mini-Fluorescence-Assisted Resection and Exploration (Mini-FLARE) image-guided surgery system as described in Chapter 11. Briefly, the system consists of two wavelength isolated light sources: a "white" light source, generating 26,600 lx of 400-650 nm light, and a "near-infrared" light source, generating 7.7 mW/cm$^2$ of 760 nm light. Color video and NIR fluorescence images are simultaneously acquired and displayed in real-time using custom optics and software that separate the color video and NIR fluorescence images. A pseudo-colored (lime green) merged image of the color video and NIR fluorescence images is also displayed. The imaging head is attached to a flexible gooseneck arm, which permits positioning

of the imaging head at extreme angles virtually anywhere over the surgical field. For intraoperative use, the imaging head and imaging system pole stand are wrapped in a sterile shield and drape (Medical Technique Inc., Tucson, USA).

## Clinical trial

The double-blind, randomized, single-institution, non-inferiority trial comparing ICG:HSA with ICG alone was approved by the Medical Ethics Committee of the Leiden University Medical Center and was performed in accordance with the ethical standards of the Helsinki Declaration of 1975. All patients planning to undergo a sentinel lymph node procedure whether for invasive breast cancer or for high-risk carcinoma *in situ* were eligible for participation in the study. Patients had clinically negative axillary nodes as assessed by palpation and ultrasonography. Exclusion criteria were pregnancy, lactation or an allergy to iodine, shellfish, or indocyanine green.

All patients gave informed consent and were anonymized. Patients were randomized by the Department of Clinical Pharmacy. Treatment allocation was performed by block randomization. Patients received the standard-of-care sentinel lymph node procedure. For our institution, this implies one periareolar injection of approximately 100 MBq $^{99m}$Technetium-nanocolloid (mean ± S.D. = 96.6 ± 14.7 MBq, no difference between treatment groups [$P$ = .47]) the day before surgery. Before the start of the operation, one mL of patent blue V was injected. Directly after patent blue injection, the surgeon injected a total of 1.6 mL of 500 μM ICG:HSA or ICG alone. Both dyes were injected intradermally and periareolarly at four sites. Gentle pumping pressure was applied to the injection site for 1 min. After surgical scrub and sterile covering of the operation field, NIR fluorescence imaging was performed with the imaging head of the Mini-FLARE at approximately 30 cm distance to the surgical field. Camera exposure times were between 5 to 200 msec. A SLN exhibiting a signal-to-background ratio (SBR) ≥ 1.1 *in situ* was considered positive by NIR fluorescence. Both the surgeon and the Mini-FLARE operator, who was responsible for analyzing the data, were blinded to the treatment allocation.

Routine histopathological frozen analysis of SLNs was performed during surgery. SLNs were fixed in formalin and embedded in paraffin for routine hematoxylin and eosin staining and immunohistopathological staining for AE1/AE3 at three levels, with an interval of 150 to 250 μm, according to the Dutch guidelines for SLN analysis. Patients underwent an axillary lymph node dissection if the SLN was found to contain metastases. If isolated tumor cells were found (< 0.2 mm), no axillary lymph node dissection was performed.

### Power calculation and statistical analysis

A power calculation based on data from our previous study[14] revealed that 18 patients are needed to achieve 91% power to detect non-inferiority using a one-sided, two-sample *t*-test (α = 0.025) with a margin of equivalence of 5.0 while assuming no difference between the SBRs of ICG:HSA and ICG alone. For statistical analysis, SPSS statistical software package (Version 16.0, Chicago, USA) was used. Graphs were generated using GraphPad Prism Software (Version 5.01, La Jolla, USA). To compare the SBR and the number of SLNs identified between ICG:HSA and ICG alone, a one-sided, two-sample *t*-test was performed. A *P*-value < .05 was considered significant.

## RESULTS

Eighteen consecutive breast cancer patients undergoing standard-of-care SLN mapping were randomized to ICG:HSA or ICG alone for NIR fluoresence SLN imaging. Patient, tumor and treatment characteristics were equally distributed over the treatment groups (Table 1). Use of the Mini-FLARE during surgery did not interfere with the standard of care. Average time between lymphatic tracer injection and skin incision was 15.6 ± 2.2 minutes (Table 2). In all patients (N = 18), NIR fluorescence imaging enabled visualization of one or more SLNs (Figure 1). In the ICG:HSA group (N = 8 subjects), a total of 11 SLNs were identified (average per patient = 1.4 ± 0.5); 9 (82%) were radioactive, 8 (73%) were blue and 11 (100%) were NIR fluorescent. In the ICG alone group (N = 10 subjects), a total of 14 SLNs were identified (average per patient = 1.4 ± 0.5); 14 (100%) were radioactive, 10 (71%) were blue and 14 (100%) were NIR fluorescent. The average number of SLNs identified was not significantly different between both groups (*P* = .74).

The primary endpoint of this study was the average brightness of the SLN in both groups, expressed in signal-to-background ratio (SBR). The results are presented in Table 2. The average SBR of ICG:HSA (8.4 ± 3.6) and ICG alone (11.3 ± 4.8) was not significantly different (*P* = .18). However, in the ICG alone group, the afferent lymphatics were significantly better visualized percutaneously compared to the ICG:HSA group (*P* = .004; Table 2 and Figure 1).

In all patients, the NIR fluorescence signal in the SLN was detected earlier in the procedure than patent blue staining. Average time between skin incision and resection of the first SLN was 11.0 ± 4.1 minutes and was not different between both groups (*P* = .74). No adverse reactions associated with the use of ICG, ICG:HSA, or Mini-FLARE occurred.

**Table 1.** Patient and tumor characteristics

| | ICG:HSA (N = 8) | | ICG alone (N = 10) | | |
|---|---|---|---|---|---|
| **Characteristic** | **N** | **%** | **N** | **%** | ***P*** |
| Age (median, range) | 59.5 (38-72) | | 57.5 (40-73) | | 0.99 |
| Menopausal state | | | | | 0.74 |
| - Premenopausal | 3 | 37.5 | 3 | 30 | |
| - Postmenopausal | 5 | 62.5 | 7 | 70 | |
| Body Mass Index (median, range) | 26 (20-41) | | 23.5 (21-30) | | 0.26 |
| Skin type | | | | | 0.40 |
| - II | 2 | 25 | 1 | 10 | |
| - III | 6 | 75 | 9 | 90 | |
| Previous procedure of breast | | | | | 0.12 |
| - Breast implants | 1 | | 0 | | |
| - Breast reduction | 0 | | 1 | | |
| - Lumpectomy | 2 | | 0 | | |
| - Radiotherapy | 0 | | 1 | | |
| - Neoadjuvant chemotherapy | 1 | | 0 | | |
| Multifocality | 0 | | 0 | | 1.00 |
| Tumor side | | | | | 0.81 |
| - Left | 2 | 25 | 3 | 30 | |
| - Right | 6 | 75 | 7 | 70 | |
| Tumor localization | | | | | 0.23 |
| - Upper outer | 6 | 75 | 4 | 40 | |
| - Lower outer | 0 | 0 | 1 | 10 | |
| - Lower medial | 1 | 12.5 | 2 | 20 | |
| - Upper medial | 0 | 0 | 3 | 30 | |
| - Central | 1 | 12.5 | 0 | 0 | |
| Type of operation | | | | | 0.15 |
| - Mastectomy | 3 | 37.5 | 1 | 10 | |
| - Wide Local Excision | 4 | 50 | 9 | 90 | |
| - SNB only | 1 | 12.5 | 0 | 0 | |
| Pathological tumor size (median, range) | 7 (5-11) | | 12 (8-15) | | 0.13 |
| Histological type | | | | | 0.62 |
| - Infiltrating ductal adenocarcinoma | 7 | 87.5 | 7 | 70 | |
| - Infiltrating lobular adenocarcinoma | 0 | 0 | 1 | 10 | |
| - Ductal carcinoma *in situ* | 1 | 12.5 | 1 | 10 | |
| - Other | 0 | 0 | 1 | 10 | |
| Histological grade | | | | | 0.15 |
| - I | 1 | 16.7 | 3 | 33.3 | |
| - II | 2 | 33.3 | 5 | 55.6 | |
| - III | 3 | 50 | 1 | 11.1 | |

ICG:HSA = indocyanine green adsorbed to human serum albumin

Skin type = American Academy of Dermatology Skin Types I-VI:
I. Pale, white skin: always burns easily; never tans (Celtic, Scandinavian, and infants)
II. White: usually burns easily; tans minimally (Northern European)
III. White (average): sometimes burns; tans gradually to light brown (Central European)
IV. Beige or lightly tanned: burns minimally; always tans to moderately brown (Mediterranean, Asian)
V. Moderate brown or tanned: rarely burns; tans well (South American, Indian, Native American)
VI. Dark brown or black: never burns; deeply pigmented (African, African-American, Aborigine)

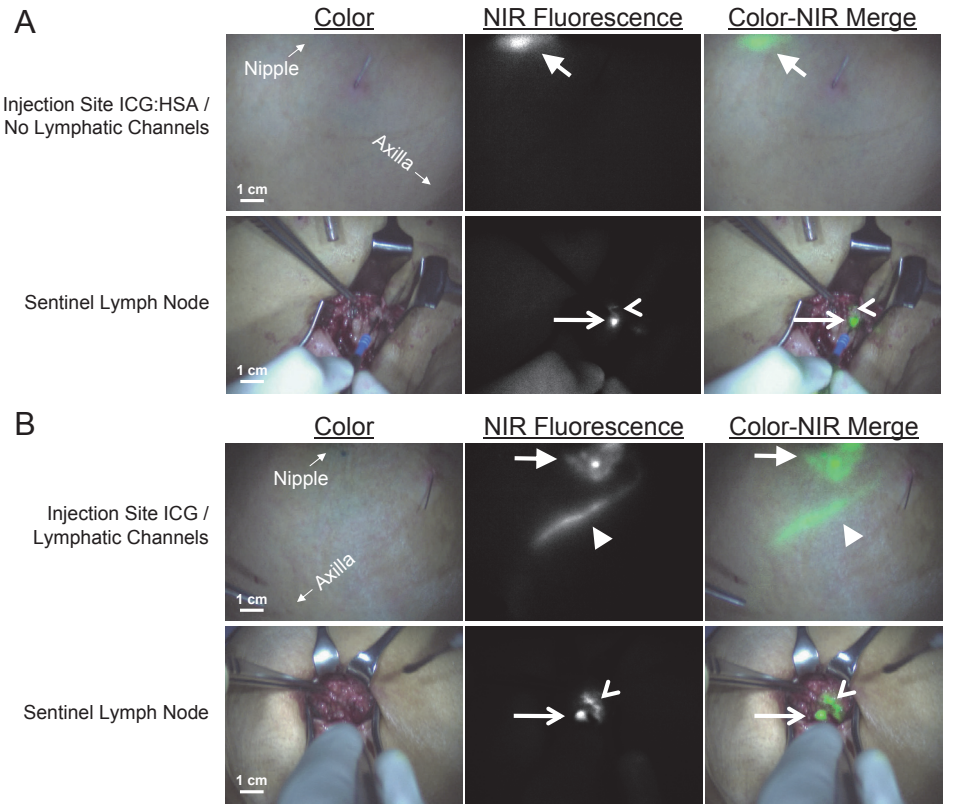


**Figure 1. NIR fluorescence imaging during sentinel lymph node mapping in breast cancer patients. A. ICG:HSA.** In the upper panel, the periareolar injection site (arrow) is shown, but percutaneously, no lymphatic channel can be visualized. In the lower panel, identification of the SLN (arrow) and an afferent lymphatic channel (open arrowhead) with NIR fluorescence imaging is demonstrated 27 min after injection of 1.6 mL of 500 μM ICG:HSA. Camera exposure times were 60 msec (top row) and 150 msec (bottom row). Scale bars represent 1 cm. **B. ICG alone.** In the upper panel, the periareolar injection site (arrow) and a lymphatic channel (arrowhead) are clearly visualized. In the lower panel, identification of the SLN (arrow) and an afferent lymphatic channel (open arrowhead) with NIR fluorescence imaging is demonstrated 28 min after injection of 1.6 mL of 500 μM ICG. Camera exposure times were 30 msec (top row) and 100 msec (bottom row). Scale bars represent 1 cm.

## DISCUSSION

The use of NIR fluorescence for SLN mapping has several advantages over conventional methods, such as better tissue penetration when compared to blue dyes, and lack of ionizing radiation and real-time visualization when compared to radiotracers. A number of clinical studies have been published on the use of NIR fluorescence in the SLN procedure in breast cancer, all of which use ICG, which is currently clinically available.[6, 9, 11, 12, 14] Preclinical studies indicated that adsorption of ICG to human serum albumin (HSA, complex is ICG:HSA), by simply mixing it, increases the fluorescence intensity and the hydrodynamic diameter, thereby providing improved detection and better retention in the SLN.[15] Our group has subsequently conducted a dose-finding

study and demonstrated that the optimal concentration of ICG:HSA for NIR-based SLN mapping in breast cancer patients lies between 400 μM and 800 μM.[14] Indeed, above 800 μM ICG:HSA, the fluorescent intensity dropped due to quenching. Based on these results a concentration of 500 μM ICG:HSA, which requires minimal manipulation of albumin volumes and uses only one vial of ICG, was chosen for further studies to identify whether premixing with albumin indeed increases the fluorescent intensity of the node in a clinical setting. In the current study, SLN mapping after ICG or ICG:HSA injection was successful in all patients. ICG showed a comparable or even slightly increased (though not significantly) brightness than ICG:HSA while identifying an equal average number of SLNs. Although no macrometastases in the SLNs were observed in the current study, our previous study showed that tumor-positive SLNs were also detected by NIR fluorescence, signifying ICG uptake.[14] However, lymph node macrometastases continue to be a contraindication for SLN mapping and preoperative staging of the axilla remains pivotal to minimize false negatives SLN mapping.

The results of our study are discordant with preclinical work in intestine, which suggested an improvement in fluorescent brightness and retention in the SLN by premixing ICG with HSA.[15] Although the current study was powered to determine non-inferiority in SBR of ICG alone when compared to ICG:HSA, it was not formally powered to assess the secondary endpoint, average number of SLNs identified. However, power analysis using data from our previous study[14] demonstrated that a difference of at least one additional SLN identified per patient could be detected with 90% power with the current sample size. The discrepancy between the current clinical results and these preclinical experiments could be caused by the increased distance that the injected dye has to travel, as the preclinical studies were performed in the bowel of healthy pigs.[15] Lymph fluid contains a high concentration of albumin, among other proteins; therefore, a longer traveling distance could aid ICG in adsorbing to albumin or other proteins, as it would after intravenous injection,[18] diminishing the need for premixing ICG with HSA. This observation implies that premixing might prove to be useful in other cancer types (such as colon cancer, for example), where ICG is less likely to completely adsorb to proteins before the SLN is reached. Therefore, the use of ICG:HSA or ICG alone should be formally tested for every anatomical site.

Although the fluorescent brightness did not differ significantly between both groups, ICG alone showed significantly improved percutaneous visibility of lymphatic channels when compared to ICG:HSA (Figure 1). It has been shown that in plasma, ICG preferably binds to $\alpha_1$-lipoprotein and γ-globulin, despite the higher concentration of albumin.[19] Previous experiments have shown a higher increase in quantum yield when ICG is mixed with serum, in comparison to HSA.[15] Therefore, the observed differences in visualization of lymphatics could likely be attributable to the protein constitution of lymph fluid. The high albumin content (20%) of ICG:HSA could also be a contributing factor, as the increased hydrodynamic diameter and higher viscosity could diminish

**Table 2.** SLN identification results

| Characteristic | Total (18 subjects) | | ICG:HSA (8 subjects) | | ICG alone (10 subjects) | | *P* |
|---|---|---|---|---|---|---|---|
| | N | % | N | % | N | % | |
| Number of SLNs identified | 25 | | 11 | | 14 | | |
| Number of SLNs identified per patient | | | | | | | 0.91 |
| - One SLN | 11 | 61 | 5 | 63 | 6 | 60 | |
| - Two SLNs | 7 | 39 | 3 | 37 | 4 | 40 | |
| Average number of SLNs identified ± S.D. | 1.4 ± 0.5 | | 1.4 ± 0.5 | | 1.4 ± 0.5 | | 0.92 |
| Method of detection | | | | | | | |
| - Radioactive | 23 | 92 | 9 | 82 | 14 | 100 | 0.18 |
| - Blue | 18 | 72 | 8 | 73 | 10 | 71 | 1.00 |
| - NIR fluorescent | 25 | 100 | 11 | 100 | 14 | 100 | 1.00 |
| Signal-to-background ratio | 10.0 ± 4.4 | | 8.4 ± 3.6 | | 11.3 ± 4.8 | | 0.18 |
| Percutaneous NIR fluorescent lymph drainage visualization | | | | | | | 0.004 |
| - Yes | 10 | 56 | 1 | 13 | 9 | 90 | |
| - Partially[a] | 3 | 17 | 3 | 38 | 0 | 0 | |
| - No | 5 | 28 | 4 | 50 | 1 | 10 | |
| Average time between injection and skin incision ± S.D. (minutes) | 15.6 ± 2.2 | | 15.3 ± 1.7 | | 15.9 ± 2.6 | | 0.55 |
| Average time between skin incision and SLN resection ± S.D. (minutes) | 11.0 ± 4.1 | | 10.6 ± 5.1 | | 11.3 ± 3.3 | | 0.74 |
| Histology | | | | | | | 0.44 |
| - Negative | 24 | 96 | 10 | 91 | 14 | 100 | |
| - Isolated tumor cells | 1 | 4 | 1 | 9 | 0 | 0 | |
| - Macrometastases | 0 | 0 | 0 | 0 | 0 | 0 | |
| Axillary lymph node dissection | | | | | | | 1.00 |
| - No | 18 | 100 | 8 | 100 | 10 | 100 | |
| - Yes | 0 | 0 | 0 | 0 | 0 | 0 | |

ICG:HSA = indocyanine green adsorbed to human serum albumin; S.D. = standard deviation; SLN = sentinel lymph node; NIR = near-infrared.
[a] Partial percutaneous visualization was noted when lymphatic channels could be visualized percutaneously from the injection site, but did not reach the axilla.

ICG uptake in lymphatic channels. It should be noted that the anatomical variation (amount of tissue overlying the lymphatic channels) is also a major influencing factor and may be primarily responsible for the observed difference.

An optimal lymphatic tracer is non-toxic, has a high quantum yield (i.e., brightness), migrates quickly to the SLN, and does not migrate to higher tier nodes. If a tracer migrates to higher tier nodes, non-sentinel lymph nodes could incorrectly be identified as SLNs, causing more nodes than necessary to be resected. ICG is far from optimal; in aqueous solution the quantum yield is relatively low and due to its small hydrodynamic diameter, it can flow to higher tier nodes, as is the case with blue

dyes. The synthesis and clinical introduction of an optimal probe will be the subject of future studies and will greatly help to confirm the clinical benefit of NIR fluorescence imaging in the SLN procedure.[15, 20]

In the current study, NIR fluorescence after ICG injection could consistently be visualized before blue dye staining could be observed, which is consistent with earlier findings.[14] Therefore, NIR fluorescence imaging has the potential to replace blue dyes in SLN mapping of breast cancer patients. Furthermore, as NIR fluorescence light penetrates relatively deep into tissue, it can potentially replace radiocolloids in SLN mapping in a selected group of patients, for example those with a low body mass index. A clinical trial on omitting blue dyes and using NIR fluorescence without the need for radiocolloids is currently ongoing (NTR2674).

In conclusion, this double-blind, randomized trial showed no advantage of ICG:HSA in comparison to ICG alone for the SLN procedure. To reduce the cost and complexity of the procedure, a dose of 500 μM ICG alone (1.6 ml) is recommended for NIR fluorescence SLN mapping in breast cancer patients. Therefore, this study has determined the optimal parameters that can be used to validate this technique in a larger series in order to investigate patient benefit.

## ACKNOWLEDGEMENTS

We thank the following individuals for the contribution to this study: Gemma Ranke, Elly Krol-Warmerdam, Annemarie Voet-van den Brink, Gerlinda van Gent-de Bruijn (Breast Cancer Unit) and Linda van der Hulst (Central Pharmacy). We thank Lindsey Gendall for editing. This work was supported in part by NIH grants R01-CA-115296 and R21-CA-130297, the Dutch Cancer Society grant UL2010-4732, the Nuts Ohra Fund, the "Maurits and Anna de Kock" Foundation and the American Women's Club of The Hague. J.S.D. Mieog is a MD-medical research trainee funded by The Netherlands Organisation for Health Research and Development (grant nr. 92003526).

## REFERENCES


1. Cox CE, Pendas S, Cox JM, et al. Guidelines for sentinel node biopsy and lymphatic mapping of patients with breast cancer. Ann Surg 1998; 227:645-51.
2. Goyal A, Newcombe RG, Chhabra A, et al. Factors affecting failed localisation and false-negative rates of sentinel node biopsy in breast cancer - results of the ALMANAC validation phase. Breast Cancer Res Treat 2006; 99:203-8.
3. Krag DN, Anderson SJ, Julian TB, et al. Technical outcomes of sentinel-lymph-node resection and conventional axillary-lymph-node dissection in patients with clinically node-negative breast cancer: results from the NSABP B-32 randomised phase III trial. Lancet Oncol 2007; 8:881-8.
4. Zavagno G, De Salvo GL, Scalco G, et al. A Randomized clinical trial on sentinel lymph node biopsy versus axillary lymph node dissection in breast cancer: results of the Sentinella/GIVOM trial. Ann Surg 2008; 247:207-13.
5. Straver ME, Meijnen P, van Tienhoven G, et al. Sentinel Node Identification Rate and Nodal Involvement in the EORTC 10981-22023 AMAROS Trial. Ann Surg Oncol 2010; 17:1854-61.
6. Kitai T, Inomoto T, Miwa M, et al. Fluorescence navigation with indocyanine green for detecting sentinel lymph nodes in breast cancer. Breast Cancer 2005; 12:211-5.
7. Murawa D, Hirche C, Dresel S, et al. Sentinel lymph node biopsy in breast cancer guided by indocyanine green fluorescence. Br J Surg 2009; 96:1289-94.
8. Tagaya N, Yamazaki R, Nakagawa A, et al. Intraoperative identification of sentinel lymph nodes by near-infrared fluorescence imaging in patients with breast cancer. Am J Surg 2008; 195:850-3.
9. Hirche C, Murawa D, Mohr Z, et al. ICG fluorescence-guided sentinel node biopsy for axillary nodal staging in breast cancer. Breast Cancer Res Treat 2010; 121:373-8.
10. Hojo T, Nagao T, Kikuyama M, et al. Evaluation of sentinel node biopsy by combined fluorescent and dye method and lymph flow for breast cancer. Breast 2010; 19:210-3.
11. Troyan SL, Kianzad V, Gibbs-Strauss SL, et al. The FLARE intraoperative near-infrared fluorescence imaging system: a first-in-human clinical trial in breast cancer sentinel lymph node mapping. Ann Surg Oncol 2009; 16:2943-52.
12. Sevick-Muraca EM, Sharma R, Rasmussen JC, et al. Imaging of lymph flow in breast cancer patients after microdose administration of a near-infrared fluorophore: feasibility study. Radiology 2008; 246:734-41.
13. Tanaka E, Choi HS, Fujii H, et al. Image-guided oncologic surgery using invisible light: completed pre-clinical development for sentinel lymph node mapping. Ann Surg Oncol 2006; 13:1671-81.
14. Mieog JS, Troyan SL, Hutteman M, et al. Towards optimization of imaging system and lymphatic tracer for near-infrared fluorescent sentinel lymph node mapping in breast cancer. Ann Surg Oncol 2011; 18:2483-91.
15. Ohnishi S, Lomnes SJ, Laurence RG, et al. Organic alternatives to quantum dots for intraoperative near-infrared fluorescent sentinel lymph node mapping. Mol Imaging 2005; 4:172-81.
16. Cherrick GR, Stein SW, Leevy CM, et al. Indocyanine green: observations on its physical properties, plasma decay, and hepatic extraction. J Clin Invest 1960; 39:592-600.
17. Fogh-Andersen N, Altura BM, Altura BT, et al. Composition of interstitial fluid. Clin Chem 1995; 41:1522-5.
18. Moody ED, Viskari PJ, Colyer CL. Non-covalent labeling of human serum albumin with indocyanine green: a study by capillary electrophoresis with diode laser-induced fluorescence detection. J Chromatogr B Biomed Sci Appl 1999; 729:55-64.
19. Sauda K, Imasaka T, Ishibashi N. Determination of protein in human serum by high-performance liquid chromatography with semiconductor laser fluorometric detection. Anal Chem 1986; 58:2649-53.
20. Hutteman M, Choi HS, Mieog JS, et al. Clinical translation of ex vivo sentinel lymph node mapping for colorectal cancer using invisible near-infrared fluorescence light. Ann Surg Oncol 2011; 18:1006-14.

# Chapter 13

## Summary and general discussion

Partly based on:
*Mieog JS, van de Velde CJ. Neoadjuvant chemotherapy for early breast cancer. Expert Opin Pharmacother 2009; 10:1423-34.*

*Schaafsma BE, Mieog JS, Hutteman M, et al. The clinical use of indocyanine green as a near-infrared fluorescent contrast agent for image-guided oncologic surgery. J Surg Oncol 2011; 104:323-32.*

This thesis consists of two parts. In part I, we have demonstrated that preoperatively administrated systemic (neoadjuvant) therapy is a feasible treatment strategy in early stage breast cancer to achieve improved surgical options and to assess tumor response. We also demonstrated that overexpression of the breast cancer stem cell marker aldehyde dehydrogenase-1 in early stage breast cancer patients is inversely associated with age and is of prognostic importance. In part II, we have demonstrated proof-of-principle of intraoperative tumor detection and image-guided tumor resection by using the novel technique of near-infrared fluorescence imaging. We have performed two clinical trials to optimize the use of indocyanine green as a near-infrared fluorescence lymphatic tracer for the sentinel lymph node procedure in breast cancer patients.

## PART I: NEOADJUVANT SYSTEMIC THERAPY

The meta-analysis described in **Chapter 2** demonstrated that neoadjuvant chemotherapy results in equivalent overall and disease-free survival rates and permits more breast-conserving therapies, while not significantly hampering loco regional control. An international expert panel recently recommended that all patients with a clear indication for adjuvant chemotherapy can be offered chemotherapy preoperatively.[1]

However, neoadjuvant therapy is still underutilized in many countries. Also, in the Netherlands, an apparent barrier exists for the routine administration of neoadjuvant strategies in the treatment of early stage breast cancer patients that might benefit from this approach. This is in spite of the obvious advantages associated with the use of neoadjuvant therapy, while little disadvantages exits (Table 1). Moreover, the compliance of patients to neoadjuvant therapy is high, thanks to the motivating decrease in tumor size that breast cancer patients can assess themselves by palpation. Even more, the indications for neoadjuvant strategies have broadened due to an increase in the availability of more tailored regimens, e.g. hormonal, chemo- and targeted therapies.

**Table 1. Advantages and disadvantages of neoadjuvant chemotherapy**

| Advantages | Disadvantages |
|---|---|
| Tumor down staging: more breast conserving surgery | Delay of adequate surgery in the case of tumor resistance |
| Nodal down staging: less axillary lymph node dissection | Loss of information on pretreatment nodal status |
| *In vivo* assessment of tumor resistance or sensitivity | |
| Tumor response as surrogate prognostic marker | |
| Rapid screening of efficiency of new drugs | |

Although the routine use of neoadjuvant therapy could be extended, an encouraging increase in the number of included patients in Dutch neoadjuvant studies is witnessed over the last years, as demonstrated in the recently closed INTENS study (BOOG 2007-02) and the lately started NEO-ZOTAC study (BOOG 2010-01). However, another national study, the TEAM-IIA trial (BOOG-2006-04a), in which the duration of neoadjuvant hormonal therapy is investigated, suffers from slow inclusion. Therefore, further research and propagation on the use of neoadjuvant systemic therapy as a powerful tool in the treatment of early stage breast cancer patients is still warranted.

Neoadjuvant hormonal therapy is an attractive alternative to neoadjuvant chemotherapy in treating women with estrogen receptor (ER) positive breast cancer because of the low toxicity of hormonal therapy and the low response rate in ER positive breast cancer (especially lobular cancer) treated with neoadjuvant chemotherapy. Neoadjuvant hormonal therapy was directly compared with neoadjuvant chemotherapy in one study demonstrating equal response rates (64%) and lower adverse events in the hormonal group.[2] Currently, the randomized NEOCENT study is underway to compare 6 cycles of neoadjuvant chemotherapy with 18-23 weeks of the aromatase inhibitor letrozole. Three randomized trials have compared 3-4 months of neoadjuvant tamoxifen with aromatase inhibitors and showed superiority of aromatase inhibitors in clinical response rate and breast conservation rate (RR, 1.36; 95% CI, 1.16- 1.59).[3] The tumor response to neoadjuvant hormonal therapy is slow, but sustained. To address the issue of the optimum duration of neoadjuvant hormonal therapy, several phase II studies have investigated the prolonged use of neoadjuvant hormonal therapy beyond 3-4 months and demonstrated response rates up to 80%. Even more, reductions in tumor volume were achieved up to 2 years of treatment.[4] For elderly women with a limited life expectancy, neoadjuvant hormonal therapy without surgery provided long-term disease control. So, these data suggest that a further reduction in tumor size can be achieved with prolonged treatment and that even surgery can be withheld for elderly women on continuing hormonal treatment. However, the optimum duration of neoadjuvant hormonal therapy remains to be established.

Several surgical aspects are associated with the use of neoadjuvant therapy. **Chapter 2** demonstrated that the major benefit of neoadjuvant chemotherapy is the down sizing effect on the primary tumor allowing for a breast conservative approach in selected patients. In addition, the total volume of excised breast tissue is significantly decreased in patients with tumors already suitable for breast-conserving surgery.[5] However, defining the optimal selection criteria for breast conservation remains a clinically relevant area of research, as breast tumors respond in a heterogeneous fashion to neoadjuvant chemo- and hormonal therapy and distinct types of regression can be recognized (Figure 1). After concentric shrinkage, the residual tumor can easily be

completely resected. However, tumors that regressed in a patchy fashion leaving scattered microscopic disease over the original tumor bed volume may predispose to a higher breast cancer recurrence rate when surgery is directed only at the 'center' of the residual tumor.[6]

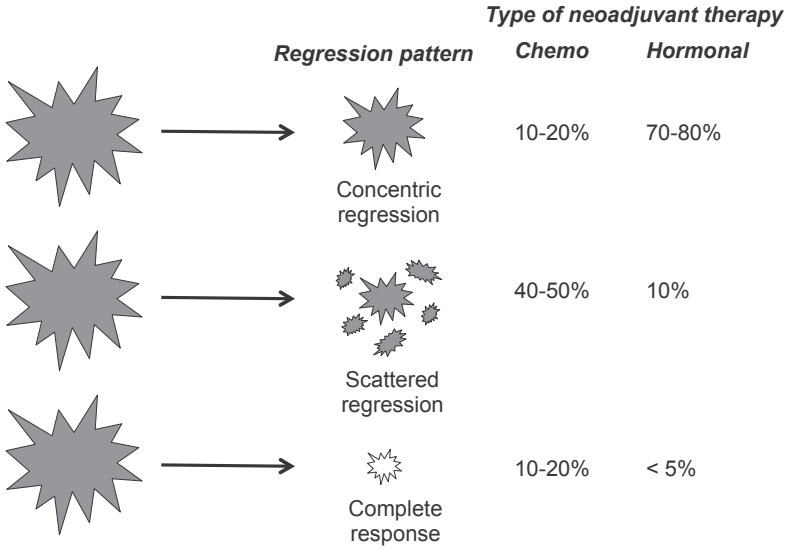


**Figure 1.** Regression patterns to neoadjuvant therapy. Adapted from [7, 8].

Conventional imaging modalities have demonstrated poor correlation between the radiological and the pathological tumor size after neoadjuvant chemotherapy.[9] **Chapter 2** demonstrated that the local recurrence rate in the neoadjuvant arm is greatly reduced after excluding studies in which patients received exclusive radiotherapy and no surgery after clinical complete tumor regression. These data emphasize the importance of incorporating surgery in the loco regional treatment after neoadjuvant chemotherapy. Otherwise stated, the current clinical assessment of tumor response is insufficiently sensitive to safely withhold surgery. Therefore, surgical planning and execution should take into account the size of the original tumor and the response to neoadjuvant chemotherapy.[1] Placement of radiopaque clips within breast lumps at the time of biopsy provides localization for subsequent surgical removal has been associated with better local control.[10] In order to improve risk assessment of a loco regional recurrence following breast-conserving surgery after neoadjuvant chemotherapy, a prognostic index has been developed, which includes four factors: clinical N2-3 disease, residual pathologic tumor size larger than 2 cm, a multifocal pattern of residual disease, and lymphovascular space invasion.[11] The index was able to predict loco regional recurrence in a retrospective study,[12] and may be useful in selecting type of surgical treatment for patients treated with neoadjuvant chemotherapy; however, confirmation in prospective patient series is warranted.

Sentinel lymph node (SLN) mapping provides the possibility of assessing the axillary lymph node status after neoadjuvant therapy. If the SLN becomes negative following neoadjuvant therapy in patients with proven nodal metastases prior to treatment, an axillary dissection could be prevented. Though, concerns exist on the accuracy of SLN mapping after neoadjuvant chemotherapy because the proposed alteration of the lymphatic network. However, scintigraphy data from patients before and after neoadjuvant chemotherapy demonstrated that the location of the SLN was the same in 99.2% of patients.[13] Moreover, a meta-analysis on SLN mapping after neoadjuvant chemotherapy reported a SLN identification rate of 91% and a false negative rate of 11%;[14] these rates are comparable in patients naïve to chemotherapy.[15] In patients with proven axillary metastases, the SLN becomes negative in approximately one-third of the cases and the SLN identification rate and false negative rate are 85% and 11%, respectively.[13] These results suggest that SLN mapping after neoadjuvant chemotherapy is feasible in node-positive patients with complete clinical response in order to avoid an axillary dissection. Currently, the prospective, multicenter SENTINA trial is accruing patients to evaluate the accuracy of the SLN procedure in both clinically node-negative and node-positive patients.

In **Chapter 3**, data are presented from the neoadjuvant chemotherapy trial EORTC 10902 that suggest that expression of the tumor suppression protein p53 is of predictive significance in anthracycline-containing chemotherapy regimens. To assess the value of p53 to predict sensitivity of anthracycline and taxane containing neoadjuvant chemotherapy regimens, the phase III randomized EORTC 10994/BIG 00-01 trial has been conducted using a functional yeast assay to detect biologically important mutations of p53. The final results of this trial were recently published and demonstrated that although p53 was highly prognostic, p53 status was not a predictive factor of sensitivity or resistance to taxanes or anthracyclines.[16]

In **Chapter 4**, the effect of chemotherapy in relation to ER status was studied in very young breast cancer patients. Patients with ER positive tumors had an improved overall survival compared to their ER negative counterparts. However, in the subgroup of patients treated with chemotherapy, no difference in overall survival was shown. These data suggest that young patients with ER positive tumors benefit less from chemotherapy than patients with ER negative tumors. Moreover, these results suggest that chemotherapy alone cannot be considered optimal adjuvant systemic treatment in very young breast cancer patients with hormone receptor positive tumors.

In **Chapter 5**, the impact of established prognostic factors was tested in very young breast cancer patients. Tumor size, nodal status and molecular subtype were independent prognostic factors. In the node negative patient group, molecular subtype was the sole prognostic factor for overall survival. These data support the use of established prognostic factors and in particular molecular subtype to plan systemic treatment strategies in these very young patients.

In **Chapter 6**, the prognostic effect of the breast cancer stem cell marker aldehyde dehydrogenase-1 (ALDH1) has been analyzed. ALDH1 expression was inversely associated with age. In elderly patients, ALDH1 status was not associated with clinical outcome. Alternatively, in young patients, ALDH1 expression was associated with poor outcome. These results support the hypothesis that breast cancer biology is different in elderly patients compared to their younger counterparts, which may be explained by differences in cellular pathways involved in cancer stem cell activity.

In **Chapter 7**, the association was studied between ALDH1 expression and the coagulation protein tissue factor (TF) and its alternatively spliced (asTF) isoform. Expression of both TF isoforms was very common in human breast cancer cells and was associated with poor histological grade. Expression of TF was associated with ALDH1 expression, whereas expression of asTF was not. Moreover, co-expression of TF and ALDH1 was strongly correlated with poor relapse-free period in patients younger than 65 years, whereas in older patients the inverse effect was demonstrated. These results provide new insights on the interaction between the tissue factor/protease activated receptor (TF/PAR) pathway and the growth potential of the cancer stem cell subset and suggest that the TF/PAR pathway is important for the cancer stem cell population in early breast cancer.[17, 18] Therefore, modulation of the activity of this pathway might interfere with survival of the cancer stem cell subset, which may subsequently improve patient survival.

Selective survival of cancer stem cells might be responsible for treatment failure witnessed in early stage breast cancer. Regrowth of tumors from this intrinsically chemotherapy-resistant subpopulation has been termed the 'dandelion hypothesis'.[19] Neoadjuvant systemic therapy offers an excellent model to test the dandelion hypothesis in breast cancer patients. By comparing the cancer stem cell content of the pretreatment specimens with the posttreatment specimens, an increase in the relative proportion of cancer stem cells is expected after neoadjuvant systemic therapy. Targeting with novel therapies of the residual cells with stem cell self-renewal properties may provide a specific approach to prevent cancer recurrence and improve long-term survival.[20]

## PART II: IMAGE-GUIDED SURGERY

In **Chapter 8**, a novel near-infrared (NIR) fluorescence imaging system, the Fluobeam®, was tested both *in vitro* and *in vivo*. This study demonstrated the technical performance of this new imaging system and its intraoperative utility in guiding resection of tumors using a protease-activatable NIR fluorescent probe. Also, this study has provided several methods for the validated testing of new NIR fluorescence imaging system.

In **Chapter 9**, the accuracy was determined of real-time NIR fluorescence imaging in obtaining tumor-free resection margins in a rat model of primary breast cancer using a protease-activatable NIR fluorescence probe. Real-time NIR fluorescence guidance

of tumor resection resulted in a complete resection of all tumors with minimal excision of normal healthy tissue (mean minimum and a mean maximum tumor-free margin of 0.2 ± 0.2 mm and 1.3 ± 0.6 mm, respectively). Histological analysis revealed that the NIR fluorescence signal was highest at the invasive tumor border and in the stromal compartment of the tumor, which correlates with the mechanism of action of protease activity.

In **Chapter 10**, the performance was assessed of antibody-based detection of breast tumor margins in the same breast cancer rat model as described in Chapter 9. The monoclonal antibody MG1, directed against epithelial rat tumor cells, was conjugated to a NIR fluorophore. All breast tumors were identified and under direct image-guidance, all tumors could be resected with a clear margin. The fluorescence signal corresponded with histological tumor demarcation. Interestingly, the control experiment with a non-targeted antibody demonstrated equal fluorescent intensity and signal-to-background ratio. This observation can be explained by the 'enhanced permeability and retention' effect, by which the conjugated antibodies passively accumulate in the tumor due to the 'leaky vessels'; the characteristic large pores seen in neovascularization. This observation may provide a simple and effective targeting strategy for NIR imaging of solid tumors.

**Chapter 8**, **Chapter 9**, and **Chapter 10** demonstrated that NIR fluorescence detection of breast tumor margins was successful in a rat model. These studies suggest that clinical introduction of intraoperative NIR fluorescence imaging has the potential to increase the number of complete tumor resections in breast cancer patients undergoing breast-conserving surgery.

In **Chapter 11**, the clinical translation of a new, portable NIR fluorescence imaging system, the Mini-FLARE™, is described in a dose optimization study of SLN mapping in breast cancer using indocyanine green (ICG) absorbed to human serum albumin (ICG:HSA) as a lymphatic tracer. The imaging system, which was developed for capturing color video and two channels of NIR fluorescence (700 nm and 800 nm), enabled visualization of lymphatic channels and SLNs in all patients. Mean number of identified SLNs was 1.45. All SLNs were NIR fluorescent. Optimal injection dose of ICG:HSA ranged between 400 and 800 μM.

In **Chapter 12**, the effect of premixing ICG to HSA for SLN mapping in breast cancer was determined in a double-blind, randomized study. No significant differences were found in signal brightness and number of detected SLNs between the ICG:HSA group and the ICG alone group. This study has demonstrated that there is no direct benefit of premixing ICG with HSA prior to injection for SLN mapping in breast cancer patients, thereby reducing the cost and complexity of the procedure.

**Chapter 11** and **Chapter 12** describe the optimization of NIR fluorescence SLN mapping using ICG in breast cancer and have paved the way for larger trials that can determine patient benefit of this technique.

The recent introduction of NIR fluorescence image guidance has provided new opportunities in cancer surgery. Several NIR fluorescence imaging systems have been designed for intraoperative clinical use.[21] Two of these imaging systems have been described in **Chapter 8** and **Chapter 11**, respectively. Although differing in their technical specifications, all of these systems provide the surgeon with an image of the NIR fluorescence signal that would otherwise be invisible to the human eye (Table 2). To permit precise localization of the NIR fluorescent signals in the context of surgical anatomy, several imaging systems acquire color video and NIR fluorescence emission simultaneously and provide overlay images.[22-24] The development of new imaging systems will further improve NIR fluorescence image-guided surgery. NIR fluorescence laparoscopic imaging systems are currently being developed, and a commercial system is already available, which will allow NIR fluorescence guided-surgery in a minimally invasive setting.[25, 26] Various techniques are being evaluated to correct photon scattering and thereby enhance the depth at which NIR fluorescent signal can be detected.[27-29]

**Table 2.** Clinically available NIR fluorescence imaging systems

| Imaging system | Excitation source | Working distance | Field of view | White light illumination of surgical field | NIR-color overlay |
|---|---|---|---|---|---|
| PDE | LED 805 nm, power NS | 15 - 25 cm | NS | No | No |
| SPY | Laser 806 nm, 2.0 W | 30 cm | 56 $cm^2$ | No | No |
| Fluobeam® | Laser 780 nm, 10mW/$cm^2$ | 22 cm | 80 $cm^2$ | Yes | No |
| HyperEye | LED 760 nm, power NS | 30 - 50 cm | 78.5 $cm^2$ | Yes | Yes |
| FLARE™ | LED 745-779 nm, 14 mW/$cm^2$ | 45 cm | 3.7 $cm^2$ - 169.5 $cm^2$ | Yes | Yes |
| Mini-FLARE™ | LED 760 nm, 8.6 mW/$cm^2$ | 30 cm | 100 $cm^2$ | Yes | Yes |
| FDPM imager | Laser 785 ± 10 nm, < 1.9 mW/$cm^2$ | <76.2 cm | Max 900 $cm^2$ | No | No |
| Munich prototype | Laser 750 nm, 300 mW | 21 cm | 1,5 $cm^2$ - 107 $cm^2$ | Yes | Yes |

PDE, Photodynamic Eye; LED, Light emitting diode; NS, not specified; FLARE, Fluorescence-Assisted Resection and Exploration; FDPM, Frequency Domain Photon Migration

Besides NIR fluorescence imaging systems, exogenous NIR fluorescent contrast agents are necessary to visualize specific tissues. The only NIR fluorescent contrast agents currently registered by the FDA and EMA for clinical applications are indocyanine green (ICG; peak emission ≈ 820 nm) and methylene blue (peak emission ≈ 700 nm).[30] ICG has preferable fluorescent characteristics because it provides a higher signal-to-background ratio as the autofluorescence is lower and tissue penetration is increased at 820 nm wavelength compared to 700 nm and ICG has a higher "brightness" (quantum yield).

ICG is a negatively charged, amphiphilic, water-soluble, tricarbocyanine with a molecular mass of 776 Da. ICG has been registered for several decades to determine cardiac output, hepatic function, and ophthalmic perfusion. ICG has a very favorable safety profile, as the number of allergic reactions, the most important side-effect, is very low (1: 10,000, as reported by manufacturer).[31] ICG is currently utilized in NIR fluorescence cancer surgery for four indications: sentinel lymph node (SLN) mapping, endoscopic marking of colorectal tumors,[32] intraoperative identification of certain solid tumors,[33] and angiography during reconstructive breast surgery.[34]

Sentinel lymph node mapping with NIR fluorescence imaging using ICG as described in **Chapter 11** and **Chapter 12** has demonstrated accuracy and percutaneous visualization of the lymphatic channels. Thereby, it can reduce time of surgery and improve localisation of the SLN so that surgical exploration can be minimized, while maintaining a high identification rate. It should be noted, however, that NIR fluorescence detection is currently in the millimetre to centimetre range, far less than radioactive tracers, which requires caution when interrogating thick tissues, for instance in patients with high body mass index. In **Chapter 11** and **Chapter 12**, it was demonstrated that NIR fluorescence using ICG could consistently be visualized before the blue dye could be observed. Therefore, NIR fluorescence imaging has the potential to replace blue dyes in SLN mapping of breast cancer patients. Whether NIR fluorescence could also replace radiocolloids is subject of an ongoing clinical trial, which is conducted by our group (NTR2674).

Intraoperative NIR fluorescence imaging tumor detection in cancer patients is currently limited because both ICG and methylene blue are so-called non-targeted probes as they cannot be conjugated to tumor-specific targets. Novel, non-toxic NIR fluorophores have been developed, such as IRDye CW800 (LI-COR Biosciences, Lincoln, USA), VivoTag family (PerkinElmer, Waltham, USA) and the 800 nm zwitterionic heptamethine indocyanine ZW-800-1 (John V. Frangioni, Center for Molecular Imaging, Boston, USA), with improved fluorescence properties for higher tissue penetration and with the ability to be conjugated to tumor-targeting ligands. Several academic and industry groups are translating these fluorophores to the clinic and the first toxicity results have been reported.[35] Once these fluorophores have obtained regulatory approval, the logical next step would be the conjugation of these fluorophores to already clinically available monoclonal antibodies, such as trastuzumab (directed to the HER2/neu receptor, which is overexpressed in 20% of breast cancer patients), cetuximab, or bevacizumab. Thereafter, novel tumor-targeting approaches should be exploited. Various mechanisms are available for tumor targeting, including the conjugation of NIR fluorophores to tumor-specific antibody, to glucose derivates in order to visualize elevated metabolic rate, and autoquenched fluorophores that can be activated by tumor-specific enzymatic cleavage in order to become fluorescent. An

important strategy is the conjugation of fluorophores to a tumor-specific antibody or ligand directed to markers overexpresed by tumors, such as the follicle-stimulating hormone receptor, which is selectively expressed by endothelial cells at the periphery in a layer of approximately one cm of a wide range of tumors.[36] Multiple targeted probes have already been developed, some of which are commercially available, and have successfully been tested in animal studies and this thesis also has provided examples of this in **Chapter 9** and **Chapter 10**. Translating these preclinical results to the clinical setting in order to improve breast cancer outcome remains a major challenge for the next decades.

NIR optical spectroscopy is a technique to non-invasively monitor tumor response to neoadjuvant therapy. The technique utilizes the differences in absorption and scattering spectra of endogenous compounds. Therefore, no contrast agents are necessary. For the breast, the major absorption chromophores are oxyhemoglobin, deoxyhemoglobin, lipids and water, which are altered by angiogenesis, tumor cell proliferation and hypoxia.[37, 38] The Softscan® (ART, Montreal, Canada) is an optical breast imaging device, which uses pulsed time domain optical spectroscopy to obtain 3D images of the breast.[39] Current imaging modalities for tumor response assessment (mammography, ultrasound, MRI) are mainly based on size measurements. However, it is expected from tumor biology data that physiological changes in the tumor can be noted long before any changes in size can be observed.[40] As the Softscan measurements are based on tissue physiology, it should theoretically be able to assess early changes in the tumor, which could indicate a good response to neoadjuvant therapy. Indeed, a small clinical trial has demonstrated that the Softscan can discriminate responders from non-responders after one cycle of neoadjuvant chemotherapy.[41] Our group is currently conducting a larger clinical trial with the Softscan to study the predictive value of early tumor response assessment to neoadjuvant therapy within the framework of the NEOZOTAC and TEAM-IIa studies. Another application of NIR imaging could be the *in vivo* monitoring of the response of axillary metastases, either by optical spectroscopy or by NIR fluorescence contrast agents either targeting apoptotic[42] or viable tumor cells. As discussed above, if axillary metastases are regressed after neoadjuvant therapy and this can be confirmed by fluorescent imaging, an axillary lymph node dissection can be prevented.

In summary, near-infrared fluorescence imaging has the potential to revolutionize human cancer surgery by providing sensitive, specific, and real-time intraoperative visualization of normal and malignant tissues, to optimize surgical removal of tumors and their (local or lymph node) metastases.

# REFERENCES


1. Kaufmann M, von Minckwitz G, Bear HD, et al. Recommendations from an international expert panel on the use of neoadjuvant (primary) systemic treatment of operable breast cancer: new perspectives 2006. Ann Oncol 2007; 18:1927-34.
2. Semiglazov VF, Semiglazov VV, Dashyan GA, et al. Phase 2 randomized trial of primary endocrine therapy versus chemotherapy in postmenopausal patients with estrogen receptor-positive breast cancer. Cancer 2007; 110:244-54.
3. Seo JH, Kim YH, Kim JS. Meta-analysis of pre-operative aromatase inhibitor versus tamoxifen in postmenopausal woman with hormone receptor-positive breast cancer. Cancer Chemother Pharmacol 2009; 63:261-6.
4. Dixon JM, Renshaw L, Macaskill EJ, et al. Increase in response rate by prolonged treatment with neoadjuvant letrozole. Breast Cancer Res Treat 2009; 113:145-51.
5. Boughey JC, Peintinger F, Meric-Bernstam F, et al. Impact of preoperative versus postoperative chemotherapy on the extent and number of surgical procedures in patients treated in randomized clinical trials for breast cancer. Ann Surg 2006; 244:464-70.
6. Buchholz TA, Lehman CD, Harris JR, et al. Statement of the science concerning locoregional treatments after preoperative chemotherapy for breast cancer: a National Cancer Institute conference. J Clin Oncol 2008; 26:791-7.
7. Thomas JS, Julian HS, Green RV, et al. Histopathology of breast carcinoma following neoadjuvant systemic therapy: a common association between letrozole therapy and central scarring. Histopathology 2007; 51:219-26.
8. Dixon JM, Renshaw L, Murray J, et al. Surgical issues surrounding use of aromatase inhibitors. J Steroid Biochem Mol Biol 2005; 95:97-103.
9. Kaufmann M, Hortobagyi GN, Goldhirsch A, et al. Recommendations from an international expert panel on the use of neoadjuvant (primary) systemic treatment of operable breast cancer: an update. J Cli nOncol 2006; 24:1940-9.
10. Oh JL, Nguyen G, Whitman GJ, et al. Placement of radiopaque clips for tumor localization in patients undergoing neoadjuvant chemotherapy and breast conservation therapy. Cancer 2007; 110:2420-7.
11. Chen AM, Meric-Bernstam F, Hunt KK, et al. Breast conservation after neoadjuvant chemotherapy: the MD Anderson cancer center experience. J Clin Oncol 2004; 22:2303-12.
12. Huang EH, Strom EA, Perkins GH, et al. Comparison of risk of local-regional recurrence after mastectomy or breast conservation therapy for patients treated with neoadjuvant chemotherapy and radiation stratified according to a prognostic index score. Int J Radiat Oncol Biol Phys 2006; 66:352-7.
13. Dixon JM, Cody HS. Role of sentinel node biopsy in patients having neoadjuvant chemotherapy. Eur J Surg Oncol 2010; 36:511-3.
14. van Deurzen CH, Vriens BE, Tjan-Heijnen VC, et al. Accuracy of sentinel node biopsy after neoadjuvant chemotherapy in breast cancer patients: a systematic review. Eur J Cancer 2009; 45:3124-30.
15. Kim T, Giuliano AE, Lyman GH. Lymphatic mapping and sentinel lymph node biopsy in early-stage breast carcinoma: a metaanalysis. Cancer 2006; 106:4-16.
16. Bonnefoi H, Piccart M, Bogaerts J, et al. TP53 status for prediction of sensitivity to taxane versus non-taxane neoadjuvant chemotherapy in breast cancer (EORTC 10994/BIG 1-00): a randomised phase 3 trial. Lancet Oncol 2011; 12:527-39.
17. Milsom C, Yu J, May L, et al. The role of tumor-and host-related tissue factor pools in oncogene-driven tumor progression. Thromb Res 2007; 120 Suppl 2:S82-91.
18. Garnier D, Milsom C, Magnus N, et al. Role of the tissue factor pathway in the biology of tumor initiating cells. Thromb Res 2010; 125 Suppl 2:S44-50.
19. Jones RJ, Matsui WH, Smith BD. Cancer stem cells: are we missing the target? J Natl Cancer Inst 2004; 96:583-5.
20. Li X, Lewis MT, Huang J, et al. Intrinsic resistance of tumorigenic breast cancer cells to chemotherapy. J Natl Cancer Inst 2008; 100:672-9.
21. Gioux S, Choi HS, Frangioni JV. Image-guided surgery using invisible near-infrared light: fundamentals of clinical translation. Mol Imaging 2010; 9:237-55.

22. Handa T, Katare RG, Nishimori H, et al. New device for intraoperative graft assessment: HyperEye charge-coupled device camera system. Gen Thorac Cardiovasc Surg 2010; 58:68-77.
23. Troyan SL, Kianzad V, Gibbs-Strauss SL, et al. The FLARE intraoperative near-infrared fluorescence imaging system: a first-in-human clinical trial in breast cancer sentinel lymph node mapping. Ann Surg Oncol 2009; 16:2943-52.
24. Mieog JS, Troyan SL, Hutteman M, et al. Toward optimization of imaging system and lymphatic tracer for near-infrared fluorescent sentinel lymph node mapping in breast cancer. Ann Surg Oncol 2011; 18:2483-91.
25. Ishizawa T, Bandai Y, Ijichi M, et al. Fluorescent cholangiography illuminating the biliary tree during laparoscopic cholecystectomy. Br J Surg 2010; 97:1369-77.
26. Tajima Y, Murakami M, Yamazaki K, et al. Sentinel node mapping guided by indocyanine green fluorescence imaging during laparoscopic surgery in gastric cancer. Ann Surg Oncol 2010; 17:1787-93.
27. Gioux S, Mazhar A, Cuccia DJ, et al. Three-dimensional surface profile intensity correction for spatially modulated imaging. J Biomed Opt 2009; 14:034045.
28. Kumar AT, Raymond SB, Bacskai BJ, et al. Comparison of frequency-domain and time-domain fluorescence lifetime tomography. Opt Lett 2008; 33:470-2.
29. Themelis G, Yoo JS, Soh KS, et al. Real-time intraoperative fluorescence imaging system using light-absorption correction. J Biomed Opt 2009; 14:064012.
30. Schaafsma BE, Mieog JS, Hutteman M, et al. The clinical use of indocyanine green as a near-infrared fluorescent contrast agent for image-guided oncologic surgery. J Surg Oncol 2011; 104:323-32.
31. Alford R, Simpson HM, Duberman J, et al. Toxicity of organic fluorophores used in molecular imaging: literature review. Mol Imaging 2009; 8:341-54.
32. Watanabe M, Tsunoda A, Narita K, et al. Colonic tattooing using fluorescence imaging with light-emitting diode-activated indocyanine green: a feasibility study. Surg Today 2009; 39:214-8.
33. Ishizawa T, Fukushima N, Shibahara J, et al. Real-time identification of liver cancers by using indocyanine green fluorescent imaging. Cancer 2009; 115:2491-504.
34. Lee BT, Hutteman M, Gioux S, et al. The FLARE intraoperative near-infrared fluorescence imaging system: a first-in-human clinical trial in perforator flap breast reconstruction. Plast Reconstr Surg 2010; 126:1472-81.
35. Marshall MV, Draney D, Sevick-Muraca EM, et al. Single-dose intravenous toxicity study of IRDye 800CW in Sprague-Dawley rats. Mol Imaging Biol 2010; 12:583-94.
36. Radu A, Pichon C, Camparo P, et al. Expression of follicle-stimulating hormone receptor in tumor blood vessels. N Engl J Med 2010; 363:1621-30.
37. Hockel M, Vaupel P. Tumor hypoxia: definitions and current clinical, biologic, and molecular aspects. J Natl Cancer Inst 2001; 93:266-76.
38. Leff DR, Warren OJ, Enfield LC, et al. Diffuse optical imaging of the healthy and diseased breast: a systematic review. Breast Cancer Res Treat 2008; 108:9-22.
39. Intes X. Time-domain optical mammography SoftScan: initial results. Acad Radiol 2005; 12:934-47.
40. Cerussi A, Hsiang D, Shah N, et al. Predicting response to breast cancer neoadjuvant chemotherapy using diffuse optical spectroscopy. Proc Natl Acad Sci U S A 2007; 104:4014-9.
41. Soliman H, Gunasekara A, Rycroft M, et al. Functional imaging using diffuse optical spectroscopy of neoadjuvant chemotherapy response in women with locally advanced breast cancer. Clin Cancer Res 2010; 16:2605-14.
42. Grimberg H, Levin G, Shirvan A, et al. Monitoring of tumor response to chemotherapy in vivo by a novel small-molecule detector of apoptosis. Apoptosis 2009; 14:257-67.

# Chapter 14

## Nederlandse samenvatting

Borstkanker is de meest voorkomende kankersoort bij vrouwen en veroorzaakt de grootste kankergerelateerde sterfte onder vrouwen. Hoewel de incidentie van borstkanker nog steeds stijgt, is het sterftecijfer de laatste decennia afgenomen voornamelijk als gevolg van verbetering van systemische therapie. Desondanks blijft chirurgisch ingrijpen de hoeksteen van de curatieve behandeling van borstkanker.

De chirurgische behandeling van borstkanker heeft de afgelopen eeuw een sterke verandering doorgemaakt, waarbij deze steeds minder uitgebreid is geworden en daardoor patiëntvriendelijker. In 1907 werd door de Amerikaanse chirurg William S. Halsted een serie patiënten beschreven die dankzij een radicale mastectomie een uitstekende lokale controle kende. Bij deze operatie werden de borstklier, beide pectoralisspieren en alle relevante lymfklierstations *en bloc* verwijderd hetgeen gepaard ging met een grote morbiditeit. Om de morbiditeit te verminderen werd de radicale mastecomie gemodificeerd naar een operatie waarbij de pectoralisspieren gespaard bleven, de gemodificeerde radicale mastectomie. In de jaren zeventig van de vorige eeuw werd borstsparende chirurgie in combinatie met radiotherapie geïntroduceerd. Dit leidde tot een betere cosmetische uitkomst en een verbetering van het zelfbeeld van de patiënt. In 1994 werd de schildwachtklierprocedure geïntroduceerd waardoor een okselklierdissectie slechts bij patiënten met een positieve schildwachtklier wordt uitgevoerd. In deze paradigmaverschuiving naar een meer conservatieve chirurgische benadering past het concept van preoperatieve systemische (ook wel neoadjuvante) therapie, omdat hierbij de systemische therapie voorafgaand aan de operatie wordt gegeven om de tumor te verkleinen en daarmee de chirurgische mogelijkheden tot minder invasief opereren vergroot.

De belangrijkste uitdaging bij de chirurgische behandeling van borstkanker is het volledig verwijderen van het tumorweefsel met in achtneming van een adequate tumorvrije marge en een acceptabel cosmetisch resultaat. Echter, de chirurg moet vertrouwen op zijn zicht en gevoel om een onderscheid te maken tussen tumor- en normaal weefsel. Bij borstsparende operaties is dit bijzonder lastig, getuige het feit dat een onvolledige (irradicale) resectie in 5-40% van de gevallen voorkomt. Irradicale resecties kunnen leiden tot lokale terugkeer van de ziekte, hetgeen geassocieerd is met een slechtere overleving. Een techniek die tijdens de operatie specifiek tumorcellen visualiseert om de chirurg te helpen de optimale resectievlakken te kiezen zou daarom van grote meerwaarde kunnen zijn. Fluorescente beeldvorming met nabij-infrarood licht is een techniek die voor dit doel zeer geschikt lijkt.

Dit proefschrift bestaat uit twee delen. In **deel I** werd de effectiviteit van neoadjuvante therapie en de aanvullende waarde van het meten van de tumorrespons beoordeeld. Bovendien werd onderzocht of kankerstamcellen van invloed zijn op de prognose van borstkankerpatiënten. In **deel II** werd de techniek van de nabij-infrarode fluorescente beeldvorming preklinisch gevalideerd en geïntroduceerd in de kliniek.

# DEEL I: NEOADJUVANTE THERAPIE, TUMORRESPONS EN KANKERSTAMCELLEN

**Hoofdstuk 1** geeft een algemene inleiding op dit proefschrift. In **Hoofdstuk 2** werd in een meta-analyse van gerandomiseerde studies aangetoond dat neoadjuvante chemotherapie vergeleken met adjuvante chemotherapie resulteert in een gelijke overleving en een toename van het aantal borstsparende operaties, terwijl de lokale controle gelijk blijft. Derhalve is in internationale richtlijnen geadviseerd om neoadjuvante chemotherapie toe te passen voor alle patiënten waarbij voorafgaand aan de operatie duidelijk is dat zij in aanmerking komen voor chemotherapie.

Dankzij neoadjuvante therapie kan uitstekend het biologisch gedrag van de tumor *in vivo* geanalyseerd worden. Immers de tumor is nog in het lichaam aanwezig en hierdoor kan de respons van de tumor op de systemische therapie direct bepaald worden. Dit in tegenstelling tot de adjuvante situatie, waarbij de therapie 'blind' wordt gegeven; de tumor is reeds verwijderd en de reactie van de tumor tijdens de behandeling kan niet worden bepaald. Hierdoor is het nog grotendeels onbekend welke vrouwen het meeste baat hebben van welke specifieke systemische therapie. In **Hoofdstuk 3** werd binnen een gerandomiseerd onderzoek van neoadjuvante chemotherapie bepaald welke tumormarkers een goede tumorrespons voorspellen. Hierbij bleek het tumorsuppressoreiwit p53 de gevoeligheid voor een anthracycline-bevattende chemotherapieschema goed te voorspellen.

In **Hoofdstuk 4** werd het effect van chemotherapie in relatie tot de hormoonreceptorstatus onderzocht in een grote groep jonge borstkankerpatiënten (< 40 jaar). Uit eerdere neoadjuvante studies is gebleken dat hormoonreceptornegatieve borstkanker beter reageert op chemotherapie dan tumoren met overexpressie van de hormoonreceptoren. Echter, borstkanker op jonge leeftijd is relatief zeldzaam (~ 5% van de gevallen), waardoor er weinig onderzoeksresultaten bekend zijn voor deze groep. Bovendien is door de slechtere overleving van deze patiëntengroep in de huidige richtlijnen jonge leeftijd als absolute indicatie voor het geven van chemotherapie opgenomen ongeacht de status van de hormoonreceptoren. Hierdoor bestaat de zorg van overbehandeling bij deze jonge (fertiele) patiëntengroep. De meta-analyse van Hoofdstuk 4 toont aan dat jonge vrouwen met hormoonreceptorpositieve borstkanker minder baat hebben bij chemotherapie dan die met hormoonreceptornegatieve borstkanker.

**Hoofdstuk 5** laat zien dat de overleving van jonge vrouwen sterk afhankelijk is van het moleculaire subtype borstkanker en dat jonge patiënten met een gunstig subtype een uitstekende lange-termijn overleving hebben. Deze resultaten benadrukken dat tumorspecifieke prognostische kenmerken moeten worden meegenomen in het behandelingsplan van jonge borstkankerpatiënten.

Ondanks de recente verbeteringen in systemische en lokale behandeling ontwikkelt een substantieel deel van de borstkankerpatiënten een lokaal recidief of metastasen op afstand. Vaak ontstaan deze na een aanzienlijke follow-up tijd; soms pas 20 jaar na de operatie. Uit recent onderzoek is gebleken dat de kankerstamceltheorie dit falen van de behandeling kan verklaren. Binnen deze hypothese worden kankerstamcellen gezien als een kleine subpopulatie van tumorcellen met stamcelachtige kenmerken, zoals het overgaan van epitheel naar mesenchym, aanzetten tot differentiatie, het overleven van chemotherapie en bestraling door onder andere specifieke transporteiwitten en reparatie van DNA-schade. Expressie van het ontgiftende enzym aldehyde dehydrogenase-1 (ALDH1) wordt als één van de meest karakteristieke kenmerken van borstkankerstamcellen gezien. De kankerstamceltheorie zou ook een verklaring kunnen bieden voor de leeftijdsspecifieke verschillen in overleving van borstkanker, waarbij vroeg-optredende tumoren (< 65 jaar) vaak agressiever zijn en snel metastaseren, terwijl laat-optredende tumoren (> 65 jaar) meer indolent zijn.

Het onderzoek in **Hoofdstuk 6** toont aan dat de expressie van ALDH1 omgekeerd evenredig is met de leeftijd bij diagnose van borstkanker. Bij patiënten jonger dan 65 jaar was ALDH1 expressie sterk geassocieerd met een slechtere overleving, terwijl bij patiënten ouder dan 65 jaar ALDH1 status geen effect had op de overleving. Dit onderzoek onderstreept de verschillen in borstkankerbiologie tussen jonge en oude patiënten, hetgeen deels verklaard kan worden door verschillen in cellulaire mechanismen betrokken bij kankerstamcelactiviteit.

In **Hoofdstuk 7** werd de rol van het stollingseiwit tissue factor (TF) en zijn alternatief-gesplitste variant (asTF) bij de formatie en groei van borstkankerstamcellen onderzocht. Beide eiwitten worden tot expressie gebracht in een groot aantal tumortypen. De activiteit van TF verloopt via een protease activated receptor-2 (PAR2) pathway, terwijl de activiteit van asTF via een integrine-afhankelijke pathway verloopt. De resultaten van Hoofdstuk 7 tonen aan dat ALDH1 expressie sterk geassocieerd is met TF expressie en niet met asTF expressie, hetgeen suggereert dat de TF-PAR2 pathway van belang is voor de activiteit van borstkankerstamcellen. Het specifiek beïnvloeden van deze pathway door nieuwe medicijnen zou theoretisch de kankerstamcellen kunnen aanpakken, hetgeen zou kunnen leiden tot verbetering van overleving van borstkankerpatiënten.

## DEEL II: IMAGE-GUIDED SURGERY

In deel II van dit proefschrift werd de intraoperatieve beeldvormende techniek van nabij-infrarood (NIR) fluorescentie onderzocht. Nabij-infrarood (NIR) licht heeft een golflengte tussen de 700 en 900 nm, hetgeen voor het menselijk oog niet zichtbaar is. Het grote voordeel van NIR licht is dat het minder wordt geabsorbeerd door weefsel, waardoor de weefselpenetratie groter is (tot enkele cm's) dan dat van zichtbaar licht.

Daarnaast is de techniek veilig en vindt de beeldacquisitie in milliseconden plaats, waardoor het 'real-time' toegepast kan worden. Bovendien wordt het operatieveld niet beïnvloed door het NIR licht, omdat het niet zichtbaar is voor het menselijk oog. Voor de intraoperatieve detectie van tumoren zijn tumorspecifieke, NIR fluorescente contrastmiddelen (probes) nodig en camerasystemen om deze stoffen zichtbaar te maken.

In **Hoofdstuk 8** werd een nieuw, 'hand-held', intraoperatief NIR fluorescentie camerasysteem getest. Met nieuw ontwikkelde methodes werd zowel *in vitro* als *in vivo* de minimale detectielimieten, resolutie en intraoperatieve toepasbaarheid bepaald met behulp van een protease-geactiveerde NIR fluorescente probe en twee syngene ratmodellen.

In **Hoofdstuk 9** werd dit camerasysteem gebruikt om in een syngeen borstkankerratmodel orthotope borsttumoren te detecteren met een protease-geactiveerde NIR fluorescente probe. Op geleide van het NIR fluorescente beeld werden alle tumoren compleet gereserceerd met een minimale hoeveelheid normaal weefsel (gemiddelde minimale en maximale tumorvrije marge van respectievelijk 0.2 ± 0.2 mm en 1.3 ± 0.6 mm).

In **Hoofdstuk 10** werd het gebruik van monoclonale antilichamen gekoppeld aan een NIR fluorescente kleurstof uitgetest in hetzelfde syngeen ratmodel. Dit onderzoek toonde aan dat zowel de specifieke als de aspecifieke antilichamen een adequate detectie van borsttumoren faciliteerden, waardoor alle tumoren compleet gereserceerd konden worden. Het feit dat ook de aspecifieke antilichamen een goed contrast gaven, kan verklaard worden door het zogenaamde 'enhanced permeability and retention effect'. Hierbij concentreren de stoffen zich in de tumor door passieve accumulatie.

Deze preklinische onderzoeken toonden de potentie van NIR fluorescente beeldvorming aan voor de intraoperatieve detectie en succesvolle resectie van tumoren in een borstkankerratmodel. Zodra de NIR fluorescente probes goedgekeurd worden voor klinische toepassing kan de waarde van NIR fluorescente beeldvorming bij de operatieve behandeling van borstkankerpatiënten bepaald worden.

Naast de intraoperatieve tumordetectie biedt NIR fluorescente beeldvorming de mogelijkheid om de schildwachtklierprocedure te verbeteren. De schildwachtklier is de eerste lymfeklier waar een tumor op draineert. Als deze klier geen tumorcellen bevat is de kans zeer groot dat de andere lymfeklieren ook geen metastasen bevatten, waardoor een ingrijpende okselklierdissectie achterwege kan worden gelaten. Om de schildwachtklier te vinden wordt tegenwoordig een radioactieve stof en een blauwe kleurstof rondom de borsttumor ingespoten. NIR fluorescente beeldvorming kan met de klinisch goedgekeurde NIR probe indocyaninegroen (ICG) een aanvulling vormen op de huidige schildwachtklier-procedure of zelfs de huidige modaliteiten vervangen. Preklinisch onderzoek heeft laten zien dat als ICG aan humaan serum albumine (HSA)

gekoppeld wordt de eigenschappen als lymfetracer verbeterd worden door een betere retentie in de schildwachtklier en een verhoogde fluorescentie.

In **Hoofdstuk 11** werd een nieuw, intraoperatief camerasysteem gebruikt dat zowel het normale kleurenbeeld als het NIR fluorescente beeld registreert, om de geïnjecteerde dosis ICG:HSA te optimaliseren bij borstkankerpatiënten. De schildwachtklier werd bij alle patiënten succesvol geïdentificeerd. De optimale dosis ICG:HSA lag tussen 400 en 800 μM. Bovendien werden de lymfebanen en in sommige gevallen de schildwachtklier percutaan gevisualiseerd.

In **Hoofdstuk 12** werd onderzocht of het vooraf koppelen van HSA aan ICG noodzakelijk is of dat injectie van alleen ICG een even goed resultaat levert. In dit geblindeerd, gerandomiseerd onderzoek werd geen verschil gevonden in fluorescent contrast of het aantal gevonden schildwachtklieren tussen de ICG:HSA groep en de ICG alleen groep. Vooraf koppelen van ICG aan HSA is dus overbodig. Dit kan verklaart worden doordat ICG zich snel bindt aan de in de lymfe aanwezige eiwitten. Deze resultaten zullen de introductie in de kliniek aanzienlijk vergemakkelijken. Of NIR fluorescente beeldvorming de radioactieve tracer en de blauwe kleurstof kan vervangen wordt momenteel door onze groep onderzocht (NTR2674).

## CONCLUSIES

Neoadjuvante therapie moet als een geaccepteerde behandelingsmodaliteit van borstkanker beschouwd worden. Deze therapievorm maakt meer borstsparende operaties mogelijk en geeft gelijke overlevingscijfers en lokale controle ten opzichte van adjuvante therapie. Daarnaast biedt neoadjuvante therapie de mogelijkheid om bij tumorresistentie van therapie te veranderen en faciliteert het translationeel onderzoek waardoor een belangrijke bijdrage geleverd wordt aan de verdere ontwikkeling van geïndividualiseerde behandelplannen voor borstkankerpatiënten.

NIR fluorescente beeldvorming is een sensitieve techniek om tijdens de operatie specifiek tumor- en normaalweefsel te visualiseren om de optimale tumorvrije marges te bepalen en de schildwachtklierprocedure te verbeteren. In de komende jaren moet blijken of deze vorm van “image-guided surgery” daadwerkelijk de chirurgische behandeling van kankerpatiënten kan optimaliseren om daarmee een verbetering van de overleving en kwaliteit van leven te bereiken.

## LIST OF PUBLICATIONS

**Mieog JS***, de Kruijf EM*, Bastiaannet E, Kuppen PJ, Sajet A, de Craen AJ, Smit VT, van de Velde CJ, Liefers GJ. Age interactions in the prognostic role of the cancer stem cell marker aldehyde dehydrogenase-1 in breast cancer. *Submitted.*

van der Vorst JR, Hutteman M, Schaafsma BE, **Mieog JS**, Liefers GJ, Hartgrink HH, Smit VT, Frangioni JV, van de Velde CJ, Vahrmeijer AL. Identification and image-guided resection of occult superficial liver metastases using indocyanine green and near-infrared fluorescence imaging. *Submitted.*

van der Vorst JR, Schaafsma BE, Hutteman M, Verbeek F, **Mieog JS**, Liefers GJ, Frangioni JV, van de Velde CJ, Vahrmeijer AL. Randomized comparison of near-infrared fluorescence imaging using indocyanine green with or without patent blue for the sentinel lymph node procedure in breast cancer patients. *Submitted.*

**Mieog JS**, Morden JP, Bliss JM, Coombes RC, van de Velde CJ. Impact of carpal tunnel syndrome and musculoskeletal symptoms in postmenopausal women with early breast cancer treated with exemestane vs. tamoxifen after 2-3 years of tamoxifen: a retrospective analysis of the Intergroup Exemestane Study. *Submitted.*

Hutteman M, van der Vorst JR, Gaarenstroom KN, Peters AA, **Mieog JS**, Schaafsma BE, Löwik CW, Frangioni JV, van de Velde CJ, Vahrmeijer AL. Optimization of near-infrared fluorescent sentinel lymph node mapping for vulvar cancer. *Am J Obstet Gynecol 2011.*

van der Vorst JR, Hutteman M, Gaarenstroom KN, Peters AA, **Mieog JS**, Schaafsma BE, Kuppen PJ, Frangioni JV, van de Velde CJ, Vahrmeijer AL. Optimization of near-infrared fluorescent sentinel lymph node mapping in cervical cancer patients. *Int J Gynecol Cancer 2011.*

van der Hage JA*, **Mieog JS***, van de Velde CJ, Putter H, Bartelink H, van de Vijver MJ. Impact of established prognostic factors and molecular subtype in very young breast cancer patients: Pooled analysis of four EORTC randomized controlled trials. *Breast Cancer Res 2011; 13:R68.*

van der Vorst JR, Hutteman M, **Mieog JS**, de Rooij KE, Kaijzel EL, Lowik CW, Putter H, Kuppen PJ, Frangioni JV, van de Velde CJ, Vahrmeijer AL. Near-infrared fluorescence imaging of liver metastases in rats using indocyanine green. *J Surg Res 2011.*

Schaafsma BE, **Mieog JS**, Hutteman M, van der Vorst JR, Kuppen PJ, Lowik CW, Frangioni JV, van de Velde CJ, Vahrmeijer AL. The clinical use of indocyanine green as a near-infrared fluorescent contrast agent for image-guided oncologic surgery. *J Surg Oncol 2011; 104:323-32.*

Hutteman M*, **Mieog JS***, van der Vorst JR, Liefers GJ, Putter H, Lowik CW, Frangioni JV, van de Velde CJ, Vahrmeijer AL. Randomized, double-blind comparison of indocyanine green with or without albumin premixing for near-infrared fluorescence imaging of sentinel lymph nodes in breast cancer patients. *Breast Cancer Res Treat 2011; 127:163-70.*

**Mieog JS***, Troyan SL*, Hutteman M*, Donohoe KJ, van der Vorst JR, Stockdale A, Liefers GJ, Choi HS, Gibbs-Strauss SL, Putter H, Gioux S, Kuppen PJ, Ashitate Y, Lowik CW, Smit VT, Oketokoun R, Ngo LH, van de Velde CJ, Frangioni JV, Vahrmeijer AL. Toward optimization of imaging system and lymphatic tracer for near-infrared fluorescent sentinel lymph node mapping in breast cancer. *Ann Surg Oncol 2011; 18:2483-91.*

Keereweer S, Kerrebijn JD, Mol IM, **Mieog JS**, van Driel PB, Baatenburg de Jong RJ, Vahrmeijer AL, Lowik CW. Optical imaging of oral squamous cell carcinoma and cervical lymph node metastasis. *Head and Neck 2011.*

Keereweer S, **Mieog JS**, Mol IM, van Driel PB, Snoeks TJ, Baatenburg de Jong RJ, Vahrmeijer AL, Kerrebijn JD, Lowik CW. Detection of oral squamous cell carcinoma and cervical lymph node metastasis using activatable near-infrared fluorescence agents. *Arch Otolaryngol Head Neck Surg 2011; 137:609-15.*

Hutteman M, van der Vorst JR, **Mieog JS**, Bonsing BA, Hartgrink HH, Kuppen PJ, Lowik CW, Frangioni JV, van de Velde CJ, Vahrmeijer AL. Near-infrared fluorescence imaging in patients undergoing pancreaticoduodenectomy. *Eur Surg Res 2011; 47:90-7.*

Hutteman M*, **Mieog JS***, van der Vorst JR, Dijkstra J, Kuppen PJ, van der Laan AM, Tanke HJ, Kaijzel EL, Que I, van de Velde CJ, Lowik CW, Vahrmeijer AL. Intraoperative near-infrared fluorescence imaging of colorectal metastases targeting integrin $\alpha_v\beta_3$ expression in a syngeneic rat model. *Eur J Surg Oncol 2011; 37:252-7.*

Hutteman M, Choi HS, **Mieog JS**, van der Vorst JR, Ashitate Y, Kuppen PJ, van Groningen MC, Lowik CW, Smit VT, van de Velde CJ, Frangioni JV, Vahrmeijer AL. Clinical translation of ex vivo sentinel lymph node mapping for colorectal cancer using invisible near-infrared fluorescence light. *Ann Surg Oncol 2011; 18:1006-14.*

Keereweer S, Kerrebijn JD, van Driel PB, Xie B, Kaijzel EL, Snoeks TJ, Que I, Hutteman M, van der Vorst JR, **Mieog JS**, Vahrmeijer AL, van de Velde CJ, Baatenburg de Jong RJ, Lowik CW. Optical image-guided surgery - where do we stand? *Mol Imaging Biol 2011; 13:199-207.*

**Mieog JS**, Hutteman M, van der Vorst JR, Kuppen PJ, Que I, Dijkstra J, Kaijzel EL, Prins F, Lowik CW, Smit VT, van de Velde CJ, Vahrmeijer AL. Image-guided tumor resection using real-time near-infrared fluorescence in a syngeneic rat model of primary breast cancer. *Breast Cancer Res Treat 2011; 128:679-89.*

Schepers A, **Mieog JS**, van de Burg BB, van Schaik J, Liefers GJ, Marang-van de Mheen PJ. Impact of complications after surgery for colorectal liver metastasis on patient survival. *J Surg Res 2010; 164:e91-7.*

**Mieog JS**, Vahrmeijer AL, Hutteman M, van der Vorst JR, Drijfhout van Hooff M, Dijkstra J, Kuppen PJ, Keijzer R, Kaijzel EL, Que I, van de Velde CJ, Lowik CW. Novel intraoperative near-infrared fluorescence camera system for optical image-guided cancer surgery. *Mol Imaging 2010; 9:223-31.*

**Mieog JS**, van de Velde CJ. Neoadjuvant chemotherapy for early breast cancer. *Expert Opin Pharmacother 2009; 10:1423-34.*

Lowik CW, Kaijzel E, Que I, Vahrmeijer AL, Kuppen PJ, **Mieog JS**, van de Velde CJ. Whole body optical imaging in small animals and its translation to the clinic: Intra-operative optical imaging guided surgery. *Eur J Cancer 2009; 45:391-3.*

**Mieog JS**, van Nes JG, van de Velde CJ. The advantages of preoperative systemic therapy in breast cancer. *Ned Tijdschr Geneeskd 2008; 152:2501-6.*

**Mieog JS**, Stoot JH, Bosch JJ, Koning OH, Hamming JF. Inflammatory aneurysm of the common iliac artery mimicking appendicitis. *Vascular 2008; 16:116-9.*

van der Hage JA, **Mieog JS**, van de Vijver MJ, van de Velde CJ. Efficacy of adjuvant chemotherapy according to hormone receptor status in young patients with breast cancer: A pooled analysis. *Breast Cancer Res 2007; 9:R70.*

**Mieog JS**, van der Hage JA, van de Velde CJ. Neoadjuvant chemotherapy for operable breast cancer. *Br J Surg 2007; 94:1189-200.*

**Mieog JS**, van der Hage JA, van de Velde CJ. Preoperative chemotherapy for women with operable breast cancer. *Cochrane Database Syst Rev 2007: CD005002.*

**Mieog JS**, van der Hage JA, van de Vijver MJ, van de Velde CJ. Tumour response to preoperative anthracycline-based chemotherapy in operable breast cancer: The predictive role of p53 expression. *Eur J Cancer 2006; 42:1369-79.*

**Mieog JS**. Carotisstenose: een oorzaak van herseninfarct. *Ned Tijdschr Geneeskd Stud 2003; 6:47-50.*

* Shared first authorship

**Selected presentations**

Five years of exemestane as initial therapy compared to 5 years of tamoxifen followed by exemestane: the TEAM trial, a prospective, randomized, phase III trial in postmenopausal women with hormone-sensitive early breast cancer - a report by the TEAM trial investigators. *European Society of Surgical Oncology Congress, Bordeaux, 2010.* Awarded with Best Paper Award.

Impact of histological grade on prognosis in very young breast cancer patients: pooled analysis of four EORTC trials. *6th European Breast Cancer Conference, Berlijn, 2008.* Awarded with Best Presented Poster Award.

## CURRICULUM VITAE

Sven Mieog werd geboren op 27 januari 1980 in Monster. Na het behalen van het VWO-diploma in 1998 aan het Zandevelt College te 's Gravenzande startte hij met de studie Biologie aan de Universiteit Leiden. In 2000 werd hij ingeloot voor de studie Geneeskunde aan diezelfde universiteit. In het collegejaar 2002-2003 was hij student assessor van het Leids Universitair Medisch Centrum (LUMC). Gedurende de studie werkte hij mee aan verschillende onderzoeken naar borstkanker bij de afdeling Heelkunde van het LUMC onder leiding van Prof. dr. C.J.H. van de Velde. Hiervoor ontving hij de Nijbakker-Morra studentenprijs. Voor zijn wetenschapsstage ter afronding van de doctoraalfase Geneeskunde verrichtte hij onderzoek bij de Cochrane Breast Cancer Group in Sydney, Australië. Voor dit onderzoek ontving hij de Dick Held junior prijs. Zijn co-assistentschappen deed hij ondermeer bij de afdeling Gynaecologie in het Diaconessenhuis in Paramaribo, Suriname en bij Dr. P. Arrindell, huisarts te St. Maarten, Nederlandse Antillen. In 2007 studeerde hij cum laude af. Aansluitend startte hij zijn promotieonderzoek bij de afdeling Heelkunde van het LUMC (promotor: Prof. dr. C.J.H. van de Velde, co-promotor Dr. A.L. Vahrmeijer), waarvan de resultaten in dit proefschrift zijn beschreven. In 2008 verkreeg hij een ZonMw assistent-geneeskundige in opleiding tot klinisch onderzoeker (AGIKO) stipendium. Sinds juli 2010 is hij in opleiding tot chirurg in het HagaZiekenhuis te Den Haag (opleider Dr. J.W.S. Merkus).

# DANKWOORD

Eerst wil ik de patiënten bedanken die deel hebben genomen aan de onderzoeken en alle co-auteurs voor hun inzet en kritische beoordeling. Prof. van de Velde, als student was ik in 2003 direct onder de indruk van uw 'onderzoeksimperium'. Zeer veel dank voor uw begeleiding en vertrouwen. Alexander, samen begonnen we aan het imaging-avontuur. Dankzij jouw enorme betrokkenheid en motto "nummer één word je niet alleen" heb je in een korte tijd een prachtige onderzoekslijn opgebouwd. Jos van der Hage, onder jouw hoede heb ik mijn eerste stappen in het wetenschappelijk bedrijf gezet. Gerrit-Jan, onze discussies over de biologie en therapie van oncologische ziektes waardeer ik bijzonder.

Veel dank gaat uit naar het Green Team! Dankzij jullie was promoveren een feest: van het croissantontbijt via de nachtelijke experimenten gevoed door quattro formaggi's met extra salami tot de champagnekurken in het raamkozijn om een publicatie te markeren. Wat een hechte vriendschap kan een 'beetje' onderzoek al niet aanrichten! Merlijn, al snel kwam je bij het team en vanuit Boston hadden we een prachtig één-tweetje om het klinische onderzoek in Leiden van de grond te krijgen. Joost, jouw humor en handigheid brachten naast MTH en Bas 'finish the situation' Rutten, ook razendsnel klinische resultaten. Bob, als eigenzinnige student begonnen heb je nu het stokje overgenomen. Zet 'm op! Floris, Mark, Sanne, Kees en Rutger-Jan, wat mooi om te zien dat het onderzoek in jullie handen voortvarend doorgaat.

Dit proefschrift is tot stand gekomen dankzij de hulp en ondersteuning van velen. Graag wil ik ook de volgende afdelingen bedanken: Heelkunde research lab, chirurgen, assistenten, promovendi en secretaressen van de afdeling Heelkunde, Moleculaire Endocrinologie, LKEB, proefdierverzorgers, Pathologie, Moleculaire Celbiologie, Datacenter, Mammapoli, Apotheek, Hematologie en Urologie. Special thanks to the Cochrane Breast Cancer Group in Sydney for the support during my stay in 2005. Also, special thanks to the lab of Prof. Frangioni in Boston for a great collaboration and a warm welcome during our visit. John, what a vibrant atmosphere in your group! Many thanks for sharing your knowledge and equipment with our team.

Caro, dank voor je artistieke omslag van mijn proefschrift.

Dries en Roderick, studiegenoten, huisgenoten, musketiers, ceremoniemeesters en dan nu paranimfen. Onze vriendschap is voor mij zeer belangrijk.

Lieve grootouders, ouders, broer en zus, heel veel dank voor jullie steun en vertrouwen. Lieve Hans en Nel, jullie aanstekelijke levensvreugde was en is een voorbeeld.

Lieve Anne, jouw liefde en enthousiasme hebben er voor gezorgd dat nu ook mijn proefschrift af is, zodat we nu kunnen gaan genieten … van ons volgende wonder.